MEMBRANE DEVELOPMENT AND FABRICATION FOR REVERSE OSMOSIS AND ULTRAFILTRATION

by

EP JACOBS and RD SANDERSON

FINAL REPORT TO THE
WATER RESEARCH COMMISSION

BY THE
INSTITUTE FOR POLYMER SCIENCE
UNIVERSITY OF STELLENBOSCH

PART 2:
STATISTICAL AND NUMERICAL TECHNIQUES IN THE OPTIMIZATION OF MEMBRANE FABRICATION VARIABLES

WRC PROJECT: 172

DEC 1987

MEMBRANE DEVELOPMENT AND FABRICATION FOR REVERSE OSMOSIS AND ULTRAFILTRATION

THIS PROJECT WAS FUNDED BY THE WATER RESEARCH COMMISSION AND CARRIED OUT AT THE INSTITUTE FOR POLYMER SCIENCE AT THE UNIVERSITY OF STELLENBOSCH

THE REPORT IS PRESENTED IN FOUR PARTS:

PART 1: EXECUTIVE SUMMARY TO THE FINAL REPORT

EP JACOBS and RD SANDERSON

PART 2: STATISTICAL AND NUMERICAL TECHNIQUES IN THE OPTIMIZATION OF MEMBRANE FABRICATION VARIABLES

EP JACOBS and RD SANDERSON

PART 3: THE CHEMISTRY OF POLY-2-VINYLIMIDAZOLINE REVERSE OSMOSIS MEMBRANES

MJ HURNDALL and RD SANDERSON

PART 4: TECHNOLOGY TRANSFER: THE DEVELOPMENT OF TUBULAR UF TECHNOLOGY FOR INDUSTRIAL USE (CLASSIFIED - NOT AVAILABLE FOR DISTRIBUTION)

NKH STROHWALD, EP JACOBS and RD SANDERSON

ACKNOWLEDGEMENT

The Steering Comittee, co-opted members and referees for this project consisted of the following persons:

Dr CF Schutte	Water Research Commission (Chairman)
Mr JP Barnard	Bakke Industries (Pty) Ltd
Prof CA Buckley	University of Natal
Mr NA Dowler	University of Stellenbosch
Prof W Engelbrecht	University of Stellenbosch
Dr PF Fuls	National Institute for Water Research
Dr OO Hart	Water Research Commission
Mr BA Hendry	Bakke Industries (Pty) Ltd
Dr MJ Hurndall	University of Stellenbosch
Dr EP Jacobs	University of Stellenbosch
Dr S Kuehl	University of Stellenbosch
Mr PE Odendaal	Water Research Commission
Dr C Patterson-Jones	University of Cape Town
Dr HS Pienaar	Universiteit van Stellenbosch
Dr LS Rayner	University of Stellenbosch
Dr RD Sanderson	University of Stellenbosch
Prof DF Schneider	University of Stellenbosch
Mr DB Smit	Bakke Industries (Pty) Ltd
Prof JJ Smit	University of Potchefstroom for CHE
Mr PL Swart	Bakke Industries (Pty) Ltd
Dr AJ van Reenen	University of Stellenbosch
Mr PW Weideman	Water Research Commission (Secretary)

The financing of the project by the Water Research Commission and the contribution by the members of the Steering Committee are acknowledged gratefully.

EXECUTIVE SUMMARY

In a semi-arid country such as South Africa we are all too often made aware, by the recurrence of drought and the imposition of water restrictions, of how essential water is to nature and man. Industrial growth proceeds with population growth and further increases the demand for the already meagre resources of water. Industrial growth areas have now to be supported by transporting water over long distances, even from neighbouring states. Water has been identified as a strategic mineral and in many quarters is seen as a growth-limiting factor. Its quality and availability need to be protected, even by legislation, as the demand will exceed supply by the year 2020 - 2030. One process which will help to augment the supply of water by recycling of wastewater, is the desalination process of reverse osmosis.

With the rapid growth of the potential of membrane desalination processes, most of the attention in literature has been focused on membrane module configurations which, by their nature, allow large membrane-to-volume packing densities, such as the spiral wrap and hollow fine fibre modules which, respectively, house flat-sheet and hollow fine-fibre membranes. Not much attention had been paid to the tubular membrane module configuration which, although it has a low packing density relative to the others, is an attractive alternative as very little pretreatment of the feed process water is required because of the open flow-channel of the tubular membrane.

Therefore, an entirely new approach to tubular membrane fabrication was necessary. The objective of this work was to develop a statistical approach in identifying and formulating membrane design criteria. We will not be interested in first principles or reasons why one, two or three factors studied are, or are not, important or interacting. We will merely identify those ones which are important and show that the use of the statistically designed-experiment approach in membrane fabrication can be a very important scientific device in applied membrane science.

As an outline of what the study entailed, the objectives are summarized below:

ASYMMETRIC CELLULOSE ACETATE MEMBRANES

The objective of this research was, with the aid of factorially designed experiments to:

i) Isolate factors important in the formulation of an asymmetric tubular cellulose acetate reverse osmosis membrane.

ii) Generate membrane performance regression equations to assist in the formulation of tubular cellulose acetate membranes with optimal flux performance in the 90 to 95% salt-rejection range.

iii) Test the design equations and approach for validity.

ULTRA-THIN FILM POLYVINYLAMIDINE MEMBRANES

The objective of this research, with the aid of a Simplex technique of self-directing optimization, was to:

i) Determine whether polyvinylamidine can be used as a precursor in the creation of a novel ultra-thin film composite reverse osmosis membrane.

ii) Determine the intrinsic salt rejection potential of the tubular polyvinylamidine ultra-thin film membrane through a membrane formulation study.

ASYMMETRIC MICRO-POROUS SUBSTRATE FOR ULTRA-THIN COMPOSITE MEMBRANES

The objective of the study, through the use of a fractional factorial designed experiment, was to;

i) Isolate fabrication variables which have a significant effect on the adherence of the micro-porous membrane to the support fabric.

ii) Determine to what extent substrate membrane fabrication variables have an effect on the performance of ultra-thin film polyvinylamidine reverse osmosis membranes

In the following paragraphs a brief outline is given of the text contained in the chapters following.

Wet-phase inversion, the process according to which the asymmetric membranes in this text are formed, is discussed in Chapter II. The literature survey covers topics such as the behaviour of polymers in solution, de-mixing of polymers and the role which casting solution and coagulant additives play in affecting membrane properties. To aid in a better understanding of results presented in Chapter VI, the chapter also includes a section of phase diagrams for the ternary polymer/solvent/non-solvent system. For the sake of completion, reference is also made to other methods by which phase inversion can be accomplished.

In Chapter III, the concept of forming an ultra-thin permselective film on the surface of an asymmetric ultrafiltration membrane is discussed. Factors involved in the formation of the permselective film are again reviewed in section 6.3.2 in Chapter VI.

In Chapter IV the topic of statistically designed experiments is introduced (and detailed with the aid of experimental results which has bearing on the text in Chapter VI), to allow the reader, not familiar with the technique, to acquaint himself with the procedures followed. These techniques were necessary to allow the maximum amount of unambiguous information to be extracted from the minimum amount of experimental work. For example, five factors were studied simultaneously in the case of the asymmetric cellulose acetate membrane in a complete 25 factorial designed experiment (section 6.1.2), nine factors were considered simultaneously in a study of the effect of membrane fabrication variables on the adhesion of poly(arylether

sulphone) micro-porous membranes to their support fabric in a sixteenth fractionally replicated 29 factorial experiment (section 6.2.2.3).

During the course of the research effort, it was necessary to design and construct equipment to facilitate the continuous or semicontinuous fabrication of tubular membranes. This, as well as equipment constructed for use in the evaluation of the membranes, is discussed in detail in Chapter V.

Chapter VI contains the results of and discussion on experiments designed to achieve objectives stated earlier. Two reverse osmosis membrane systems were studied. In the first section of the chapter, the reader is introduced to aspects regarding the formulation of the well-known cellulose acetate membrane. The intention of this research was not to determine the optimal intrinsic performance of tubular CA membranes as such (well documented in the open and patent literature for flat-sheet CA membranes), but rather to relate fabrication variables to tubular membrane performance by means of regression procedures. Numerical optimization was performed on the regression equations obtained through factorial designed experiments, to forecast formulations of membranes with optimal flux performances for specified rejections. Two grades of cellulose acetate membrane materials were used in this study.

In sections 6.2 and 6.3 aspects concerning the research and development of a novel ultra-thin film composite membrane receive attention. In section 6.2 formulation of the micro-porous substrate membrane on which the ultra-thin film reverse osmosis membrane is created is discussed. One problem in creating this membrane was the poor adherence between the poly(bisphenol-A-sulphone) substrate membrane and the poly(ethylene terephthalate) support fabric used. As no solution to this problem was presented in the literature, and as various membrane formulations offered for flat-sheet micro-porous membranes did not solve the tubular membrane adherence problem, a simultaneous study (in the form of a fractionally replicated factorial experiment) of a large number of fabrication variables was conducted to relate their effect on substrate membrane/fabric adherence quantitatively. No attempt at a mechanistic study of the problem was made.

In section 6.3 the formation of novel ultra-thin film polyvinylamidine composite reverse osmosis membranes is discussed and the intrinsic (optimum) salt rejection performance of the membranes determined by means of a self-directing optimization approach. Additional factors, such as post-treatment of the membrane and the role of substrate membrane formulations, and their effect on the reverse osmosis performance of the membrane also receive attention.

The work proved the following:

TUBULAR CELLULOSE ACETATE MEMBRANES

i) The applicability of statistical techniques and statistical designed experiments to the generation of fabrication formulations for tubular cellulose acetate membranes was illustrated. (Sections 6.1.2 and 6.1.3)

ii) It was proved that the multiple-linear regression models, which were developed to represent the permeate flux and salt rejection responses of tubular cellulose acetate membranes, can be manipulated mathematically to predict fabrication formulations to achieve optimal permeate flux performances for specified salt rejections. (Sections 6.1.2.4 and 6.1.2.5).

iii) A Taylor series, expanded to include quadratic terms, proved sufficient for modelling the permeate flux and salt rejection responses of tubular cellulose acetate membranes. (Section 6.1.3.5).

iv) It was shown further that by changing the grade of cellulose acetate used from 398-10 to 400-25, a different set of design equations, which showed better performance in different ranges of usage, was obtained. (Preamble to section 6.1.3 and 6.1.3.6).

ASYMMETRIC MICRO-POROUS TUBULAR SUBSTRATE MEMBRANES

i) Although micro-porous substrate membranes, used in ultra-thin film composite membrane fabrication, were successfully produced from the well documented Udel 1700P and 3500P poly(bisphenol A sulphone) dissolved in a mixture of N-methyl, 2-pyrrolidone and 1,4-dioxane, the adhesion of these membrane systems to the porous non-woven Viledon FO2406 poly(ethylene terephthalate) support fabric was as unsatisfactory. This inadequacy in membrane adherence was overcome by the use of a different substrate membrane which was developed from a study of membrane-forming polymers, casting solution compositions and fabrication conditions. These membranes were produced from Victrex 4800G poly(arylether sulphone), dissolved in either N-methyl, 2-pyrrolidone or a mixture of N-methyl, 2-pyrrolidone and N,N-dimethyl formamide, with polyvinyl-pyrrolidone and lithium chloride additives. The bond-strength of these membranes to the support fabric was more than twenty times greater than that of the Udel 1700P and 3500P membranes. (Section 6.2.2.4).

ii) In a simultaneous study of nine factors (Section 4.3.4), only thirty-two experiments were needed to establish that an inverse relationship existed between the substrate membrane permeate flux performance and the adherence of the substrate membrane to the non-woven support tube.

ULTRA-THIN FILM POLYVINYLAMIDINE MEMBRANES

i) It was demonstrated with the polyvinylamidine ultra-thin film composite reverse osmosis membrane system that up to twelve membrane formulation variables can be studied simultaneously in a self-directing optimization approach to yield a membrane with optimum performance. (Sections 6.3.2 and 6.3.3). This study was successfully concluded even though the synthesis of the polyvinylamidine precursor was still under development and random variability in the quality of the material was known to exist.

ii) It was shown that ultra-thin film composite membranes with extremely good reverse osmosis properties (in the optimum case a sodium chloride salt rejection of 99,1% and a permeate flux performance of 860 liters per square metre per day), can be fabricated in tube form. (Section 6.3.7.3). Although the ultra-thin film composite membrane study was mainly directed towards a better understanding of factors at play in the formulation of the membrane it was shown unequivocally that a novel ultra-thin film tubular composite membrane can be made with more than adequate performance characteristics to warrant its use as a commercial brack-water desalting membrane.

iii It was also shown that the chemistry of the approximately 200 nanometre ultra-thin membrane film can be changed or improved by further post-chemical reaction(s). Examples were the improved permeate flux performance which resulted by reaction of the membrane with glyoxal, and the improved dry storage-life obtained with diaminobenzene treatment. (Section 6.3.7).

LIST OF CONTENTS

LIST OF FIGURES

LIST OF TABLES

LIST OF SYMBOLS AND ABBREVIATIONS

A,B,...	Factors (defined as feature of a designed experiment, which can be varied from experiment to experiment, such as temperature, concentration *etc.*) are denoted by capital letters.
CA	Cellulose acetate
DMAc	Dimethyl acetamide
DMF	N,N-Dimethyl formamide
F-ratio	Variance ratio, the test statistic of the F-test. The F-test checks the difference between two variances in terms of the F-distribution. $F(\phi_1,\phi_2)_\alpha$ is the critical value for the F-test, ϕ_1 df (degrees of freedom) in the numerator, ϕ_2 df in the denominator.
H_o	Null hypothesis.
H_1	Alternative hypothesis
Level	Value of variable x assigned to a factor for the purpose of experimentation. Typically factor-levels are -1, +1, or 0. When decoded, they represent the actual experimental value, *i.e.* degrees Celcius or mass percent for temperature and concentration, *etc.*
lmd	Membrane permeation rate, litres per square metre per day
lpm	Litres per minute
MSS	Mean sum of squares, variance
n	Sample size, number of factors under consideration in an experiment or number of independent measurements.
P	Probability
NMP	N-methyl-2-pyrrolidone
PPO	Poly(2,6-dimethyl 1,4-phenylene oxide)
PS	Poly(bisphenol-A-sulphone)
PES	Poly(arylether sulphone)
PET	Poly(ethylene terephthalate), polyester
PVAM	Polyvinylamidine
PWP	Pure water permeability
RO	Reverse osmosis
SCL	m-Chlorosulphonyl benzoylchloride
SDO	Self-directing optimization
SS	Sum of squares, $\Sigma(x - \bar{x})^2$, variation
SST	Total sum of squares
t-Test	Test statistic to check the equality of two means in terms of the Student distribution
UF	Ultrafiltration
UTF	Ultrathin-film
VAR	Variance = σ^2
c	Number of columns in the one-way analysis of variance
df	Degrees of freedom
r	Number of rows in the two-way analysis of variance, or number of replicates in two-level factorial experiments
s	Standard deviation of a sample
s^2	Variance of a sample
$s_{\bar{x}}^2$	Variance of the arithmetic mean in a sample
s_p^2	Pooled variance
x	Independent measurements of a variable

x	Independent variable
y	Response observed
Y	Response in regression
y^*	Fitted value of Y
α	Level of significance, Type I error, probability of rejecting a valid null hypothesis, also Population regression intercept.
β	Probability of retaining an invalid null hypothesis and commit a Type II error, also Population regression slope.
σ	Standard deviation of a population
σ^2	Variance of a population
μ	Arithmetic mean of population
Σ	Summation, *e.g.* Σx^2 means, add up the squares of all the x's
Δ	Difference
$\longrightarrow$	Estimate of the quantity to the right

CHAPTER I

INTRODUCTION AND OBJECTIVES

In a semi-arid country such as South Africa we are all too often made aware, by the recurrence of drought and the imposition of water restrictions, of how essential water is to nature and man. Industrial growth proceeds with population growth and further increases the demand for the already meagre resources of water. Industrial growth areas have now to be supported by transporting water over long distances, even from neighbouring states. Water has been identified as a strategic mineral and in many quarters is seen as a growth-limiting factor. Its quality and availability need to be protected, even by legislation, as the demand will exceed supply by the year 2020 - 2030. One process which will help to augment the supply of water by recycling of wastewater, is the desalination process of reverse osmosis.

Much of the literature on membrane research and development which relates to fabrication procedures mainly concerns membranes other than of the tubular configuration, *e.g.* the hollow fine-fibre and flat-sheet configurations. Where the published research is directed at membranes of tubular geometry, the literature becomes sparse; in fact there has been no useful physico-chemical approach involving statistical experimental design to study tubular membrane fabrication variables. This thesis makes a contribution to scientific knowledge regarding the engineering, chemical and physical aspects of polymers related to tubular reverse osmosis membrane research and development.

The science of any membrane system involves a multitude of formulation variables. On this premise, membrane research involves a study of these variables and their interactions in order, either to generate an understanding of the science involved, or to exercise control over desired properties.

Two levels or strategies have been employed in order to develop design criteria for the fabrication of membranes which meet the specific needs of the user. The starting point is the identification of those specific factors which are known to be present in any membrane, for optimal performance in the end-use situation. An example of such a variable might be the pore size of a micro-filtration membrane. Thus, for optimal end-use performance, one identifies factors such as the temperature at which the membrane will be used, the type and size of the material to be filtered, and the permeability which is required to make the separation process economically feasible.

The process of membrane design starts with a search for a membrane forming and membrane support material which have the right properties and which can be manipulated to incorporate the structural characteristics deemed valuable or necessary in the specific end-use application.

The fine toning of these structural characteristics, be they related to a particular size, shape or number, can be approached by the two strategies mentioned earlier. One is an *ab initio* or first-principles type of approach whereby, in the most simple case, only a few variables, which are known to be directly related to the physics of the membrane material or the physics of the interactions between the membrane and the solvent, are identified and studied independently, so that general guidelines can be formulated from which the specific type of structure required can be realized. In practice this approach has been the one used most in the membrane-design field. This has resulted in many models of membrane behaviour such as the capillary or solution-diffusion models for example. In this way, the mechanisms of the transport process are identified on purely physical and microscopic levels, and the fabrication procedures are built around and arise from these microscopic criteria. When too many structural characteristics are imposed on the membrane, and where many of these cannot be optimized independently of other desired structures, the first-principles approach fails to aid in membrane fabrication. Such problems have been identified in many fields of science, *e.g.* agriculture and biology.

One technique which can aid in processes of optimization, especially in the presence of obscure interaction among variables, is the statistically designed or factorial designed experiment. This is not a first-principles approach, but one in which the user identifies a regime of desired structures, translated into an input variable, which one wants to incorporate into the membrane.

When some of the input parameters are coupled and where there is no obvious correlation between the effects of slight changes in an initially chosen input variable on another variable, and where there is even less of a correlation between the set of chosen variables and the optimized response, then one wishes to employ an iterative procedure by which each variable is changed independently around some given initial condition, the others remaining constant. In practice this is sometimes still too complicated as very many tightly controlled experiments must be performed.

Alternatively, one can use first principles to make assumptions about the relative importance which some of the independent variables have on the response, and about possible interactions between independent variables. Then a statistically designed experiment can be performed by which, by symmetrical considerations of the designed experiment *etc.*, the number of experiments can be reduced. The statistical approach of factorially designed experiments has been used in establishing fabrication procedures for flat-sheet membranes. As example, factors considered for analysis might be the chemical composition of the coagulant, temperature of the casting solution and coagulant, membrane-forming polymer concentration, substrate thickness, membrane thickness, environmental controlling factors such as humidity, temperature and drying.

As an example of the interaction between independent variables, consider the cross-effects on the kinetics of the gelation process with coagulant temperature and coagulant solubility parameter, in a study of the effect of these independent variables on membrane/support fabric adhesion. One might wonder if changing the coagulant solubility parameter in one direction increases the membrane flux, while at the same time reducing the membrane/support fabric adhesion. Ultimately, the mechanical integrity, solute retention and permeate

flux are responses to be optimized, but this in turn is related to many optimizations on a microscopic level, some possibly being mutually exclusive.

With the rapid growth of the potential of membrane desalination processes, most of the attention in literature has been focused on membrane module configurations which, by their nature, allow large membrane-to-volume packing densities, such as the spiral wrap and hollow fine fibre modules which, respectively, house flat-sheet and hollow fine-fibre membranes. Not much attention had been paid to the tubular membrane module configuration which, although it has a low packing density relative to the others, is an attractive alternative as very little pretreatment of the feed process water is required because of the open flow-channel of the tubular membrane.

Therefore, an entirely new approach to tubular membrane fabrication was necessary. The objective of this work was to develop a statistical approach in identifying and formulating membrane design criteria. We will not be interested in first principles or reasons why one, two or three factors studied are, or are not, important or interacting. We will merely identify those ones which are important and show that the use of the statistically designed-experiment approach in membrane fabrication can be a very important scientific device in applied membrane science.

As an outline of what the study entailed, the objectives are summarized below:

Asymmetric cellulose acetate membranes

The objective of this research was, with the aid of factorially designed experiments to:

i) Isolate factors important in the formulation of an asymmetric tubular cellulose acetate reverse osmosis membrane.
ii) Generate membrane performance regression equations to assist in the formulation of tubular cellulose acetate membranes with optimal flux performance in the 90 to 95% salt-rejection range.
iii) Test the design equations and approach for validity.

Ultra-thin film polyvinylamidine membranes

The objective of this research, with the aid of a Simplex technique of self-directing optimization, was to:

i) Determine whether polyvinylamidine can be used as a precursor in the creation of a novel ultra-thin film composite reverse osmosis membrane.
ii) Determine the intrinsic salt rejection potential of the tubular polyvinylamidine ultra-thin film membrane through a membrane formulation study.

Asymmetric micro-porous substrate for ultra-thin composite membranes

The objective of the study, through the use of a fractional factorial designed experiment, was to;

i) Isolate fabrication variables which have a significant effect on the adherence of the micro-porous membrane to the support fabric.

ii) Determine to what extent substrate membrane fabrication variables have an effect on the performance of ultra-thin film polyvinylamidine reverse osmosis membranes

As was mentioned earlier, the bulk of the available published information on asymmetric reverse osmosis and ultrafiltration membrane formulations, stems from research conducted on flat-sheet membranes. Since this thesis considers tubular membrane formulation variables, it must be borne in mind that continuous flat-sheet membrane fabrication allows for fine control of the immediate environment from the moment the nascent membrane film has been produced until it is fully coagulated. The situation is different in the case of tubular membrane fabrication in the sense that the processes of film extrusion and gelation take place in the self-created environment of the 12,7mm tube bore. Furthermore, in the case of flat-sheet membranes the angle and rate of nascent membrane entry into the coagulant can be introduced as factors for study; in the case of the tubular membranes under study, the membranes enter the coagulant bath vertically at a fixed rate. (The support tube rotates by nature of the way in which it is fabricated, *i.e.* the faster the rate of entry, the faster the rotational speed).

The physical differences which exist between the two membrane configurations would naturally result in different responses in membrane performance to alterations in the levels of factors studied in their fabrication. However, information can be drawn from the flat-sheet membrane literature as to which factors are of importance in flat-sheet membrane formulation and as such be applied in a study of their effect on tubular membrane performance.

In the following paragraphs a brief outline is given of the text contained in the chapters following.

Wet-phase inversion, the process according to which the asymmetric membranes in this text are formed, is discussed in Chapter II. The literature survey covers topics such as the behaviour of polymers in solution, de-mixing of polymers and the role which casting solution and coagulant additives play in affecting membrane properties. To aid in a better understanding of results presented in Chapter VI, the chapter also includes a section of phase diagrams for the ternary polymer/solvent/non-solvent system. For the sake of completion, reference is also made to other methods by which phase inversion can be accomplished.

In Chapter III, the concept of forming an ultra-thin permselective film on the surface of an asymmetric ultrafiltration membrane is discussed. Factors involved in the formation of the permselective film are again reviewed in section 6.3.2 in Chapter VI.

In Chapter IV the topic of statistically designed experiments is introduced (and detailed with the aid of experimental results which has bearing on the text in Chapter VI), to allow the reader, not familiar with the technique, to acquaint himself with the procedures followed. These techniques were necessary to allow the maximum amount of unambiguous information to be extracted from the minimum amount of experimental work. For example, five factors were studied simultaneously in the case of the asymmetric cellulose acetate membrane in a complete 2^5 factorial designed experiment (section 6.1.2), nine factors were considered simultaneously in a study of the effect of membrane fabrication variables on the adhesion of poly(arylether

sulphone) micro-porous membranes to their support fabric in a sixteenth fractionally replicated 2^9 factorial experiment (section 6.2.2.3).

During the course of the research effort, it was necessary to design and construct equipment to facilitate the continuous or semicontinuous fabrication of tubular membranes. This, as well as equipment constructed for use in the evaluation of the membranes, is discussed in detail in Chapter V.

Chapter VI contains the results of and discussion on experiments designed to achieve objectives stated earlier. Two reverse osmosis membrane systems were studied. In the first section of the chapter, the reader is introduced to aspects regarding the formulation of the well-known cellulose acetate membrane. The intention of this research was not to determine the optimal intrinsic performance of tubular CA membranes as such (well documented in the open and patent literature for flat-sheet CA membranes), but rather to relate fabrication variables to tubular membrane performance by means of regression procedures. Numerical optimization was performed on the regression equations obtained through factorial designed experiments, to forecast formulations of membranes with optimal flux performances for specified rejections. Two grades of cellulose acetate membrane materials were used in this study.

In sections 6.2 and 6.3 aspects concerning the research and development of a novel ultra-thin film composite membrane receive attention. In section 6.2 formulation of the micro-porous substrate membrane on which the ultra-thin film reverse osmosis membrane is created is discussed. One problem in creating this membrane was the poor adherence between the poly(bisphenol-A-sulphone) substrate membrane and the poly(ethylene terephthalate) support fabric used. As no solution to this problem was presented in the literature, and as various membrane formulations offered for flat-sheet micro-porous membranes did not solve the tubular membrane adherence problem, a simultaneous study (in the form of a fractionally replicated factorial experiment) of a large number of fabrication variables was conducted to relate their effect on substrate membrane/fabric adherence quantitatively. No attempt at a mechanistic study of the problem was made.

In section 6.3 the formation of novel ultra-thin film polyvinylamidine composite reverse osmosis membranes is discussed and the intrinsic (optimum) salt rejection performance of the membranes determined by means of a self-directing optimization approach. Additional factors, such as post-treatment of the membrane and the role of substrate membrane formulations, and their effect on the reverse osmosis performance of the membrane also receive attention.

In Chapter VII the conclusions are drawn, suggestions are made for further research and the relevance which the text has to membrane science is highlighted.

CHAPTER II

ASYMMETRIC MEMBRANES

2.0 INTRODUCTION

Reverse osmosis [RO] is a pressure-driven process used for the separation of water from a saline solution across semipermeable membranes, the pressure being adequate to exceed the osmotic pressure of the saline solution and to provide an economically acceptable flux. This is a short description of a unit process that has come of age as a result of research findings and developments since the early 1960s. Although microfiltration membranes have been in commercial use for many years *(1)*, the era of reverse osmosis and ultrafiltration [UF] as commercially viable unit processes came about as result of the development of methods for producing asymmetric membranes.

Since its inception, and as a result of research and development, the asymmetric membrane has found widespread application, not only in the technological fields of reverse osmosis and ultrafiltration separation *(2)(3)(4)(5)*, but also in processes such as active transport *(6)*, pervaporation *(7)*, gas separation *(8)*, analytical separation techniques, *e.g.* field flow fractionation *(9)* and many others *(10)*.

All of the above development was initiated in 1959 by Reid and Breton *(11)* who reported that homogeneous films prepared from cellulose acetate [CA] exhibited permselective properties. The films, cast from a binary cellulose acetate/acetone solution, retained inorganic salts to a high degree, but because of the high density of the films, the water transport across the films was commercially unattractive.

The significance of this discovery owes its importance to the work of Loeb and Sourirajan *(12)* who, by casting a membrane from a quaternary solution, increased the rate of water transport across the films by an order of magnitude, without affecting the selective properties of the membrane. The casting solution consisted of the polymer, acetone (solvent) and aqueous magnesium perchlorate (swelling agent). This method of membrane preparation was later simplified by Manjikian *et al (13)* who used a ternary casting solution consisting of the polymer, acetone and formamide (non-solvent), with which the membranes could be fabricated at room, rather than at sub-zero, temperatures.

Films cast by the above methods are not homogeneous as the dense films of Reid were, but are anisotropic *(14)*; the bulk of the membrane sub-structure is porous, becoming progressively less and less porous as the dense membrane surface region -the skin- is approached. Salt rejection is imparted by the integrated dense skin (0,1 - 1,0μm thick), whereas the bulk of the membrane (100 - 200μm) merely acts as a mechanical

support for the skin. Resistance to diffusive and convective transport of permeate is reduced as a result of the decrease in the relative thickness of the dense portion of the membranes, and the higher rates of permeation make these membranes commercially more attractive for use in brack-water desalination.

In general, membranes which exhibit this anisotropic nature, dense skins, integrated with, and supported by, a micro-porous or porous substructure (see Figure 2.1), are referred to as asymmetric membranes.

In order to enable sea water to be desalinated in a single pass, reverse osmosis membranes must have the capacity to retain more than 99,5% of the salts (concentration level, 3,5% by mass) present in sea water. The performances of the existing membranes fell short of this requirement by 1 to 2% at the time, and efforts directed at reducing imperfections, as well as the thickness of the dense permselective skin, led to an important conceptual development, namely, the composite laminated membrane, and membranes capable of single-pass sea water desalination. Riley *(15)* successfully *modelled the anisotropic nature of the Loeb-Sourirajan membrane by laminating a near-perfect ultrathin, dense, cellulose acetate film onto a microporous cellulose acetate support membrane. (The support membrane was not capable of retaining any salt). The film was prepared by solution-spreading techniques *(16)*, that is, by floating an extremely thin cellulose acetate film from dilute cyclohexanone solutions on a water surface.

A further important conceptual development regarding cellulosic-type reverse osmosis membranes came about by the introduction of blend membranes *(17)*. These asymmetric membranes, prepared from a mixture of cellulose di- and tri-acetate, outperformed membranes prepared from these components used singly.

Membrane development did not revolve around only cellulosic materials, as the formation of reverse osmosis membranes from non-cellulosic materials also received attention. Asymmetric aromatic polyamide *(18)* membranes were the first to be introduced commercially, followed by other membranes such as polyimide *(19)* and polybenzimidazole *(20)*.

The concept of the composite-laminate cellulose acetate membrane was reintroduced in a different form, that of the synthetic (non-cellulosic) ultrathin film [UTF] composite membrane *(21)(22)*. In this approach an ultrathin (<200nm) film of cross-linked polymer was created by a chemical reaction on the surface of an asymmetric substrate membrane. The substrate membrane, prepared from a synthetic polymer, was an ultrafiltration membrane not capable of retaining salt, but the composite membrane as such was capable of single-pass desalination of sea water.

Another field of reverse osmosis membrane development centres on the use of charged *(23)(24)* polymers or ionomers. As an example, synthetic hydrophobic polymers which exhibit no permselectivity (*e.g.* polysulphones or poly(phenylene oxide) are modified chemically (*e.g.* sulphonated) *(25)* to render hydrophilic asymmetric membranes capable of desalinating brack water. In yet another membrane concept, that of the on-line, *in-situ*, dynamically formed membrane, a composite permselective matrix is formed on an asymmetric membrane or on a sintered stainless steel support *(26)*. Poly(acrylic acid) and other *(27)* ionically charged synthetic polymers, together with hydrous oxides, are employed for preparing these membranes.

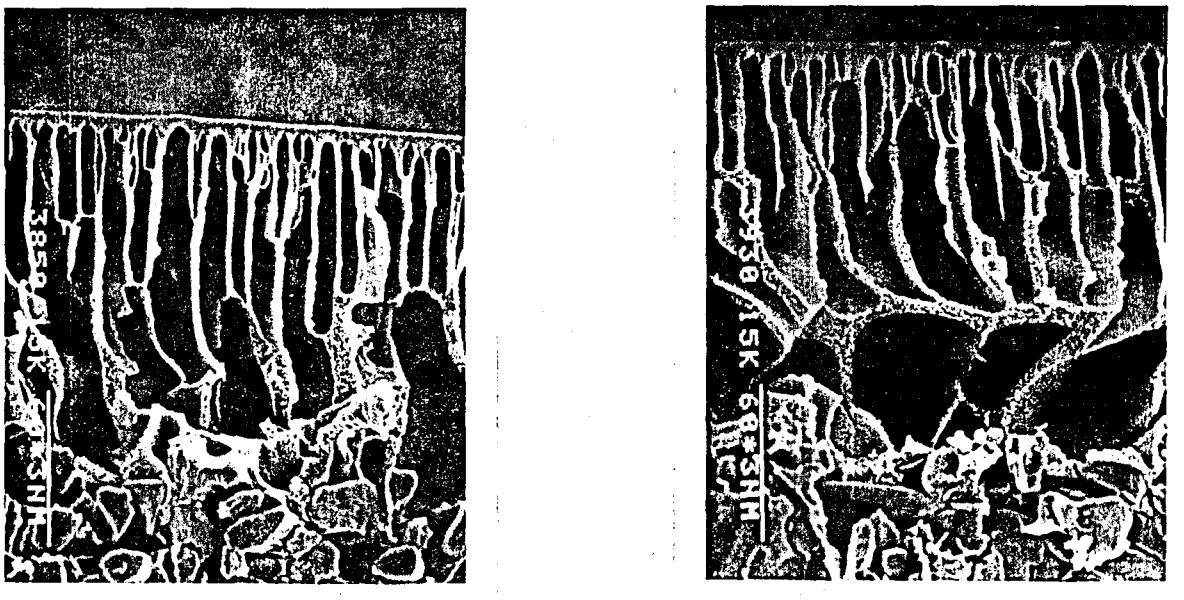

Cross-section of ultrafiltration membranes

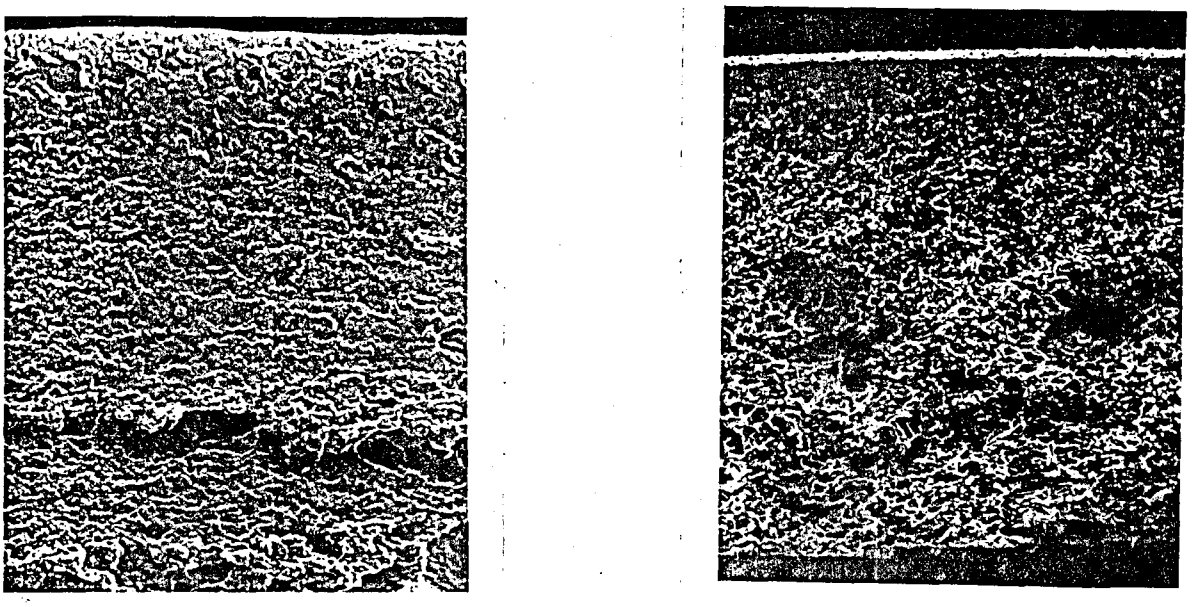

Cross-section of cellulose acetate reverse osmosis membranes

FIGURE 2.1: SCANNING ELECTRON MICROGRAPHS OF ASYMMETRIC UF AND RO MEMBRANES

2.1 TRANS-MEMBRANE FLUX

Membrane separation processes involving microfiltration and ultrafiltration operate on the mechanism of size-exclusion (*i.e.*, their selectivity is primarily a function of the hydrodynamic diameter of the solute and the size distribution of the diameters of the pores in the membrane skin *(28)*. The nominal pore size of ultrafiltration membranes plays an important role in the characterization of these membranes and their suitability for a specific application *(29)*. No universal method by which ultrafiltration membranes are characterized exists *(30)*, and various analytical methods are used to estimate the sizes of the skin-surface pores *(31)(32)(33)*.

Microfiltration involves the removal of particles in the 0,01 to 10μm size range, at trans-membrane pressure differences of 40 to 200kPa. In the ultrafiltration process, macromolecular solutes in the molecular mass range from 1 000 daltons to several hundred thousand daltons can be removed at operating pressures ranging from 200kPa to 1 000kPa. The nominal radii of pores in ultrafiltration membranes can range from 0,05nm upwards, where a membrane with a nominal pore radius of 7nm will retain 95% of a solute with a molecular mass of 200 000 *(34)*. (Pore diameters above 10nm fall within the limits of resolution of scanning and transmission electron microscopy *(28)*).

Whether reverse osmosis membranes have pores in the strict sense of the word, is debatable *(35)*, and the numerous models which have been developed for the interpretation of mass transport across reverse osmosis membranes are a strong reflection of this uncertainty. These models basically involve either pore flow and/or diffusive flow *(36)*. In a capillary-diffusion model, based on the existence of pores, separation is described by assuming a preferentially absorbed *(37)(38)(39)* layer of pure water on the membrane surface, mass transport of which takes place through the capillaries *(40)(41)* by fluid permeation under pressure. The model, based on the assumption that the membrane contains fine pores, considers frictional drag between the permeating species themselves and between the species and the polymer matrix to be the basis of separation *(42)*.

In a solution-diffusion model *(43)(44)*, it is assumed that the reverse osmosis membrane does not have these pores and that each component in the feed dissolves and diffuses in the membrane independently of the others. Based on this assumption (that the flows of water and salt are uncoupled), the respective transport equations for water and salt flux through a membrane of effective thickness Δx are given by;

Water flux:

$$J_1 = D_1 c_1 V_1 (\Delta P - \Delta\pi)/RT\Delta x \qquad [g.cm^{-2}s^{-1}]$$
$$= A(\Delta P - \Delta\pi)$$

Salt flux:

$$J_2 = D_2 K \Delta c_2/\Delta x \qquad [g.cm^{-2}s^{-1}]$$
$$= B\Delta c_2$$

A	$\equiv D_1 c_1 V_1/RT\Delta x$, the water permeability constant $[g.cm^{-2}s^{-1}atm^{-1}]$
B	$\equiv D_2 K_2/\Delta x$, the salt permeability constant [cm/s]
c_1	concentration of water in the membrane $[g/cm^3]$
Δc_2	difference in salt concentration across the membrane $[g/cm^3]$
D_1	diffusion coefficient of water in the membrane $[cm^2/s]$
D_2	diffusion coefficient of salt in the membrane $[cm^2/s]$
$D_1 c_1$	water permeability $[g.cm^{-1}s^{-1}]$
$D_2 K$	salt permeability coefficient $[cm^2/s]$
K	membrane/water partition coefficient for salt

Although the various models do not always fulfil specific requirements *(45)*, their use is important with respect to membrane research and development as well as to membrane plant design *(46)(47)(48)*.

The operating pressure in the reverse osmosis process is largely a function of the osmotic pressure of the process stream, that is, the pressure that theoretically must be exceeded to induce the transport of water across the membrane. For the desalination of sea water the trans-membrane pressure may be as high as 7MPa, whereas in the desalination of brack water, it may be as low as 1,5MPa.

In the operation of ultrafiltration and reverse osmosis membrane processes, the principle of cross-flow filtration is adopted, *i.e.* the pressurized process fluid is directed along the membrane surface, perpendicularly to the direction of flow of the permeate. This cross-flow is used in all the various modules which accommodate the membranes of different configurations used in separation processes *i.e.*, the tubular membrane module *(49)*, the spiral-wrap *(50)* which houses flat sheet membranes, and hollow fine-fibre *(51)* modules. The linear cross-flow velocity is important from a boundary-layer point of view, since it has an effect on phenomena such as concentration polarization *(52)* and steady-state fouling *(53)(54)*, which may impair membrane performance.

2.2 PHASE INVERSION PROCESSES

Asymmetric membranes are produced by a process called phase inversion, and although different fabrication techniques apply to produce the membranes in their various configurations, the asymmetry of these membranes arises as a result of phase inversion. The process is also referred to as binodal or spinodal decomposition *(55)*.

Phase inversion is a process *(56)* by which a homogeneous single-phase polymer solution undergoes transition into a heterogeneous, metastable solution of two interdispersed liquid phases, which subsequently forms a gel. Whereas the solvent forms the continuum in the homogeneous polymer solution, the polymer becomes the continuous phase during gel formation. It is important, therefore, that the polymer phase should remain coherent, as an incoherent phase will result in a powdery, instead of a semi-rigid, structure.

In the following paragraphs, three different phase-inversion processes are described. The only thermodynamic assumption for all three processes is that the Gibbs free energy of mixing of the membrane-forming polymer solution must be negative only under certain conditions of temperature and/or composition, *i.e.* a solubility or miscibility gap *(57)(58)(59)* must exist over a defined temperature and/or composition range.

2.2.1 ADDITION OF A NON-SOLVENT

A solvent for a polymer is a liquid whose force-fields are so similar to that of the polymer, that polymer molecules cannot distinguish between themselves and the solvent. Solvent molecules can therefore diffuse between the polymer chains and ease them far enough apart to cause the polymer to be solubilized. The addition of non-solvent to a polymer solution will have the reverse effect. The polymer chains will shrink up and coil in amongst themselves as they seek like sites in an unlike medium. A point is reached at which the solution no longer has the necessary solvating power and the polymer then precipitates.

This, in principle, is the technique followed in the preparation of wet-phase-inversion membranes, which is the most commonly used method for the preparation of asymmetric membranes.

2.2.1.1 Solubility parameters

For polymer/solvent mixing to be possible, the Gibbs free energy of mixing, ΔG_m, must be negative at constant pressure *(60)*:

$$\Delta G_m = \Delta H_m - T\Delta S_m < 0$$

The entropy change, ΔS_m, of a polymer/solvent mixing process is usually small and positive, as the macromolecules are allowed greater freedom of movement than they are when they are in the solid state, in which molecular motion is limited to segmental Brownian movement. Miscibility therefore depends on the enthalpy term, ΔH_m, which is also referred to as heat of mixing. When this term is positive and less than the $T\Delta S_m$ term, or negative, mixing can occur.

The solubility behaviour of polymers can be predicted to a reasonable extent by the relationship of Hildebrandt *(61)* who connected the energy of mixing of two compounds to their respective energies of vaporization *(62)*:

$$\Delta H_m = V_m \nu_1 \nu_2 \left[\sqrt{(\Delta E_1/V_1)} - \sqrt{(\Delta E_2/V_2)}\right]^2$$

V_m	Total molar volume of mixture
V_i	Molar volume of component
ν_i	Volume fraction components, i=1 (solvent), i=2 (polymer)
ΔE_i	Energy of vaporization [J/mol]

The cohesive energy density ($\Delta E/V$), that is, the cohesive forces keeping the molecules together, is quantified by the energy to overcome all the intermolecular forces (vaporization of the liquid) and is expressed in terms of pressure [MPa]. The square root of this quantity is defined as the cohesion parameter, also called the solubility parameter, δ:

$$\delta = (\Delta E/V)^{1/2} \qquad [MPa^{1/2}]$$

The expression for the heat of mixing can now be rearranged in terms of solubility parameters:

$$\Delta H/(V_m \nu_1 \nu_2) = (\delta_1 - \delta_2)^2$$

If, therefore;

$\lvert\delta_1-\delta_2\rvert > 0$	$\Delta G < 0$, if the difference is small, and mixing will occur;
$\lvert\delta_1-\delta_2\rvert \gg 0$	$\Delta G > 0$ and mixing will not occur.

Hansen introduced partial solubility parameters by dividing the total cohesive energy density into three attributes *(63)*:

$$\Delta E_T/V = \Delta E_D/V + \Delta E_P/V + \Delta E_H/V$$

in which

ΔE_D	dispersion forces
ΔE_P	permanent di-pole, permanent di-pole forces
ΔE_H	donor/acceptor or hydrogen-bonding forces

which give rise to the following relationship:

$$\delta_T^2 = \delta_D^2 + \delta_P^2 + \delta_H^2$$

where δ_T^2 is the Hildebrandt cohesive parameter *(64)*.

The use of the solubility parameter concept has far-reaching implications in the field of polymer science. Apart from providing insight into polymer/solvent-system miscibility and compatibility, it can be used to establish other cohesion parameters such as surface free-energy *(65)(66)*. In membrane research *(67)* partial solubility parameters are used in the selection of solvents and non-solvents *(68)* and in the characterization of membrane materials *(69)*.

2.2.1.2 Solubility maps

Organic agents will affect polymers in a number of ways; they may be regarded as solvents, latent solvents (mixing depends on thermal energy or mixing is achieved only at high polymer concentration) *(70)*, or as non-solvents. Vincent *(71)* classed organic liquids according to those that dissolve the polymer (true solvents) and those that are stress-inducing. When the difference between the solubility parameter of an organic liquid and that of the polymer is small, the liquid will promote stress-cracking, whereas stress-crazing will be promoted when the difference is high.

A region referred to as the solubility envelope can be described graphically on the basis of partial solubility parameters; this illustrates the behaviour of the polymer in organic liquid medium. Liquids which fall within this region will generally dissolve the polymer and those that fall outside it, will not.

As an approximation, the three-dimensional solubility region of a polymer may be seen as a sphere, which can be projected onto three planes to provide circular regions of solubility in two dimensions. (See Figure 2.2) *(72)*. The miscibility potential of a solvent then depends on the distance of its co-ordinates (${}^{S}\delta_{P}$, ${}^{S}\delta_{H}$, ${}^{S}\delta_{D}$) from the centre point (${}^{P}\delta_{P}$, ${}^{P}\delta_{H}$, ${}^{P}\delta_{D}$), of the solute sphere of solubility, which is:

$$ {}^{S}P_{R} = \sqrt{[4({}^{S}\delta_{D} - {}^{P}\delta_{D})^{2} + ({}^{S}\delta_{P} - {}^{P}\delta_{P})^{2} + ({}^{S}\delta_{H} - {}^{P}\delta_{H})^{2}]} $$

Thus, when ${}^{S}P_{R}$ is less than that of the solute sphere of solubility, the likelihood of polymer/solvent miscibility is high. Likewise, when it is greater, it is not expected that the polymer and solvent will be miscible *(71)*.

Various approaches are followed by which partial solubility parameters are used to depict the solubility region of a polymer graphically *(73)(74)*. In one approach *(75)*, the partial solubility parameters of the organic liquids are plotted on a triangular diagram. The partial solubility parameters which represent each solvent or solvent mixture are first transformed by the first-power relationship:

$$ F_{i} = [\delta_{i}/(\delta_{D} + \delta_{P} + \delta_{H})]100\% = [\delta_{i}/\delta_{T}]100\% $$

where F_{i} represents the three axes of the triangle, F_{D}, F_{P} and F_{H}. The partial solubility parameters of solvent-mixtures are calculated from:

$$ {}^{M}\delta_{i} = \Sigma \nu_{j} \delta_{ij} $$

${}^{M}\delta_{i}$	partial solubility parameter of the mixture
ν_{j}	volume fraction of the j^{th} solvent component
δ_{ij}	partial solubility parameter (δ_{H}, δ_{P} and δ_{H}) of the j^{th} solvent component in the mixture

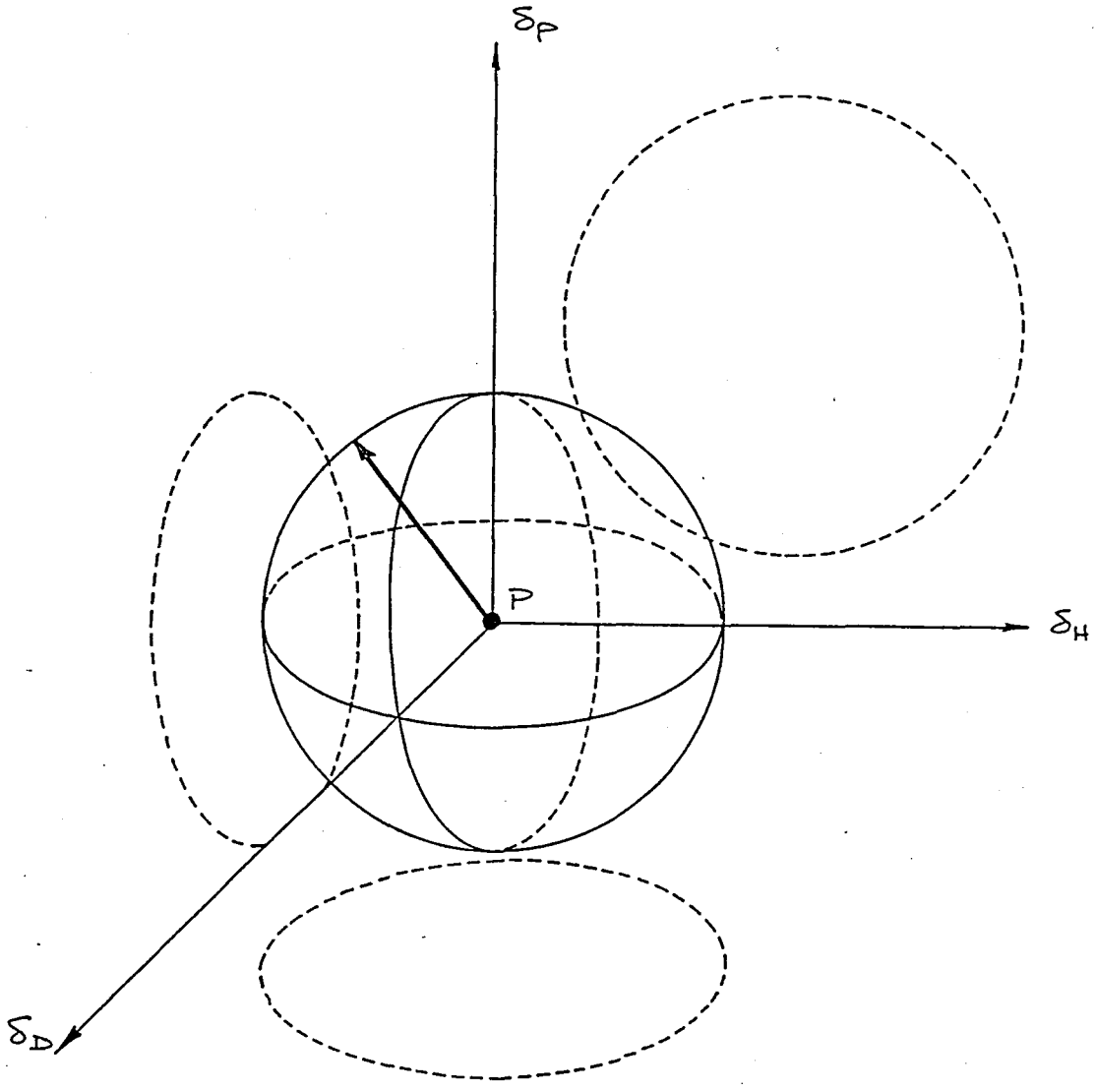

FIGURE 2.2: TWO-DIMENSIONAL PROJECTION OF THE SOLUBILITY SPHERE OF A POLYMER

This graphical method has been used to develop a solvent system for the preparation of asymmetric sulphonated poly(arylether sulphone) membranes *(76)* which consisted of a true non-solvent (formamide) and a swelling agent (tetrahydrofuran). The solubilities of these two liquids were such as to be located on either side of the polymer solubility region, and by mixing the two liquids in the proper proportions, a co-solvent mixture resulted which was a solvent for the polymer. The solubility diagram also assisted in locating a non-solvent coagulant, iso-propanol, based on its position on the solubility diagram.

In Figure 2.3 and 2.4 diagrams are shown which represent the solubility regions of poly(bisphenol-A-sulphone) (Udel 1700P) on the different maps.

2.2.1.3 Phase diagrams

The solvent component used in the preparation of homogeneous membrane-forming solutions (referred to as casting solutions) may contain a single solvent (binary solution) *(77)(78)* or a solvent mixture consisting of a solvent(s) and a non-solvent(s) (ternary solution) *(79)*. Non-solvent or swelling agent additives are referred to as porosity-enhancing agents as their addition leads to an increase in membrane flux *(80)*.

Thus, in the case of cellulose acetate a ternary solution is prepared from the polymer, acetone (solvent) and formamide (non-solvent) *(13)*, and water is used as the coagulation non-solvent medium. In the case of poly(bisphenol-A-sulphone) [PS] a binary casting solution may be prepared from N,N-dimethylformamide [DMF], N,N-dimethyl acetamide or N-methyl-2-pyrrolidone [NMP], or a ternary solution may be prepared by the addition of non-solvents such as sulpholane, methyl cellusolve or 1,4-dioxane to the above binary solutions. Water is usually used as the coagulation medium.

Ternary phase diagrams are commonly used in discussions of asymmetric membrane-formation mechanisms. In the following paragraphs, the experimental procedure *(77)(81)* followed to create a phase diagram for a polymer/solvent/non-solvent system will be described with the help of Figure 2.5.

In Figure 2.5, points 1, 2 and 3 represent homogeneous casting-solution compositions on the solvent (or co-solvent system) (S) and polymer (P) tie-line; the third corner of the diagram, N-S, represents the non-solvent coagulant, *i.e.* water. Small quantities of the non-solvent are added to a weighed sample of the polymer solution and stirred vigorously at a controlled temperature until the first permanent sign of cloudiness appears (cloud-point). The composition of the cloud-points (1_C, 2_C and 3_C), which mark the miscibility border (binodal curve), is obtained by mass balance. The solution will most probably be in a metastable state at this point and will not separate spontaneously into two distinct phases. (These points are referred to as critical points *(82)*, the tie-line between the phases being a point and the compositions of the phases are similar).

A further fixed quantity of non-solvent is added to the cloud-point mixtures and the final compositions of these mixtures are represented by points 1_M, 2_M and 3_M. As the region of immiscibility has been entered, the mixture will spontaneously separate into two phases, namely, a polymer-rich phase (represented by points 1_P, 2_P and 3_P), and the polymer-poor phase (represented by points 1_L, 2_L and 3_L). The two phases are separated by filtration or centrifugation in order to determine their actual compositions.

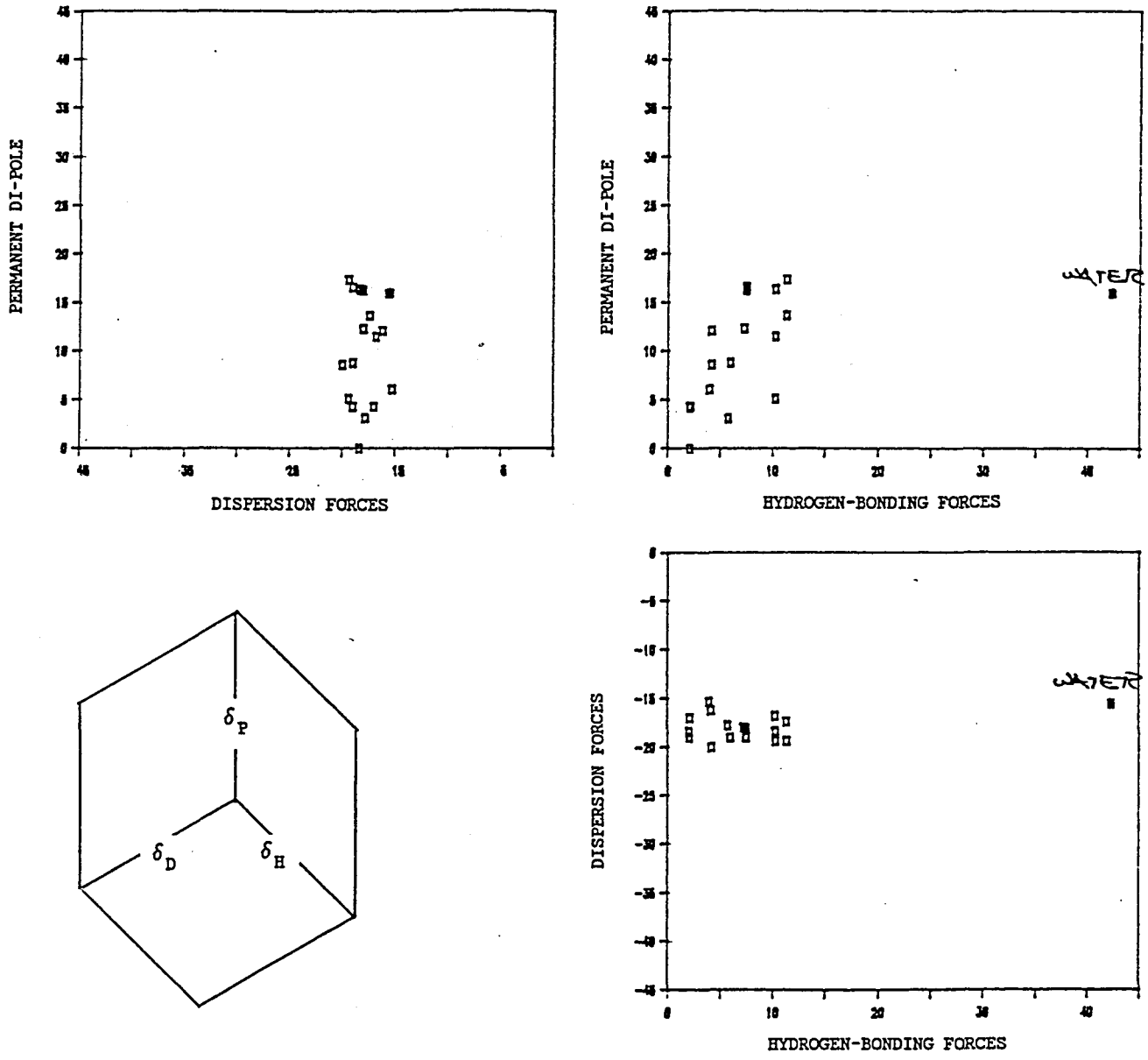

FIGURE 2.3: SOLUBILITY MAP FOR POLY(BISPHENOL-A-SULPHONE) (UDEL 1700P), TWO-DIMENSIONAL MAP

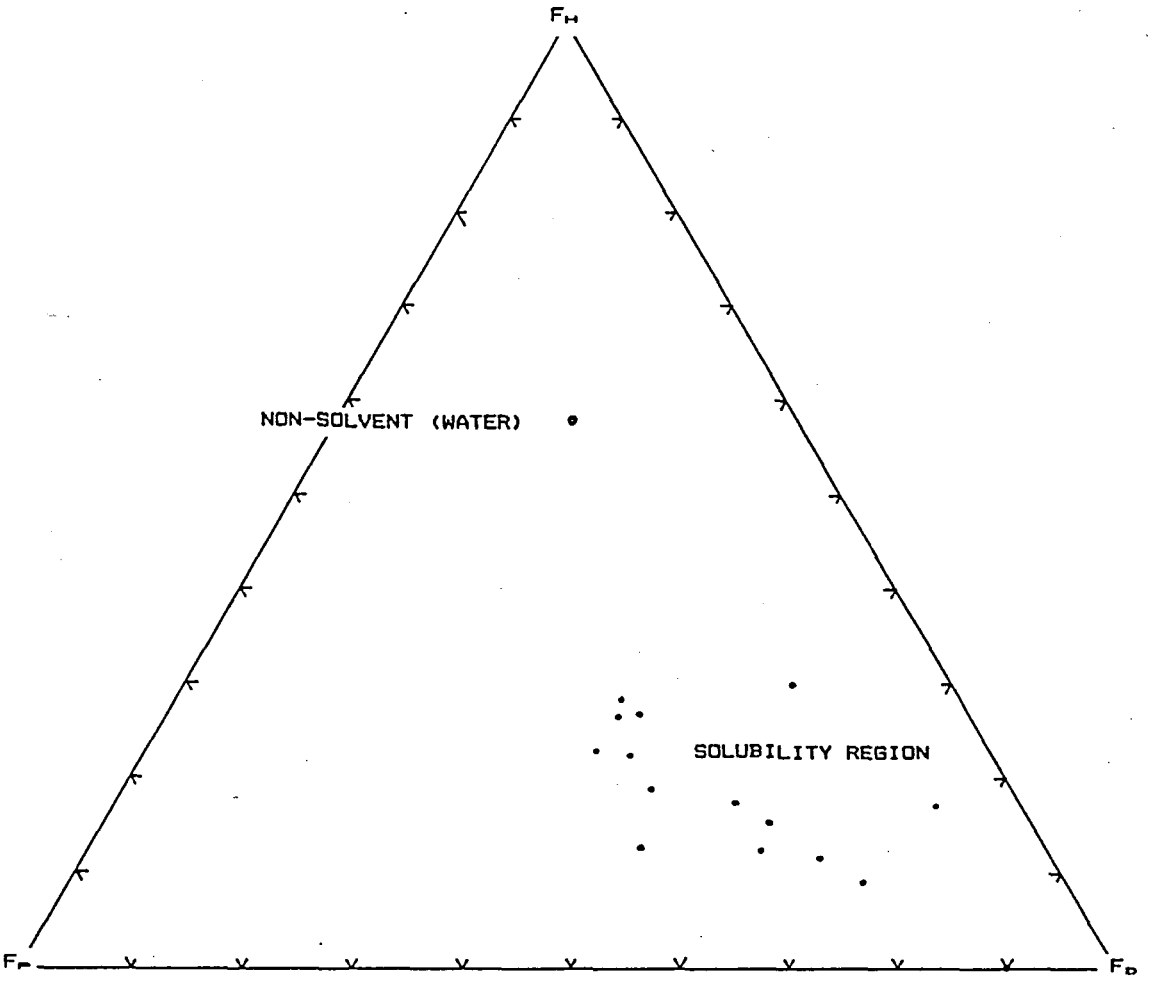

FIGURE 2.4: SOLUBILITY MAP FOR POLY(BISPHENOL-A-SULPHONE), TERNARY DIAGRAM

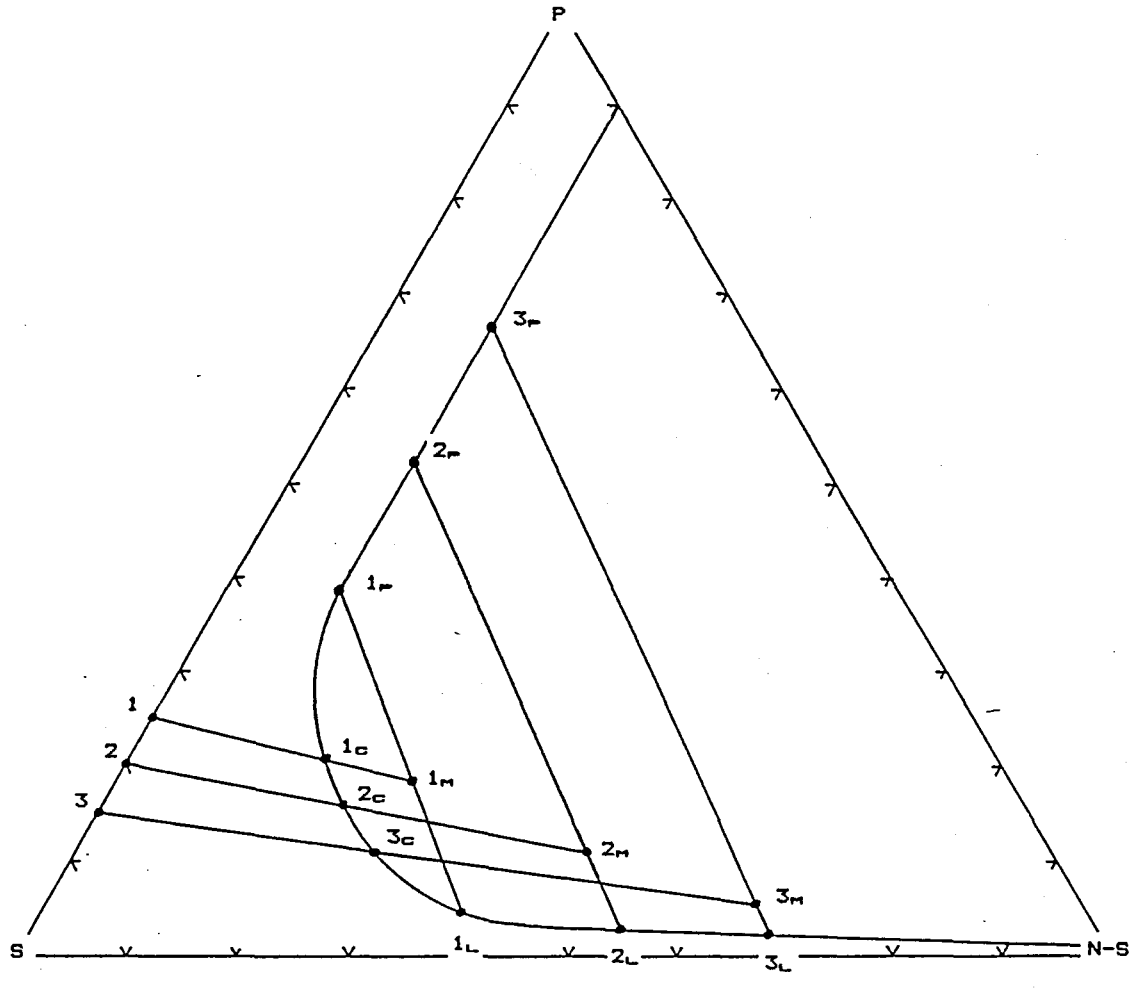

FIGURE 2.5: A TERNARY POLYMER/SOLVENT/NON-SOLVENT PHASE DIAGRAM, ILLUSTRATING THE POLYMER, POLYMER SOLVENT-SYSTEM AND COAGULANT

The compositions of points representing the polymer-rich phase are determined by analyzing one portion of the sample for non-solvent content and the other portion for polymer content. The solvent content of the solid phase is determined by mass balance. As water is used as the non-solvent, its concentration in the sample can be determined by radio chemistry, *i.e.* if it was marked initially. The polymer content of the sample is determined gravimetrically by evaporation to complete dryness.

The water content in the liquid phase is determined by Karl Fischer titration and the polymer content gravimetrically. The solvent content is determined by mass balance.

Strathmann *(81)* remarked that deviations of up to 8% must be expected when this approach is used since (i) cloud-point determination is problematic, especially when concentrated polymer solutions are used; (ii) problems arise in the determination of the water concentration in the polymer-rich phase, and (iii) commercial polymers are not pure and because of the molecular mass distribution, will show different solvation behaviour.

However, the accuracy of the experimental procedure can be tested in that the tie-line 1_P-1_L should join through point 1_M and like-wise the 2_P-2_L and 3_P-3_L tie-lines should join through points 2_M and 3_M.

2.2.1.4 Coagulation and gelation

Asymmetric membrane formation by the wet-phase-inversion process involves the application of a film of homogeneously dissolved polymer to a support (fabric material or glass plate) by means of a doctor blade. After this, the polymer film may undergo an evaporation step *(83)(84)*. This is not always a prerequisite for the formation of either the skin or the asymmetric sub-structure *(85)(86)(87)*. The next step, the principal step, in the formation of the asymmetric structure, is the immersion of the film in a non-solvent coagulant. During this step the exchange that takes place between the solvent and non-solvent (solvent outflow/non-solvent inflow) leads to phase transformations, and an asymmetric *(88)(89)* porous polymer structure results; this is the membrane.

Certain membrane types (*e.g.* cellulose acetate *(90)* and aromatic polyamide *(91)* reverse osmosis membranes) require heat treatment as a final step in their preparation. During this process, called annealing, the already formed structure of the membrane skin is densified further to achieve the reverse osmosis rejection performances required. Densification is both a result of shrinkage of the membrane and a rearrangement of inter- and intra-molecular hydrogen bonding which introduces domains of crystallinity.

The relative porosities of surfaces and subsurfaces of membranes prepared from a specific polymer depends to a large extent on the relative rates at which phase inversion occurs *(92)*. In general, a fast phase-inversion rate will favour the formation of a thin dense membrane skin and reduced rates of water permeation; the reverse applies when the rate of phase-inversion is reduced.

Thus by reducing the activity of the coagulant, (*e.g.* decreasing the temperature, addition of inorganic solutes) *(78)*, the rate of phase separation is reduced because of a smaller chemical potential difference between the

coagulant and membrane solution. The choice of a coagulant is primarily dependent on its position on a solubility map relative to that of the polymer/solvent mixture. Another requirement is that the coagulant must be miscible, in all proportions, with the casting solution solvents. The choice of water as a coagulant has become customary, apart from relative cost considerations.

Modifications to the composition of the casting solution have a more pronounced effect on membrane morphology and the rate at which a solution phase separates, than do modifications to a specific coagulant medium. For example, by merely increasing the viscosity *(93)* of a casting solution (either by means of additives or by increasing the polymer concentration), the rate of phase separation is reduced. Increasing the solution viscosity *(94)* has proved to be an effective means of suppressing the formation of finger-like macrovoids (associated with high rates of membrane precipitation) and alteration of the membrane sub-surface morphology. (See Figure 2.6). According to thin-film-coating theories, free-energy perturbations *(95)* which develop at solution/air interfaces after the thin films have been created, as well as the Marangoni effect *(96)*, which develop as a result of surface cohesive energy effects, are reduced by increase in the viscosity. The same applies to membrane films, and surface deformations and macro-void formation will also be reduced if the casting solution viscosity is increased.

Solvents *(97)* also play a major role in influencing the rate of phase separation, and not only because of their relative solvating power and effect on solution viscosity *(98)*. Their affinity for the coagulant and the heat that develops when they are mixed with the coagulant are of prime importance *(99)*. Solvents which exhibit higher heats of mixing will, for example, favour the formation of membranes of greater porosity.

It is common to add inorganic solutes to casting solutions, either as an aid in solvating the polymer *(100)*, or increasing the porosity of the membrane *(93)(101)*. Inorganic additives enhance phase separation as they decrease the tolerance of the polymer solution to water intrusion, and a more porous membrane results *(102)(103)*; the reverse occurs when inorganic solutes are added to the coagulation medium.

Mathematical modeling of the phase-inversion process lags behind the amount of research information available regarding the process. Researchers do not agree generally *(104)*, when relating the mechanism of phase inversion to the resulting asymmetric structure of membranes, or to the occurrence of large, finger-like, sub-structure voids. Although some qualitative models have been developed to explain the process of phase inversion *(88)(105)*, no attempt has been made as yet to relate the mechanism of formation to ultimate membrane performance.

Most polymers are capable of ordered agglomeration or precipitation when the thermodynamic quality of the polymer solution is lowered by the introduction of a non-solvent, or by evaporation of a volatile solvent component. When the solution becomes thermodynamically unstable, the free enthalpy of mixing of the original solution can be reduced by separation of the solution into two phases, a process which is referred to as liquid-liquid phase separation. Two mechanisms for liquid-liquid phase separation have been proposed: nucleation, and growth *(106)* (particularly in the case of crystalline polymers *(80)*, namely, poly(2,6-dimethyl 1,4-phenylene oxide [PPO]) of the second phase (followed by coalescence and gelation of the polymer

phase), or spinodal decomposition *(105)(107)*. The phase-separation process was elucidated by Koenhen *(82)* in the light of the Flory-Huggins equation for the Gibbs free enthalpy of mixing change for a polymer and a solvent (see paragraph 2.2.3).

Koenhen's theory of nucleation and growth for the ternary solvent/polymer/non-solvent system is discussed below. Two possibilities are offered in the nucleation and growth mechanism, depending on whether

i) the miscibility gap is entered on the 'dilute' side of the critical point (refer paragraph 2.2.1.3), or
ii) the phase border is entered on the 'concentrated' side.

In case (i), nuclei of the concentrated phase will be formed with a composition very different from that of the original solution. The dilute phase will change continuously in composition, and become more and more dilute; that is, nucleation and growth of the concentrated phase will occur. The process will continue until the spheres of the concentrated phase, dispersed in a dilute solution, coalesce into an open-pore structure which will have some some strength *(108)*. (See Figure 2.7).

In case (ii), nuclei of the dilute phase will be formed while the concentrated phase can change continuously; that is, nucleation and growth of the dilute phase will occur. The process will continue and the spheres of dilute solution, surrounded by the concentrated phase, will gel into a spherical cell structure.

The mode of formation of the dense membrane skin layer seems to be a matter of conjecture. Some researchers regard an evaporation step as being necessary for the formation of the dense skin layer, which is true in certain cases (*83*), but is not always a prerequisite for formation of the skin.

Casting-solution compositions are normally located near the edge of the polymer solubility region and on that side of the solubility map which faces the area in which the non-solvent coagulant is situated. Evaporation of a volatile solvent component will reduce the thermodynamic quality of the polymer in solution, but will also cause a shift in solution composition towards the gel region. Gelation is therefore regarded as the mechanism by which the skin is formed.

Gelation is also regarded as the mechanism *(109)* by which the nascent film, in direct contact with the non-solvent medium, coagulates and gels. This process is instantaneous and is regarded as being too rapid to support the nucleation and growth mechanisms. However, this gelated region of the film, the skin, must have a fine-mazed structure as it must facilitate transport of process water. The skin-layer also influences the kinetics of sub-surface coagulation. It acts as a barrier through which the coagulant and solvent(s) exchange by diffusion, reducing the rate of diffusion to an extent that equilibrium between the phases in the sub-surface region is maintained, and coagulation is brought about by liquid-liquid phase separation *(110)*.

Figure 2.8 shows ternary polymer/solvent/non-solvent phase diagrams, indicating the metastable region which exists between the binodal and spinodal curves, as well as the critical point.

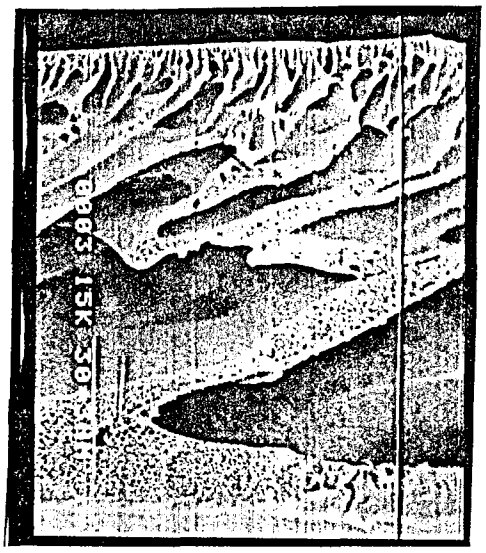

15% PES in NMP
(viscosity 310 cP)

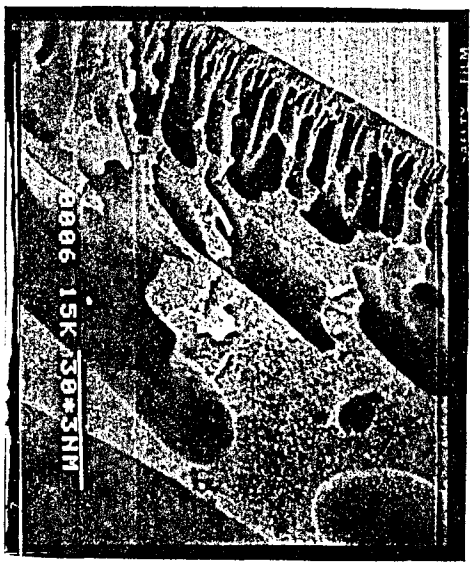

20% PES in NMP
(viscosity 1 250 cP)

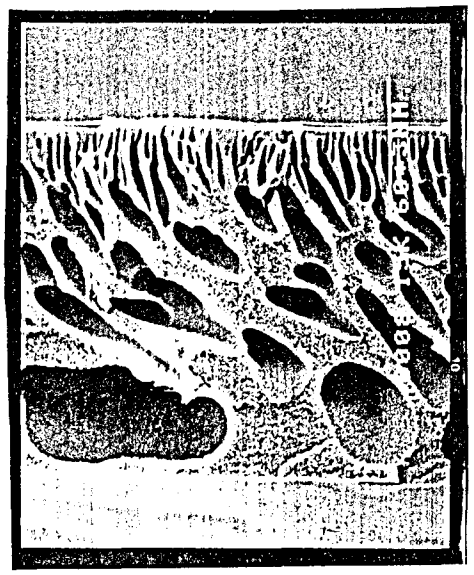

20% PES, 5% PVP 44K in NMP
(viscosity 12 760 cP)

FIGURE 2.6: VICTREX 4800G POLY(ARYLETHER SULPHONE) ULTRA-FILTRATION MEMBRANES

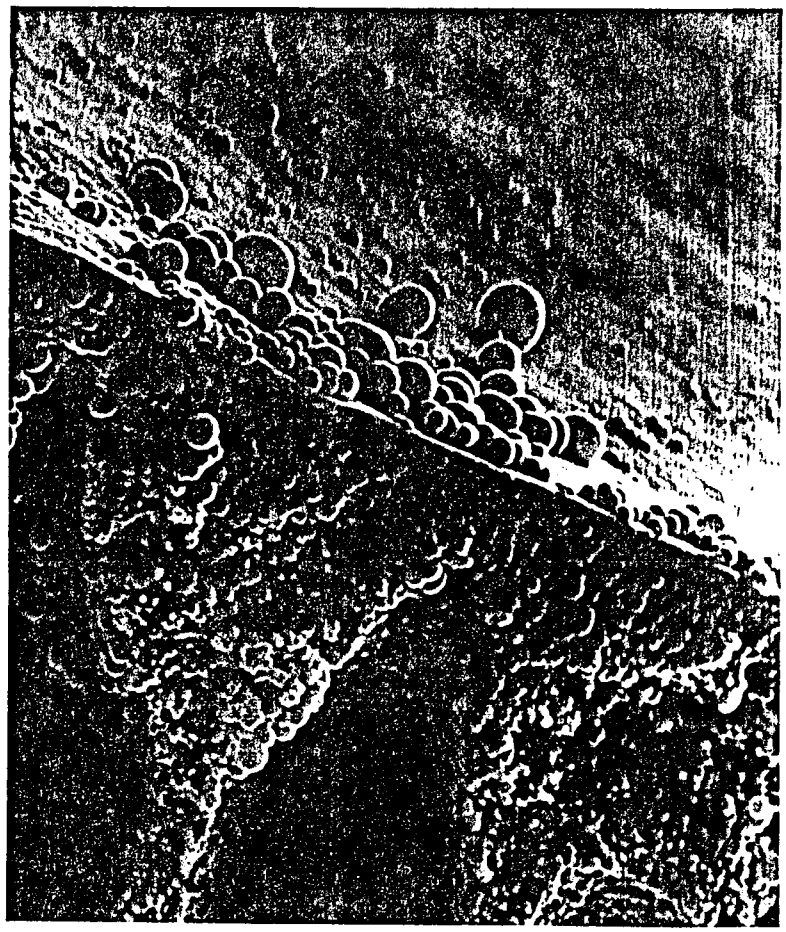

FIGURE 2.7: SCANNING ELECTRON MICROGRAPH OF THE NODULAR STRUCTURE IN AN ASYMMETRIC MEMBRANE

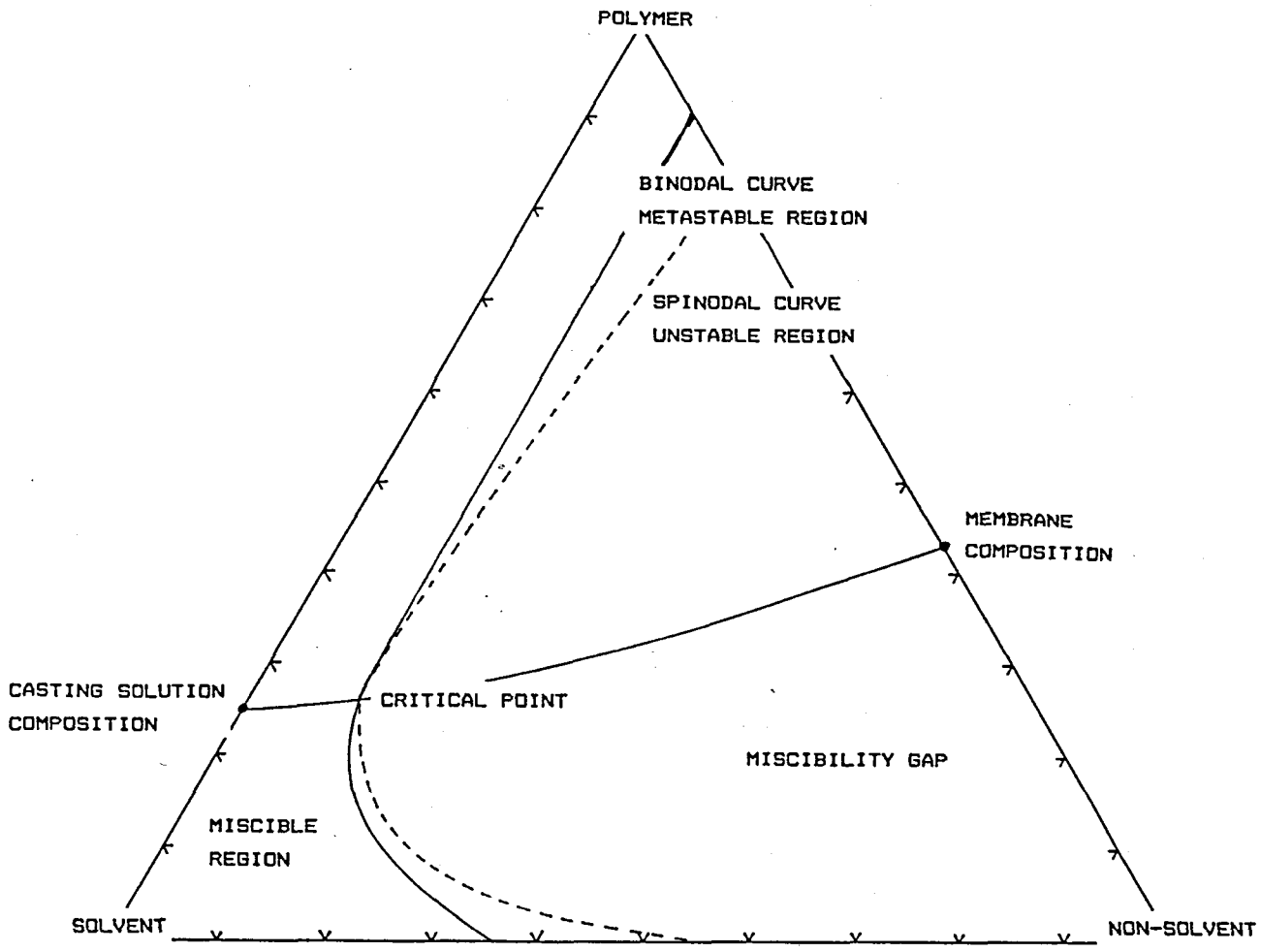

FIGURE 2.8: ILLUSTRATION OF THE BINODAL AND SPINODAL BOUNDARIES IN A TERNARY PHASE DIAGRAM

2.2.2 PHASE INVERSION BY COMPLETE SOLVENT EVAPORATION

This technique has a long history and was first used in the preparation of microfiltration membranes *(111)*. Since then it has been used by Kesting in the preparation of both reverse osmosis and ultrafiltration membranes *(112)(113)(114)*.

The technique involves complete evaporation of a solvent from a ternary polymer solution consisting of the low boiling-point solvent, a high boiling-point non-solvent (swelling agent) and the polymer (See Figure 2.9)

The ternary mixture is completely miscible over a certain solvent composition range, but shows a misciblity gap over another composition range, similar to that shown by the wet-phase-inversion technique discussed above. Evaporation of the solvent in this instance reduces the solvating power of the remaining solvent mixture, and the miscibility border is crossed. When there is complete removal of the solvent component of the casting solution mixture, represented in Figure 2.9 by A, the composition will change to that of B. At point B the mixture consists of a polymer phase, represented by point B^{II} and the liquid phase, represented by B^{I}.

2.2.3 THERMAL PHASE INVERSION

As was described earlier, the existence of a miscibility gap in a solvent system is the first requirement for wet-phase inversion, and thermally induced inversion *(115)* is no different. The technique depends on the choice of a latent solvent which is a solvent for the polymer at elevated temperatures, but which is a non-solvent at lower temperatures. When the solution is cooled, the thermodynamic quality of the solvent is reduced to such an extent that phase separation takes place.

As high temperatures are normally employed (>150°C), further considerations are that the polymer must not decompose at high temperatures and that the latent solvent must have a high boiling point *(116)*. The technique has been found to be particularly useful in the preparation of asymmetric membranes from polymers which have poor solubility, such as polyethylene *(117)* and polypropylene, but the technique is applicable to other polymers as well *(118)*.

Koenhen *(119)* explained the process of thermal phase inversion in the light of the Flory-Huggins equation for the Gibbs free energy of mixing change for a polymer and a solvent, with the following relationship:

$$\Delta G_M/RT = \omega_o \ln\omega_o + \Sigma M_o/M_i \omega_i \ln\omega_i + g\Sigma\omega_i\omega_o$$

where	ΔG_M	free energy of mixing
	R	universal gas constant
	T	absolute temperature
	ω_o	weight fraction of solvent
	ω_i	weight fraction of polymer species i
	M_o	molecular mass of solvent
	M_i	molecular mass of polymer species i
	g	empirical correction factor
	entropy term	$\omega_o \ln\omega_o + \Sigma M_o/M_i \omega_i \ln\omega_i$
	enthalpy term	$g\Sigma\omega_i\omega_o$

In non-ideal mixtures the Gibbs free-energy change for the mixing process is not equal to the ideal value and Figure 2.10 illustrates the miscibility gap which exists in a non-ideal polymer solution.

The mechanism *(120)* of nucleation and growth for a binary system is described with the aid of Figure 2.11. Points A and D are the common tangents of the ΔG_M curve. The points have identical chemical potentials and form phases in equilibrium. The free enthalpy of mixing of any composition between points A and D can be lowered by separating it into phases with compositions A and D. Compositions between A and B (the points of inflection) on one side of the de-mixing region and C and D, on the other side, are in a metastable state. De-mixing occurs when a nucleus is formed which has a composition which is close enough to the composition on the other side of the immiscibility gap. These nuclei grow further until a complete de-mixing into phases A and D has taken place. The compositions between points B and C are unstable to small fluctuations. Such compositions would give rise to instantaneous demixing, the so-called spinodal decomposition.

The morphology of the resulting membrane is a function of the rate of cooling, as it affects the liquid-liquid phase-separation mechanism *(118)*. At low rates of cooling, binodal decomposition occurs by the nucleation and growth mechanisms, and results in the formation of an open-pore membrane structure. At relatively high rates of cooling, spinodal decomposition takes place and the resultant membrane structure has a lacy appearance. The permeability of membranes with a lacy structure is higher than the permeability of membranes with a porous structure. Figure 2.12 shows electron micrographs of thermal phase-inversion poly(arylether sulphone) membranes, depicting the two different structures *(121)*.

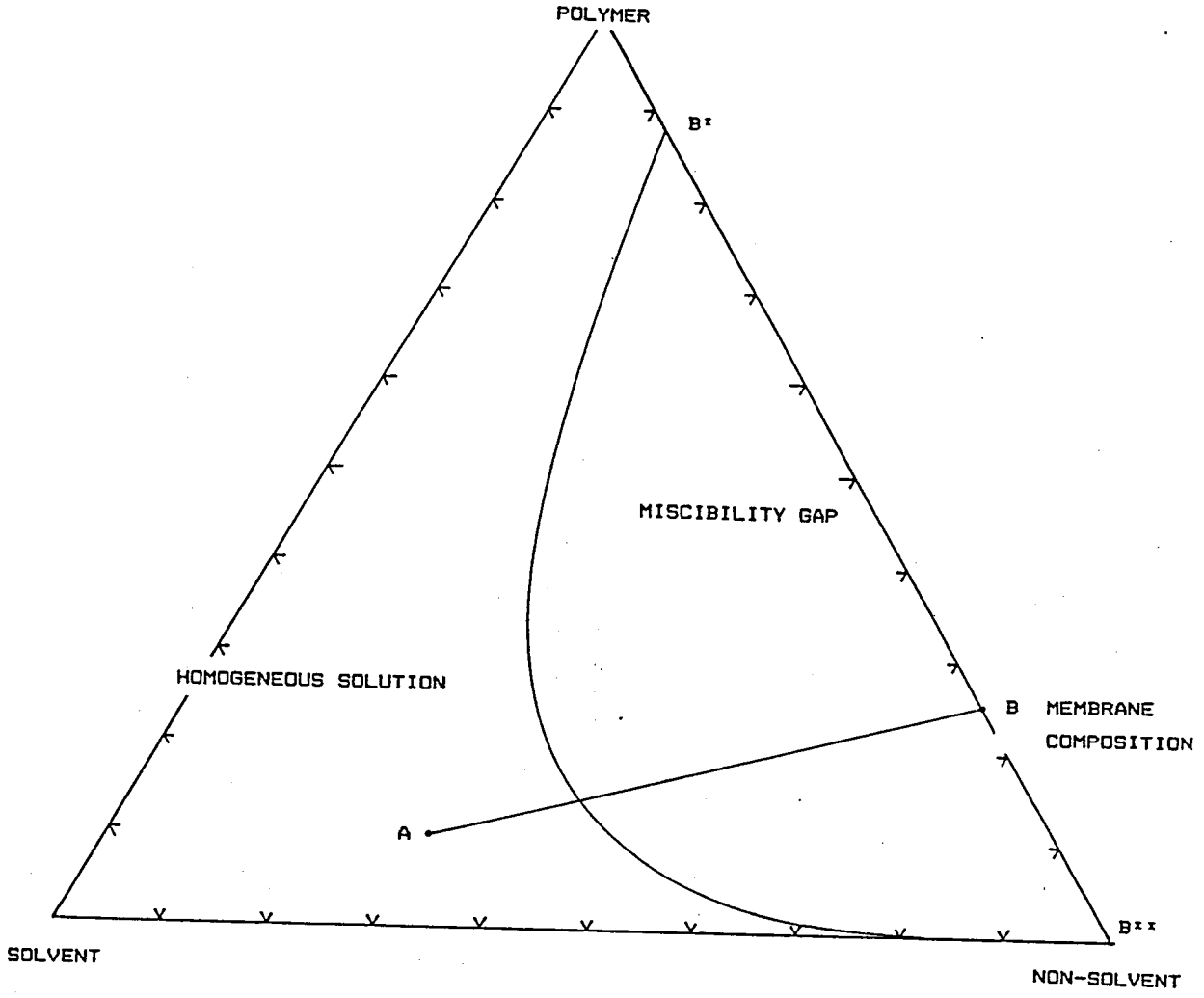

FIGURE 2.9: ISOTHERMAL PHASE DIAGRAM - PHASE-INVERSION BY COMPLETE EVAPORATION

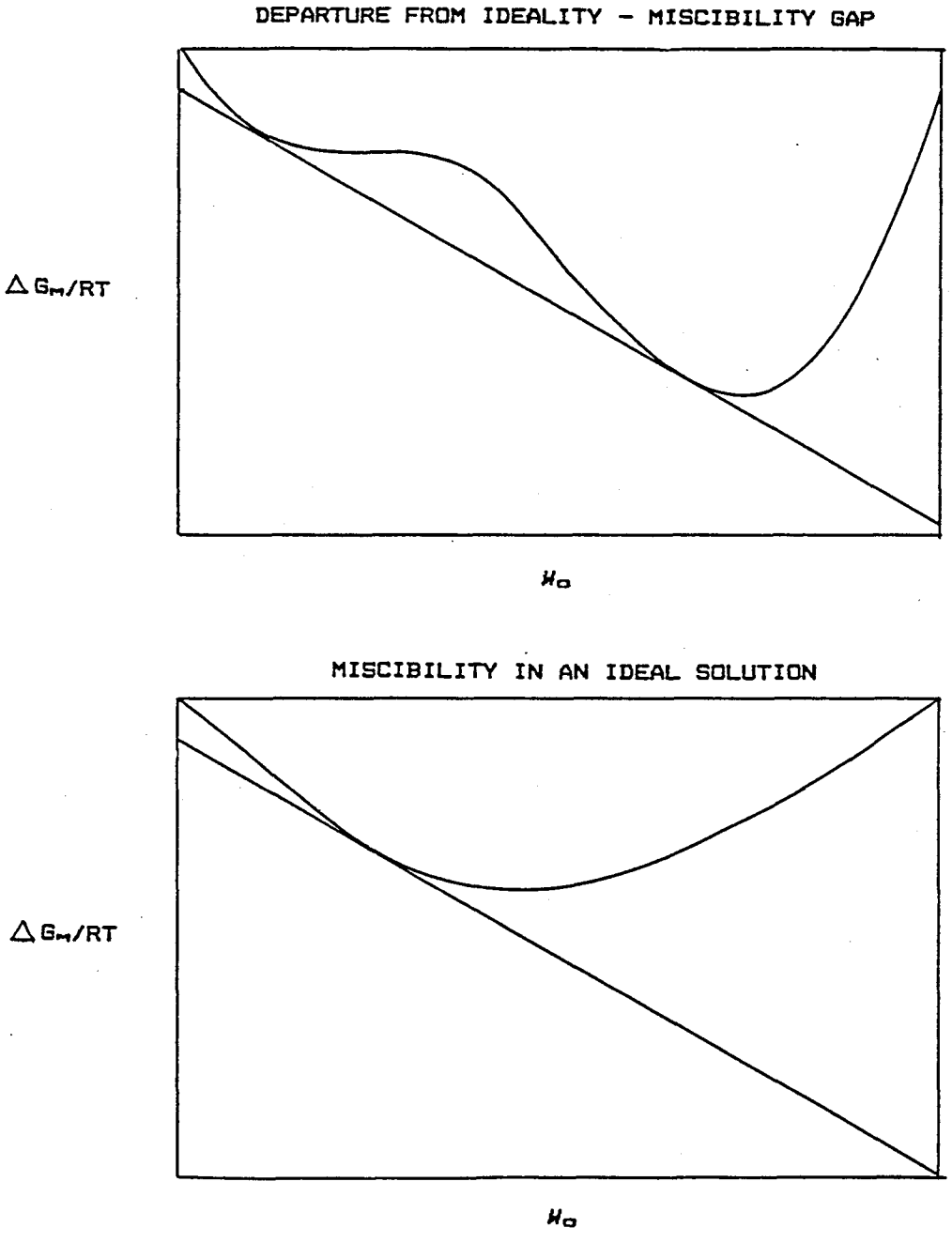

FIGURE 2.10: GIBBS FREE ENERGY OF A POLYMER MIXTURE, MISCIBILITY GAP IN A NON-IDEAL SOLUTION

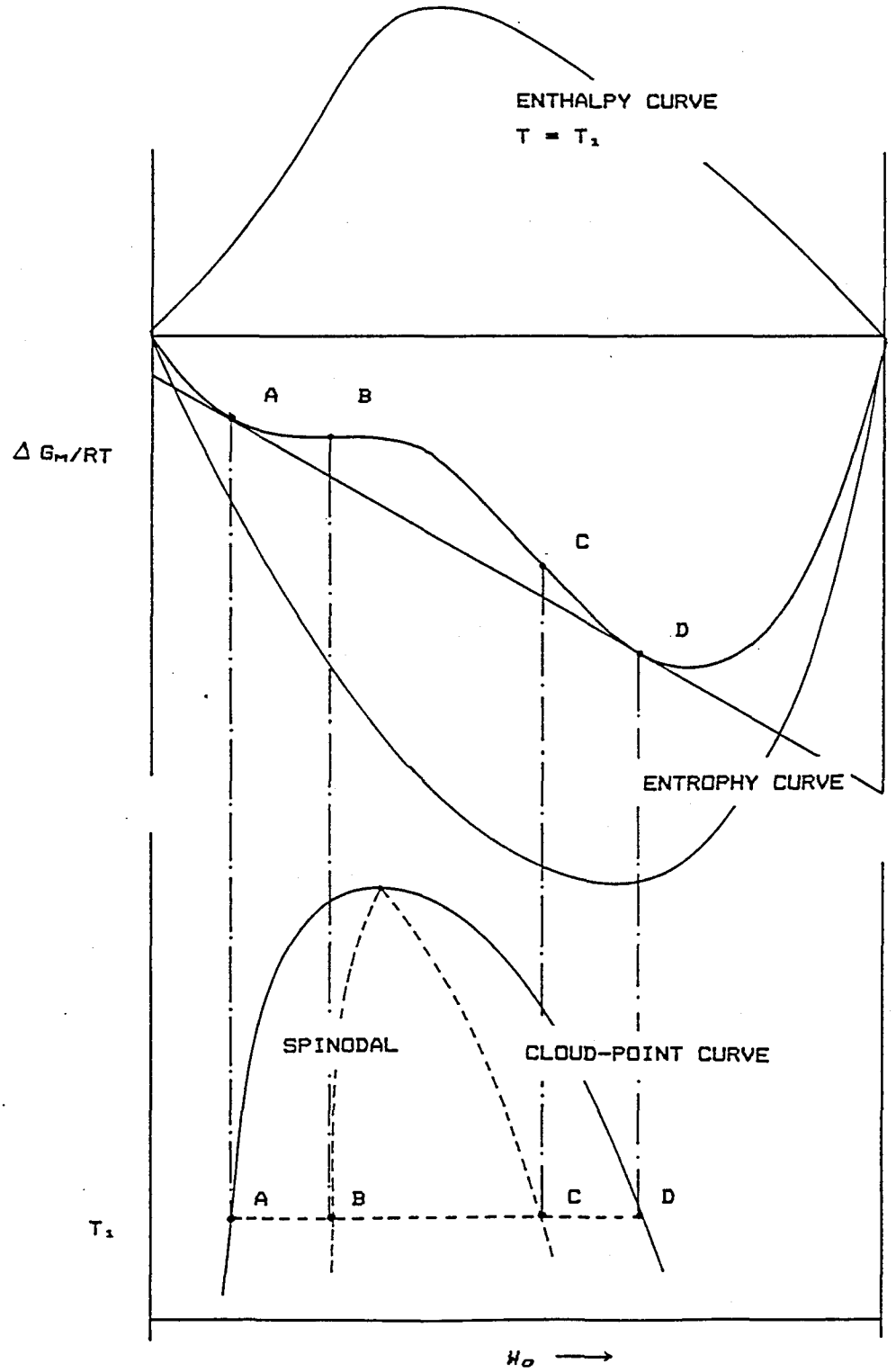

FIGURE 2.11: MISCIBILITY GAP IN THERMAL PHASE INVERSION

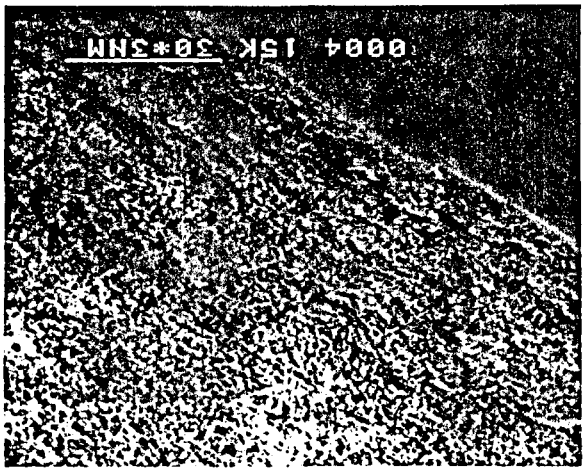

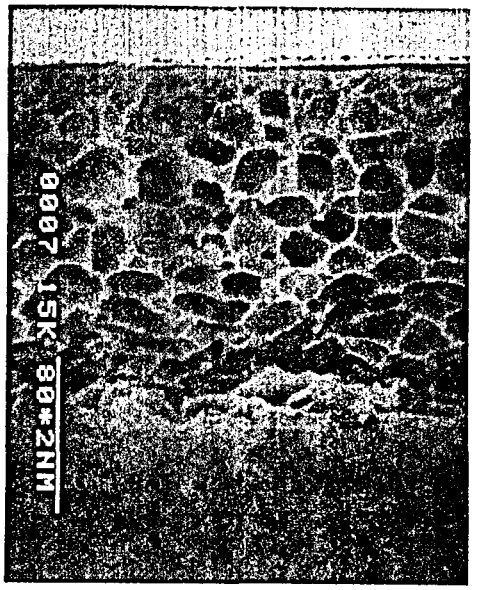

FIGURE 2.12: SCANNING ELECTRON MICROGRAPHS OF VICTREX 4800G POLY(ARYLETHER SULPHONE) THERMAL INVERSION MEMBRANES

2.3 MEMBRANE MATERIALS

Various synthetic polymers have been introduced as membrane-forming materials, since the use, first of all, of cellulose acetate as a reverse osmosis material and cellulosic derivatives as ultrafiltration membrane materials. Apart from yielding an anisotropic structure when prepared by a phase inversion process, polymers must also satisfy other requirements before they can be regarded as possible membrane materials. These requirements are, *inter alia*, that:

i) The material should be hydrolytically stable and show resistance to attack by organic liquids. The latter is particularly important in the case of ultrafiltration membrane materials because of their use in industrial applications. The former is more important in reverse osmosis applications.

ii) The molecular mass should preferably be high (from the advantage point of higher casting solution viscosities) and the distribution of molecular mass low (which reduces the tendency of micro-bead formation during the coagulation process). Wettability is another important requirement, particularly in the case of reverse osmosis membrane materials. In general, materials used for ultrafiltration are more hydrophobic than are those used for reverse osmosis.

iii) The material must be resistant to deformation. Water acts as a plasticizer, and by virtue of its association with hydrophilic materials, will render them more prone to viscoelastic flow than less hydrophilic materials will.

The relative degree to which a polymeric membrane is permeable to water depends not only on the overall porosity and surface characteristics of the membrane, but also on the material of construction. The functionality of the polymer determines to which degree, if at all, water will associate with the polymer matrix. On the one hand, there are those materials, *e.g.* poly(tetrafluoro ethylene), for which water has no affinity. Water is transported through finely porous media of such materials only with difficulty. On the other hand, there are the hygroscopic polymers, *e.g.* polyamines, which dissolve readily in water, unless they are cross-linked. Between these two extremes are polymers with the correct hydrophilic/hydrophobic balance for the fabrication of asymmetric reverse osmosis and ultrafiltration membranes *(122)*.

Water molecules are highly orientated within the confines of a hydrophilic membrane surface matrix due to their capacity to form hydrogen bonds with the polymer. Calorimetric studies *(123)(124)* produced proof of the existence of bound (or highly ordered) water structures within the membrane surface-matrix, and related to solute-rejecting characteristics of cellulose acetate reverse osmosis membranes. Because of their interaction with the polymer, water molecules lose part of their energy of hydration. This leads to a reduction in hydration potential and entry of ionized species into the surface matrix is hindered. Water passes through the membrane by translation.

Using activity coefficients (ion potentials within capillaries and near phase boundaries), Glueckauf *(40)* calculated surface pore radii for cellulose acetate reverse osmosis membranes, effective in NaCl rejection, to be 0,6nm. This he compared with the radii of unhydrated Li^+ (0,06nm), Na^+ (0,095nm), K^+ (0,133nm) ion and that of a water molecule (0,2nm). Water sorption isotherm studies (a review by Pusch) *(125)* indicate the existence of pore radii of the order of 4nm in homogeneous cellulose acetate membranes. Pores of the same

dimensions may also exist on the surface of asymmetric membranes, but the indications are that they range in size from 10 to 300nm.

The above pore sizes should be compared with those of a hydrophobic ultrafiltration membrane, in which 95% of a 50 000 molecular-mass polymer will be retained by a membrane with pore radii of the order of 4nm *(126)*. These membranes are, however, not capable of retaining salt to the same extent due to the hydrophobic nature of ultrafiltration membrane materials. Water does not associate with a hydrophobic polymer matrix to the same degree. By the time random movement and cluster formation are so restricted by the confines of the available space that solvation of ionic species is no longer possible, viscous transport of water through the membrane would no longer be possible either. At this stage the membrane can be used to separate gases *(127)*.

Figure 2.13 shows a graphical representation of the partial solubility parameters (δ_H, δ_P) for a range of reverse osmosis and ultrafiltration membrane materials. An arbitrary circle, outside which ultrafiltration materials lie, has been inserted. The key to the solubility parameters *(69)(70)* and abbreviations used in the map, is given in Table 2.1.

TABLE 2.1: SOLUBILITY PARAMETERS AND ABBREVIATIONS OF MEMBRANE-FORMING POLYMERS (FIGURE 2.13)

Membrane forming material	Abbreviation	Solubility parameter			
		δ_T	δ_D	δ_P	δ_H
polyvinylchloride	PVC		18,2	7,5	8,3
poly(methyl methacrylate)	PMMA	20,3	16,5	7,6	9,0
cellulose acetate (398)	CA	25,9	15,6	16,1	12,9
cellulose triacetate	CTA	24,6	15,6	14,9	11,9
cellulose	C	49,3	15,1	40,2	24,2
poly(bisphenol A sulphone)	PS	25,8	18,4	16,5	7,5
polypropylene (isotactic)	PP	16,4	15,7	4,9	0,0
aromatic polyamide	PA 55	32,5	19,0	18,3	19,0
polyurea (NS-100)	PU	25,0	16,1	14,2	12,8
polybenzimidazolone	PBIL	35,0	19,1	24,6	16,0
aromatic polyimide	PI	38,9	19,9	28,8	16,8
poy(arylether sulphone)	PES	28,4	18,7	18,9	9,8
poly(phenylene oxide)	PPO	13,5	12,3	2,7	4,9
sulphonated PS	SPS	28,9	18,1	19,3	11,5
polyacrylonitrile	PAN	29,4	17,4	22,5	7,5
poly(ethylene terephthalate)	PET	21,6	19,5	3,5	8,6
poly(vinylidene fluoride)	PVDF	19,2	13,7	10,6	8,2

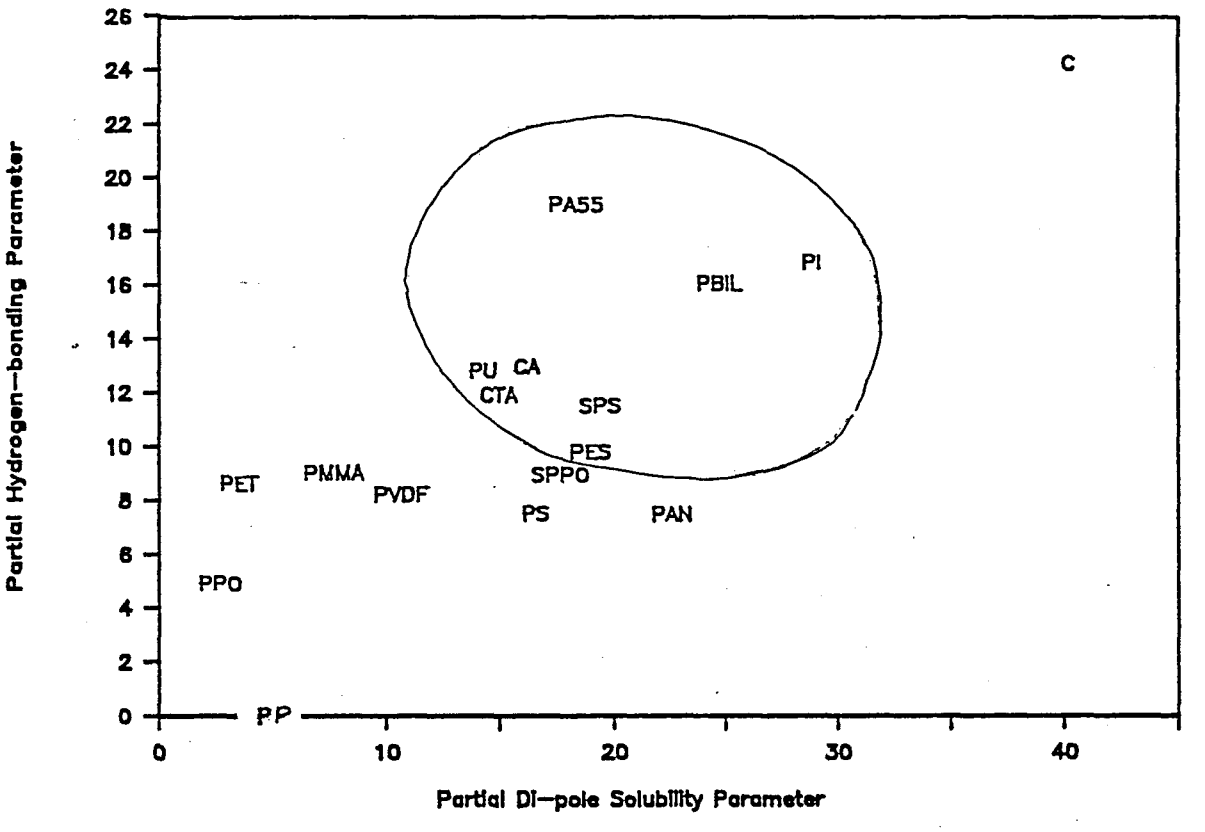

FIGURE 2.13: MAP OF THE PARTIAL SOLUBILITY PARAMETERS, δ_H, δ_P, FOR A RANGE OF ASYMMETRIC MEMBRANE-FORMING MATERIALS

LIST OF REFERENCES

1. Ferry, J.D., Chem. Rev., 18(1936)373-455
2. Rogers, A.N., Conf.: Synth. Membr. Processes: Fundam. Water Appl., Ed. Belfort, G., (1984)437-477
3. Anon, Industrial application of RO technology, Bulletin 608 (1981), Trace Metal Data Inst., El Paso, Texas
4. Gregor, H.P., Gregor, C.D., Sci. Amer., 239(1978)88-101
5. Cartolano, A.R., Design and operation of UF systems for water treatment, PhD Dissertation, (1984), Columbia University
6. Sakamoto, H., Kimura, K., Shono, T., Eur. Polym. J., 22,2(1986)97-101
7. Mulder, M.H.V., Smolders, C.A., J. Membrane Science, 17(1984)289-307
8. Malon, R.F., Zampini, A., US Patent 4 486 202 (Dec 1984)
9. Caldwell, K.D., Chem. Anal., Mod. Meth. Ed., 73(1984)211-250
10. Lonsdale, H.K., J. Membr. Sci., 10(1982)81-181
11. Reid, C.E., Breton, E.S., J. Appl. Polym. Sci., 1(1959)133-143
12. Loeb, S., Sourirajan, S., Advan. Chem. Ser., 38(1962)117-132; US Patent 3 133 132 (1964)
13. Manjikian, S., Loeb, S., McCutchan, J.W., Proc. 1st Int. Symp. Desaln., 2(1965)159173, Washington, D.C.
14. Riley, R.L., Merten, U., Gardner, J.O., Desalination, 1(1966)30-34
15. Riley, R.L., Lonsdale, Lyons, C.R., Merten, U., J. Appl. Polym. Sci., 11(1967)2143-2158
16. Salemme, R.M., Browall, W.R., US Patent 4 155 793 (May 1979)
17. King, W.M., Hoernschemeyer, D.L., Saltonstall, C.W., Reverse osmosis membrane research, Ed. Lonsdale, H.K., Podall, H.E., (1972), Plenum Press, NY
18. Richter, J.W., Hoehn, H.H., U.S. Patent 3 567 632, (1972)
19. Panar, M., Hoehn, H.H., Herbert, R.R., Macromolecules, 6(1973)777-780
20. Murakami, H., Igarashi, N., Ind. Eng. Chem. Prod. Res. Dev., 20,3(1981)501-508
21. Riley, R.L., Fox, R.L., Lyons, C.R., Milstead, C.E., Seroy, W.M., Tagami, M., Desalination, 19(1976)113
22. Rozelle, L.T., Cadotte, J.E., Cobian, K.E., Kopp, C.V., Ch. 12, Ed. Sourirajan, S., Reverse Osmosis and Synthetic Membranes, (1977), Nat. Res. Council Canada
23. Meares, P., NATO ASI Ser., Ion Exch., Sci. Techn., 107(1986)529-558
24. Hann, R.A., Eur. Patent Appl., 843 078 22.1 (Nov. 1984)
25. Schwarz, H., Kudela, V., Lukas, J., Vacik, J., Collect. Czech. Chem. Commun., 51,3(1986)539-544
26. Marcinkowsky, A.E., Krans, K.A., Phillips, H.O., Johnson, J.S., J. Am. Chem. Soc., 88(1966)5744
27. Van Reenen, A., PhD-thesis in Preparation, Proposed Title "Polyacrylic acid co- and terpolymer dynamic membranes" (1988), Inst. Polym. Sci., Univ. Stel.
28. Zeman, L., Tkacik, G., ACS Symp. Ser., 269(1985)339-350
29. Jonsson, G., Desalination, 53(1985)3-10
30. Tragardh, G., Desalination, 53(1985)25-35
31. Smolders, C.A., Vugteveen, E., ACS Symp. Ser., 269(1985)327-338
32. Push, W., Walch, A., J. Membr. Sci., 10(1982)325-360
33. Yasuda, H., Tsai, J. Appl. Polym. Sci., 18(1974)805-819
34. Sarbolouki, M.N., Sepn. Sci. Techn., 17,2(1982)381-386
35. Katz, M.G., Proc. 15th Conf.: Water Desalination and Re-use, (May 1983)229-243, Jerusalem,
36. Staverman, A.J., J. Membr. Sci., 16(1983)7-20
37. Sourirajan, S., Reverse osmosis, (1970), Academic Press, NY
38. Sourirajan, S., Ind. Eng. Chem., Fundam., 2(1963)51
39. Sourirajan, S., Pure & Appl. Chem., 50(1978)593-615
40. Glueckauf, E., Proc. 1st Int. Symp., Water Desaln., (1965)143-150, OSW, Washington, DC
41. Kimura, S., Sourirajan, S., J. Am. Inst. Chem. Engnrs., 13(1967)497-503
42. Johnson, J.S., McCutchan, J.W., Bennion, D.N., Report UCLA-ENG 7139, Univ. of UCLA, California
43. Lonsdale, H.K., Merten, U., Riley, R.L., J. Appl. Polym. Sci., 9(1965)1341-1362
44. Lonsdale, H.K., Transport properties of osmotic membranes; Ed. Merten, U., Desalination by reverse osmosis, Ch. 4, (1966), M.I.T. Press, Cambridge
45. Mazid, M.A., Sepn. Sci. & Techn., 19(1984)357-373
46. Sikar, K.K., 3rd World Filtr. Congr., (1982)564-571, Uplands Press, UK; Sikar, K.K., Rao, G.H., Ind. Eng. Chem., Process Des. Dev., 20(1981)116-127
47. Goel, V., McCutchan, W., Use of simulation for specification of RO membrane and operating parameters, Paper presented at the Summer Simulation, (1977)250-255, Chicago
48. Murkes, J., Bohman, H., Desalination, 11(1972)269-301
49. Putter, W.J., Patent: Ger. Offen 2 529 515 (Jan. 1976)
50. Larson, T.J., Gibbons, B.C., Report 442 (Jun. 1969), OWRT, USA
51. Rosenblatt, N.W., et al, Report PB 252 597, (1975), OWRT, USA
52. Jonsson, G., Boesen, C.E., Synth. Membr. Processes, Fund. & Water Appl., (1984)101-130, Academic Press, Inc.
53. Potts, D.E., Ahlert, R.C., Wang, S.S., Desalination, 36(1981)325-264
54. Probstein, R.F., Cohen, R.D., NTIS Report: PB 86-126 182 (Nov. 1985)
55. Cahn, J.W., Acta. Metall., 9(1961)795-801
56. Kesting, R. E., ACS Symp. Ser., 269(1985)119-164
57. Koningsveld, R., Kleintjens, L.A., Macromolecules, 4,5(1971)637-641
58. Scott, R.L., J. Chem. Phys., 17,3(1949)268-279
59. Scott. R.L. J. Chem. Phys., 17,3(1949)279
60. Rabek, J.F., Experimental methods in polymer chemistry, 1st Ed., (1980), John Wiley & sons
61. Hildebrandt, J.H., Scott, R.L., The solubility of non-electrolytes, 3rd Ed., (1949), Dover, NY
62. Barton, A.M.F., Handbook of solubility parameters, p8, (1983), CRC Press, Inc., Florida
63. Hansen, C.M., J. Paint Techn., 42(1970)660-664
64. Hildebrandt, J.H., Prausnitz, J.M., Scott, R.L., Regular and related solutions, (1970), Reinhold Princeton, NY
65. Jackson, L.C., Adhesives Age, (Oct. 1976)17-19
66. Barton, A.M.F., Handbook of solubility parameters, p425-435, (1983), CRC Press, Inc., Florida
67. Ventoza, T.P., Gouye, S.A., Lloyd, D.R., ACS Symp. Ser., 51(1984)713-717, ACS, Washington

68. Klein, E., Smith, J.K., Ind. Eng. Chem., Prod. Res. Dev., 11(1972)207-210
69. Matsuura, T., Sourirajan, S., Characterization of membrane materials for reverse osmosis, Anon.Report; p1188-1199, Div. of Chem., Nat. Res. Counc. Canada, Ontario
70. Barton, A.M.F., Handbook of solubility parameters, p308-317 (1983), CRC Press, Inc., Florida
71. Vincent, P.I., Raha, S., Polymer, 13(1972)283-287
72. Barton, A.M.F., Handbook of solubility parameters, Ch. 8, (1983), CRC Press, Inc., Florida
73. Barton, A.M.F., Handbook of solubility parameters, Ch. 15, (1983), CRC Press, Inc., Florida
74. Cowley, J.D., Teague, G.S., Lowe, J.W., J. Paint Techn., 39(1967)19-27
75. Teas, J.P., J. Paint Techn., 40(1968)19-25
76. Kinzer, K.E., Lloyd, D.R., J. Membrane Sci., 22(1985)1-29
77. Wijmans, J.G., Kant, J., Mulder, M.H.V., Smolders, C.A., Polymer, 26(1985)1539-1545
78. Bottino, A., Capannelli, G., Munari, S., J. Appl. Polym. Sci., 30(1985)3009-3022
79. Chauhan, B.D., Mehta, D.J., Indian J. of Techn., 22(1984)474-476
80. Wijmans, J.G., Rutten, H.J.J., Smolders, C.A., J. Polym. Sci., Polym. Phys. Ed., 23(1985)1941-1955
81. Strathmann, H., Habilitationsschrift, (1981)51-54, Univ. Tubingen, FRG
82. Koenhen, D.M., Mulder, M.H.V., Smolders, C.A., J. Appl. Polym. Sci., 21(1977)199-215
83. Lemoyne, C., Friedrich, J.L., Halary, C.N., Monnerie, L., J. Appl. Polym. Sci., 25(1980)1883-1913
84. Kamide, K., Manabe, S., Polym. Mater. Sci. Eng., 50(1984)156-160
85. Sikar, K.K., Agarwal, N.K., Rangaiah, G.P., J. Appl. Polym. Sci., 22(1978)1919-1944
86. Sarbolouki, M.N., J. Polym. Sci., Lett. Ed., 11(1973)753
87 Sarbolouki, M.N., J. Appl. Polym. Sci., 29(1984)743-753
88. Neogi, P., J. AIChE., 29(1983)402-410
89. McHugh, A.J., Yilmaz, L., J. Polym. Sci., 23(1985)1271-1274
90. Mysels, K.J., Lonsdale, H.K., Want, D.E., ACS Symp. Ser., 281(1985)201-208
91. Buckfelder, J.J., Schleinitz, H.M., Eur. Patent Appl. 85/112312 (Sept. 1986)
92. Frommer, M.A., Lancet, D., Reverse osmosis membrane research, Ed. Lonsdale, H.K., Podall, H.E., P85-110, (1972), Plenum Press, NY
93. Friedrich, C., Driancourt, A., Noel, C., Monnerie, L., Desalination, 36(1981)39-62
94. Ramsbotham, J., Prog. in Org. Coatings, 8(1980)113-141
95. Ray, R.J., Kranz, W.B., Sani, R.L., Linear stability model for finger formation in asymmetric membranes, Annual Meet. A.I.Ch.E. (1984), NY
96. Stevens, W.E., Dunn, C.S., Petty, C.A., Paper presented at the 73rd Annual Meeting AIChE, (1980), Chicago
97. Uragami, T., Ohsumi, y., Sugihara, M., Polymer, 23(1982)999-1004
98. Munari, S., Bottino, A., Capanelli, G., J. Membr. Sci., 16(1983)181-193; Desalination, 53(1985)11-23
99. Strathmann, H., Von Mylius, U., 5th Int. Symp on Fresh Water from the Sea, 4(1976)189-199
100. Sundet, S.A., Eur. Patent Appl., 851 040 93.1, (Apr. 1985)
101. Congjie, G. Xueren, L., Xiuzhen, S., Desalination, 62(1987)89
102. Halary, J.L., Noel, C., Monnerie, L., Desalination, 13(1973)251
103. Strathmann, H., Schneible, P., Baker, R.W., J. Appl. Polym. Sci., 15(1971)811-828
104. Yilmaz, L., McHugh, A.J., J. Membr. Sci., 28(1986)287-310
105. Cohen, C., Tanny, G.B., Prager, S., J. Polym. Sci., 17(1979)477-489
106. Broens, L., Altena, F.W., Smolders, C.A., Desalination, 32(1980)33-45
107. Cahn, J.,W., Acta. Metall., 9(1961)795-801
108. Sanderson, R.D., Pienaar, H.S., Desalination, 25(1978)281-301
109. Koenhen, D.M., Mulder, M.H.V., Smolders, C.A., J. Appl. Polym. Sci., 21(1977)199-215
110. Caneba, G.T., Soong, D.S., Macromolecules, 18(1985)2545-2555
111. Zsigmondy, R., Carius, C., Chem. Ber., 60B(1927)1047
112. Kesting, R., J. Appl. Polym. Sci., 17(1973)1771-1784
113. Kesting, R., Anon., NTIS Report PB 300 488 (1979)
114. Kesting, R., US Patent 3 884 801 (1975)
115. Castro, A.J., US Patent 4 247 498 (1981)
116. Gerlach, K., Kessler, E., US Patent 4 564 488 (1986)
117. Mizuo, S., Takashi, Y., Hisayoshi, Y., Eur. Patent Appl., 0 050 399/A1, (Jul. 1981)
118. Hiatt, W.C., Vitzthum, G.H., Wagener, K.B., Gerlach, K., Josefiak, C., ACS Symp. Ser., 269(1985)229-244
119. Koenhen, D.M., Mulder, M.H.V., Smolders, C.A., J. Appl. Polym. Sci., 21(1977)199-215
120. Strathmann, H., ACS Symp. Ser., 269(1985)165-195
121. Kuhl, S., Unpublished results, Institute for Polymer Science, University of Stellenbosch
122. Matsuura, T., Blais, P., Sourirajan, S., J. Appl. Polym. Sci., 20(1976)1515-1531
123. Burghoff, H.G., Push, W., J. Appl. Polym. Sci., 23(1979)473-484
124. Burghoff, H.G., Push, W., Polym. Eng. Sci., 20(1980)305
125. Pusch, W., Walch, A., J. Membr. Sci., 10(1982)325-360
126. Sarbolouki, M.N., Sepn. Sci. & Techn., 17(1982)381-386
127. Finken, H., Asymmetric membranes for gas separation, Report, GKSS 85/E/22, GKSS-Forschungszentrum, Geesthacht, FRG

CHAPTER III

COMPOSITE MEMBRANES

3.0 INTRODUCTION

A composite reverse osmosis membrane consists of an ultra-thin (20 - 200nm) permselective layer of polymer deposited and immobilized on the surface of a microporous substrate membrane. When the composite membrane is compared with the Loeb-Sourirajan asymmetric phase-inversion membrane, the ultra-thin perm-selective polymer-film represents the much thicker desalting skin section (0,1 - 1,0μm) *(1)* of the cellulose acetate reverse osmosis membrane. The substrate membrane beneath it merely acts as a support for the thin film and does not contribute to the salt rejection performance of the thin permselective layer.

As indicated earlier (section 2.2), the method by which asymmetric membranes are formed is essentially a one-step procedure, that is, coagulation and gelation of a film produced from a polymer solution. The fabrication of composite membranes, on the other hand, is a two-step procedure, consisting of the formation of the substrate membrane, followed by a step(s) to create the desalting ultra-thin film [UTF] on the skin-surface of the substrate membrane.

3.1 UTF MEMBRANE PREPARATION

3.1.1 METHODS

Different methods *(2)* can be used to create various kinds of permselective ultra-thin desalting layers on the surface of substrate membranes:

i) Coating of the substrate membrane with a reactive monomer, oligomer or polymer, followed by an interfacial poly-condensation reaction to cross-link the film chemically *(3)*.

This method is important to the text and will be discussed in the next section and also later in Chapter VI.

ii) Coating of the substrate membrane with a reactive monomer, oligomer or polymer solution, followed by thermal or ionic cross-linking.

An example of a composite RO membrane produced in this fashion, is the NS-200 furfuryl alcohol membrane. This composite membrane is produced by coating a substrate membrane with a 2:2:1 solution of furfuryl

alcohol:sulphuric acid:Carbowax 20M in 80:20 water:isopropanol. Oven-curing of the coated substrate membrane at 125 - 140°C produces the characteristic black sulphonated polyfurane UTF permselective matrix *(4)*.

Composite sulphonated polysulphone membranes are another example of thermally cross-linked UTF membranes. Polysulphone can be sulphonated to such a degree that it becomes water-soluble. Composite UTF membranes are formed by coating a substrate membrane with an aqueous solution of the sulphonated material. Heat treatment (100 - 140°C) immobilizes the coated hydrophilic polymer film by the formation of sulphone cross-links *(5)*.

Composite permselective films may also be formed by insolubilizing hydrophilic (water-soluble) polymers by contacting the film with polyvalent metal ions, such as barium or aluminium. An example of such a membrane is a composite permselective film formed from poly(acrylic acid), with the water-soluble film being fixed by ionic cross-linking, for example, with aluminium *(6)*. The same process was followed to insolubilize a water-soluble membrane performance restorative coating on the surface of CA RO membranes *(7)*.

iii) Gas-phase deposition by the use of glow discharge plasma *(8)(9)*.

Vinyl monomers, or any monomer with an adequate vapor pressure, can be used to deposit a permselective barrier on a substrate membrane. Additional copolymers could be formed by inclusion of nitrogen in the reagent gases. The plasma reactions are heterogeneous and involve polymerization, depolymerization, as well as reactions with the support membrane polymer *(10)*.

3.1.2 INTERFACIAL CONDENSATION REACTIONS

The first of the methods described above, namely, that of producing a UTF composite RO membrane by chemical reactions, performed *in situ* on the surface of the substrate membrane, is widely used for the fabrication of RO membranes *(11)*.

In the fabrication of this class of membrane, the rapid condensation reaction between acyl halides or isocyanates and amines is exploited, to form, respectively, amide and urea bonds. Cross-linking, to immobilize the water-soluble amine precursors, is achieved by proper choice of the cross-linking reagent functionality.

An interface for the chemical reaction is created by using two immiscible solvents for the reacting species, *i.e.* aqueous phase for the water-soluble amine precursor and organic phase (hexane) for the cross-linking reagent.

3.1.2.1 Polymeric precursor

One of the first successful interfacial UTF composite membranes produced was fabricated from a polyamine. In the fabrication of the NS-101 UTF polyamide membrane, an aqueous film of poly(ethylene imine) is interfacially reacted with isopthaloyl chloride [IPC] to insolubilize the hydrophilic polymer. The polyurea

analog [NS-100], is obtained by substituting IPC by 1,3-toluene di-isocyanate [TDI] as the cross-linking reagent. As a final step in the preparation of the UTF composite RO membrane, the membrane is cured thermally (110°C) to induce further cross-linking by means of a condensation reaction between primary amine groups *(12)*.

3.1.2.2 Oligomeric precursor

Amine-terminated oligomers have also been used in the preparation of UTF composite membranes *(13)*. In the case of piperazine-based *(14)* UTF composite membranes, monomeric piperazine or a prepolymer version, have been used in the preparation of composite membranes. The secondary-amine-terminated oligomer is obtained by reacting excess piperazine with a tri-functional acyl halide (tri-mesoyl chloride [TMC]) or a mixture of TMC/IPC in an inert solvent such as di-chloro ethane *(5)*.

In the first case the RO membrane is prepared by chemical cross-linking di-functional piperazine monomer with tri-functional TMC. Di-functional IPC is used to cross-link the tri-functional oligomeric version of piperazine.

Another example of a membrane prepared from an oligomeric precursor is the aliphatic tri-functional amine, di-ethylene tri-amine [DETA]. To prepare the oligomer, excess DETA is reacted with IPC in an inert solvent. The reactive tri-functional primary-amine-terminated oligomer is cross-linked with IPC to form the UTF composite RO membrane *(15)*.

3.1.2.3 Monomeric precursor

A commercially successful membrane (FT30), is prepared solely from monomeric reagents. In the fabrication of these membranes, an aromatic diamine, 1,3-diaminobenzine, is reacted with TMC on the surface of a PS substrate membrane to produce the UTF composite RO membrane *(16)*. The resulting aromatic polyamide membrane is capable of single-pass sea water desalination *(17)*, with salt rejection capabilities exceeding 99%.

LIST OF REFERENCES

1. Riley, R.L., Gardner, J.O., Merten, U., Science, 143(1964)801
2. Cadotte, J.E., Evolution of composite RO membranes, Materials science of synthetic membranes, Ed. Lloyd, D.R., ACS Symp. Ser. 269(1985)273-294
3. Cadotte, J.E., Cobian, K., Forester, R., Peterson, R., Final Report to OWRT, Contract No. 14-30-3298, (April 1976).
4. Cadotte, J.E., US Patent 3 926 798, (1975)
5. Cadotte, J.E., Steuck, M.J., Petersen, R.J., Research on in-situ formed condensation polymer for RO membranes, NTIS Rep. No. PB-288287, (1977), OWRT Contract No. 14-34-0001-6521, Washington, DC
6. Huang, R.Y.M., Gao, C.J., Kim, J.J., J. Appl. Pol. Sci., 28(1983)3064-3073
7. Pienaar, H.S., The synthesis and physical properties of semipermeable membranes used in water purification by the process of RO, PhD-thesis, (1977), University of Stellenbosch
8. Yasuda, H., Sourirajan, S., Reverse osmosis synthetic membranes, Report No. 15427, (1977), National Research Council Canada, Ottawa
9. Yasuda, H., Composite RO membranes prepared by plasma polymerization; Ed., Sourirajan, S., Synthetic RO membranes, p263-294 (1977), NRCC, Ottawa
10. Yasuda, H., Marsh, H.C., J. Appl. Polym. Sci., 20(1976)543-555
11 Lonsdale, H.K., J. Membrane Sci., 33(1987)121-136
12. Rozelle, L.T., Cadotte, J.E., Cobian, K.E., Kopp, C.V., Jr., Nonpolysaccharide membranes for reverse osmosis: NS-100 membranes for RO and synthetic membranes, Ed., Sourirajan, S., p249-261 (1977), NRCC, Ottawa
13. Wolfe, J.F., Jones, R.S., Sybert, P.D., Novel polymers for RO membranes, NTIS Rep. PB83-173237, (Nov. 1982), OWRT Contract, DI-14-34-0001-0465, Washington, DC
14. Cadotte, J.E., Cobian, K.E., Forester, R.H., Petersen, R.J., Continued evaluation of in-situ formed condensation polymers for RO membranes, NTIS Report No. PB 253193 (1976), OWRT Contract No. 14-30-3298, Washington, DC
15. Lu, E.K., Babcock, W.C., Novel composite membranes, NTIS Report No. PB83-243170 (Apr. 1983), Washington, DC
16. Cadotte, J.E., US Patent 4 277 344, (1981)
17. Larson, R.E., Cadotte, J.E., Petersen, R.J., Desalination, 38(1981)473

CHAPTER IV

STATISTICALLY DESIGNED EXPERIMENTS

4.0 INTRODUCTION

Statistical planning of experiments *(1)* and statistical analysis of results *(2)(3)* can contribute in large measure to the success of any research effort, since they allow the maximum amount of unambiguous information to be extracted from the minimum amount of experimental work.

The characteristic of the statistical approach in experimental design is the pre-planning or formal arrangement of experimental trials, called the designed experiment; there is a broad field of statistics which is devoted wholly to the planning of such experiments *(4)*. The technique of statistically designed experiments (first introduced in agricultural research) *(5)* offers solutions to problems with which researchers are faced daily:

i) Screen a list of possible factors and isolate those that truly affect the measured quantity/quality.
ii) Determine in what/which way the outcome is affected by the factors.
iii) Determine the direction in which the factor levels (variables) should be altered to obtain wanted properties.
vi) Find those factor levels (variables) that would yield the best property.

A method commonly used in obtaining wanted properties is the univariant approach *(6)*, in which the level of one of n factors is varied, while the other n-1 factors are kept at a constant level (Figure 4.1). The method has the disadvantage that convergence to a solution is not particularly rapid and does not converge at all in certain cases (Figure 4.2). Important, though, is the lost opportunity to research more factors in the same amount of time, and to learn something about possible interactions between the factors.

A more certain way of finding wanted or better properties would be to explore the whole n-dimensional experimental region in a grid-pattern search. This is the basis of statistically designed experiments, namely, the construction of a low-density grid of experimental points which covers the experimental region. The factorial design *(7)* is one approach which can be used to isolate important factors, introduce untested factors, and create a basis of understanding and knowledge, all while the route to better properties is followed.

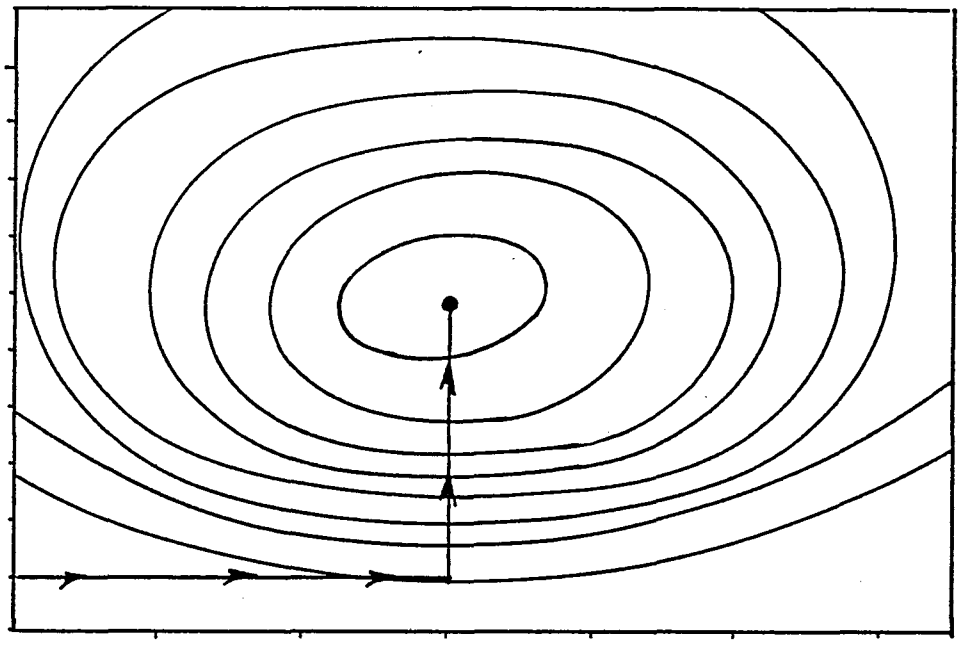

FIGURE 4.1: ILLUSTRATION OF THE UNIVARIANT SEARCH TECHNIQUE, INVOLVING TWO FACTORS

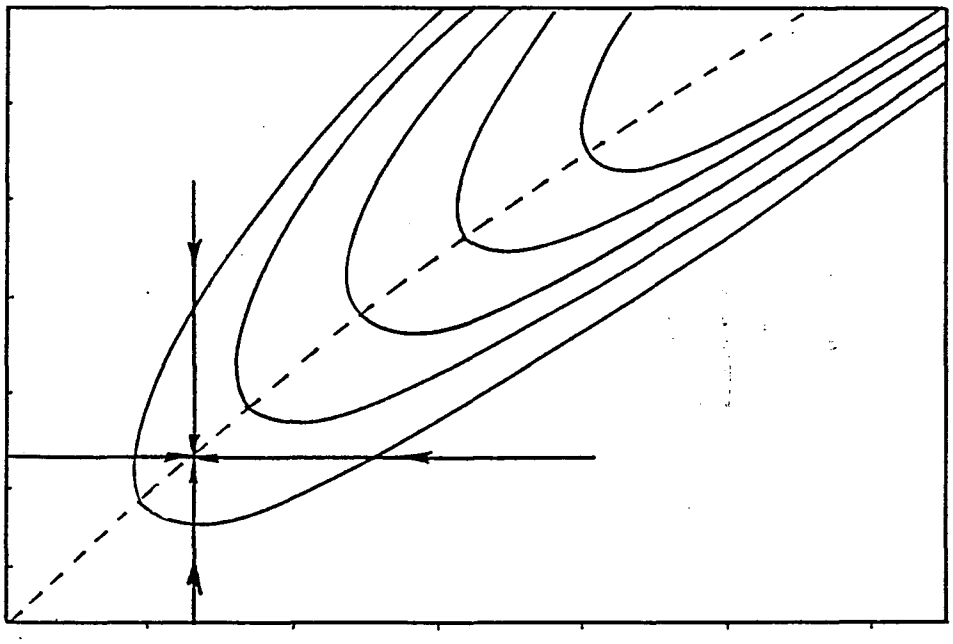

FIGURE 4.2: FAILURE OF THE UNIVARIANT SEARCH IN CONVERGING

There are different types of factorial experimental designs *(1)*, one of which is the 2-level factorial design (2^n factorial), in which each factor is tested at two levels. In the exploration of the experimental region using this approach, all the possible combinations of the different factors are investigated at the two levels to elucidate the effect of each factor and the possible interactions between the factors. The main effects of the factors can be determined with the same accuracy as if only one factor had been varied at a time *(8)(9)*.

4.1 STATISTICAL QUANTITIES

4.1.1 DEFINITIONS *(10)*

Deviation is the difference between a particular measurement and the mean calculated from a set of measurements of the same quantity. The standard deviation (defined as the root-mean-square average of the deviations from the mean) for n independent measurements of equal validity is:

$$\sigma = \sqrt{[\Sigma(x_i - \bar{x})^2/n]}$$

The square of this quantity, σ^2, is called the variance. To obtain an estimate of the variance of the parent population, the sample variance is modified:

$$\sigma^2_{\text{Parent}} = [n/(n - 1)]\sigma^2_{\text{Sample}}$$

replacing n by (n - 1) in the definition for standard deviation for n observations:

$$s = \sqrt{[\Sigma(x_i - \bar{x})^2/(n - 1)}$$

which allows s^2 to become an unbiased estimator of the parent population variance, σ^2 *(11)*. The estimator used for a series of n identical, independent measurements of a quantity 'x' is:

$$\bar{x} = \Sigma x_i/n$$

The standard deviation is related to the average error of each measurement, and the standard error (deviation) of the mean is:

$$\Delta\bar{x} = \sqrt{(s^2/n)} = \sqrt{[\Sigma(\bar{x} - x_i)^2/n(n - 1)]}$$

The deviation of the mean from the population mean decreases as the number of observations increases, but only as the square root of the number of observations.

4.1.2 SIZE OF AN EXPERIMENT

The probability of detecting a real difference between two sources of data is a function of:

i) the magnitude of that difference,
ii) the standard deviation of the single observations, and
iii) the amount of data collected from each source.

The sizes of experiments are correlated with the magnitude of the difference (δ) to be detected, and with the random error (σ) of each of the observations, and not necessarily with the number of variables *(12)(13)(14)*.

To illustrate: consider an experiment in which the aim was to determine whether the rate at which a PS membrane phase separated was any different from the rate at which a PES membrane phase separated. Eight experiments *(15)* must be conducted with each polymer (16 experiments in total) to detect a difference of 8 seconds ($\delta = 8$) in the rate at which the membrane will phase-separate, with a known error of deviation of $\sigma = 4$ seconds. (Probability of committing Type I and II errors (section 4.1.3.1), respectively, chosen at the 5% level).

[Note at this stage that 16 experiments are required to conduct a complete 2^4 factorial experiment in which four factors can be studied simultaneously. At hardly any expense in time, three more factors may be included in the above study, with the advantage that an assessment can be made of all these factors as well as of possible interactions between them].

4.1.3 ANALYSIS OF RESULTS

4.1.3.1 Errors of a statistical test

When a statistical test is conducted, the experimental results are in some form or other compared with a statistical norm in a fair test of significance. The outcome of the test can be that the results differ from the norm to such an extent that it is highly probable that the differences observed are not solely due to experimental error. It must then be accepted that a true difference does exist.

When one hypothesis is tested against another, the hypothesis is either rejected or accepted, at the risk of committing one of two kinds of error. For example, if the Null Hypothesis, (H_0: $\mu_A - \mu_B = 0$) that is, that the means (μ) are equal, is erroneously rejected, in favour of the alternative hypothesis, (H_1: $\mu_A > \mu_B$), a Type I error is committed. If the Null Hypothesis is false, and it is erroneously accepted, a Type II error is committed. The probability of this occurring is β. Table 4.1 illustrates the two kinds of error *(14)*.

TABLE 4.1: ERRORS - TYPE I AND TYPE II

Real Situation	Concluded from Data	
	Not reject H_o $\mu_1 - \mu_2 = 0$	Reject H_o $\mu_1 - \mu_2 = 0$
	Correct	Wrong
True $H_o: \mu_1 - \mu_2 = 0$	Probability= $1 - \alpha$ (Confidence level)	Type I error Probability= α (Level of test)
False $H_1: \mu_1 > \mu_2$		
	Wrong	Correct
True $H_1: \mu_1 > \mu_2$	Type II error Probability= β	$1 - \beta$ Probability= (Power of test)
False $H_o: \mu_1 - \mu_2 = 0$		

4.1.3.2 Paired comparison *(16)*

Invariably the question "is there a difference?" arises when sets of data are compared *(17)*. It is important to have a strategy by which to ascertain whether the difference between sets of observed responses is due to random variation, resulting from within the experiment (experimental error), or from an external source (possible effect of a factor on the data recorded).

To answer the question whether the rates at which the PS and PES membranes phase-separate differ, the rates are compared in a test of significance, such as the Student's t-test *(18)*:

$$t_o = {}^{\text{Mean}}/_{\text{Standard error of the mean}}$$

If the calculated value of t_o exceeds that of the tabled critical values of t at specified levels of significance, it is declared that there is a significant difference between the sets of data, and that the difference between the means is real and due not only to random error contribution.

In the case under consideration, the difference between pairs of observed responses is compared in a test of significance. The assumption is that the differences between the data pairs are normally distributed about the means, which, if there was no difference, would be zero. The statistical test performed is contained in Table 4.2.

Test the Hypothesis, H_o: $\mu = 0$, against the alternative, $\mu \neq 0$ at the 95% level of significance. The critical value (c) in this double-sided test, obtained from the distribution tables *(19)*:

$$P(T \leq c_1) = {}^{\alpha}/_{2} = 2{,}5\% \quad \text{and} \quad P(T \leq c_2) = 1 - {}^{\alpha}/_{2} = 97{,}5\%$$

is for n - 1 = 7 df, c = ± 2,36. Since t_o = 2,81 lies outside this region, the Null Hypothesis is rejected. The two sets of data therefore do differ significantly.

[The two membrane-forming materials have been compared and found to differ with regard to the rate at which they phase-separate. The results shown above have been extracted from a 2^4 factorial experiment in which other factors were also studied. The complete experiment will be analyzed later in section 4.2.3].

4.1.4 ANALYSIS OF VARIANCE *(20)(21)*

In section 4.1.3.2 the t-test was used in a paired comparison of the means of two sets of data of equal size. When comparing more than two sets of data, it is most important to have a strategy by which to ascertain whether the differences between means are due to random variation or whether they result from the effect which a factor has on the recorded data. This is accomplished through a procedure known as analysis of variance *(22)(23)*, by which several means are compared.

Analysis of variance is based on a decomposition of the sum of squares [SS] of the deviations between the sample values and the sample mean.

TABLE 4.2: t-TEST FOR PAIRED DIFFERENCES - TIME IN SECONDS TO COMPLETE PHASE SEPARATION

	Membrane Polymers		Difference
	PS	PES	(d)
	47,6	45,0	2,6
	65,4	64,3	1,1
	49,7	49,2	0,5
	72,9	68,4	4,5
	55,5	47,9	7,6
	92,1	72,6	19,5
	57,9	47,5	10,4
	90,0	65,3	24,7
Mean:	66,4	57,5	8,86

Variance of the mean difference: $s_d^2 = \Sigma(d - \bar{d})^2/(n-1)$

$\bar{d}$ mean difference
d difference between data pairs
n number of observations

$s_d^2 = 1/7[(2,6 - 8,86)^2 + (1,1 - 8,86)^2 + \ldots + (24,7 - 8,86)^2]$
$= 79,48$

Standard deviation: $s_d = \sqrt{s_d^2} = 8,92$

t-ratio: $t_o = \bar{d}/(s_d/\sqrt{n}) = 2,81$

In the one-way analysis of variance, the interest lies in analysing the effect of one factor, and the total sum of squares [SST] is decomposed into two parts, one corresponding to the factor whose effect is being investigated, and the other to random variation.

In the two-way analysis of variance, the effects of two factors are investigated, the SST being decomposed into attributes due to each factor and to random variation.

An extension of the two-way classification is the investigation of interactions between factors for which no provision is made in the formal two-way classification. This approach is used in the analysis of variance of 2-level factorial designs.

In the case of 2-level factorial designs, the concept of balance of the designs simplifies the calculations tremendously, and simple calculations provide answers to questions such as:

i) Does a factor have an effect on the response?
ii) How real is this apparent effect?
iii) Does the effect of one factor depend on the level of other factors, *i.e.* are there indications of interaction between factors?
iv) How real is the interaction?
v) What are the confidence limits of each of the observed effects?

The algebraic formula used in the calculation of variance is:

$$s^2 = \frac{\Sigma(x - \bar{x})^2}{n - 1} = \frac{[\Sigma(x^2) - (\Sigma x)^2/n]}{n - 1}$$

where the numerator is the variation between observed values and the mean (sum of squares). The sum of squares [SS] divided by degrees of freedom [df] is the mean sum of squares [MSS], which is equivalent to variance.

4.1.4.1 One-way analysis of variance

As an example of a situation to which the one-way analysis of variance would apply, consider the question: do RO modules produced over a five-day period differ in rejection performance?

The essential aspect of this method of analysis is that the deviations of the observed values from the overall mean (total sum of squares) [SST] is decomposed into two attributes:

$$SST = SS_{Explained} + SS_{Unexplained}, \text{ or;}$$

$$SST = SS_{Between\ columns} + SS_{Within\ columns}$$

$$\sum_i \sum_j (x_{ij} - \bar{x})^2 = n \sum_{i=1}^{c} (\bar{x}_i - \bar{x})^2 + \sum_{i=1}^{c} \sum_{j=1}^{n} (x_{ij} - \bar{x}_i)^2$$

where the $SS_{Between}$ entity refers to the SS of the deviations of the means between the groups (production days in the example, Table 4.4), columns in the array below;

$$\begin{array}{cccc} x_{11} & x_{12} & \cdots & x_{1j} \\ \cdot & \cdot & \cdot & \cdot \\ \cdot & \cdot & \cdot & \cdot \\ \cdot & \cdot & \cdot & \cdot \\ x_{i1} & x_{i2} & \cdots & x_{ij} \end{array}$$

and the SS_{Within} entity, which refers to the SS of the deviations within the different batches of RO modules produced on each of the production days (*i.e.* rows). Since this variation cannot be explained, it is known as the error sum of squares [SSE]. Table 4.3 shows a summary of the one-way analysis of variance for samples of equal size.

We refer back to the example of membrane modules. Table 4.4 lists the rejection performance of five batches of modules produced on five consecutive days. The question whether there is any significant difference in module performance will be answered by means of the analysis of variance table (Table 4.3).

The variation is calculated as follows:

Between columns

$$\text{Variation} = n\sum_{i=1}^{c} (\bar{x}_i - \bar{\bar{x}})^2$$

$$= 5[(96,0 - 96,116)^2 + (95,78 - 96,116)^2 + \ldots + (95,92 - 96,116)^2]$$
$$= 3,318$$

Within columns

$$\text{Variation} = \sum_{i=1}^{c}\sum_{j=1}^{n}(x_{ij} - \bar{x}_i)^2$$

$$= (95,4 - 96,0)^2 + (96,0 - 96,0)^2 + \ldots + (94,9 - 95,92)^2$$
$$= 8,816$$

Total

$$\text{Total Variation} = \sum_{i}\sum_{j}(x_{ij} - \bar{\bar{x}})^2$$

$$= (95,4 - 96,116)^2 + \ldots + (94,9 - 96,116)^2$$
$$= 12,134$$

In the statistical test performed, the Null Hypothesis H_o: $\mu_1 = \mu_2$ (that the means are equal) is tested against the alternative, H_1: $\mu_1 > \mu_2$. The critical point on the F-distribution curve for rejecting the Null Hypothesis *(24)*, for 4 and 20 df at the 0,05 and 0,01 levels are, $F(4,20)_{0,05}$ = 2,87 and $F(4,20)_{0,01}$ = 4,43, respectively. The F-ratio calculated in Table 4.4 lies well within the acceptance region and it can therefore be concluded that there is no significant difference between the batches of modules produced.

TABLE 4.3: ONE-WAY ANALYSIS OF VARIANCE

Source of Variation	Variation SS	df	Variance MSS	F-ratio
Explained Between (Columns)	$n\sum_{i=1}^{c}(\bar{x}_i - \bar{\bar{x}})^2$	c-1	$SS/(c-1) = ns_{\bar{x}}^2$	
Unexplained Within (Columns)	$\sum_{i=1}^{c}\sum_{j=1}^{n}(x_{ij} - \bar{x}_i)^2$	c(n-1)	$SS/c(n-1) = s_p^2$	$\frac{VAR_{Expl}}{VAR_{Unexpl}}$
Total	$\sum_{i}\sum_{j}(x_{ij} - \bar{\bar{x}})^2$	nc-1		

TABLE 4.4: RO MODULE PERFORMANCE - FIVE SETS OF MODULES PRODUCED ON FIVE CONSECUTIVE DAYS

		Production Batches (day number)				
	S M	[1]	[2]	[3]	[4]	[5]
	a o	95,4	96,0	97,1	96,2	96,1
	m d	96,0	96,0	95,9	96,0	97,3
	p u	95,8	94,9	97,1	96,0	96,7
	l l	96,2	95,5	97,2	95,9	94,6
	e e	96,6	96,5	96,8	96,2	94,9
Column total		480,0	478,9	484,1	480,3	479,6
Column mean:	$\bar{x}_i$	96,00	95,78	96,82	96,06	95,92
Grand total		2402,9				
Grand mean:	$\bar{\bar{x}}$	96,116				

ANALYSIS OF VARIANCE TABLE (From Table 4.3)

Source of Variation	Variation	df	Variance	F-ratio
<u>Explained</u> Between Columns	3,318	4	0,829	1,88
<u>Unexplained</u> Within Columns	8,816	20	0,441	
Total	12,134	24		

4.1.4.2 Two-way analysis of variance

The model associated with the two-way analysis of variance is;

Observed value	=	Overall mean	+	Row effect	+	Column effect	+	Experimental error

and the sum of squares total [SST] is again decomposed into variations that can be explained, rows [SSR] and columns [SSC], and that which cannot be explained: variation caused by experimental error [SSE]:

$$SST = SS_{Explained} + SS_{Unexplained}$$

$$SST = SSR_{Row} + SSC_{Column} + SSE$$

$$\sum_{ij}^{rc}\sum(x_{ij} - \bar{\bar{x}})^2 = c\sum_{i}^{r}(\bar{x}_{i.} - \bar{\bar{x}})^2 + r\sum_{j}^{c}(\bar{x}_{.j} - \bar{\bar{x}})^2 + \sum_{ij}^{rc}\sum(x_{ij} - \bar{x}_{i.} - \bar{x}_{.j} + \bar{\bar{x}})^2$$

Under the proviso that interaction between factors are not expected, single observations are organised in an array of cells in r-rows and c-columns. (The entry in each cell may be an average of a number of observations).

$$\begin{array}{ccccccc}
x_{11} & x_{12} & \cdots & x_{1j} & \cdots & x_{1c} \\
x_{21} & x_{22} & \cdots & x_{2j} & \cdots & x_{2c} \\
\vdots & \vdots & & \vdots & & \vdots \\
x_{i1} & x_{i2} & \cdots & x_{ij} & \cdots & x_{ic} \\
\vdots & \vdots & & \vdots & & \vdots \\
x_{r1} & x_{r2} & \cdots & x_{rj} & \cdots & x_{rc}
\end{array}$$

The analysis of variance table for the two-way analysis of variance is given in Table 4.5.

This method of analysis can, for example, be used to determine whether the performance of RO membranes produced on two machines by different operators differ in salt rejection, and at the same time, evaluate the consistency in performance of membranes produced over a period of a week.

In the following illustrative example, membranes produced on two machines (each with its own operator) are compared over a period of five production days to determine whether there is any significant difference in the quality of the membranes produced over the 5-day period, and whether there is any appreciable difference in the salt rejection performance of the membranes produced on two machines by the different operators.

	Production day number					
Machine	[1]	[2]	[3]	[4]	[5]	Total
I	*93,9%	94,7	95,0	94,3	94,2	472,1
II	94,1%	96,0	95,1	94,9	93,8	473,9
Total	188,0	190,7	190,1	189,2	188,0	946,0

(* Cell entries are average salt rejection performances obtained from six randomly selected 1m membrane sections)

The SS values of the various contributors are calculated below by means of a simplified version *(25)* of the formulas shown in Table 4.5, and summarized in the analysis of variance table, Table 4.6.

$$SST = \sum_{i=1}^{r}\sum_{j=1}^{c} x_{ij}^2 - T_{..}^2/rc$$
$$= (93,9)^2 + (94,7)^2 + \ldots + (94,9)^2 + (93,8)^2 - (946)^2/10$$
$$= 4,100$$

$$SSR = \sum_{i=1}^{r} T_{i.}^2/c - T_{..}^2/rc$$
$$= [(472,1)^2 + (473,9)^2]/5 - (946)^2/10$$
$$= 0,324$$

$$SSC = \sum_{j=1}^{c} T_{.j}^2/r - T_{..}^2/rc$$
$$= [(188)^2 + \ldots + (188)^2]/2 - (946)^2/10$$
$$= 2,970$$

$$SSE = SST - SSR - SSC$$
$$= 4,1 - 0,324 - 2,97$$
$$= 0,806$$

Since F_{Col} = 3,69 is less than the critical value for F of $F(4,4)_{0,1}$ = 4,11 and F_{Row} = 1,60 is less than the critical value of $F(1,4)_{0,1}$ = 4,54, it can be concluded that there is not enough evidence to reject the Null Hypothesis, $H_o: \mu_1 = \mu_2$, (even at the 10% level). There is no difference between membranes produced on the various days and the two operators (machines) produce membranes of equal standard.

TABLE 4.5: TWO-WAY ANALYSIS OF VARIANCE

Source of Variation	Variation SS	df	Variance MSS
Explained Between (Rows)	$c\sum_{i=1}^{r}(\bar{x}_{i.} - \bar{\bar{x}})^2$	(r-1)	SSR/(r-1) $= cs^2_{xi.}$
Explained Between (Columns)	$r\sum_{j=1}^{c}(\bar{x}_{.j} - \bar{\bar{x}})^2$	(c-1)	SSC/(c-1) $= rs^2_{x.j}$
Unexplained Residual variation, Random fluctuation	$\sum_{i=1}^{r}\sum_{j=1}^{c}(x_{ij} - \bar{x}_{i.} - \bar{x}_{j.} + \bar{\bar{x}})^2$	(r-1)(c-1)	SSU/(r-1)(c-1) $= s^2$
Total	$\sum_{i=1}^{r}\sum_{j=1}^{c}(x_{ij} - \bar{\bar{x}})^2$	(rc-1)	

TABLE 4.6: TWO-WAY ANALYSIS OF VARIANCE - COMPARISON OF PERFORMANCE OF PRODUCTION EQUIPMENT OVER FIVE PRODUCTION DAYS.

Source of Variation	Variation SS	df	Variance MSS	F-ratio
Days (Columns)	2,970	4	0,743	3,69
Machines (Rows)	0,324	1	0,324	1,60
Error	0,806	4	0,202	
Total	4,100	9		

4.2 2-LEVEL FACTORIAL DESIGN OF EXPERIMENTS

4.2.1 NOTATION

A factorial design having n factors, each at two levels, requires 2^n measurements (trials) for one complete replicate, *i.e.* all combinations of the n factors. The term "factor" is used to denote any feature the experimenter wishes to incorporate into an experiment, and may be continuous, namely, temperature, concentration, *etc.*, or discrete, *e.g.*, polymer A *versus* polymer B or absence *versus* presence, *etc.*

The n factors, as well as their interactions are designated by capital letters, A, B, C,... and AB, AC,..., BC,... and ABC,... *etc.*, and there are;

n	main effects
n(n - 1)/2	two-factor interactions
n(n - 1)(n - 2)/6	three-factor interactions
n(n - 1)...(n - h - 1)/h!	h-factor interactions

Lower-case italicized letters are used to denote the different treatment combinations that constitute the various experimental trials of the factorial design. The presence of a letter indicates the high level of that factor, its absence the low level. The symbol 'I' is that treatment at which all the factors are considered at their low levels.

Therefore in an experiment involving three factors (A, B, and C), the treatment combination '*ac*' indicates that factors A and C are considered at their respective high levels and that factor B is considered at its low level.

The various treatment combinations that constitute a 2^n factorial are normally arranged in standard order when presented (refer to Table 4.7). Two methods are used to arrange the trials in this order;

Sign notation:

Factor A -1 and +1, alternating, starting -1
Factor B -1 -1 and +1 +1, alternating, starting -1 -1
Factor C -1 -1 -1 and +1 +1 +1, alternating, starting -1 -1 -1
etc.

Alpha notation:

Every new letter introduced is followed by its combination with all previous treatment combinations, starting first with the identity "I".

TABLE 4.7: 2^3 FACTORIAL EXPERIMENT

	Factors	Levels -1	Levels +1	
A	PS concentration	14,0	18,0	Mass %
B	LiCl concentration	0	0,2	Mass %
C	PVP^{10K} concentration	1,0	10,0	Mass %

Treatment	Factors A	B	C	Gelation time (sec)
I	-1	-1	-1	47,6
a	+1	-1	-1	65,4
b	-1	+1	-1	49,7
ab	+1	+1	-1	72,9
c	-1	-1	+1	55,5
ac	+1	-1	+1	92,1
bc	-1	+1	+1	57,9
abc	+1	+1	+1	90,0

	Factors	Levels -1	Levels +1	
A	PES concentration	14,0	18,0	Mass %
B	LiCl concentration	0	0,2	Mass %
C	PVP^{10K} concentration	1,0	10,0	Mass %

Treatment	Factors A	B	C	Gelation time (sec)
I	-1	-1	-1	45,0
a	+1	-1	-1	64,3
b	-1	+1	-1	49,2
ab	+1	+1	-1	68,4
c	-1	-1	+1	47,9
ac	+1	-1	+1	72,6
bc	-1	+1	+1	47,5
abc	+1	+1	+1	65,3

The levels of a factor constitute the high or low end of the range over which the factor is varied, and is denoted by variables which take on the value of: +1 (high-level), 0 (mid-level, or base-level), -1 (low-level). A linear transformation is used to calculate the variables associated with the factor levels:

$$X^* = c_1 x + c_2$$

where

X^*	Factor level
x	Variable level
c_1	Unit
c_2	Base

4.2.2 DESIGN OF A 2^3 FACTORIAL EXPERIMENT

For the purpose of this illustration, consider the case where it was important to determine to what extent the concentration of a membrane-forming polymer and the concentrations of two casting-solution additives influenced the rate at which the membrane phase separated. Eight different casting solution compositions (2^3 factorial) can be prepared by adding smaller or larger quantities of each of the three components to the mixture (See Table 4.7). (The components may be qualitative, *i.e.*, present or absent, or quantitative, *i.e.* presentable on a scale such as, in this case, mass percent).

There will therefore be four mixtures in which each one of the three components will be present at a low concentration (low-level) and four mixtures in which it will be present at a high concentration (high-level). The difference in the effect observed, apart from random fluctuations, between these two sets of four trials each, must therefore be ascribed to that particular solution component by which they differ. Furthermore, this comparison will have the same precision as if the eight trials had been devoted to testing the influence of one single component.

In the two 2^3 factorial experiments (detailed in Table 4.7), membrane films were produced from the various casting solutions, and the time-period between onset of phase separation and completion of the process (which renders the membrane), was determined under identical conditions. The only difference between the two experiments was that different membrane-forming materials were used: poly(bisphenol-A-sulphone) [PS] in the first case, and poly(arylether sulphone) [PES] in the second.

(The original intention was to investigate whether there was a difference in the rates at which PS and PES membranes phase-separated. The scope of the same experiment had been widened to include other casting solution components, which will also be evaluated, in the same number of experimental trials. The gain in added information within the same number of experiments is obvious).

4.2.3 ANALYSIS OF EXPERIMENTAL RESULTS *(26)*

The data presented in Table 4.7 resulted from a 2^4 factorial design (shown in Table 4.8), in which the low level of factor D represents PS and the high level PES. (See section 6.2.2.2 for a discussion of the experiment and results).

4.2.3.1 Calculation of effect totals and effects

The effect of a variable is determined by comparing averages of the response at one level of the independent variable against the averages of the outcome at another level of the same independent variable. (Figure 4.3). The average effect of a factor is called the main effect of that factor.

To find the main effect of factor A in Table 4.8 for example, it is first of all necessary to compute the difference in the average of the responses (gelation time in this case) at the high level of factor A (*i.e.* treatment combinations which contain the letter '*a*') and the average of the responses at the low level of factor A (*i.e.* treatment combinations that do not contain the letter '*a*').

Convenient symbolic expressions are given below which can be used, after algebraic expansion, to calculate the effect totals and the effects for n factors, A, B, C, ..., Q of a 2^n factorial. The effects are obtained by dividing the effect totals by 2^{n-1}.

$$\begin{aligned}
&\text{Effect Total A} && = (a - I)(b + I)(c + I)\ldots(q + I)\\
&\text{Effect Total AB} && = (a - I)(b - I)(c + I)\ldots(q + I)\\
&&& \vdots\\
&\text{Effect Total AB...Q} && = (a - I)(b - I)(c - I)\ldots(q - I)
\end{aligned}$$

If the effect of one factor is different at different levels of another factor, the two factors are said to interact. In this experiment there was an interaction between factors C and D. The effect which the CD interaction has on the gelation time of the membranes is illustrated in Table 4.9.

$$\begin{aligned}
\text{Effect CD} &= 1/2^{n-1}\,(a + I)(b + I)(c - I)(d - I)\\
&= 1/8\,(I + a + b + ab - c - ac - bc - abc - d - ad - bd - abd + cd\\
&\qquad + acd + bcd + abcd)\\
&= -6,7
\end{aligned}$$

Method I

One method for computing the effect totals of factors and their respective interactions from the experimental data, is by forming linear combinations of the treatment totals (Table 4.10). In this table the levels of factors A, B, C and D are presented by minus (-) and plus (+) signs, as in Table 4.8. Table 4.10 also contains columns of signs representing interactions between factors. The signs in the respective interaction columns (*e.g.* AB, AC *etc.*) are obtained by cross-multiplying the signs in the four columns in pairs, threes and then all four together. (The combination of signs for any interaction or main effect can also be obtained by algebraic expansion of the symbolic expressions for the different effect totals, shown earlier).

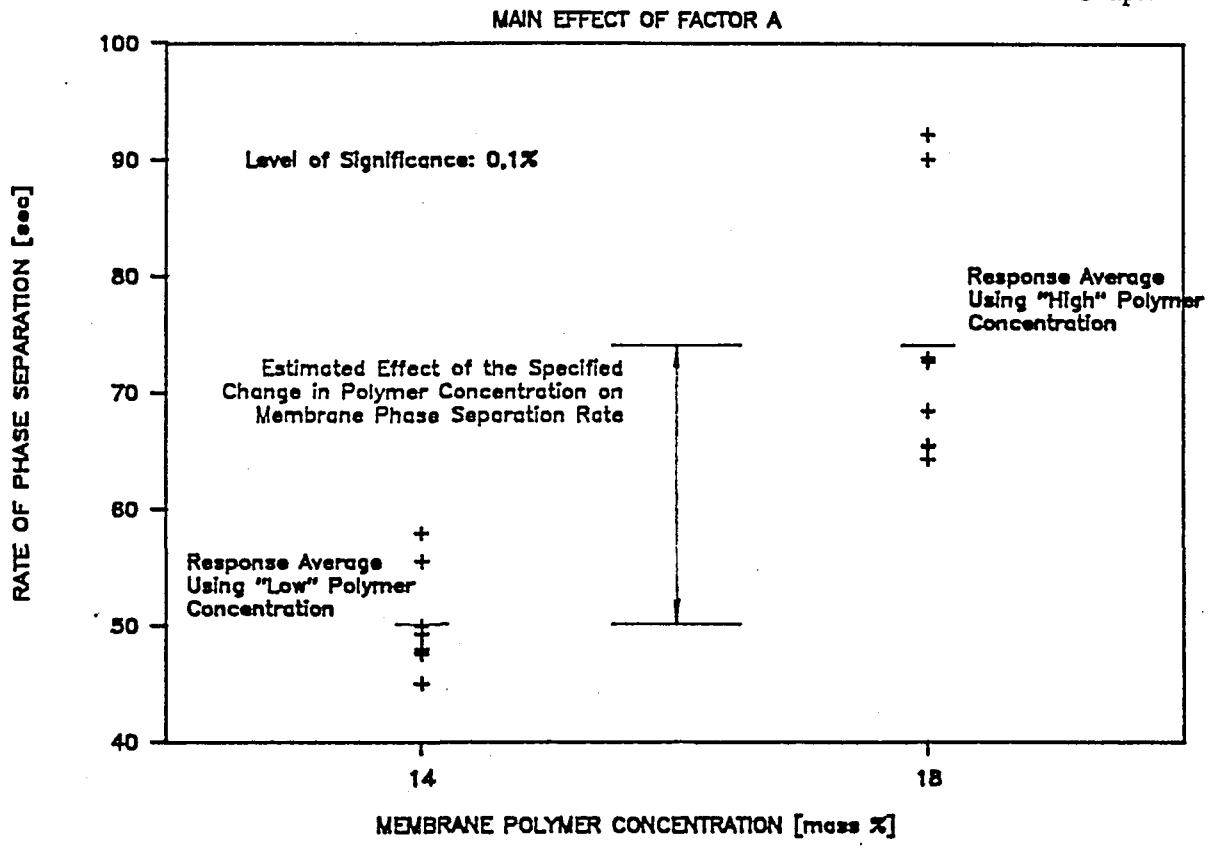

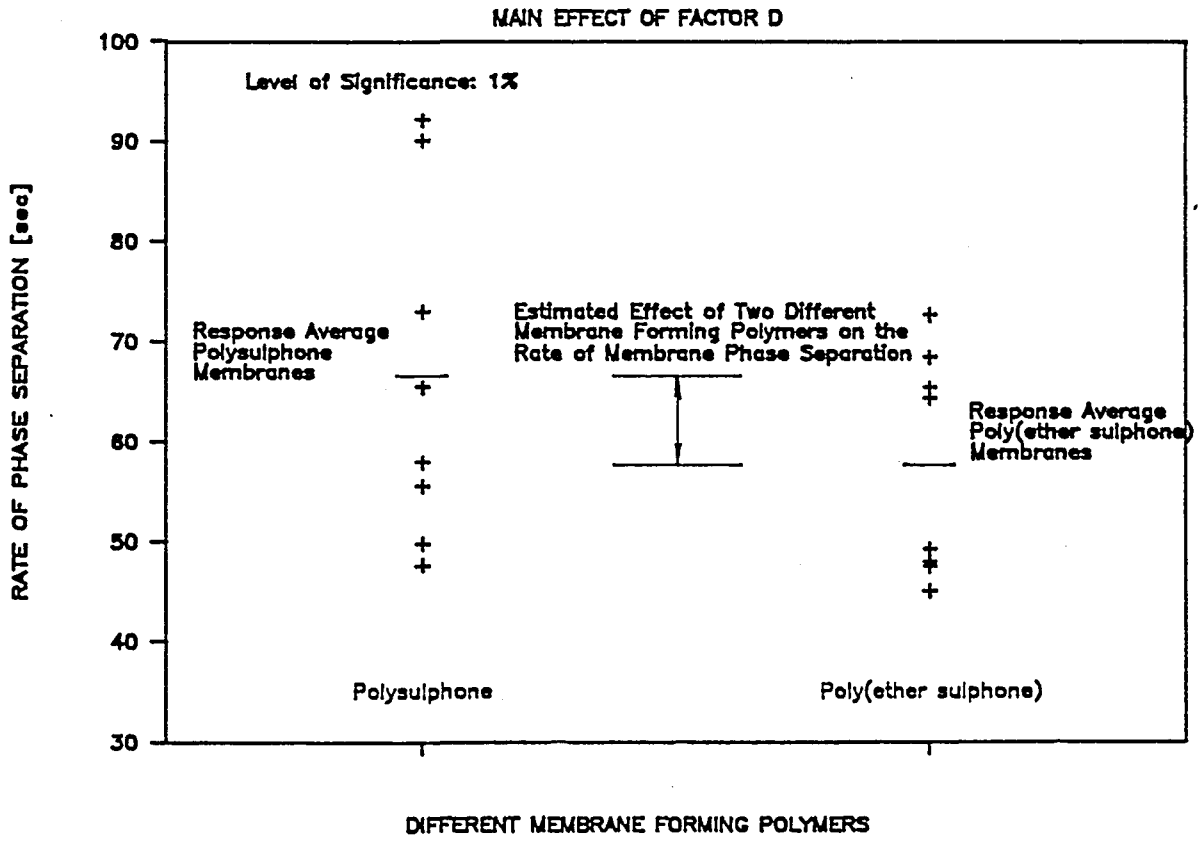

FIGURE 4.3: EFFECT: THE DIFFERENCE IN THE AVERAGE RESPONSE MEASURED AT TWO FACTOR-LEVELS

TABLE 4.8: 2^4 FACTORIAL EXPERIMENT - MEMBRANE GELATION TIME

	Factors	Levels -1	Levels +1	
A	Polymer concentration	14,0	18,0	Mass %
B	LiCl concentration	0	0,2	Mass %
C	PVP^{10K} concentration	1,0	10,0	Mass %
D	Membrane-forming polymer	PS	PES	

Treatments	Factors A	B	C	D	Gelation time (sec)
I	-1	-1	-1	-1	47,6
a	+1	-1	-1	-1	65,4
b	-1	+1	-1	-1	49,7
ab	+1	+1	-1	-1	72,9
c	-1	-1	+1	-1	55,5
ac	+1	-1	+1	-1	92,1
bc	-1	+1	+1	-1	57,9
abc	+1	+1	+1	-1	90,0
d	-1	-1	-1	+1	45,0
ad	+1	-1	-1	+1	64,3
bd	-1	+1	-1	+1	49,2
abd	+1	+1	-1	+1	68,4
cd	-1	-1	+1	+1	47,9
acd	+1	-1	+1	+1	72,6
bcd	-1	+1	+1	+1	47,5
abcd	+1	+1	+1	+1	65,3

TABLE 4.9: EFFECT OF THE INTERACTION CD ON THE RATE OF MEMBRANE PHASE-SEPARATION.

			FACTOR [D]			
			Membrane forming polymer			
			PS		PES	
		Levels	[-]		[+]	
F	P		47,6		45,0	
A	V	[-]	65,4	Ave	64,3	Ave
C	P	1%	49,7	= 58,9	49,2	= 56,7
T			72,9		68,4	
O	C					
R	O		55,5		47,9	
	N	[+]	92,1	Ave	72,6	Ave
[C]	C	10%	57,9	= 73,9	47,5	= 58,3
			90,0		65,3	

$$\text{Effect CD} = 1/2\ (58,9 - 56,7 - 73,9 + 58,3)$$
$$= -\ 6,7$$

TABLE 4.10: TABLE OF SIGNS FOR CALCULATING MAIN AND INTERACTION EFFECTS IN A 2^2 2^3 AND 2^4 FACTORIAL

Treatment	Main Effects and Interactions																Treatment Total
		2^2			2^3				2^4								
	Total	A	B	AB	C	AC	BC	ABC	D	AD	BD	ABD	CD	ACD	BCD	ABCD	
I	+	-	-	+	-	+	+	-	-	+	+	-	+	-	-	+	47,6
a	+	+	-	-	-	-	+	+	-	-	+	+	+	+	-	-	65,4
b	+	-	+	-	-	+	-	+	-	+	-	+	+	-	+	-	49,7
ab	+	+	+	+	-	-	-	-	-	-	-	-	+	+	+	+	72,9
c	+	-	-	+	+	-	-	+	-	+	+	-	-	+	+	-	55,5
ac	+	+	-	-	+	+	-	-	-	-	+	+	-	-	+	+	92,1
bc	+	-	+	-	+	-	+	-	-	+	-	+	-	+	-	+	57,9
abc	+	+	+	+	+	+	+	+	-	-	-	-	-	-	-	-	90,0
d	+	-	-	+	-	+	+	-	+	-	-	+	-	+	+	-	45,0
ad	+	+	-	-	-	-	+	+	+	+	-	-	-	-	+	+	64,3
bd	+	-	+	-	-	+	-	+	+	-	+	-	-	+	-	+	49,2
abd	+	+	+	+	-	-	-	-	+	+	+	+	-	-	-	-	68,4
cd	+	-	-	+	+	-	-	+	+	-	-	+	+	-	-	+	47,9
acd	+	+	-	-	+	+	-	-	+	+	-	-	+	+	-	-	72,6
bcd	+	-	+	-	+	-	+	-	+	-	+	-	+	-	+	-	47,5
abcd	+	+	+	+	+	+	+	+	+	+	+	+	+	+	+	+	65,3

The main and interaction effects are calculated by associating the sign in the respective columns with the values in the treatment totals column (response) and sum, which give the respective effect totals. When the signs in Table 4.10 are applied, the effect totals, or contrast sums *(27)*, are calculated as follows:

A = - 47,6 + 65,4 - 49,7 + 72,9 - 55,5 + ... + 65,3 = 190,7
B = - 47,6 - 65,4 + 49,7 + 72,9 - 55,5 - ... + 65,3 = 10,5
CD = + 47,6 + 65,4 + 49,7 + 72,9 - 55,5 - ... + 65,3 = -53,5
ABC = - 47,6 + 65,4 + 49,7 - 72,9 + 55,5 - ... + 65,3 = -16,7 *etc.*

To obtain the effects, the effect totals are divided by $2^{4-1} = 8$ (in general by 2^{n-1}), as was shown earlier. The effects of the above main factors and interactions are therefore: A = 23,84, B = 1,31 and the effect of the interactions CD = -6,69 and ABC = -2,09, *etc.*

Method II

Yates *(28)* developed a systematic tabular approach which simplifies the calculation of effect totals. This technique has become standard practice in the calculation of effect totals and effects.

The technique is illustrated in Table 4.11. The treatment combinations are presented in standard order in the first column of the table and their respective treatment totals (responses) are given in the second column. The quantities in column no. 1 were obtained by adding the treatment totals in pairs, *i.e.*, 47,6 + 65,4 = 113, 49,7 + 72,9 = 122,6, *etc.*, making the top eight entries in this column. The entries in the bottom half of column no. 1 were obtained by subtracting the treatment totals, again in pairs, the first from the second in each case, again starting from the top, *i.e.* 65,4 -47,6 = 17,8, 72,9 - 49,7 = 23,2 *etc.*, thus completing the entries in the bottom half of the column. The entries in columns nos. 2 to 4 were obtained by repeating the procedure, using the values generated in the columns to their left. In general, the procedure is repeated n times, where n equals the number of factors under consideration.

4.2.3.2 Analysis of variance *(29)*

The procedure used in the analysis of variance of 2-level factorial experimental data is a logical extension of the approach used earlier in section 4.1.2.1 in the two-way analysis of variance. The mathematical computations are, however, simplified in that the SS contribution of the various treatments to the total observed variation [SST], is calculated from the respective factorial effect totals, obtained by methods illustrated above.

Two situations present themselves, namely, that of an non-replicated complete factorial, and that of a replicated complete factorial. Both cases will be exemplified in the following text.

TABLE 4.11: ILLUSTRATION OF THE YATES METHOD FOR CALCULATING MAIN AND INTERACTION EFFECTS IN A 2^4 FACTORIAL (FROM TABLE 4.8)

	Treatment				Effect Total			
Treatment	Total	[1]	[2]	[3]	[4]			Effect
I	47,6	113,0	235,6	531,1	991,0	=	Total	
a	65,4	122,6	295,5	460,2	190,7	=	8A	23,84
b	49,7	147,6	226,9	109,7	10,5	=	8B	1,31
ab	72,9	147,9	233,3	81,0	-6,1	=	8AB	-0,76
c	55,5	109,3	41,0	9,9	66,3	=	8C	8,29
ac	92,1	117,6	68,7	0,6	31,7	=	8AC	3,96
bc	57,9	120,5	38,5	0,9	-25,3	=	8BC	-3,16
abc	90,0	112,8	42,5	-7,0	-16,7	=	8ABC	-2,09
d	45,0	17,8	9,6	59,9	-70,9	=	8D	-8,86
ad	64,3	23,2	0,3	6,4	-28,7	=	8AD	-3,59
bd	49,2	36,6	8,3	27,7	-9,3	=	8BD	-1,16
abd	68,4	32,1	-7,7	4,0	-7,9	=	8ABD	-0,99
cd	47,9	19,3	5,4	-9,3	-53,5	=	8CD	-6,69
acd	72,6	19,2	-4,5	-16,0	-23,7	=	8ACD	-2,96
bcd	47,5	24,7	-0,1	-9,9	-6,7	=	8BCD	-0,84
abcd	65,3	17,8	-6,9	-6,8	3,1	=	8ABCD	0,39

Non-replicated 2-level factorial

The deviations of the treatment totals from the overall mean [SST] is, as before, decomposed into its attributes, which are:

$$SST = SS_{Treatments} \ (+ SSE)$$

The $SS_{Treatments}$ can be decomposed further into its respective attributes which are the SS contributions of the various main and interaction effects:

$$SS_{Treatments} = SS_A + \ldots + SS_{AB} + \ldots + SS_{ABC} + \ldots + SS_{ABCD}$$

etc.

In non-replicated designs, the contribution of the factorial effects to the $SS_{Treatments}$ can be calculated from the expression:

$$SS = [\text{Effect Total}]^2/2^n$$

Likewise, the respective effects can be calculated from the expression:

$$\text{Effect} = [\text{Effect Total}]/2^{n-1}$$

By applying these expressions to the effect totals calculated in Table 4.11 (column no. 4), for the gelation-time experiment contained in Table 4.8, the SS contributions of the main and interaction effects, summarized in Table 4.12, are obtained.

In the absence of resources on which to base the estimate of error variation [SSE] (which replication of the experiment could have provided), it is customary to accept, *a priori*, that higher-order interaction effects (*e.g.* the three-factor and four-factor interaction effects) are not significant, in which case their observed variation can be ascribed to experimental error. By dividing their combined variation (Table 4.12), SSE (= 59,85), by their number of df (= 5), an estimate of the mean error variance, MSE (= 11,97) is arrived at from within the experiment *(30)*.

The F-ratio (variance ratio) is obtained by dividing the MSS by the MSE. The critical values of the F distribution for 1 and 5 df at the 10%, 5% and 0,1% levels are $F(1,5)_{0,1}$ = 4,06, $F(1,5)_{0,05}$ = 6,61 and $F(1,5)_{0,01}$ = 16,3, respectively. The levels of significance, corresponding to the respective factorial effects, are shown in Table 4.12.

Replicated 2-level factorial

The following example illustrates the procedure followed in the analysis of variance of a replicated 2-level factorial experiment. The data used was acquired from a 2^4 factorial experiment (replicated twice), designed to determine the possible effect of casting solution components on the linear shrinkage of wet-phase-separated PS and PES substrate membranes. The responses shown in Table 4.13 were arrived at by expressing the width of a coagulated flat-sheet membrane as a percentage of its cast (nascent) width (section 6.2.2.1).

TABLE 4.12: UNREPLICATED 2^4 FACTORIAL - ANALYSIS OF VARIANCE - EFFECT OF CASTING SOLUTION COMPONENTS ON THE GELATION TIME OF SUBSTRATE MEMBRANES

Variation Source		Effect	SS	df	MSE	F-ratio	Level
Main effects							
Pol conc.	A	23,84	2272,91	1	2272,91	189,1	0,1%
LiCl conc.	B	1,31	6,89	1	6,89	0,58	
PVP conc.	C	8,29	274,73	1	274,73	22,95	1%
PS/PES	D	-8,86	314,18	1	314,18	26,25	1%
Interactions							
	AB	-0,76	2,33	1	2,33	0,19	
	AC	3,96	62,81	1	62,81	5,25	10%
	AD	-3,59	51,48	1	51,48	4,30	10%
	BC	-3,16	40,01	1	40,01	3,34	
	BD	-1,16	5,41	1	5,41	0,45	
	CD	-6,69	178,89	1	178,89	14,89	5%
	ABC	-2,09	17,43				
	ABD	-0,99	3,90				
	ACD	-2,96	35,11	=5	11,97		
	BCD	-0,84	2,81				
	ABCD	0,39	0,60				

TABLE 4.13: 2^4 FACTORIAL EXPERIMENT - LINEAR MEMBRANE SHRINKAGE

	Factors	Levels -1	+1	
A	Polymer concentration	14,0	18,0	Mass %
B	LiCl concentration	0	0,2	Mass %
C	PVP^{10K} concentration	1,0	10,0	Mass %
D	Membrane polymer	PS	PES	

Final membrane width (percentage of wet width)

Treatment	Rep 1	Rep 2	Treatment Total
I	87,94%	88,11%	176,05%
a	88,86	88,13	176,99
b	88,00	88,90	176,90
ab	88,69	88,70	177,39
c	87,70	87,21	174,91
ac	88,03	88,41	176,44
bc	87,60	87,90	175,50
abc	88,11	88,05	176,16
d	84,45	88,33	172,78
ad	87,70	87,92	175,62
bd	87,09	86,73	173,82
abd	87,23	87,88	175,11
cd	87,19	87,03	174,22
acd	87,27	87,33	174,60
bcd	87,52	86,73	174,25
abcd	89,16	86,89	176,05
Total	1402,54	1404,25	2806,79

As for the two-way analysis of variance, the total sum of squares [SST] for a replicated factorial can be decomposed into three attributes, namely, variation among treatments, replicates and one measuring the experimental error:

$$SST = SS_{Treatments} + SS_{Replicates} + SSE$$

Analyzing the data first as showed for the 2-way analysis of variance (section 4.1.4.2) with 16 treatments (rows) and two replicates (columns), the error variation may be found by subtraction.

$$SST = \sum_{i=1}^{16}\sum_{j=1}^{2} x_{ij}^2 - T_{..}^2/2.16$$

$$= (87,94)^2 + (88,86)^2 + \ldots + (86,73)^2 + (86,89)^2 - 2806,79)^2/32$$

$$= 23,82$$

$$SS_{Treatments} = \sum_{i=1}^{16} T_{i.}^2/2 - T_{..}^2/32$$

$$= [(176,05)^2 + \ldots + (176,05)^2]/2 - (2806,79)^2/32$$

$$= 12,17$$

$$SS_{Replicates} = \sum_{j=1}^{2} T_{.j}^2/16 - T_{..}^2/32$$

$$= [(1402,54)^2 + (1404,25)^2]/16 - (2806,79)^2/32$$

$$= 0,09$$

$$SSE = SST - SS_{Treatments} - SS_{Replicates}$$

$$= 23,82 - 12,17 - 0,09$$

$$= 11,56$$

Next, as in the case of non-replicated 2-level factorial designs, the contribution of the factorial effects to the $SS_{Treatments}$ is obtained from the effect totals by use of the following generalized expression:

$$SS = [\text{Effect Total}]^2/2^n r$$

whereas the factorial effects are obtained from the effect totals as:

$$\text{Effect} = [\text{Effect Total}]/2^{n-1} r$$

To obtain the factorial effect totals, the method outlined in Table 4.11 may be used. In the case of replicated designs, however, the responses observed for the various treatment combinations are added, as shown in the treatment total column (Table 4.13) before the method of Yates can be used to calculate the effect totals.

Table 4.14 shows the analysis of variance table for the experiment, the effect totals calculated for the factors and their interactions are included in the second column of the table.

TABLE 4.14: REPLICATED 2^4 FACTORIAL - ANALYSIS OF VARIANCE - EFFECT OF CASTING SOLUTION COMPONENTS ON THE LINEAR SHRINKAGE OF SUBSTRATE MEMBRANES

Variation Source	Effect totals	SS	df	MSS	F-ratio	Level
Main Effects						
A	9,93	3,081	1	3,081	4,00	10%
B	3,57	0,398	1	0,398	<1	
C	-2,53	0,200	1	0,200	<1	
D	-13,89	6,029	1	6,029	7,83	5%
Two-factor interactions						
AB	-1,45	0,066	1	0,066	<1	
AC	-1,19	0,044	1	0,044	<1	
AD	2,69	0,226	1	0,226	<1	
BC	0,01	0,000	1	0,000	<1	
BD	0,45	0,006	1	0,006	<1	
CD	6,11	1,167	1	1,167	1,52	
Three-factor interactions						
ABC	2,55	0,203	1	0,203	<1	
ABD	1,19	0,044	1	0,044	<1	
ACD	-2,71	0,230	1	0,230	<1	
BCD	1,89	0,112	1	0,112	<1	
Four-factor interactions						
ABCD	3,39	0,359	1	0,359	<1	
Treatment total		12,17	15			
Replicates		0,09	1	0,090	<1	
Residual Error		11,56	15	0,771		
Total		23,82	31			

TABLE 4.15: GENERAL FORM OF THE ANALYSIS OF VARIANCE TABLE FOR A 2^n FACTORIAL WITH REPLICATES

Variation Source	Variation SS	df	Total df	Variance MSS	F-ratio
Main Factors					
A		1			
B		1			
.		.	n		
.		.			
.		.			
Two-factor Interactions					
AB		1			
AC		1			
.		.	n(n - 1)/2		
.		.			
.		.			
Three-factor Interactions					
ABC		1			
ABD		1			
.		.	n(n - 1)(n - 2)/6		
.		.			
.		.			
k-factor Interactions					
.		1			
.		.	n(n - 1)...(n - k - 1)/k!		
.		.			
$SS_{Treatments}$			$2^n - 1$		
$SS_{Replicates}$			r - 1		
SSE			$(r - 1)(2^n - 1)$		
SST			$(r2^n - 1)$		

The critical value $F(1,15)_{0,1} = 3,07$ and $F(1,15)_{0,05} = 4,54$. The effect of factor A is therefore barely significant (10% level), whereas the effect of factor D is significant at the 5% level.

In general, the analysis of variance table for a 2^n complete factorial, with r replicates, assumes the form shown in Table 4.15

4.3 2-LEVEL FACTORIAL DESIGNS, BLOCK AND FRACTIONAL REPLICATION

4.3.1 CONFOUNDING - BLOCKS

It is very often not possible to conduct a complete factorial experiment under uniform conditions. In such cases the factorial should be divided up into smaller experimental units, called blocks, within which uniform experimental conditions can be maintained.

This is accomplished by a process referred to as 'confounding', which Davies *(31)* defines as the process by which unimportant comparisons are deliberately confused for the purpose of assessing the more important comparisons with greater precision. In other words, interaction effects unlikely to be important (*i.e.* higher-order interactions) are confounded in order that the factorial can be subdivided, rather than to sacrifice information on, say, two-factor interactions which are more likely to be important.

Consider a 2^3 factorial and suppose that the eight treatment combinations that constitute the design are to be divided into two blocks, allocating four treatment combinations to each of the blocks. One possible allocation of the treatment combinations to the two blocks are shown below.

Furthermore, because of non-uniformity in experimental conditions which exists between the two blocks, the observed values in Block II are increased by a quantity, say, x.

Block I	Block II
I	*abc*
ab	*a*
ac	*b*
bc	*c*

Block I	Block II
I	*abc* + *x*
ab	*a* + *x*
ac	*b* + *x*
bc	*c* + *x*

The block effect total is obtained as follows for the second case presented:

$$\begin{aligned}\text{Block effect total} &= [(abc + x) + (a + x) + (b + x) + (c + x)] \\ &\quad - [I + ab + ac + bc] \\ &= [abc + a + b + c - I - ab - ac - bc] + 4x\end{aligned}$$

Comparison of the signs of the treatments of a complete unconfounded 2^3 design with those of the ABC interaction (refer Table 4.10), shows that the block-effect total contains the ABC-effect total in addition to the quantity 4x, thus;

$$\text{Block - effect total} = (\text{ABC - effect total}) + 4x$$

The ABC-interaction effect is therefore completely confounded with the block effect, and the effect of the ABC interaction cannot be determined independently of the block effect.

The main effects of factors A, B and C, as well as the other interaction effects can be determined independently since they are not confounded with the block effect. Consider the linear combination of treatment totals used in the calculation of the AB interaction effect total. The AB interaction effect total, in the case of a complete, unconfounded design, is calculated as:

$$\begin{aligned}\text{AB effect total} &= (a - 1)(b - 1)(c + 1) \\ &= (ab - b - a + 1)(c + 1) \\ &= (abc - bc - ac + c + ab - b - a + I)\end{aligned}$$

and in the case of the example where block confounding has been introduced, the linear combination of treatment totals to obtain the AB effect total is:

$$\begin{aligned}\text{AB effect total} &= [(abc + x) + (c + x) + ab + I] - [(bc + ac + (b + x) \\ &\quad + (a + x)] \\ &= (abc - bc - ac + c + ab - b - a + I)\end{aligned}$$

The block effect cancels out in the second case (the two linear combinations of treatment totals are the same) and the AB interaction effect is therefore free of block effects. This applies equally to the main effects A, B, C, as well as to the remainder of the two-factor interaction effects. These interactions are therefore orthogonal to block effects.

In the case of the example, the ABC interaction (or any other interaction(s) chosen to be confounded with the block effect(s)), is called the defining contrast.

(By partial confounding *(32)(33)* some information on confounded interactions may be recovered if the experiment is replicated. This is achieved by confounding one interaction in the first replicate and another in the second, partly recovering lost information).

4.3.2 DEFINING CONTRASTS

In general, if a 2^n factorial is to be sub-divided into 2^p blocks, a set of $(2^p - 1)$ defining contrasts must be obtained. Of these, p may be chosen as generators (provided they are independent), while the remaining $(2^p - 1 - p)$ are obtained as a consequence *(34)(35)*.

Independence is ensured if the "generalized interaction" *(36)* of the chosen p generators is not the product of any two in the group. Factorial effects may be treated as a finite multiplication group *(34)* and the n factors of a 2^n factorial regarded as generators. Forming all possible products of the n generators, A, B, C, ... subject to $A^2 = B^2 = C^2 = ... = I$, the following elements of a 2^3 factorial are obtained:

I, A, B, C, AB, AC, BC, ABC

	Elements of the group	How obtained
Generators	A, B, C	
Products two at a time	AB	A x B = AB
	AC	A x C = AC
	BC	B x C = BC
Products three at a time	ABC	A x B x C = ABC
Any element with itself	I	A x A = I

The procedure is applied in the same way to obtain the set of defining contrasts in any system of confounding, by first choosing the p generators and obtaining the remaining $(2^p - 1 - p)$ factorial effects (which are also confounded), as a result.

As an example, a 2^4 factorial design will be subdivided into four blocks with four treatment combinations in each block. As a start two $(2^2 = 4)$ generators must be selected, which will result in a third also being confounded.

The choice of the ABC and ABCD factorial effects as generators is obviously unsuitable since it implies that the main effect D $(= ABC \times ABCD = A^2B^2C^2D = D)$ is also confused with block effects and hence cannot be determined.

A better choice would be to choose ABD and ACD as generators; this will lead to the automatic confusion of a two-factor interaction (unavoidable in this case) with block effects.

	Elements of the group	How obtained
Generators	ABD, ACD	
Products two at a time	BC	ABD x ACD = BC
Unity	I	ABD x ABD = I

In this design the effect of the interaction BC cannot be assessed independently of block effects, which is an improvement on the earlier choice where a main effect could not be determined.

4.3.3 ORTHOGONALITY

Orthogonality ensures that all main and interaction effects can be estimated independently, without entanglement. Orthogonality is crucially important when it is decided which treatment combinations should be grouped together in the respective blocks. One approach which is used to ensure that the orthogonal character of the design is maintained will be illustrated in this section.

Any effect and treatment combination may be written in the following forms *(37)*:

$$A^p\ B^q\ C^r\ D^s \ldots \quad \text{and} \quad a^w\ b^x\ c^y\ d^z \ldots$$

where the exponents are restricted to 0 or 1. The treatment combination $a^w\ b^x\ c^y\ d^z$ is orthogonal to the effect $A^p\ B^q\ C^r\ D^s$ if the following equation is satisfied *(34)*:

$$L = pw + qx + ry + sz = 0 \ (\text{Modulo } 2)$$

and when this rule is applied in the example, the defining contrasts follow as:

$$I = A^p\ B^q\ D^s = A^p\ C^r\ D^s$$

and the blocks are derived by evaluating

$$L_1 = p + q + s \ (\text{Modulo } 2)$$
$$L_2 = p + r + s \ (\text{Modulo } 2)$$

The treatment combinations of the 2^4 factorial are given below in standard order, and are considered in turn in the light of the above two expressions:

	$A^pB^qD^s$ $L_1 = p+q+s$			$A^pC^rD^s$ $L_2 = p+r+s$		
I:	$L_1 = 0+0+0$	$= 0$	(Mod 2)	$L_2 = 0+0+0$	$= 0$	(Mod 2)
a:	$L_1 = 1+0+0$	$= 1$	(Mod 2)	$L_2 = 1+0+0$	$= 1$	(Mod 2)
b:	$L_1 = 0+1+0$	$= 1$	(Mod 2)	$L_2 = 0+0+0$	$= 0$	(Mod 2)
ab:	$L_1 = 1+1+0$	$= 2 = 0$	(Mod 2)	$L_2 = 1+0+0$	$= 1$	(Mod 2)
c:	$L_1 = 0+0+0$	$= 0$	(Mod 2)	$L_2 = 0+1+0$	$= 1$	(Mod 2)
ac:	$L_1 = 1+0+0$	$= 1$	(Mod 2)	$L_2 = 1+1+0$	$= 2 = 0$	(Mod 2)
bc:	$L_1 = 0+1+0$	$= 1$	(Mod 2)	$L_2 = 0+1+0$	$= 1$	(Mod 2)
abc:	$L_1 = 1+1+0$	$= 2 = 0$	(Mod 2)	$L_2 = 1+1+0$	$= 2 = 0$	(Mod 2)
d:	$L_1 = 0+0+1$	$= 1$	(Mod 2)	$L_2 = 0+0+1$	$= 1$	(Mod 2)
ad:	$L_1 = 1+0+1$	$= 2 = 0$	(Mod 2)	$L_2 = 1+0+1$	$= 2 = 0$	(Mod 2)
bd:	$L_1 = 0+1+1$	$= 2 = 0$	(Mod 2)	$L_2 = 0+0+1$	$= 1$	(Mod 2)
abd:	$L_1 = 1+1+1$	$= 3 = 1$	(Mod 2)	$L_2 = 1+0+1$	$= 2 = 0$	(Mod 2)
cd:	$L_1 = 0+0+1$	$= 1$	(Mod 2)	$L_2 = 0+1+1$	$= 2 = 0$	(Mod 2)
acd:	$L_1 = 1+0+1$	$= 2 = 0$	(Mod 2)	$L_2 = 1+1+1$	$= 3 = 1$	(Mod 2)
bcd:	$L_1 = 0+1+1$	$= 2 = 0$	(Mod 2)	$L_2 = 0+1+1$	$= 2 = 0$	(Mod 2)
abcd:	$L_1 = 1+1+1$	$= 3 = 1$	(Mod 2)	$L_2 = 1+1+1$	$= 3 = 1$	(Mod 2)

and the blocks are derived by grouping the treatments as follows:

Block I	Block II	Block III	Block IV
$L_1 = 0$ $L_2 = 0$	$L_1 = 1$ $L_2 = 0$	$L_1 = 0$ $L_2 = 1$	$L_1 = 1$ $L_2 = 1$
I	*b*	*ab*	*a*
abc	*ac*	*c*	*bc*
ad	*abd*	*bd*	*d*
bcd	*cd*	*acd*	*abcd*

A further method of constructing the various blocks in a confounded system (*34*) revolves around the principal block which contains the identity I. The treatment combinations in this block may be found easily since they are all orthogonal to the group of defining contrasts, *i.e.* they have an even number of, or no, letters in common with the defining contrasts. (In the table above, $L_1 = 0, L_2 = 0$). The treatment combinations of the remainder of the blocks may be derived from the principal block if elements in the principal block are multiplied by elements not contained in the principal block or any other block already established. The procedure by which blocks II, III and IV are derived from the principal block is illustrated below:

Principal Block	Multiply by (say)	Resulting Treatment	Block Derived
I	*a*	*a*	
abc	*a*	*bc*	Block IV
ad	*a*	*d*	
bcd	*a*	*abcd*	
I	*b*	*b*	
abc	*b*	*ac*	Block II
ad	*b*	*abd*	
bcd	*b*	*cd*	
I	*ab*	*ab*	
abc	*ab*	*c*	Block III
ad	*ab*	*bd*	
bcd	*ab*	*acd*	
I	*bcd*	*bcd*	*Principal*
abc	*bcd*	*ad*	*Block,*
ad	*bcd*	*abc*	*Closed to*
bcd	*bcd*	*I*	*Multiplication*

4.3.4 CONFOUNDING - FRACTIONAL REPLICATION *(38)*

In membrane research one is very often faced with a bewildering array of factors, all of which must be investigated. Even when 2-level factorial designs are used, in which each factor is considered at two levels only, the practical impossibility of investigating all treatment combinations of say nine factors (512 experiments) or seven factors (128 experiments) are obvious in most situations.

However, the complete factorial can be reduced, by fractional replication, to a more manageable size still large enough to investigate the relative importance of the main effects and of some of their interactions. Should the need arise to analyze a larger number of interaction effects, the size of the designed experiment can be increased (doubled) by means of procedures indicated earlier.

The principles involved in designing and constructing a fractional factorial are the same as used in subdividing a complete factorial into blocks. When a factorial is subdivided into two blocks, each block will constitute a half-replicate of the complete factorial, if into four block, each block will constitute a quarter-replicate of the complete factorial, and so on. There is one difference though; in subdividing a factorial into blocks, interaction effects of higher order are confounded with block effects, whereas in a fractional replicated design, interactions are confounded with themselves. This gives rise to the so-called alias sets (see section 4.3.4.4).

The procedures followed in the construction of a fractional replicated design will be illustrated next by example of a $1/16^{th}$ replicate of a 2^9 factorial experiment (2^{9-4} factorial design), used for the simultaneous study of nine factors (see section 6.2.2.3).

4.3.4.1 Defining contrasts - fractional designs

The construction of a $1/16^{th}$ replicate of a 2^9 factorial is equivalent to dividing the complete factorial into 2^p ($2^4 = 16$) blocks of 2^{n-p} ($2^{9-4} = 32$) treatment combinations each. The group of defining contrasts will comprise $2^p - 1$ ($2^4 - 1 = 15$) elements of which p (= 4) are the generators and $2^p - p - 1$ (= 11) are determined as a consequence. Any of the 16 blocks derived may be used for experimentation, and the principal block may be obtained by multiplying the elements in the block in turn by any other element within the same block.

The single most important aspect of constructing a fractional replicate is the choice of which interactions to use as generators for the group of defining contrasts, since this choice affects the alias structure, *i.e.* which effects are confounded with each other. It is therefore important that the comparisons for main effects do not include other main effects or two-factor interactions, and *vice versa*, in their alias structure. The underlying assumption in designing the defining contrasts are that three- and higher-factor interaction effects are negligible and that main effects and two-factor interaction effects should be confounded with those terms in order to make an estimate of the more important effects possible.

As before, none of the generators chosen must be the generalized product of any other two. The choice of the following four interactions as generators,

$$ABCD,\ ABEF,\ BCFHJ,\ ACEHJ$$

is therefore not correct since they are not independent. The product of two of these generators, *e.g.*:

$$ABEF \times BCFHJ = AB^2CEF^2HJ = ACEHJ$$

is already a member of the group.

After careful consideration, the following interactions were chosen as generators, and Table 4.16 shows how the remaining contrasts were obtained.

The complete group of defining contrasts is:

$$I = ABCD = ABEF = BCEG = EFGHJ = CDEF = ADEG = ABCDEFGHJ = ACFG = ABGHJ$$
$$= BCFHJ = BDFG = CDGHJ = ADFHJ = ACEHJ = BDEHJ$$

TABLE 4.16: DEFINING CONTRASTS FOR A 2^{9-4} FACTORIAL

	Elements of Group	How obtained
Generators:	ABCD, ABEF, BCEG, EFGHJ	
Product:	CDEF	ABCD x ABEF = CDEF
twos	ADEG	ABCD x BCEG = ADEG
	ABCDEFGHJ	ABCD x EFGHJ = ABCDEFGHJ
	ACFG	ABEF x BCEG = ACFG
	ABGHJ	ABEF x EFGHJ = ABGHJ
	BCFHJ	BCEG x EFGHJ = BCFHJ
Product:	BDFG	ABCD x ABEF x BCEG = BDFG
threes	CDGHJ	ABCD x ABEF x EFGHJ = CDGHJ
	ADFHJ	ABCD x BCEG x EFGHJ = ADFHJ
	ACEHJ	ABEF x BCEG x EFGHJ = ACEHJ
Product: fours	BDEHJ	ABCD x ABEF x BCEG x EFGHJ = BDEHJ
Identity	I	ABCD x ABCD = I

4.3.4.2 Construction of a fractional replicate

To construct the 16 blocks that constitute the complete replicate, the procedure illustrated earlier (section 4.3.3.) may be used, from which the defining contrasts follow as:

$$I = A^rB^sC^tD^u = A^rB^sE^vF^w = B^sC^tE^vG^x = E^vF^wG^xH^yJ^z$$

and the design is constructed by evaluating

$L_1 = r + s + t + u$ (Modulo 2)
$L_2 = r + s + v + w$ (Modulo 2)
$L_3 = s + t + v + x$ (Modulo 2)
$L_4 = v + w + x + y + z$ (Modulo 2)

with each treatment combination in turn, following which the treatment combinations are assigned to blocks according to the following scheme:

Block 1:	$L_1 = 0$,	$L_2 = 0$,	$L_3 = 0$,	$L_4 = 0$	Principal Block
Block 2:	$L_1 = 1$,	$L_2 = 0$,	$L_3 = 0$,	$L_4 = 0$	
Block 3:	$L_1 = 0$,	$L_2 = 1$,	$L_3 = 0$,	$L_4 = 0$	
Block 4:	$L_1 = 1$,	$L_2 = 1$,	$L_3 = 0$,	$L_4 = 0$	
Block 5:	$L_1 = 0$,	$L_2 = 0$,	$L_3 = 1$,	$L_4 = 0$	
Block 6:	$L_1 = 1$,	$L_2 = 0$,	$L_3 = 1$,	$L_4 = 0$	
Block 7:	$L_1 = 0$,	$L_2 = 1$,	$L_3 = 1$,	$L_4 = 0$	
Block 8:	$L_1 = 1$,	$L_2 = 1$,	$L_3 = 1$,	$L_4 = 0$	
Block 9:	$L_1 = 0$,	$L_2 = 0$,	$L_3 = 0$,	$L_4 = 1$	
Block 10:	$L_1 = 1$,	$L_2 = 0$,	$L_3 = 0$,	$L_4 = 1$	
Block 11:	$L_1 = 0$,	$L_2 = 1$,	$L_3 = 0$,	$L_4 = 1$	
Block 12:	$L_1 = 1$,	$L_2 = 1$,	$L_3 = 0$,	$L_4 = 1$	
Block 13:	$L_1 = 0$,	$L_2 = 0$,	$L_3 = 1$,	$L_4 = 1$	
Block 14:	$L_1 = 1$,	$L_2 = 0$,	$L_3 = 1$,	$L_4 = 1$	
Block 15:	$L_1 = 0$,	$L_2 = 1$,	$L_3 = 1$,	$L_4 = 1$	
Block 16:	$L_1 = 1$,	$L_2 = 1$,	$L_3 = 1$,	$L_4 = 1$	

Another method for constructing the various blocks according to the defining contrasts chosen, is to use a table of signs as shown in Table 4.10. In this approach the complete factorial is first divided into two blocks (obtaining two $^1/_2$ replicates), following which one of these blocks is again sub-divided into two blocks (two $^1/_4$ replicates) ... the process being repeated until two $1/16^{th}$ replicates are obtained. The method is simple: the sign in the interaction column beneath the defining contrast, say ABCD, is used to split the complete factorial into two blocks, effectively confounding the ABCD interaction. Those treatment combinations that have a "+" sign in the ABCD interaction-column are assigned to the one block and those that have a "-" sign to the other. The process is repeated in turn with the defining contrasts ABEF, BCEG and EFGHJ to obtain two $1/16^{th}$ replicates.

All the treatment combinations associated with a complete 2^9 factorial are listed in Table 4.17. Those treatment combinations that conform to a $1/16^{th}$ fractional replicate, defined by the above contrasts, are marked in Table 4.17 and summarized in Table 4.18.

TABLE 4.17: TREATMENT COMBINATIONS OF A COMPLETE 2^9 FACTORIAL

*I	g	h	gh	j	gj	*hj	ghj
a	ag	ah	agh	aj	agj	ahj	aghj
b	bg	bh	bgh	bj	bgj	bhj	bghj
ab	abg	abh	*abgh	abj	*abgj	abhj	abghj
c	cg	ch	cgh	cj	cgj	chj	cghj
ac	acg	ach	acgh	acj	acgj	achj	acghj
bc	bcg	bch	bcgh	bcj	bcgj	bchj	bcghj
abc	abcg	abch	abcgh	abcj	abcgj	abchj	abcghj
d	dg	dh	dgh	dj	dgj	dhj	dghj
ad	adg	adh	adgh	adj	adgj	adhj	adghj
bd	bdg	bdh	bdgh	bdj	bdgj	bdhj	bdghj
abd	abdg	abdh	abdgh	abdj	abdgj	abdhj	abdghj
cd	cdg	cdh	*cdgh	cdj	*cdgj	cdhj	cdghj
acd	acdg	acdh	acdgh	acdj	acdgj	acdhj	acdghj
bcd	bcdg	bcdh	bcdgh	bcdj	bcdgj	bcdhj	bcdghj
*abcd	abcdg	abcdh	abcdgh	abcdj	abcdgj	*abcdhj	abcdghj
e	eg	eh	egh	ej	egj	ehj	eghj
ae	aeg	aeh	aegh	aej	aegj	aehj	aeghj
be	beg	beh	begh	bej	begj	behj	beghj
abe	abeg	abeh	abegh	abej	abegj	abehj	abeghj
ce	ceg	ceh	cegh	cej	cegj	cehj	ceghj
ace	aceg	*aceh	acegh	*acej	acegj	acehj	aceghj
bce	*bceg	bceh	bcegh	bcej	bcegj	bcehj	*bceghj
abce	abceg	abceh	abcegh	abcej	abcegj	abcehj	abceghj
de	deg	deh	degh	dej	degj	dehj	deghj
ade	*adeg	adeh	adegh	adej	adegj	adehj	*adeghj
bde	bdeg	*bdeh	bdegh	*bdej	bdegj	bdehj	bdeghj
abde	abdeg	abdeh	abdegh	abdej	abdegj	abdehj	abdeghj
cde	cdeg	cdeh	cdegh	cdej	cdegj	cdehj	cdeghj
acde	acdeg	acdeh	acdegh	acdej	acdegj	acdehj	acdeghj
bcde	bcdeg	bcdeh	bcdegh	bcdej	bcdegj	bcdehj	bcdeghj
abcde	abcdeg	abcdeh	abcdegh	abcdej	abcdegj	abcdehj	abcdeghj
f	fg	fh	fgh	fj	fgj	fhj	fghj
af	afg	afh	afgh	afj	afgj	afhj	afghj
bf	bfg	bfh	bfgh	bfj	bfgj	bfhj	bfghj
abf	abfg	abfh	abfgh	abfj	abfgj	abfhj	abfghj
cf	cfg	cfh	cfgh	cfj	cfgj	cfhj	cfghj
acf	*acfg	acfh	acfgh	acfj	acfgj	acfhj	*acfghj
bcf	bcfg	*bcfh	bcfgh	*bcfj	bcfgj	bcfhj	bcfghj
abcf	abcfg	abcfh	abcfgh	abcfj	abcfgj	abcfhj	abcfghj
df	dfg	dfh	dfgh	dfj	dfgj	dfhj	dfghj
adf	adfg	*adfh	adfgh	*adfj	adfgj	adfhj	adfghj
bdf	*bdfg	bdfh	bdfgh	bdfj	bdfgj	bdfhj	*bdfghj
abdf	abdfg	abdfh	abdfgh	abdfj	abdfgj	abdfhj	abdfghj
cdf	cdfg	cdfh	cdfgh	cdfj	cdfgj	cdfhj	cdfghj
acdf	acdfg	acdfh	acdfgh	acdfj	acdfgj	acdfhj	acdfghj
bcdf	bcdfg	bcdfh	bcdfgh	bcdfj	bcdfgj	bcdfhj	bcdfghj
abcdf	abcdfg	abcdfh	abcdfgh	abcdfj	abcdfgj	abcdfhj	abcdfghj
ef	efg	efh	*efgh	efj	*efgj	efhj	efghj
aef	aefg	aefh	aefgh	aefj	aefgj	aefhj	aefghj
bef	befg	befh	befgh	befj	befgj	befhj	befghj
*abef	abefg	abefh	abefgh	abefj	abefgj	*abefhj	abefghj
cef	cefg	cefh	cefgh	cefj	cefgj	cefhj	cefghj
acef	acefg	acefh	acefgh	acefj	acefgj	acefhj	acefghj
bcef	bcefg	bcefh	bcefgh	bcefj	bcefgj	bcefhj	bcefghj
abcef	abcefg	abcefh	abcefgh	abcefj	abcefgj	abcefhj	abcefghj
def	defg	defh	defgh	defj	defgj	defhj	defghj
adef	adefg	adefh	adefgh	adefj	adefgj	adefhj	adefghj
bdef	bdefg	bedfh	bdefgh	bdefj	bdefgj	bdefhj	bdefghj
abdef	abdefg	abdefh	abdefgh	abdefj	abdefgj	abdefhj	abdefghj
*cdef	cdefg	cdefh	cdefgh	cdefj	cdefgj	*cdefhj	cdefghj
acdef	acdefg	acdefh	acdefgh	acdefj	acdefgj	acdefhj	acdefghj
bcdef	bcdefg	bcdefh	bcdefgh	bcdefj	bcdefgj	bcdefhj	bcdefghj
abcdef	abcdefg	abcdefh	*abcdefgh	abcdefj	*abcdefgj	abcdefhj	abcdefghj

TABLE 4.18: TREATMENT COMBINATIONS OF A 2^{9-4} FRACTIONAL REPLICATE

I	*abgh*	*abgj*	*hj*
abcd	*cdgh*	*cdgj*	*abcdhj*
bceg	*aceh*	*acej*	*bceghj*
adeg	*bdeh*	*bdej*	*adeghj*
acfg	*bcfh*	*bcfj*	*acfghj*
bdfg	*adfh*	*adfj*	*bdfghj*
abef	*efgh*	*efgj*	*abefhj*
cdef	*abcdefgh*	*abcdefgj*	*cdefhj*

TABLE 4.19: MODIFIED STANDARD ORDER, THE MEASURED EFFECTS AND ALIAS STRUCTURE OF THE 2^{9-4} FRACTIONAL REPLICATE

[1]	[2]	[3]	[4]
I		I	
a	abcd	*abcd*	A
f	cdef	*cd*	F
af	ab ef	*abef*	AF≡BE≡CG
g	bc e g	*bceg*	G
ag	a de g	*adeg*	AG≡DE≡CF
fg	b d fg	*bdfg*	FG≡AC≡BD
afg	a c fg	*acfg*	C
h	b de h	*bdeh*	H
ah	a c e h	*aceh*	AH
fh	bc f h	*bcfh*	FH
afh	a d f h	*adfh*	DJ
gh	cd gh	*cdgh*	GH
agh	ab gh	*abgh*	BJ
fgh	efgh	*efgh*	EJ
afgh	abcdefgh	*abcdefgh*	CH
j	b de j	*bdej*	J
aj	a c e j	*acej*	AJ
fj	bc f j	*bcfj*	FJ
afj	a d f j	*adfj*	DH
gj	cd g j	*cdgj*	GJ
agj	ab g j	*abgj*	BH
fgj	efg j	*efgj*	EH
afgj	abcdefg j	*abcdefgj*	CJ
hj	hj	*hj*	HJ
ahj	abcd hj	*abcdhj*	BG≡DF≡CE
fhj	cdef hj	*cdefhj*	EG≡AD≡BC
afhj	ab ef hj	*abefhj*	D
ghj	bc e ghj	*bceghj*	EF≡CD≡AB
aghj	a de ghj	*adeghj*	B
fghj	b d fghj	*bdfghj*	E
afghj	a c fghj	*acfghj*	AE≡BF≡DG

4.3.4.3 Effect totals, Yates's method

As a prerequisite for the calculation of effect totals and for determination of the alias structure, the treatment combinations listed in Table 4.18 must be reorganized into their standard order. Although apparently complicated, the procedure is quite simple.

For a 2^{n-p} fractional factorial (in this case, n = 9, p = 4), a modified standard order can be obtained by noting that the block chosen (any of the 16 blocks) contains a subset of n - p (= 5) letters which form a complete replicate of a 2^{n-p} (= 2^5) factorial. The modified standard order is then obtained by using only these letters at first, appending the remaining p (= 4) letters to obtain the treatment combinations required. In Table 4.19, column [1] shows the five chosen letters (a, f, g, h, j) arranged in standard order. Column [2] shows the treatment combinations of Table 4.18 with the letters corresponding to column [1] highlighted; the treatment combinations in column [3] are arranged according to this "modified" standard order.

4.3.4.4 Alias sets *(39)*

In a randomized complete factorial, each main and interaction effect can be determined independently with equal accuracy. In a design in which the factorial is subdivided into blocks, some of the interaction effects are confounded with block effects and consequently cannot be measured. In fractional replication, interaction effects are confounded with each other (its so-called aliases); the different comparisons therefore contain contributions of the effect to be assessed as well as its aliases.

The whole system of confounding is dependent on the defining contrasts, and effects confused with any given effect in fractional replication can be obtained by multiplying the defining contrasts by the given effect.

The comparisons arrived at by multiplying the defining contrasts in turn with main effects, and the various interactions, are called the alias sets. These comparisons measure the sums and differences of the aliases.

In a half-replicate each effect is confused with another (an alias pair); in a quarter-replicate the alias set comprises four effects, *etc.* In the case of the present example an alias set consists of 16 aliases.

The alias sets for the present example are easily determined. The sets are derived by multiplying the group of defining contrasts successively by the effects based on the letters (column [1] of Table 4.19), used to arrange the treatment combinations in "modified" standard order. By multiplying the defining contrasts in turn with the main effect A (second row in Table 4.19), for example, the following alias structure is obtained:

$$A \equiv AEFGHJ \equiv ACDGHJ \equiv BGHJ \equiv DFHJ \equiv ABCFHJ \equiv ABDEHJ \equiv CEHJ \equiv BCD \equiv BEF$$
$$\equiv ACDEF \equiv ABCEG \equiv DEG \equiv CFG \equiv ABDFG \equiv BCDEFGHJ$$

The AFG interaction (eighth row in the table), in turn has the alias set shown below. The main effect of factor C is measured by this comparison;

$$AFG \equiv AEHJ \equiv ACDFHJ \equiv BFHJ \equiv DGHJ \equiv ABCGHJ \equiv ABDEFGHJ \equiv CEFGHJ \equiv BCDFG \equiv BEG \equiv ACDEG \equiv ABCEF \equiv DEF \equiv C \equiv ABD \equiv BCDEHJ$$

In this 2^{9-4} factorial design, three-factor and higher-factor interaction effects are confounded with main effects. Two-factor interaction effects are also confounded with higher-order interactions, except those that are confounded amongst themselves. The latter effects can therefore not be determined independently as their effect totals are numerically equal. The AF interaction effect (fourth row in Table 4.19), which has the alias structure shown below, is one example:

$$AF \equiv AEGHJ \equiv ACDGFHJ \equiv BFGHJ \equiv DHJ \equiv ABCHJ \equiv ABDEFHJ \equiv CEFHJ \equiv BCDF \equiv BE \equiv ACDE \equiv ABCEFG \equiv DEFG \equiv CG \equiv ABDG \equiv BCDEGHJ$$

The last column in Table 4.19, column [4] shows the effect(s) regarded as measurable, on the assumption that three- and higher-order effects are negligible.

4.3.5 ANALYSIS OF VARIANCE

The analysis of variance of a fractional factorial is similar to that of a complete factorial, but for the existence of alias sets which can complicate a discussion of the results obtained.

Replication of a complete factorial, if time and man-power permit, is advisable, even if only from the point of view of the availability of a larger number of df for estimation of error variance. Replicating the same design in the case of a fractional factorial does not, however, have the same implication, especially if some of the two-factor interactions, confounded as in the present example, are significant. It would rather pay to repeat the other half of the replicate (*i.e.* when the two replicates are combined, a 2^{n-p+1} fractional replicate), in order to unconfound some of the two-factor interactions.

The approach used in the analysis of variance of a factorial confounded into blocks *(40)(41)* is in principle similar to the techniques used in the analysis of variance of a complete 2^n factorial. As previously, the sum-of-squares total [SST] is divided into its contributing entities, and with replication is:

$$SST = SS_{Blocks} + SS_{Treatments} + SS_{Replicates} + SSE$$

The SST and SS_{Blocks} are obtained in the usual manner. The SS_{Blocks} quantity is the sum contribution of all the unconfounded factorial effects and is obtained by any method previously identified. The SS of the confounded effects are not calculated as their SS contributions are already accounted for in the blocks sum of square [S_{Blocks}]. The SS_{Blocks} is calculated as if the experiment consisted of pr blocks, rather than p blocks in each of r replicates *(42)*. If there are replicates, the error variation [SSE] is found by subtraction; if there is no replication, the error variance (mean sum of errors, [MSE]) is found by pooling the SS of higher-order interactions, divided by their total df.

4.4 THE RESPONSE

4.4.1 INTRODUCTION

The most common way of presenting changes in the level of a dependent variable (y, response), to changes in the level of an independent variable (x), is by graphic illustration of the function;

$$Y = \phi(x_1, \ldots, x_n), \quad i = 1, \ldots, n.$$

If i = 1, and the data can be presented by a straight line, the response function is modelled by the relation;

$$Y = \alpha + \beta_1 x_1$$

If i = 1, and the data can be presented by a curve, the response function can be modelled by the relation;

$$Y = \alpha + \beta_1 x_1 + \beta_{11} x^2$$

Similarly, when i = 2, any combination of the two independent variables, x_1 and x_2, defines a response, y, perpendicular to the x_1x_2 plane. As one moves in the x_1, x_2 factor space, the response changes continuouly and the resulting response surface can be represented by a plane, Figure 4.4, if there is no interaction between the two variables, and the function can be modelled by;

$$Y = \beta_o + \beta_1 x_1 + \beta_2 x_2$$

The function takes the form of a twisted plane if the two variables interact (Figure 4.4) and the model of the function becomes;

$$Y = \beta_o + \beta_1 x_1 + \beta_2 x_2 + \beta_{12} x_1 x_2$$

Curvature of the response surface can be modelled by including quadratic terms in the model, as with the single variable. The function of the response surface, presented as a contour diagram in Figure 4.5, can be modelled by a regression model of the form;

$$Y = \beta_o + \beta_1 x_1 + \beta_2 x_2 + \beta_{12} x_1 x_2 + \beta_{11} x_1^2 + \beta_{22} x_2^2$$

When regression analysis is performed on data to obtain a regression equation, a suitable regression model must first be selected. In linear regression analysis, the empirical model below is useful;

$$\beta_o + {}^{n}\Sigma_{i=1}\beta_i x_i + {}^{n}\Sigma_{j=i+1}{}^{n}\Sigma_{i=1}\beta_{ij} x_i x_j + {}^{n}\Sigma_{k=j+1}{}^{n}\Sigma_{j=j+1}{}^{n}\Sigma_{i=1}\beta_{ijk} x_i x_j x_k + \ldots + {}^{n}\Sigma_{i=1}\beta_{ii} x_{ii}^2$$

since it can be interpreted as a Taylor series expansion of the true response about the points $x_i = 0$, i = 1,...n.

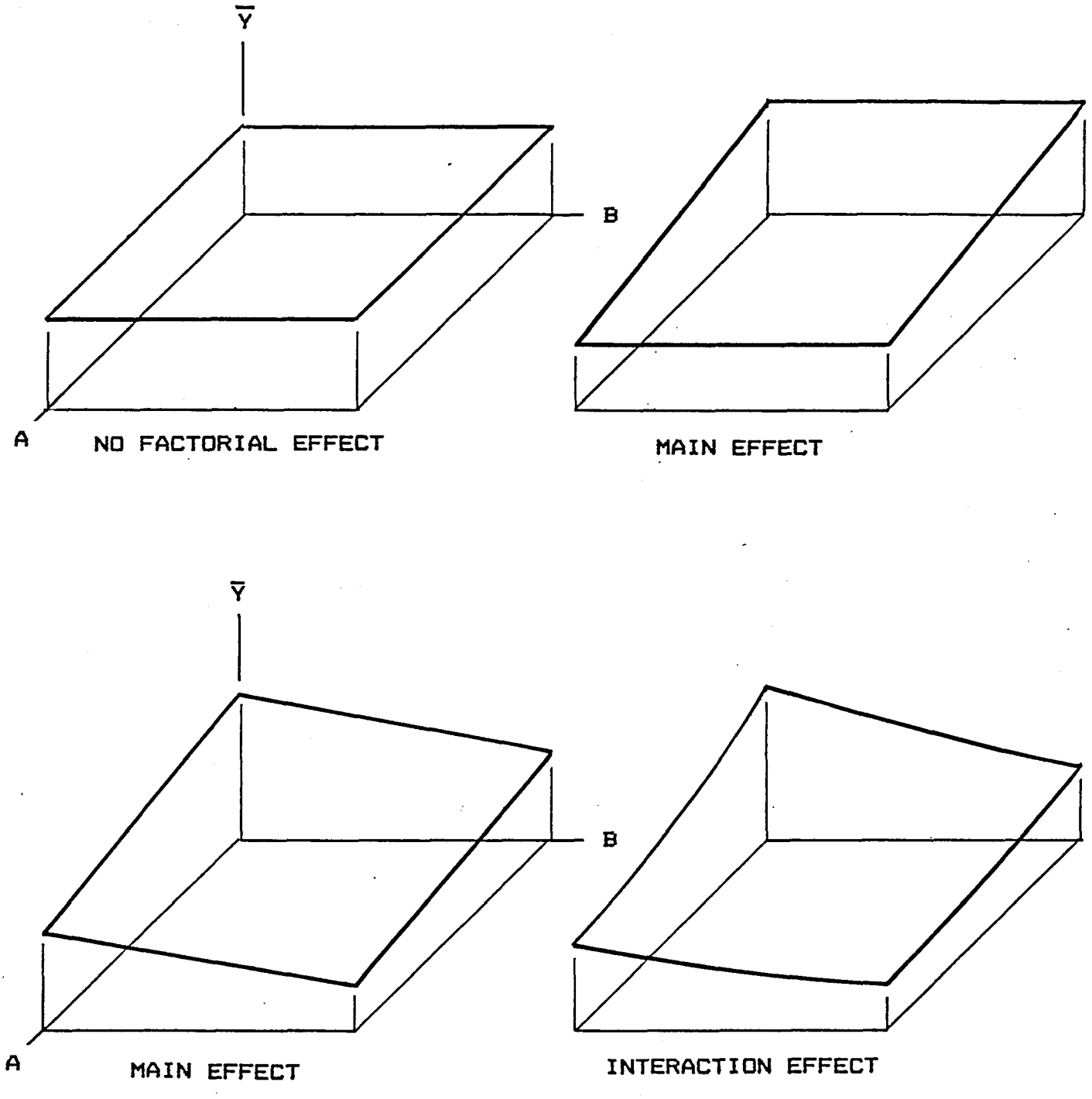

FIGURE 4.4: RESPONSE SURFACE IN THE EXPERIMENTAL REGION OF TWO FACTORS

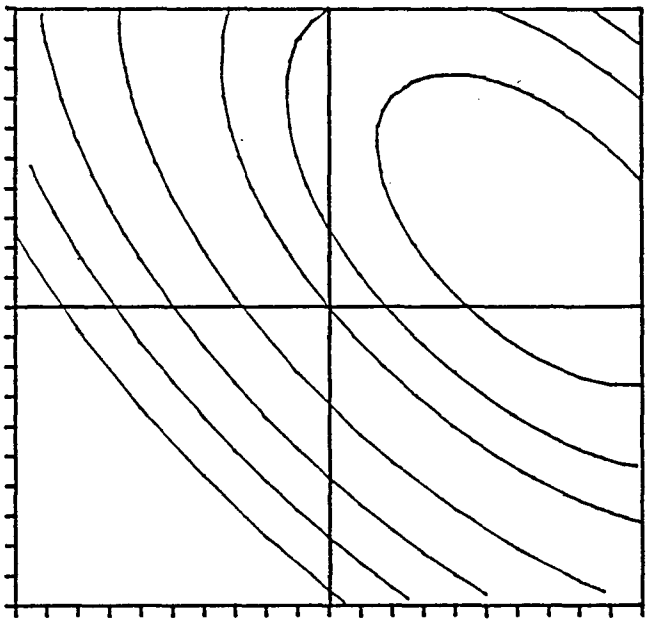

FIGURE 4.5: CONTOUR DIAGRAM OF THE RESPONSE SURFACE AT THE OPTIMUM

In a situation involving three factors, the factor space of a 2^3 factorial can be represented geometrically by a cube, Figure 4.6. The centre of the design has the co-ordinates (0,0,0), and the 8 experiments that constitute the design are conducted at the corners of the regular geometric figure.

Regression analysis can play an important role in the optimization procedure, since it allows the use of numerical techniques to determine the combination of factor levels (variables) that yield the "best" response. It is particularly useful when responses observed are inversely related, as with the rate of salt and water transport through a CA RO membrane.

The 2-level factorial approach used in experimental design simplifies multi-variable linear regression analysis calculations; the results are mathematically and numerically equivalent to those obtained on a main-frame computer with a multiple linear-regression analysis program such as SSPS *(43)*. Unfortunately, as the 2-level design considers the factors at only two levels, the quadratic term in the model given earlier cannot be estimated. The universally true response can be therefore approximated by means of a plane or twisted plane surface, due to the inclusion of only the main and first-order interaction terms. However, the 2-level factorial design is augmented by additional experimental points (2n + 1 more experiments), the so-called composite designs, which allow the inclusion of quadratic terms into the model and thus modelling of curvature.

4.4.2 REGRESSION ANALYSIS *(44)*

4.4.2.1 Linear regression

A straight line, $y = a + bx$, describes the linear relationship between the dependent (random) variable, y, and the independent variable (not random) x; the mean of the distribution of the y's, for any given x, Y, is given by the regression model;

$$Y = \alpha + \beta x$$

where α and β must be estimated from n sets of data points, (x_i, y_i), i = 1,...,n. If the estimates of α and β are denoted by 'a' and 'b' in the regression line, the estimated response, y^*, is obtained:

$$y^* = a + bx$$

For each pair of the data points, the following relation is satisfied:

$$y_i = a + bx_i + \epsilon_i$$

where ϵ_i is the residual that must be minimized, as can be seen in the following illustration.

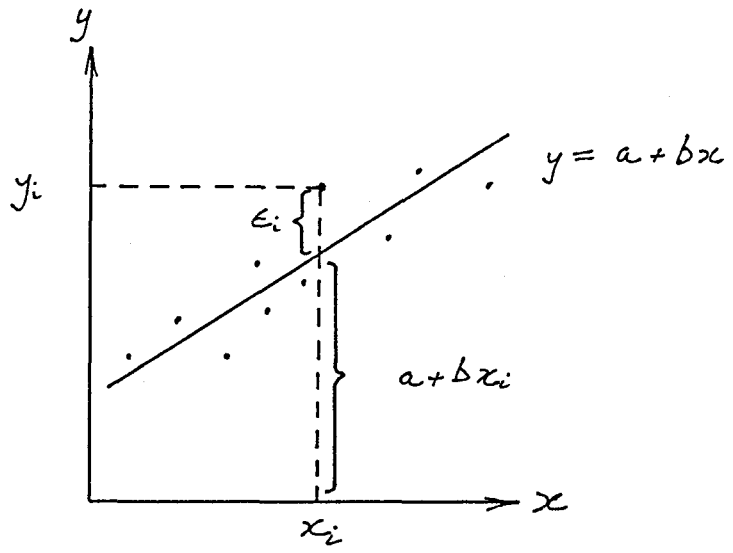

The method by which the residuals are minimized to estimate 'a' and 'b', is called the method of least squares. The sum of squares of the deviations of the observed values from the regression line;

$$SSE = \Sigma \epsilon_i^2 = \Sigma[y_i - (a + bx_i)]^2$$

is differentiated with respect to 'a' and 'b' and the partial derivatives are set equal to zero;

$$\frac{\partial(SSE)}{\partial a} = 0, \qquad \frac{\partial(SSE)}{\partial b} = 0$$

Solution and rearrangement of the two equations, give the two so-called normal equations:

$$na + b\Sigma x_i^2 = \Sigma y_i$$

which is equivalent to:

$$a + b\bar{x} = \bar{y},$$

and:

$$a\Sigma x_i + b\Sigma x_i^2 = \Sigma x_i y_i$$

The latter two equations are rewritten to obtain the estimated regression coefficient, b, of y upon x, as a ratio of the sum of products of the deviations of the x's and y's from their respective means, to the sum of squares of the x's about their means;

$$b = \Sigma(x - \bar{x})(y - \bar{y})/\Sigma(x - \bar{x})^2$$

In general, for computation of 'a' and 'b', the following two equations are used;

$$b = \frac{n\Sigma xy - \Sigma x\Sigma y}{n\Sigma x^2 - \Sigma x}$$

$$a + b\bar{x} = \bar{y}$$

4.4.2.2 Multiple linear regression *(45)*

In a situation where more than one independent variable is investigated, a multiple regression model is needed. If there are n independent variables, x_i, i = 1,...,n, the mean of Y is given by the multiple linear regression model:

$$Y = \beta_o + \beta_1 x_1 + \ldots + \beta_n x_n$$

and the estimated response is obtained from the sample regression equation;

$$y^* = b_o + b_1 x_1 + \ldots + b_n x_n$$

where each regression coefficient β_i is estimated by b_i from the data, by the method of least sum-of-squares (one of the regression methods *(46)* which can be used).

If the plane, supported by the above model, is to be fitted to the experimental data generated from n independent variables,

$$(x_{1i}, x_{2i}, \ldots, x_{ni}, y_i), \; i = 1, \ldots, k, \; k > n$$

where y_i is the observed response corresponding to the independent variables x_{ji}, j = 1,..., n, i = 1,..., k, each observation satisfies the equation;

$$Y_i = \beta_o + \beta_1 x_{1i} + \ldots + \beta_n x_{ni} + E_i$$
$$y_i = b_o + b_1 x_{1i} + \ldots + b_n x_{ni} + \epsilon_i$$

where E_i is the random error and ϵ_i is the residual of the response y_i. As before, the SS of the residual;

$$SSE = \Sigma \epsilon_i^2 = \Sigma [y_i - (b_o + b_1 x_{1i} + \ldots + b_n x_{ni})]^2$$

is minimized by partial differentiation with respect to b_i.

By equating to zero, the set of n + 1 normal equations is generated, which for n = 2 independent variables, are:

$$\begin{aligned} nb_o &+ b_1 \Sigma x_{1i} &+ b_2 \Sigma x_{2i} &= \Sigma y_i \\ b_o \Sigma x_{1i} &+ b_1 \Sigma x_{1i}^2 &+ b_2 \Sigma x_{1i} x_{2i} &= \Sigma x_{1i} y_i \\ b_o \Sigma x_{2i} &+ b_1 \Sigma x_{1i} x_{2i} &+ b_2 \Sigma x_{2i}^2 &= \Sigma x_{2i} y_i \end{aligned}$$

By solving these equations for b_o, b_1, and b_2, the estimates of the regression coefficients, β_o, β_1 and β_2 are obtained.

The same procedure is followed to obtain the normal equations for any other linear regression model postulated. For example, to determine the normal equations for a quadratic regression model, the Taylor series:

$$\beta_o + {}^{n}\Sigma_{i=1}\beta_i x_i + {}^{n}\Sigma_{j=i+1}{}^{n}\Sigma_{i=1}\beta_{ij} x_i x_j + {}^{n}\Sigma_{k=j+1}{}^{n}\Sigma_{j=j+1}{}^{n}\Sigma_{i=1}\beta_{ijk} x_i x_j x_k + \ldots + {}^{n}\Sigma_{i=1}\beta_{ii} x_{ii}{}^{2}$$

for two independent variables (x_1, x_2), where Y_i, i = 1,...,n is the response to independent variable combinations (x_{1i}, x_{2i}), reduces to;

$$Y_i = \beta_o + \beta_1 x_{1i} + \beta_2 x_{2i} + \beta_{12} x_{1i} x_{2i} + \beta_{11} x_{1i}{}^{2} + \beta_{22} x_{2i}{}^{2} + E_i$$

The least-squares normal equations are shown below, and the estimates of the coefficients, b_i, can be solved for by matrix inversion *(47)*. Since there are six parameters to estimate, n must be at least equal to six, and as quadratic terms are included for both variables, at least three levels must be tested for each variable.

$$b_o n + b_1 \Sigma x_{1i} + b_2 \Sigma x_{2i} + b_{11} \Sigma x_{1i}{}^{2} + b_{22} \Sigma x_{2i}{}^{2} + b_{12} \Sigma x_{1i} x_{2i} = \Sigma y_i$$

$$b_o \Sigma x_{1i} + b_1 \Sigma x_{1i}{}^{2} + b_2 \Sigma x_{1i} x_{2i} + b_{11} \Sigma x_{1i}{}^{3} + b_{22} \Sigma x_{1i} x_{2i}{}^{2} + b_{12} \Sigma x_{1i}{}^{2} x_{2i} = \Sigma x_{1i} y_i$$

$$b_o \Sigma x_{2i} + b_1 \Sigma x_{1i} x_{2i} + b_2 \Sigma x_{2i}{}^{2} + b_{11} \Sigma x_{1i}{}^{2} x_{2i} + b_{22} \Sigma x_{2i}{}^{3} + b_{12} \Sigma x_{1i} x_{2i}{}^{2} = \Sigma x_{2i} y_i$$

$$b_o \Sigma x_{1i}{}^{2} + b_1 \Sigma x_{1i}{}^{3} + b_2 \Sigma x_{1i}{}^{2} x_{2i} + b_{11} \Sigma x_{1i}{}^{4} + b_{22} \Sigma x_{1i}{}^{2} x_{2i}{}^{2} + b_{12} \Sigma x_{1i}{}^{3} x_{2i} = \Sigma x_{1i}{}^{2} y_i$$

$$b_o \Sigma x_{2i}{}^{2} + b_1 \Sigma x_{1i} x_{2i}{}^{2} + b_2 \Sigma x_{2i}{}^{3} + b_{11} \Sigma x_{1i}{}^{2} x_{2i}{}^{2} + b_{22} \Sigma x_{2i}{}^{4} + b_{12} \Sigma x_{1i} x_{2i}{}^{3} = \Sigma x_{2i}{}^{2} y_i$$

$$b_o \Sigma x_{1i} x_{2i} + b_1 \Sigma x_{1i}{}^{2} x_{2i} + b_2 \Sigma x_{1i} x_{2i}{}^{2} + b_{11} \Sigma x_{1i}{}^{3} x_{2i} + b_{22} \Sigma x_{1i} x_{2i}{}^{3} + b_{12} \Sigma x_{1i}{}^{2} x_{2i}{}^{2} = \Sigma x_{1i} x_{2i} y_i$$

The coefficients b_i can be determined through matrix inversion.

4.4.3 MULTIPLE LINEAR REGRESSION, 2-LEVEL FACTORIAL *(48)(49)*

4.4.3.1 First-order terms, 2^3 factorial

Fitting a first-order regression model

$$\beta_o + {}^{n}\Sigma_{i=1}\beta_i x_i + {}^{n}\Sigma_{j=i+1}{}^{n}\Sigma_{i=1}\beta_{ij} x_i x_j + {}^{n}\Sigma_{k=j+1}{}^{n}\Sigma_{j=j+1}{}^{n}\Sigma_{i=1}\beta_{ijk} x_i x_j x_k$$

to data originating from factorial designs is a simple process. The least-squares estimates of the constants in the normal equations are orthogonal linear functions of the observations, and because of this, each coefficient may be calculated separately as if the constant were the only one estimated from the data. Each estimate b_i is then given by the sum of the products of the observations (*y*'s) with the elements of the appropriate independent variable *x*, divided by the sum of squares of the elements of this independent variable, so that, in general,

$$b = \Sigma xy / \Sigma x^2$$

If the situation is considered for a complete 2^n factorial, the contrast sums (a routine calculation as part of the analysis of variance), divided by 2^n, gives the estimate of the respective coefficients.

Consider a 2^3 factorial, to which a second-order regression model of the form below is to be fitted;

$$Y = \beta_o x_o + \beta_1 x_1 + \beta_2 x_2 + \beta_3 x_3 + \beta_{12} x_1 x_2 + \beta_{13} x_1 x_3 + \beta_{23} x_2 x_3 + \beta_{11} x_1^2 + \beta_{22} x_2^2 + \beta_{33} x_3^3$$

(The dummy variable x_o is introduced as a matter of convenience and is set equal to unity, $\beta_o = \beta_o x_o$).

Table 4.20 lists the values of the independent variables, interactions and the responses obtained from a 2^3 factorial experiment.

By applying the formula given earlier, the estimators (b_i) of the coefficients (β_i) are obtained;

$$b_o = (1.y_1 + 1.y_2 + 1.y_3 + 1.y_4 + 1.y_5 + 1.y_6 + 1.y_7 + 1.y_8)/8 = \bar{y}$$

$$b_1 = (-1.y_1 + 1.y_2 - 1.y_3 + 1.y_4 - 1.y_5 + 1.y_6 - 1.y_7 + 1.y_8)/8$$

etc.

However, as only eight experiments (2^3) had been conducted, no more than eight coefficients could be estimated. From Table 4.20 it is evident that columns 5, 6, 7 and 1 are identical, so that;

$$b_o \longrightarrow \beta_o + \beta_{11} + \beta_{22} + \beta_{33}$$

where the arrow indicates that bo is an estimate of the quantity on the right *(8)*. This implies that b_o can be an unbiased estimate of β_o only if β_{11}, β_{22} and β_{33} are zero, *i.e.* that the response surface is a plane or twisted plane and that $\bar{y} = b_o$, the value of the response at the centre of the design. Curvature of the response surface will result in the mean of the responses being either an over- or an underestimate of the response at the centre of the design.

4.4.3.2 Second-order terms - 2^3 factorial

As was seen in the previous section, the 2-level factorial, where each factor is evaluated at two levels only, does not provide for the estimation of second-order coefficients. Each factor must be tested at at least three points to ensure an unbiased estimate of β_{11}, β_{22} and β_{33} and to allow curvature of the response surface to be modelled.

An extension of the 2-level factorial, the so-called rotatable composite design (*8*), provides the necessary complementary experimental points to allow a separate estimation of second-order coefficients to be made for incorporation into the first-order regression model.

These additional (2n+1) experiments, are conducted in pairs along the co-ordinate axis, x_1, x_2 and x_3 and at distances $\pm\sqrt{\alpha_i}$ away from the centre of the design. One further experiment is conducted at the centre of the design. Figure 4.7 is a geometrical illustration of the so-called star-points of the composite design of a 2^3 factorial.

The co-ordinates of the design are illustrated in Table 4.21, and suggested values for the star-points *(50)(51)*, α_i, are shown in Table 4.22.

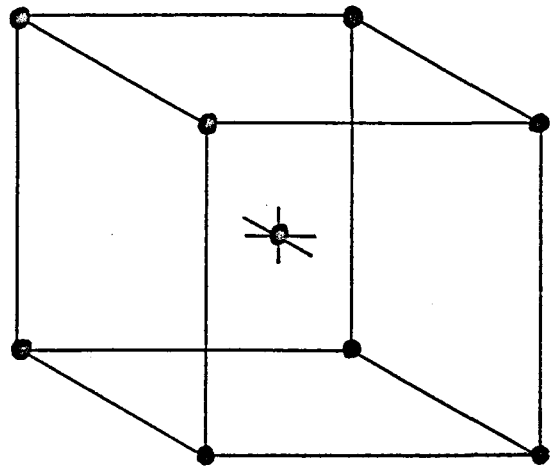

FIGURE 4.6: EXPERIMENTAL REGION OF A 2^3 FACTORIAL, EXPERIMENTS CONDUCTED AT THE CORNERS

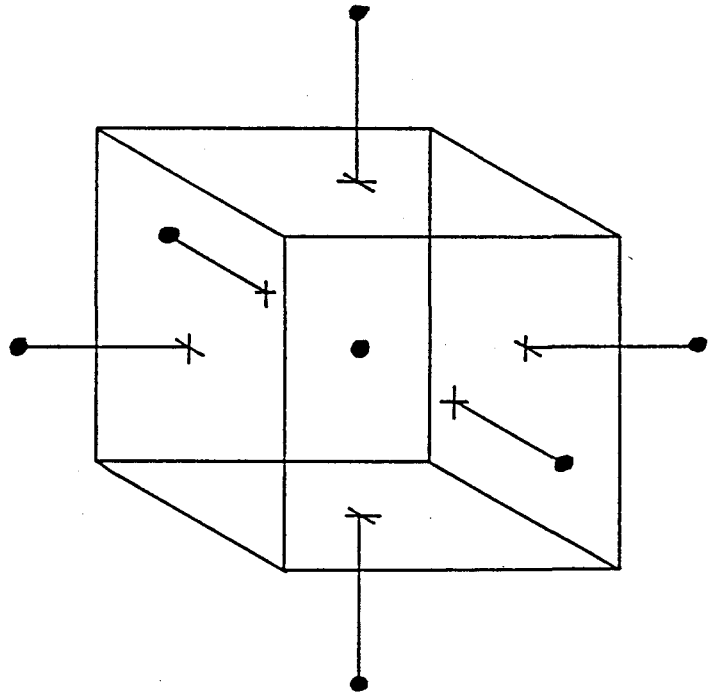

FIGURE 4.7: EXPERIMENTAL REGION OF THE ROTATABLE COMPOSITE DESIGN - 2^3 FACTORIAL

TABLE 4.20: THREE-FACTOR DESIGN

	[1]	[2]	[3]	[4]	[5]	[6]	[7]					Response
Trial	x_o	x_1	x_2	x_3	x_1^2	x_2^2	x_3^2	x_{12}	x_{13}	x_{23}	x_{123}	y
1	1	-1	-1	-1	1	1	1	1	1	1	-1	y_1
2	1	1	-1	-1	1	1	1	-1	-1	1	1	y_2
3	1	-1	1	-1	1	1	1	-1	1	-1	1	y_3
4	1	1	1	-1	1	1	1	1	-1	-1	-1	y_4
5	1	-1	-1	1	1	1	1	1	-1	-1	1	y_5
6	1	1	-1	1	1	1	1	-1	1	-1	-1	y_6
7	1	-1	1	1	1	1	1	-1	-1	1	-1	y_7
8	1	1	1	1	1	1	1	1	1	1	1	y_8
Σx	8	0	0	0	8	8	8	0	0	0	0	
Σx^2	8	8	8	8	8	8	8	8	8	8	8	

TABLE 4.21: COMPOSITE DESIGN - 2^3 FACTORIAL

Factor level		
x_1	x_2	x_3
0	0	0
$-\alpha_1$	0	0
α_1	0	0
0	$-\alpha_2$	0
0	α_2	0
0	0	$-\alpha_3$
0	0	α_3

TABLE 4.22: COMPOSITE ROTATABLE DESIGNS, STAR-POINT CO-ORDINATES

No of factors	No of experiments		Value of α	
n	2^n factorial	Star	Davies	Cochran
2	$2^2 = 4$	4+1	1,0	
3	$2^3 = 8$	6+1	1,215	1,682
4	$2^4 = 16$	8+1	1,414	2,000
5	$2^5 = 32$	10+1	1,547	2,000
6	$2^6 = 64$	12+1		2,378

Consider again the second-order regression model:

$$Y = \beta_o x_o + \beta_1 x_1 + \beta_2 x_2 + \beta_3 x_3 + \beta_{12} x_1 x_2 + \beta_{13} x_1 x_3 + \beta_{23} x_2 x_3 + \beta_{11} x_1^2 + \beta_{22} x_2^2 + \beta_{33} x_3^3$$

As is seen from Table 4.20, the sum of each of the independent variables, x_1, ...,x_1x_2, ...,$x_1x_2x_3$ is zero over the points of the design. In order to estimate the second-order coefficients, the regression model above is modified slightly;

$$Y = \beta_o' x_o + \beta_1 x_1 + \beta_2 x_2 + \beta_3 x_3 + \beta_{12} x_1 x_2 + \beta_{13} x_1 x_3 + \beta_{23} x_2 x_3 + \beta_{11} x_{11} + \beta_{22} x_{22} + \beta_{33} x_{33}$$

where $$x_{11} = x_{12} - \Sigma x_{12}/n \text{ } etc.$$

and β_o' is not estimated directly, but by means of the relation;

$$b_o = \bar{y} - b_{11}\Sigma x_1^2/n - b_{22}\Sigma x_2^2/n - b_{33}\Sigma x_3^2/n$$

As before, the estimates of the first-order main and interaction effects can be estimated as before, simply by taking the sums of the products of the responses with the elements of the appropriate independent variable and dividing by the sum of squares of the elements of the independent variable. To obtain the coefficients of the second-order effects, a set of four linear equations is obtained, the solution of which gives the estimates, b_o, b_{11}, b_{22}, and b_{33}. (In general, for k independent variables, k+1 equations *(50)(51)* need to be solved to obtain the estimates b_o, b_{11}, ...,b_{kk}).

In the example, the four equations are;

$$\begin{aligned}
C_{oo}\ b_o + C_{11o}\ b_{11} + C_{22o}\ b_{22} + C_{33o}\ b_{33} &= C_o\ y \\
C_{o11}\ b_o + C_{1111}\ b_{11} + C_{2211}\ b_{22} + C_{3311}\ b_{33} &= C_{11}\ y \\
C_{o22}\ b_o + C_{1122}\ b_{11} + C_{2222}\ b_{22} + C_{3322}\ b_{33} &= C_{22}\ y \\
C_{o33}\ b_o + C_{1133}\ b_{11} + C_{2233}\ b_{22} + C_{3333}\ b_{33} &= C_{33}\ y
\end{aligned}$$

where the coefficients, C, are the sums of products between pairs of the independent variables, x_o, x_1^2, x_2^2 and x_3^2 and the response y. For example, C_{oo} is the sum of the products of the independent variable x_o, C_{33o} is the sum of the products between the independent variable x_o and x_{32} and $C_{33}y$ is the sum of the products between the independent variable x_3^2 and the response.

If the number of equations prohibits their solution by elimination, matrix inversion is used *(52)*. In this example, a 4x4 matrix must be inverted (in general, an [n+1] x [n+1] matrix) to estimate the coefficients. Once the matrix for a specific experimental design has been inverted, the results can be used again, if the same experimental design matrix is used. Cochran *(53)* lists a number of 2-level factorial and their composite designs, complete with solutions for the direct estimation of first- and second-order regression coefficients.

4.4.3.3 Example - 2^5 factorial

To illustrate the foregoing, a multiple linear regression model of the form

$$\beta_o + {}^{n}\Sigma_{i=1}\beta_i x_i + {}^{n}\Sigma_{j=i+1}{}^{n}\Sigma_{i=1}\beta_{ij}x_i x_j + {}^{n}\Sigma_{k=j+1}{}^{n}\Sigma_{j=j+1}{}^{n}\Sigma_{i=1}\beta_{ijk}x_i x_j x_k + \ldots + {}^{n}\Sigma_{i=1}\beta_{ii}x_{ii}{}^{2}$$

was fitted to factorial experimental data, the experiment conducted to establish the relative importance of CA membrane fabrication variables on the rejection performance of the membrane (section 6.1.3). The five factors considered were: membrane polymer concentration, mole ratio between solvent and non-solvent in the casting solution, the temperature at which the membrane was annealed, the temperature at which the casting-room was controlled, and the volume flow of drying air.

2^5 Factorial Design

Table 4.23 shows the levels chosen for the factors investigated in the 2^5 factorial.

In units of the design, the transformed values for the variables are (see section 4.2.1);

$$x_1 = (A - 1,2)/0,2$$
$$x_2 = (B - 25,0)/2,0$$
$$x_3 = (C - 0,25)/0,1$$
$$x_4 = (D - 85,0)/3,0$$
$$x_5 = (E - 21,0)/3,0$$

and the transformed values for the variables are shown in Table 4.24 (see also Tables 6.20 and 6.23), together with the measured salt rejection responses. The experiment was replicated once and the five four-factor and one five-factor interactions were used to determine levels of significance for the remainder of the effects. Only those effects that proved significant at the 10% level (see Table 6.25 and 6.26, experimental section), were introduced into the regression model, and from the relationship;

$$b = \Sigma xy/\Sigma x^2 \quad \text{or,}$$
$$= [\text{Effect total}]/\Sigma x^2$$
$$= [\text{Effect total}]/32$$

the regression coefficients are estimated, *eg.*:

$$b_o = 2654,7/32 = 82,96 \quad \textit{etc.}$$

As was indicated earlier, the effect totals are best obtained through the method of Yates, which forms the only major part of the calculations to estimate the first-order regression coefficients (see Table 6.24 where the effect totals, calculated for salt rejection, are listed).

TABLE 4.23: FACTOR LEVELS FOR THE 2^5 FACTORIAL EXPERIMENT. CA MEMBRANE CASTING CONDITIONS

Factor		Factor level		Base	Unit
		-1	+1		
Casting solution components					
A	Formamide/acetone mole ratio	1,0	1,4	1,2	0,2
B	CA concentration [mass%]	23,0	27,0	25,0	2,0
Fabrication conditions					
C	Drying-air flow rate [lpm]	0,15	0,35	0,25	0,1
D	Annealing temperature [°C]	82,0	88,0	85,0	3,0
E	Casting-room temperature [°C]	18,0	24,0	21,0	3,0

TABLE 4.24: 2^5 FACTORIAL DESIGN. CA 398-10 FABRICATION VARIABLES

Treatm.	Trial	x_o	x_1	x_2	x_3	x_4	x_5	Rej[%]
I	1	1	-1	-1	-1	-1	-1	35,8
a	2	1	1	-1	-1	-1	-1	85,3
b	3	1	-1	1	-1	-1	-1	79,3
ab	4	1	1	1	-1	-1	-1	95,1
c	5	1	-1	-1	1	-1	-1	35,2
ac	6	1	1	-1	1	-1	-1	86,8
bc	7	1	-1	1	1	-1	-1	82,8
abc	8	1	1	1	1	-1	-1	94,7
d	9	1	-1	-1	-1	1	-1	61,4
ad	10	1	1	-1	-1	1	-1	92,4
bd	11	1	-1	1	-1	1	-1	95,3
abd	12	1	1	1	-1	1	-1	96,5
cd	13	1	-1	-1	1	1	-1	69,1
acd	14	1	1	-1	1	1	-1	93,3
bcd	15	1	-1	1	1	1	-1	96,6
abcd	16	1	1	1	1	1	-1	96,5
e	17	1	-1	-1	-1	-1	1	52,7
ae	18	1	1	-1	-1	-1	1	90,9
be	19	1	-1	1	-1	-1	1	78,5
abe	20	1	1	1	-1	-1	1	94,9
ce	21	1	-1	-1	1	-1	1	53,3
ace	22	1	1	-1	1	-1	1	90,4
bce	23	1	-1	1	1	-1	1	80,0
abce	24	1	1	1	1	-1	1	95,3
de	25	1	-1	-1	-1	1	1	73,2
ade	26	1	1	-1	-1	1	1	92,9
bde	27	1	-1	1	-1	1	1	96,0
abde	28	1	1	1	-1	1	1	96,7
cde	29	1	-1	-1	1	1	1	75,9
acde	30	1	1	-1	1	1	1	94,5
bcde	31	1	-1	1	1	1	1	96,4
abcde	32	1	1	1	1	1	1	97,0
Σx^2		32	32	32	32	32	32	
Σ		32						2654,7

The first-order regression equation, by which the salt rejection performance of the membrane is modelled, is given by;

$$\begin{aligned}\text{Rejection} = \quad & 82,96 + 10,366x_1 + 9,016x_2 + 0,653x_3 + 6,022x_4 + 1,953x_5 \\ & - 6,503x_{12} - 4,372x_{14} - 1,203x_{15} - 1,622x_{24} - 2,078x_{25} - 0,609x_{45} \\ & + 0,809x_{124} + 1,466x_{125} - 0,466x_{235} + 0,884x_{245}\end{aligned}$$

When the estimated $b_o = 82,96$ of β_o is compared with the response (91,9%), obtained from an experiment conducted at the centre (base) of the factorial design (*i.e.* $x_1 = x_2 = x_3 = x_4 = x_5 = 0$), it appears that b_o is a biased estimate of β_o and that second-order effects have to be introduced into the regression model to improve its accuracy.

Rotatable Composite Design

Five pairs of additional experiments were conducted on the five co-ordinate axis, at co-ordinate points $\alpha = \pm\sqrt{2}$. A further experiment was conducted at the centre of the design. The factor levels that corresponded to the unit of the design were obtained from the transformations used earlier and are shown in Table 4.25. Table 4.26 lists the independent variables and the responses obtained from the 11 trials that constituted the composite design.

The estimates of the coefficients b_o, b_{11}, b_{22}, b_{33}, b_{44} and b_{55} are obtained by solving the following equations:

$$\begin{aligned}
C_{oo}b_o + C_{11o}b_{11} + C_{22o}b_{22} + C_{33o}b_{33} + C_{44o}b_{44} + C_{55o}b_{55} &= C_o y \\
C_{o11}b_o + C_{1111}b_{11} + C_{2211}b_{22} + C_{3311}b_{33} + C_{4411}b_{44} + C_{5511}b_{55} &= C_{11}y \\
C_{o22}b_o + C_{1122}b_{11} + C_{2222}b_{22} + C_{3322}b_{33} + C_{4422}b_{44} + C_{5522}b_{55} &= C_{22}y \\
C_{o33}b_o + C_{1133}b_{11} + C_{2233}b_{22} + C_{3333}b_{33} + C_{4433}b_{44} + C_{5533}b_{55} &= C_{33}y \\
C_{o44}b_o + C_{1144}b_{11} + C_{2244}b_{22} + C_{3344}b_{33} + C_{4444}b_{44} + C_{5544}b_{55} &= C_{44}y \\
C_{o55}b_o + C_{1155}b_{11} + C_{2255}b_{22} + C_{3355}b_{33} + C_{4455}b_{44} + C_{5555}b_{55} &= C_{55}y
\end{aligned}$$

which when Tables 4.24 and 4.26 are considered together, result in;

$$\begin{aligned}
43b_o + 36b_{11} + 36b_{22} + 36b_{33} + 36b_{44} + 36b_{55} &= 3619,9 \\
36b_o + 40b_{11} + 32b_{22} + 32b_{33} + 32b_{44} + 32b_{55} &= 2984,9 \\
36b_o + 32b_{11} + 40b_{22} + 32b_{33} + 32b_{44} + 32b_{55} &= 2988,3 \\
36b_o + 32b_{11} + 32b_{22} + 40b_{33} + 32b_{44} + 32b_{55} &= 3022,3 \\
36b_o + 32b_{11} + 32b_{22} + 32b_{33} + 40b_{44} + 32b_{55} &= 3010,1 \\
36b_o + 32b_{11} + 32b_{22} + 32b_{33} + 32b_{44} + 40b_{55} &= 3014,5
\end{aligned}$$

The equations can be written in matrix form, $Cb = R$, and the estimates for the coefficients are obtained through the inverse of matrix C, *i.e.* C^{-1}, since $b = C^{-1}R$ *(47)*:

TABLE 4.25: FACTOR LEVELS FOR THE ROTATABLE COMPOSITE DESIGN, CA MEMBRANE CASTING CONDITIONS

	Factor	Factor level		Base	Unit
		$-\sqrt{2}$	$+\sqrt{2}$		
	Casting solution components				
A	Formamide/acetone mole ratio	0,92	1,48	1,2	0,2
B	CA concentration [mass%]	22,2	27,8	25,0	2,0
	Fabrication conditions				
C	Drying-air flow rate [lpm]	0,10	0,40	0,25	0,1
D	Annealing temperature [°C]	80,8	89,2	85,0	3,0
E	Casting-room temperature [°C]	16,8	25,2	21,0	3,0

TABLE 4.26: 2^5 COMPOSITE DESIGN - CA 398-10 MEMBRANE FABRICATION VARIABLES

Trial	x_o	x_1	x_2	x_3	x_4	x_5	Rejection Observed
33	1	$-\sqrt{2}$	0	0	0	0	69,1
34	1	$+\sqrt{2}$	0	0	0	0	96,0
35	1	0	$-\sqrt{2}$	0	0	0	70,7
36	1	0	$+\sqrt{2}$	0	0	0	96,1
37	1	0	0	$-\sqrt{2}$	0	0	91,4
38	1	0	0	$+\sqrt{2}$	0	0	92,4
39	1	0	0	0	$-\sqrt{2}$	0	82,0
40	1	0	0	0	$+\sqrt{2}$	0	95,7
41	1	0	0	0	0	$-\sqrt{2}$	86,4
42	1	0	0	0	0	$+\sqrt{2}$	93,5
43	1	0	0	0	0	0	91,9
Σ							965,2

$$C = \begin{bmatrix} 43 & 36 & 36 & 36 & 36 & 36 \\ 36 & 40 & 32 & 32 & 32 & 32 \\ 36 & 32 & 40 & 32 & 32 & 32 \\ 36 & 32 & 32 & 40 & 32 & 32 \\ 36 & 32 & 32 & 32 & 40 & 32 \\ 36 & 32 & 32 & 32 & 32 & 40 \end{bmatrix} \qquad b = \begin{bmatrix} b_o \\ b_{11} \\ b_{22} \\ b_{33} \\ b_{44} \\ b_{55} \end{bmatrix}$$

$$R = \begin{bmatrix} 3619,9 \\ 2984,9 \\ 2988,3 \\ 3022,3 \\ 3010,1 \\ 3014,5 \end{bmatrix}$$

$$C^{-1} = \begin{bmatrix} 0,2258 & -0,0484 & -0,0484 & -0,0484 & -0,0484 & -0,0484 \\ -0,0484 & 0,1116 & -0,0134 & -0,0134 & -0,0134 & -0,0134 \\ -0,0484 & -0,0134 & 0,1116 & -0,0134 & -0,0134 & -0,0134 \\ -0,0484 & -0,0134 & -0,0134 & 0,1116 & -0,0134 & -0,0134 \\ -0,0484 & -0,0134 & -0,0134 & -0,0134 & 0,1116 & -0,0134 \\ -0,0484 & -0,0134 & -0,0134 & -0,0134 & -0,0134 & 0,1116 \end{bmatrix}$$

The coefficients are calculated as follows:

$$b_o = (0,2258.3619,9) + (-0,0484.2984,9) + (-0,0484.2988,3) + (-0,0484.3022,3) + (-0,0484.3010,1) + (-0,0484.3014,5) = 90.618$$

etc., and, in summary, the second-order estimates which are to be incorporated into the first-order regression model already obtained, are:

$$\begin{aligned} b_o &\longrightarrow \beta_o = 90,618 \\ b_{11} &\longrightarrow \beta_{11} = -3,972 \\ b_{22} &\longrightarrow \beta_{22} = -3,502 \\ b_{33} &\longrightarrow \beta_{33} = 0,748 \\ b_{44} &\longrightarrow \beta_{44} = -0,777 \\ b_{55} &\longrightarrow \beta_{55} = -0,227 \end{aligned}$$

Four-dimensional Representation of the Response Surface

To enable the rejection performance of the CA membrane to be visualized, a graphic illustration was constructed with the aid of the regression equation, as shown in Figure 4.8.

The rate of air flow to facilitate drying (factor C), was kept constant at 1,2 lpm, *i.e.* $x_3 = 0$. The horizontal and vertical axes of the chart in Figure 4.8 (x_4 and x_5, respectively) constitute the annealing temperature (factor D) and casting-room temperature (factor E), respectively. The contour diagrams, placed at co-ordinates (0, 0), (-1, -1), (-1, +1), (+1, -1) and (+1, +1) in the E-D factor space (x_4, x_5 axis), represent the casting solution composition, obtained by varying the acetone/formamide ratio (factor A) and cellulose acetate concentration (factor B) over the x_1 and x_2 variable range, -1 to +1.

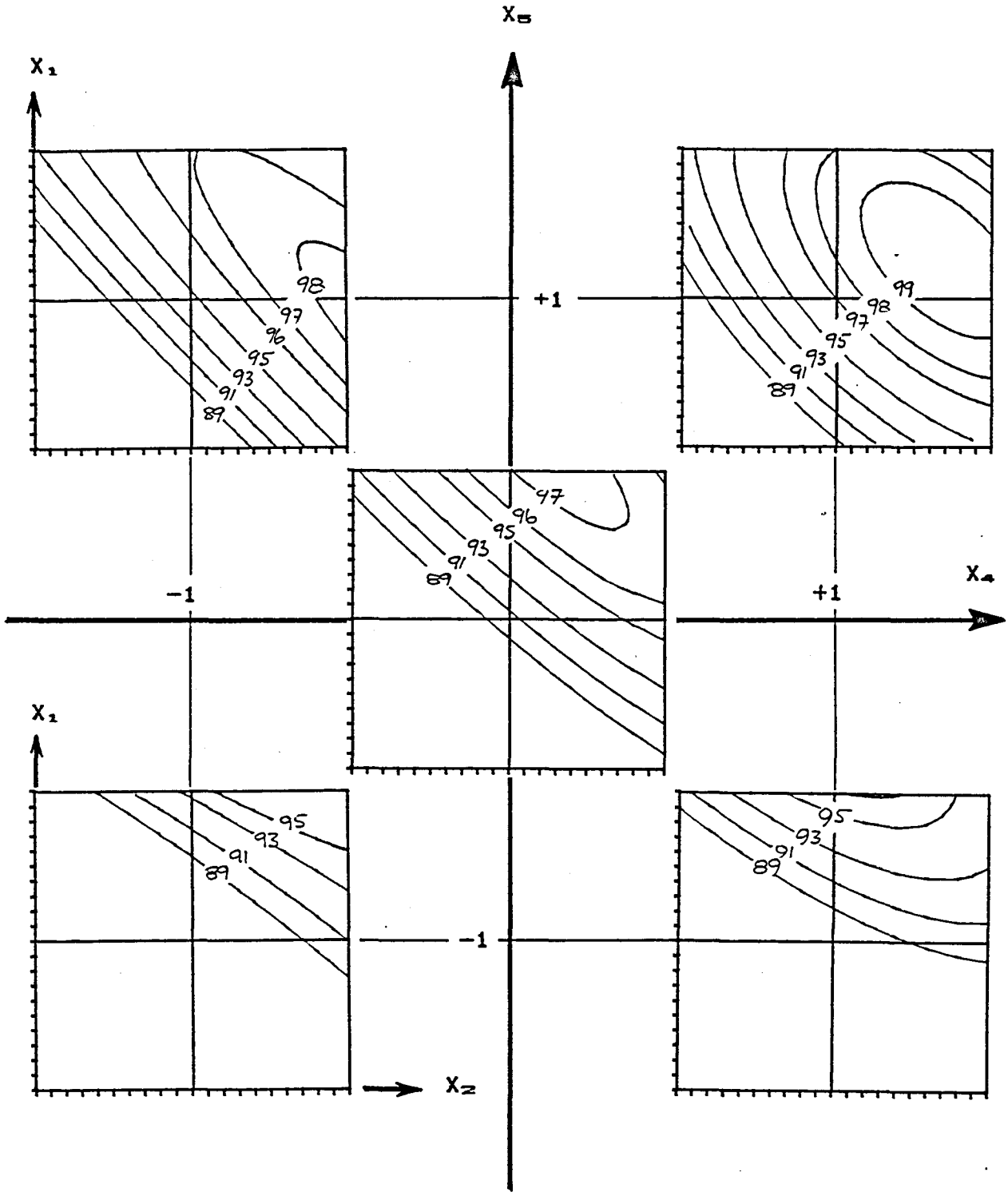

FIGURE 4.8: FOUR-DIMENSIONAL CONTOUR DIAGRAM REPRESENTING CA MEMBRANE FORMULATION VARIABLE RANGES

4.4.4 OPTIMIZATION

Optimization in itself is a necessary but time-consuming task, mainly because it is necessary, first of all, to identify all the significant factors, before the factor space can be searched for the optimum. Since identification of these factors depends upon some fundamental understanding of what physical/chemical processes are at work during, say the membrane-forming process, it is easy, in an empirical situation, to leave one or more key factors out of the investigation. This obviously results, at best, in a sub-optimum set of fabrication variables.

Nonetheless, apart from improvements normally achieved through optimization, the amount of knowledge gained of the physical/chemical processes involved, especially when statistically designed experiments are used, alone justifies the effort expended.

4.4.4.1 Numerical approach *(54)(55)(56)(57)*

This technique implies that a mathematical model of the response surfaces, say, of flux and rejection, is available and that these models are optimized numerically (*i.e.* maximized with respect to, say, membrane flux). However, the regression model of the response surface in the vicinity of the optimum must first be established.

The strategy followed with statistically designed experiments involves conducting a series of sequentially designed experiments, until there is convergence to the optimum. At a point in the factor space away from the optimum, the response can be adequatly modelled by means of the first-order terms of a Taylor series. The gradient of this tangent or twisted plane gives an indication of the direction in which improvements in the response values will lie. In the region of, or at, the optimum, this model will no longer provide an adequate estimate of the experimental mean (*i.e.* it will deviate significantly from the response obtained at the centre of the design) and the experiment must be augmented with a composite design to allow the regression model to be expanded to include the second-order terms of the Taylor series.

During the development of techniques and formulations for the fabrication of tubular CA RO membranes, the intention of the study involving membrane fabrication formulations was to establish a mathematical model of trans-membrane flux and salt rejection behaviour and, by use of numerical techniques, to forecast the optimum membrane flux and fabrication conditions, for rejection performances specified in the 90-95% range.

The numerical procedure used was to maximize membrane flux, by use of the Complex algorithm of Box *(58)(59)*:

$$\text{Maximize flux: } Y_F\ (x_1, x_2, x_3, x_4, x_5)$$

subject to the constraints

$$\text{Rejection: } Y_R^{I} < Y_R(x_1, x_2, x_3, x_4, x_5) < Y_R^{II}$$
$$-1 \leq x_i < +1 \qquad i = 1,\ldots,5$$

where Y_F and Y_R are the mathematical models for membrane flux and salt rejection, respectively. Y_R^{I} is the lower limit imposed on the rejection function and Y_R^{II} an arbitrarily imposed upper limit. (Maximum membrane flux gain lies in the direction of lower rejection, and the solution will converge to the lower rejection limit set, Y_R^{I}, see section 6.1.1.3).

The computer program used was a modified version *(60)* of the Complex algorithm of Box, listed by Kuester *(61)*.

4.4.4.2 Simplex approach in self-directing optimization

The above approach was not used in optimizing UTF composite RO membrane fabrication formulations. A UTF composite membrane has an intrinsic maximum rejection and flux capability which is highly dependent on the chemicals from which the desalting matrix is formulated. The intention with the optimization of the UTF membrane was therefore to determine what the upper limit in salt rejection was and to establish the fabrication formulation of such a membrane.

From this the conclusion could be drawn that an optimized UTF composite membrane is regarded as a membrane with the best achievable mechanical, physical and chemical performances obtainable with a given set of membrane chemicals *(62)*. Any deviation from the 'optimum' would result in a membrane of lower quality.

The simplex technique of self-directing optimization [SDO] was used, which in essence, is an easy approach to empirical optimization of a system involving multiple factors. The method does not become unmanageable when large numbers of variables are included in the study; on the contrary, the method was designed specifically to accommodate such situations. It progresses towards the optimum along the route of steepest ascent and converges reasonably rapidly.

This method takes a regular geometric figure (known as the simplex) as a basis. With two factors, the simplex is arranged in the form of an equilateral triangle. To arrange the initial simplex, n+1 trials in n dimensions (n = number of factors) are set up in such a way that orthogonality between factors and their effects is ensured. Arrangement of more than the necessary n+1 trials will only decrease the rate of progression. From the size of the design it is evident that these designs can be highly confounded; main effects are confounded with two-factor interactions, *etc.*

Hendrix *(63)* proposed the following schemes by which the co-ordinates of the initial simplex should be arranged;

i) if n = 2, use simplex;
ii) if n = 3, use saturated 2-level factorial;
iii) if $4 \leq n \leq 7$, use fractional factorial for 8 factors;

iv) if $8 \leq n \leq 11$, use Plackett-Burman *(64)* plan in 12 experiments;

v) if $12 \leq n \leq 15$, use fractional factorial for 16 variables, and,

vi) if $n = 16$, use saturated 2-level factorial.

In order to form a basis by which the significance of the main effects of factors in the first simplex can be judged, dummy factors can be incorporated into the design, *i.e.* choose the design larger than is required for the number of factors studied, to give additional degrees of freedom by which error can be assessed *(65)*.

Lowe *(66)(67)* used the following approach to establish the six co-ordinates of a five-factor simplex;

X_{11}	X_{21}	X_{31}	X_{41}	X_{51}
X_{12}	X_{21}	X_{31}	X_{41}	X_{51}
$(X_{11} + X_{12})/2$	X_{22}	X_{31}	X_{41}	X_{51}
$(X_{11} + X_{12})/2$	$(X_{21} + X_{22})/2$	X_{32}	X_{41}	X_{51}
$(X_{11} + X_{12})/2$	$(X_{21} + X_{22})/2$	$(X_{31} + X_{32})/2$	X_{42}	X_{51}
$(X_{11} + X_{12})/2$	$(X_{21} + X_{22})/2$	$(X_{31} + X_{32})/2$	$(X_{41} + X_{42})/2$	X_{52}

In the notation used, the first letter of the subscript denotes the input factor, and the second subscript the factor level used in the experiment. In the sign notation used thus far to denote the factor variables, the co-ordinate system of Lowe would be as follows for the five-factor simplex in the example given above;

x_1	x_2	x_3	x_4	x_5
-1	-1	-1	-1	-1
+1	-1	-1	-1	-1
0	+1	-1	-1	-1
0	0	+1	-1	-1
0	0	0	+1	-1
0	0	0	0	+1

Movement from the one simplex to the other is governed by the following rules *(68)*:

i) In a simplex, discard the point(s) with the least acceptable response and replace it (them) by its (their) mirror image. The co-ordinates of the new point(s) are given by: twice the average of the co-ordinates of the remaining points, minus the co-ordinates of the rejected point.

ii) When a newly generated point has the least acceptable response, care must be exercised that when this point is rejected the new point generated is not its mirror image. This will cause oscillation between two points. Retain the point for one more simplex and rather discard the second-least acceptable response.

Progress towards the optimum may be represented graphically by plotting the average simplex value of the response(s) against the simplex numbers. Movement within each factor space can like-wise be presented.

The simplex technique recovers rapidly from wrong decisions taken in creating new points and thus also has a capacity to accommodate experimental error to a large extent.

LIST OF REFERENCES

1. Davies, O.L., The design of industrial experiments, 2nd Ed, (1978), Longman Inc, NY
2. Brownlee, K.A., Industrial experimentation, 4th Ed., (1953) Chem. Pub. Co., NY
3. Lindman, H. R., Analysis of variance in complex experimental designs, (1974), W.H. Freeman & Co
4. Cochran, W.G., Cox, G.M., Experimental designs, 2nd Ed, (1957), John Wiley & Son, NY
5. Yates, F., The design and analysis of factorial experiments, Technical Communication No. 35 (1937), Publ. Imp. Bureau of soil science, London
6. Beveridge, G.S.G., Schechter, R.S., Optimization: Theory and Practice, Int. Students Ed., p363-366 (1970), McGraw-Hill
7. Sachs, L., Applied statistics, A handbook of techniques, Translation of: Angewandte Statistik, 5th Ed, p558-566 (1978), (1982), Springer-Verlag, NY
8. Box, G.E.P, Wilson, K.B., J of the Royal Statistical Soc., Series B, 13, 1 (1951)
9. Fisher, R.A., The design of experiments, 8th Ed, p95-108 (1965), Oliver and Boyd
10. Meyer, S.L., Data analysis for scientists and engineers, Ch. 7, (1975), John Wiley & Sons
11. Meyer, S.L., Data analysis for scientists and engineers, p269-273 (1975), John Wiley & Sons
12. Davies, O.L., Design of industrial experiemnts, 2nd Ed., p30-39 (1978), Longman Inc., NY
13. Sachs, L., Applied statistics, A handbook of techniques, Translation of: Angewandte Statistik, 5th Ed, p124-129 (1978), (1982), Springer-Verlag, NY
14. Wonnacott, T.H., Wonnacott, R.J., Introductory statistics, 3rd Ed., p252-260 (1977), John Wiley & Sons Inc.
15. Davies, O.L., The design of industrial experiments, 2nd Ed., p610-611 (1978), Longman Inc., NY
16. Kreyszig, E., Introductory mathematical statistics - Principles and methods, p209-212 (1970), John Wiley & Son
17. Davies, O.L., Goldsmith, P.L., Statistical methods in research and production, 4th Ed., p69-75 (1972), Oliver & Boyd
18. Meyer, S.L., Data analysis for scientists and engineers, Ch. 27, p274-282 (1975), John Wiley & Son
19. Wonnacott, T.H., Wonnacott, R.J., Introductory statistics, 3rd Ed., Table V, p613 (1977), John Wiley & Sons, Inc.
20. Davies, O.L., Goldsmith, P.L., Statistical methods in research and production, 4th Ed., p162-166 (1972), Oliver & Boyd, NY
21. Sachs, L., Applied statistics - A handbook of techniques, 5th Ed., p501-541 (1978), (1982), Springer-Verlag Inc, NY
22. Kreyszig, E., Introductory mathematical statistics, Ch. 16: Analysis of variance, p262-284 (1970), John Wiley & Son
23. Walpole, R.E., Meyer, R.H., Probability and statistics for engineers and scientists, Ch. 10-11, p365-451 (1972), Macmillan Publishing Co., Inc.
24. Wonnacott, T.H., Wonnacott, R.J., Introductory statistics, 3rd Ed., Table VII, p616-617 (1977), John Wiley & Sons, Inc., NY
25. Davies, O.L., Goldsmith, P.L., Statistical methods in research and production, 4th Ed., p125-128 (1972), Oliver & Boyd, London
26. Cochran, W.G., Cox, G.M., Experimental designs, 2nd Ed., Ch.5, (1957), John Wiley & Sons Inc.
27. Davies, O.L., The design and analysis of industrial experiments, 2nd Ed., p259-263 (1978), Longman Inc., NY.
28. Yates, F., Design and analysis of factorial experiments, Technical Communication, 35(1937)15, Publ. Imperial Bureau of Soil Science (London)
29. Miller, I., Freund, J.E., Probability and statistics for engineers, 2nd Ed., p375-401 (1977), Prentice-Hall Inc.
30. Cochran, W.G., Cox, G.M., Experimental designs, 2nd Ed., p262 (1957), John Wiley & Son, NY
31. Davies, O.L., The design of industrial experiments, 2nd Ed., Ch. 9, (1978), Longman Group, Ltd.
32. Davies , O.L., The design of industrial experiments, 2nd Ed., p380 (1978), Longman Group, Ltd.
33. Cochran, W.G., Cox, G.M., Experimental designs, 2nd Ed., p185 (1957), John Wiley & Sons, Inc.
34. Davies, O.L., The design of industrial experiments, 2nd Ed., p418-427 (1978), Longman Group, Ltd.
35. Box, G.E.P., Hunter, J.S., The 2^{k-p} fractional factorial designs. Part I, Technometrics, 3(Aug. 1961)311
36. Miller, I., Freund, J.E., Probability and statistics for engineers, 2nd Ed., p406, Prentice-Hall Inc.
37. Walpole, R.E., Myers, R.H., Probability and statistics for engineers and scientists, 2nd Ed., p456 (1978), Macmillan Pub. Co., Inc., NY
38. Cochran, W.G., Cox, G.M., Experimental designs, 2nd Ed., Ch. 6a, (1957), John Wiley & Sons, Inc.
39. Davies, O.L., The design of industrial experiments, 2nd Ed., p451-454 (1978), Longman Group, Ltd.
40. Cochran, W.G., Cox, G.M., Experimental designs, 2nd Ed., p219-221 (1957), John Wiley & Sons, Inc.
41. Yates, F., The design and analysis of factorial experiments, Technical Communication no. 35, p23-31 (1937) Imperial Bureau of Soil Science (London)
42. Miller, I., Freund, J.E., Probability and statistics for engineers, 2nd Ed., p407-411 (1977), Prentice-Hall Inc.
43. Nie, N.H., Hull, C.H., Jenkins, J.G., Steinbrenner, K. Statistical package for social sciences, 2nd Ed., (1975), Mc Graw-Hill.
44. Walpole, R.E., Myers, R.H., Probability and statistics for engineers and scientists, 2nd Ed., Ch. 8, (1978), Macmillan Publishing Co.
45. Walpole, R.E., Myers, R.H., Probability and statistics for engineers and scientists, 2nd Ed., Ch. 9, (1978), Macmillan Publishing Co.
46. Davies, O.L., Goldsmith, P.L., Statistical methods in research and production, 4th Ed., p264-268 (1972), Oliver and Boyd
47. Dorf, R.C., Marix algebra: a programmed introduction, (1969), Wiley and Son, Inc., NY
48. Davies, O.L., The design and analysis of industrial experiments, 2nd Ed., Ch. 11, (1978) Longman Group
49. Cochran, W.G., Cox, G.M., Experimental designs, 2nd Ed. p342-354 (1957), John Wiley and Son
50. Davies, O.L., The design and analysis of industrial experiments, 2nd Ed., p534-536 (1978), Longman group
51. Cochran, W.G., Cox, G.M., Experimental designs, 2nd Ed., p347-348 (1957), John Wiley and Son
52. Walpole, R.E., Myers, R.H., Probability and statistics for engineers and scientists, 2nd Ed., p321 (1978), Macmillan Publishing Co.
53. Cochran, W.G., Cox, G.M., Experimental designs, 2nd Ed., p370-375 (1957), John Wiley and Son
54. Grethlein, H.E., Statislical design of experiments for optimizing the casting variables for CA membranes; Ch 6, RO synthetic membranes, Ed., Sourirajan, S., p111-128, (1977)
55. Chian, E.S.K., Fang, H.H.P., J. Applied Polym. Sci., 19(1975)251-263
56. Fang, H.H.P., Chian, E.S.K., Optimization of NS-100 membrane for RO, J. Applied Polym. Sci., 20(1976)303-314
57. Fahey, P.M., Grethlein, H.E., Improved CA membranes for RO, Desalination, 8(1971)297
58. Box, J.M., A new method of constrained optimization and a comparison with other methods, Computer J., 8(1965)42
59. Beverage, G.S.G., Schechter, R.S., Optimization: Theory and practise, Student Ed., p453-456 (1970), Mc Graw-Hill

60. Jacobs, E.P., Sanderson, R.D., Botha, G.R., Development of membrane support systems and modules, Final Report, (1982), Water Research Commission, Pretoria
61. Kuester, J.C., Mize, J.H., Optimization techniques with Fortran, (1973), Mc Graw-Hill
62. Sanderson, R.D., Private Communications, Institute Polymer Science, University of Stellenbosch
63. Hendrix, C., Internal Report, Union Carbide, Research and Development, South Charleston, West Virginia, USA.
64. Plackett, R.L., Burman, J.P., Biometrika, 33(1946)305
65. Stowe, A.S., Mayer, R.P., Ind. Engnr. Chem., 50(1966)36-44
66. Lowe, C.W., Trans. Instn., Chem. Engrs., 45(1967)t3-t8.
67. Lowe, C.W., Trans. Instn., Chem. Engrs., 42(1964)332-340
68. Beveridge, G.S.G., Schechter, R.S., Optimization: Theory and practice, Student Ed., p367-383 (1970), Mc Graw-Hill.

CHAPTER V

EXPERIMENTAL

MEMBRANE FABRICATION EQUIPMENT AND PROCEDURES

5.0 INTRODUCTION

During the course of the study on membrane fabrication techniques and formulations, which will be discussed in the following chapter, various equipment was designed and constructed to meet the processing needs as the research progressed. In this section, the operation of the more important equipment will be described; their principles of operation are detailed in illustrations. The techniques and equipment used in the synthesis of the various chemical components used for fabricating UTF composite membranes do not form part of this study and is documented elsewhere *(1)*.

5.1 TUBULAR PHASE-INVERSION MEMBRANES

The fabrication of tubular phase-inversion membranes is a continuous process, and the sequence of events:

i) fabrication of the helically wound membrane support tube;
ii) extrusion of a thin membrane casting-solution film onto the inside wall of the support tube, and
iii) phase separation, to create the membrane,

are all stages in the continuous process.

5.1.1 SUPPORT TUBE FABRICATION

The design of the tube-winding machine [TWM] on which the support tube is produced, is based on the same principle of operation as that of the so-called "core-winder", a machine used in the production of cardboard tubes.

The tubular membranes are fabricated downwardly on the TWM, straight into a coagulation tank situated beneath the TWM. No mechanical means for conveying the membranes are therefore needed as it would have been if the support tubes were produced horizontally.

The porous membrane support tube is produced from a 31mm wide filter fabric ribbon. This ribbon, made from a thermoplastic material, is dispensed from a tensioned feed-roller, and is guided along rubber rollers and tensioning devices to a stationary mandrel. A rubber-coated drive-belt, folded around the mandrel, is used to feed the fabric helically down along the mandrel (see Figure 5.1). The relative angle between the drive belt and the mandrel, the width of the drive-belt, diameter of the mandrel and the width of the fabric ribbon, all affect the amount by which the fabric edge overlaps. The ribbon is fused ultrasonically into a tube along this overlapping edge.

The belt passes over two drums (situated on either side of the mandrel) which are mounted on a common, movable platform. One of the drums is motorized, the speed of rotation being controlled by a stepless gearbox, whereas the other drum runs freely.

An overlap of 0,5mm ensures the best mechanical strength when the Branson B12 sonifier, which operates at 20kHz with a maximum output of 150 watt, is operated at 35% of its output. A standard half-inch flat-tipped horn is used for welding.

5.1.2 MEMBRANE EXTRUSION

The membrane-casting solution is conveyed through the centre of, and to the bottom end of, the hollow mandrel on which the support tube is formed; here an extrusion die applies a membrane film of the required thickness to the inside wall of the support tube. The casting solution is conveyed either by air pressure or by a precision-gear metering pump *(2)(3)(4)*.

With lower-viscosity casting solutions (< 5 000cP) it was found best to maintain a low liquid head (2cm) within the extrusion cavity to prevent the casting solution from bleeding through the fabric.

This is accomplished by introducing the solution at the bottom-end of the cavity, allowing the liquid level to rise to the correct height, and to maintain it at that head by accurate control. (See Figures 5.2 to 5.4 for different mandrel assemblies) With the CA casting solutions of much greater viscosity (>50 000cP), this kind of control is not necessary and the cavity in extrusion die designs, such as shown in Figure 5.5, can be filled completely with casting solution.

Air-drying is accomplished by passing conditioned air, *via* a narrow bore tube, into the nascent membrane area. (See Figure 5.6). To prevent the level of coagulant inside the membrane tube from being unduly depressed, the return of the drying air is vacuum-assisted. The level of the leach front inside the membrane can be controlled by careful adjustment of the air pressure inside the membrane tube. The position of the leach front is read from a manometer, which also indicates disturbances such as oscillations of the leach front, which is one cause of membrane imperfections.

A 3,5m-long tank, which contains the coagulant, is situated vertically beneath the tube-winding machine. The coagulant is circulated by means of a pump and the coagulant temperature is controlled to $\pm$0,5°C of the set point, which normally is 20°C.

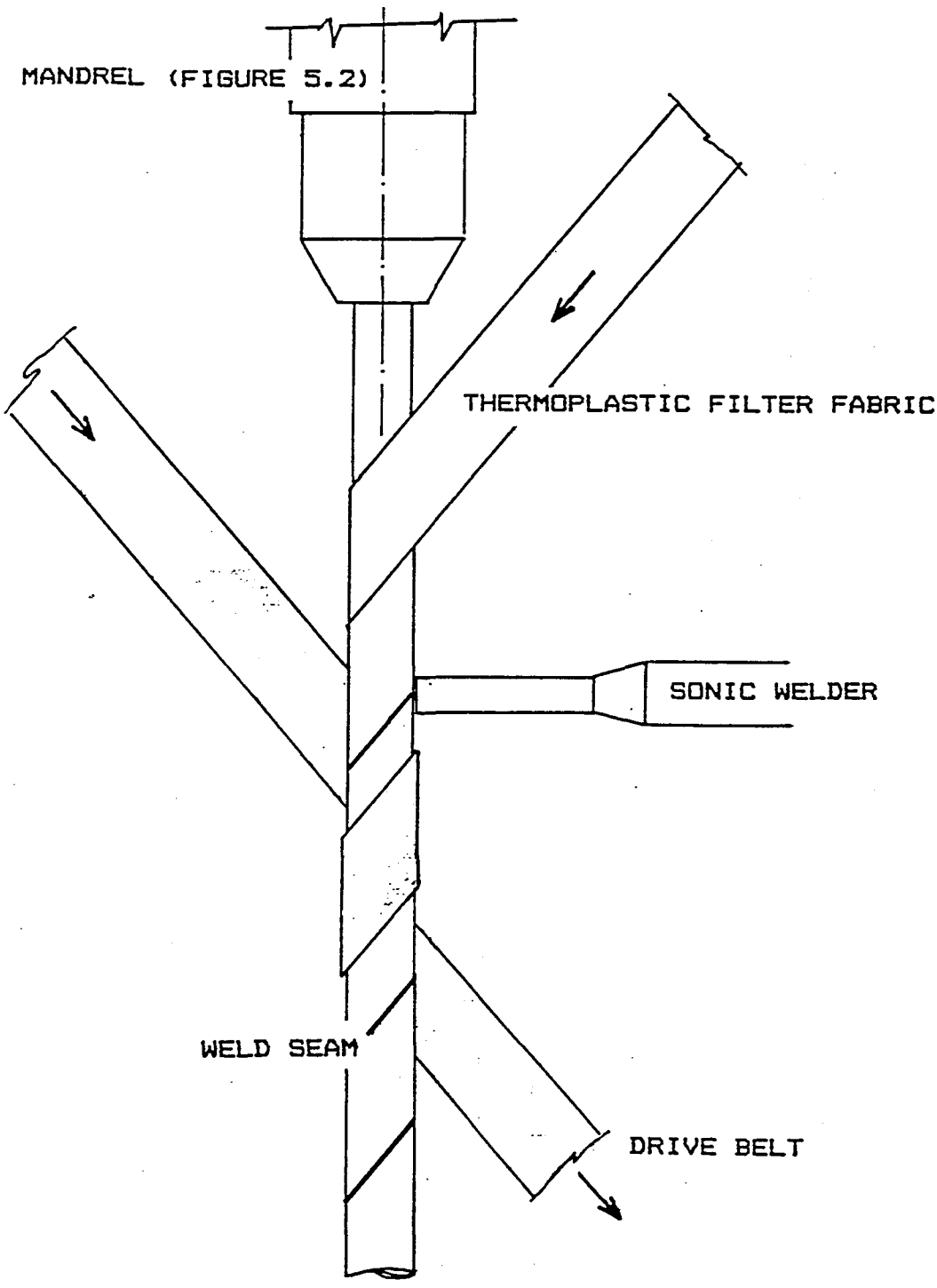

FIGURE 5.1: THE TUBE WINDING PRINCIPLE

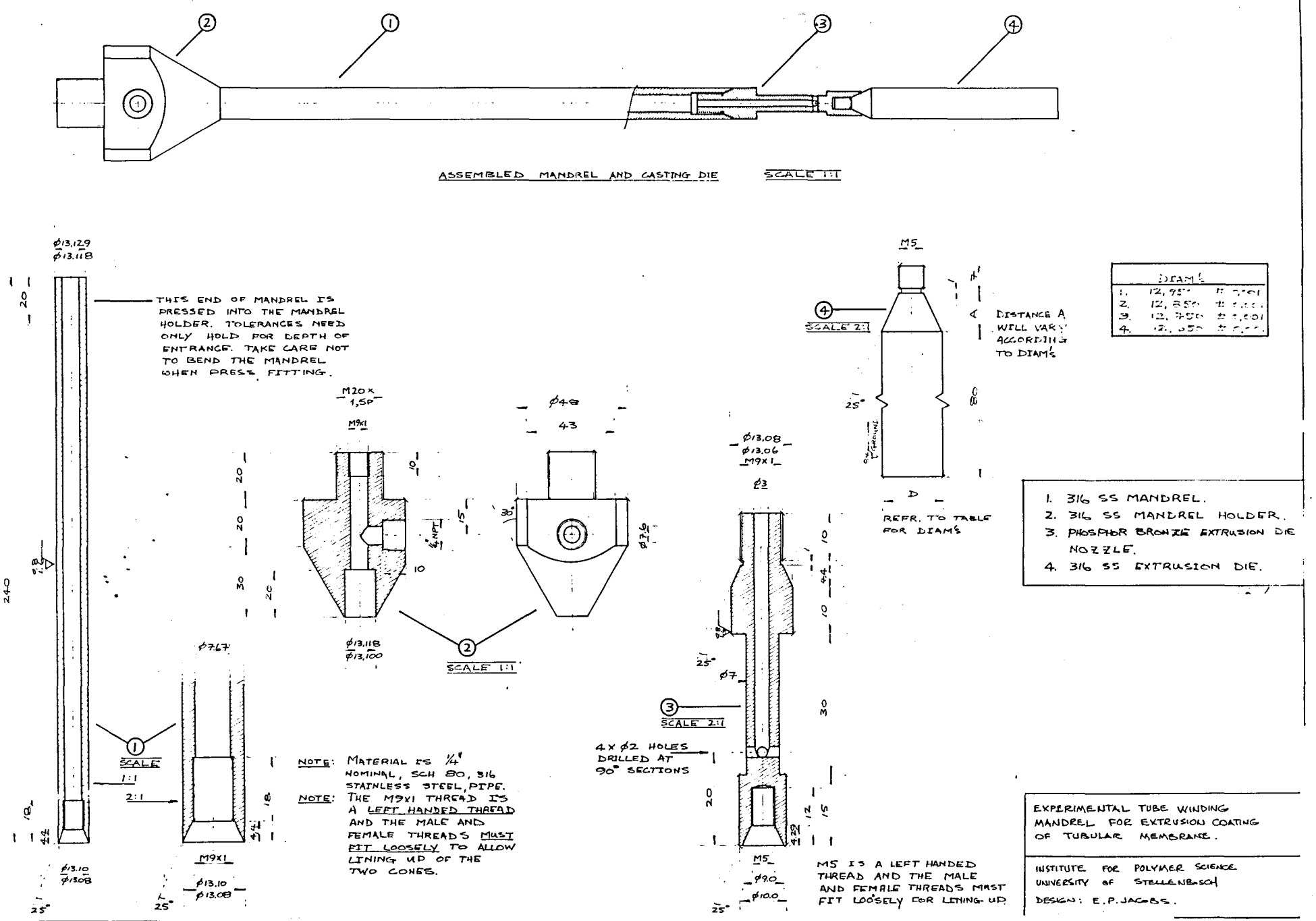

FIGURE 5.2: MANDREL FOR LOW VISCOSITY EXTRUSION - NO AIR DRYING

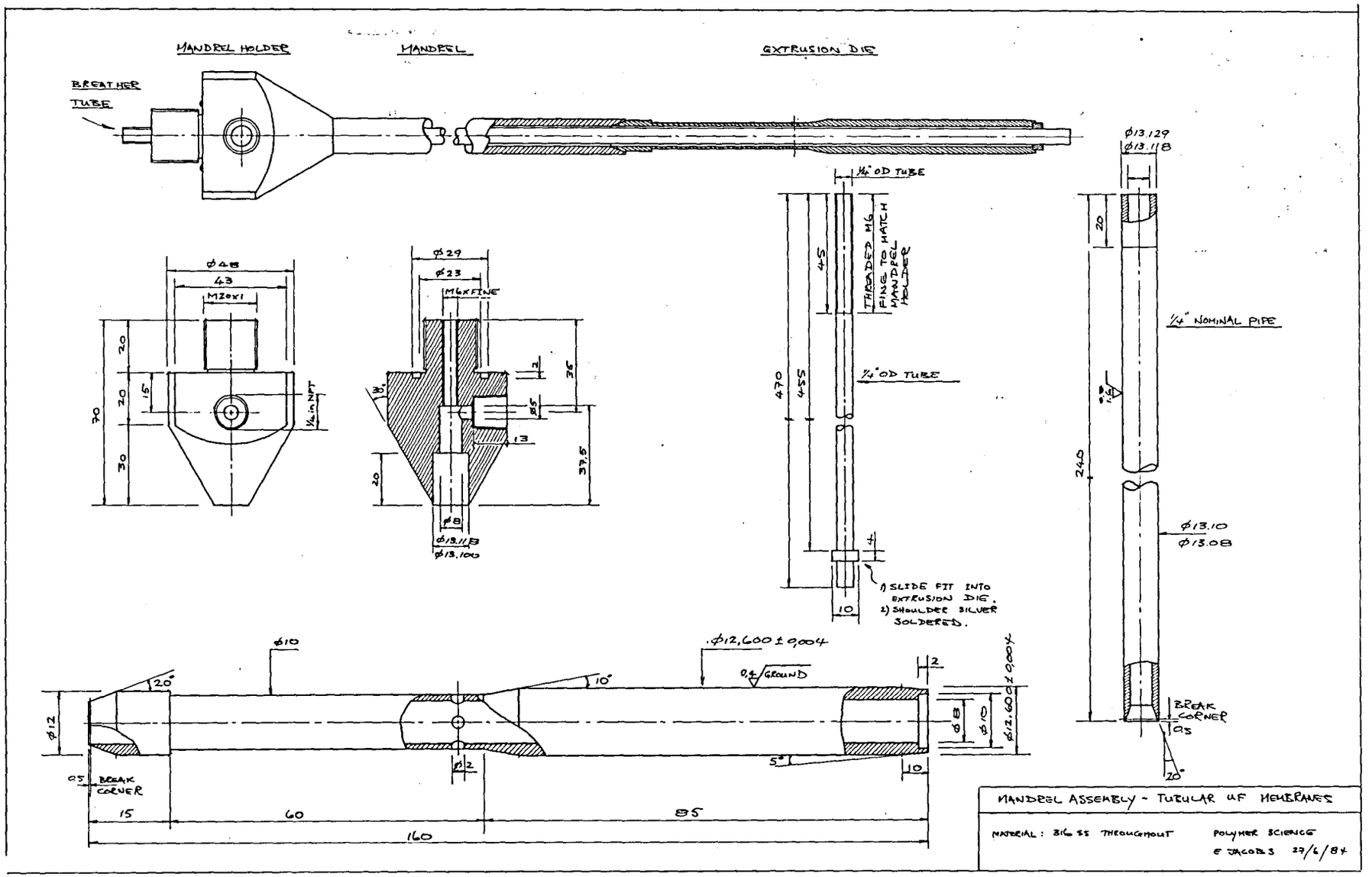

FIGURE 5.3: MANDREL FOR LOW VISCOSITY EXTRUSION WITH AIR DRYING

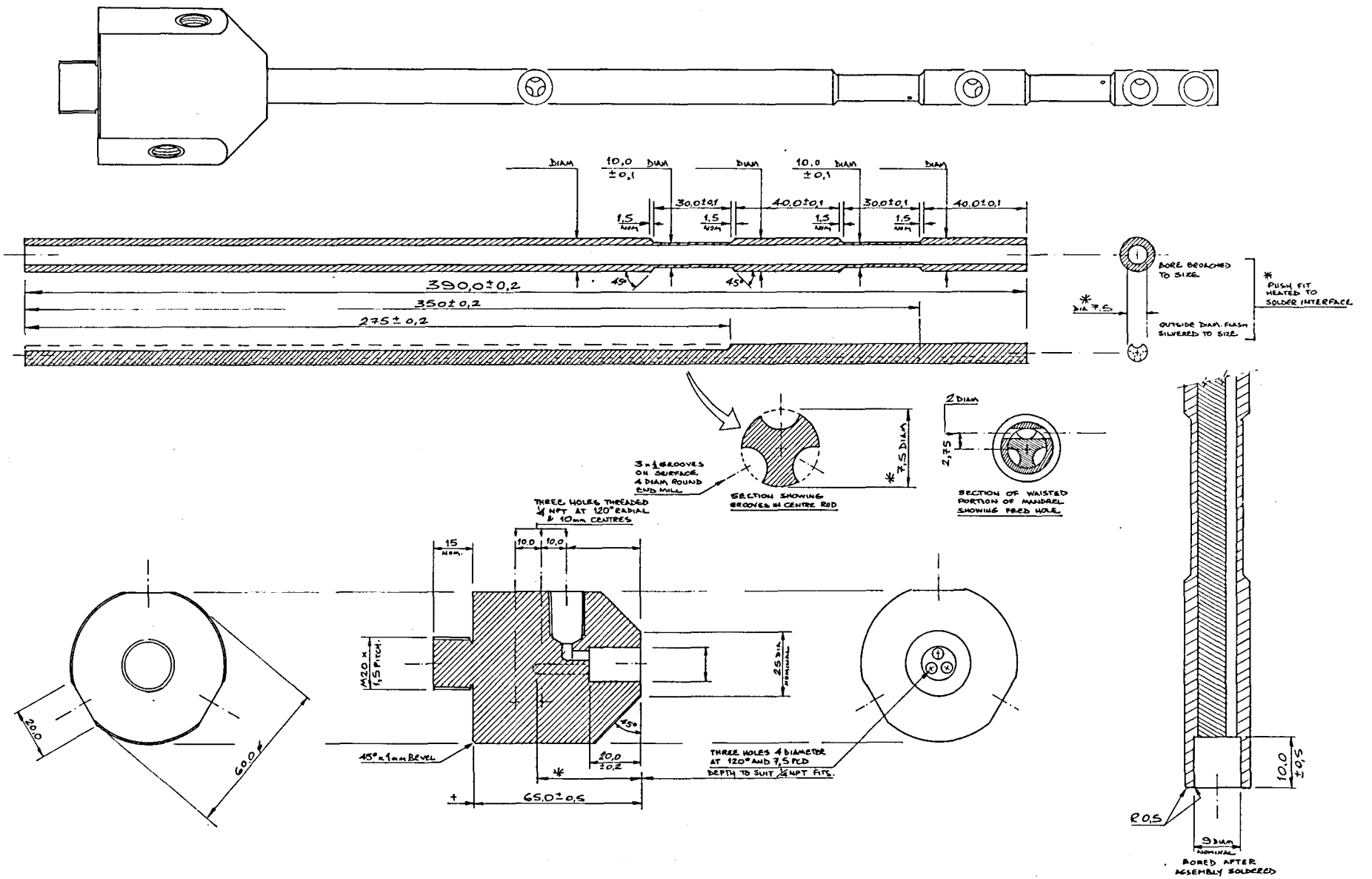

FIGURE 5.4: MANDREL FOR LOW VISCOSITY CO-AXIAL EXTRUSION - AIR DRYING

EXPERIMENTAL TUBE WINDING MANDREL FOR CO-EXTRUSION COATING AND INTERNAL AIR DRYING OF TUBULAR MEMBRANES	INSTITUTE FOR POLYMER SCIENCE UNIVERSITY OF STELLENBOSCH DESIGN: C. Sidney 21-02-1986

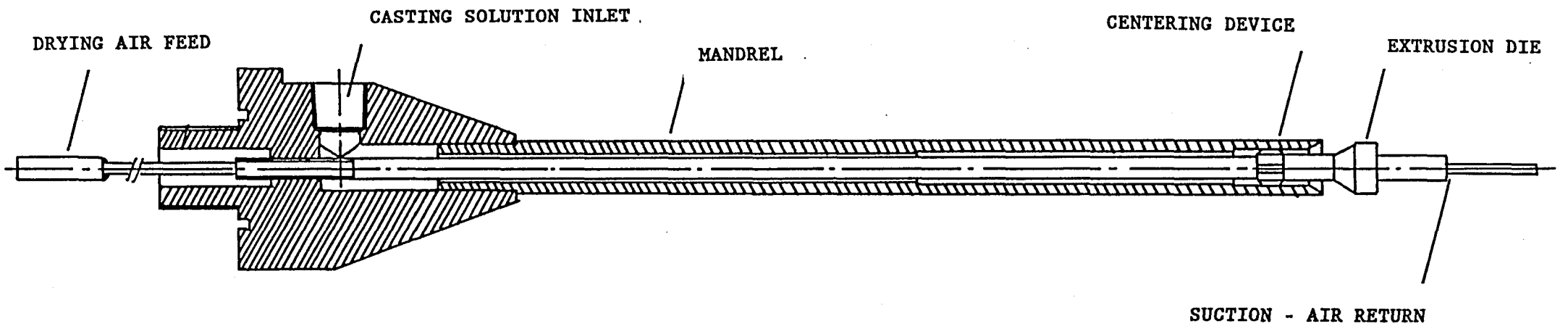

FIGURE 5.5: MANDREL ASSEMBLY FOR HIGH VISCOSITY EXTRUSION WITH AIR DRYING

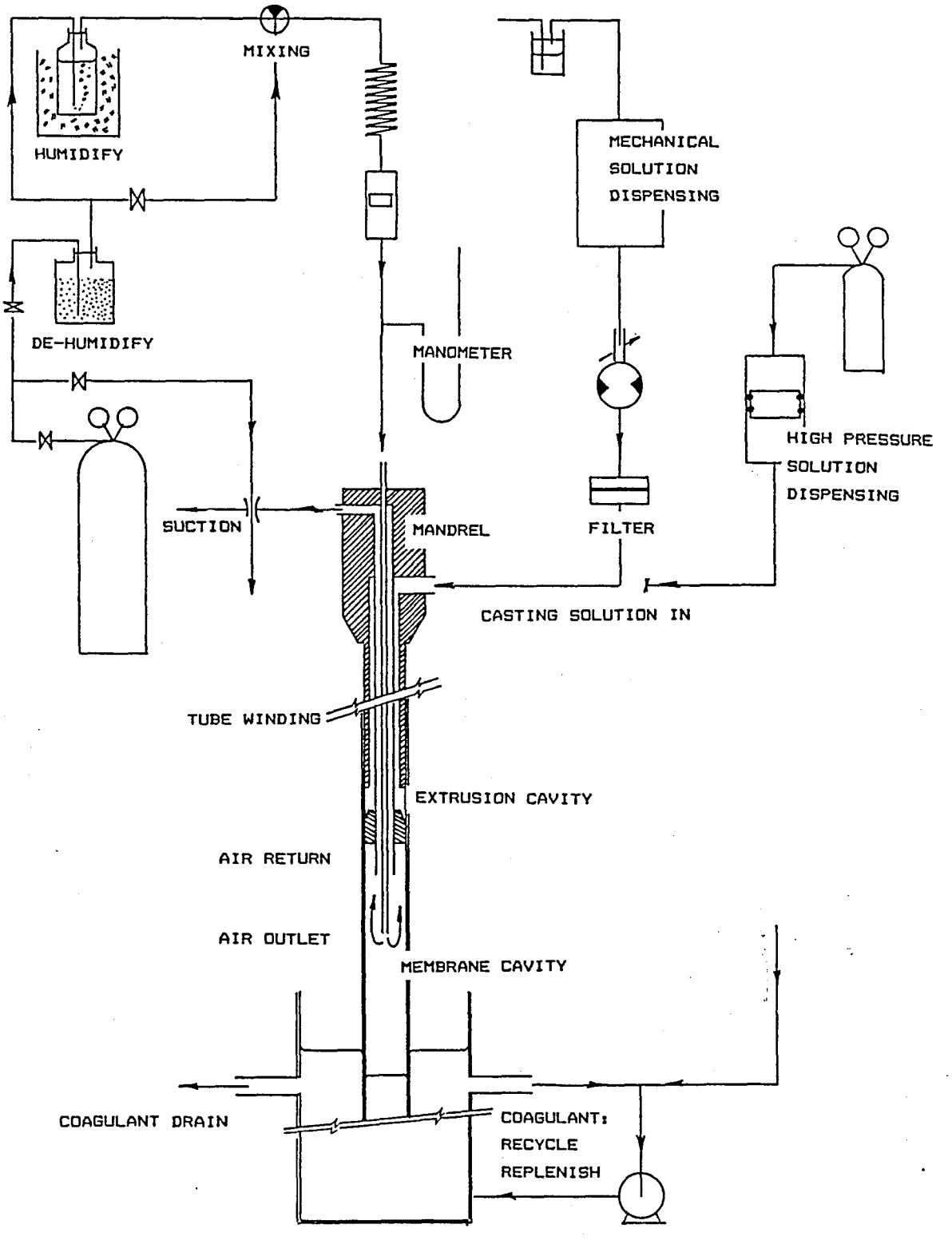

FIGURE 5.6: TECHNIQUES IN TUBULAR MEMBRANE FABRICATION

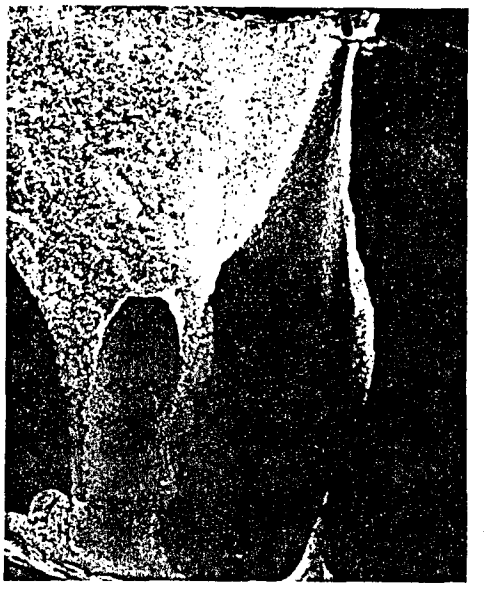

FIGURE 5.7: SUBSTRATE MEMBRANE IMPERFECTIONS

5.1.3 ANNEALING

Heat treatment of CA membranes plays an important role in final adjustment of the salt rejection and permeate flux capabilities of this RO membrane. By heat treatment of the CA membrane at temperatures above its second relaxation temperature *(5)*, the less porous skin section of the membrane is densified further due to segmental chain motion and intermolecular bonding. Crystallization can also occur if the membranes are annealed for periods longer than 20min at temperatures above 90°C.

Annealing is effected in a stainless steel annealing tank, with pH adjusted (pH 5,5 - 6) distilled water, containing 1-5%, by mass of ethylene glycol. Water is drawn from the top of the tank and, after it has been passed through a bank of electrical heaters mounted within the pipe-line, is returned to a bottom inlet of the annealing tank. The total output of the electrical heaters is adjustable by means of a temperature controller. The temperature is controlled to ±0,2°C of set-point. There is a temperature differential of 1°C between the bottom and top ends of the tank.

5.2 TUBULAR UTF COMPOSITE MEMBRANES

The open literature contains very few references regarding UTF composite membrane fabrication techniques *per se*. A small number of NTIS reports have appeared on aspects regarding flat sheet UTF composite membrane fabrication, and even less has appeared regarding tubular UTF composite membranes.

The geometry of the flat sheet membrane lends itself to a continuous approach in the creation of the thin-film desalting barrier. This is not so with the tubular membranes, and although the support membrane can be extruded onto the inside of the support fabric liner continuously, deposition of the thin desalting film onto the support membrane remains essentially a batch process.

At the start of the investigation into possible methods of UTF composite membrane fabrication, certain criteria were laid down according to which the techniques were to be judged. These criteria were, *inter alia*, that:

i) the process must be amenable to automation or at least to semi-automation;
ii) direct contact with the membranes during the fabrication process must be limited, if not avoided, because of the toxic nature of the chemicals;
iii) the process must be technically feasible;
iv) the equipment used must be reliable, low in cost and simple to operate;
v) the process must not be labour-intensive and handling of full-length membranes, 3m, must not be troublesome.
vi) small amounts of the reactants must be used;
vii) the process must lead to the formation of membranes with consistent RO performance and the desalting film must be homogeneously cross-linked.

The deposition of the precursor and reaction with the cross-linking agent can be accomplished in a number of ways *(4)*. In two techniques, the precursor film is formed by draining a solution-wetted substrate membrane under gravity. These two techniques, which differ in the way that the substrate membrane is wetted with the reactants, were used in the study on UTF composite membranes (section 6.3). In the text following, the fabrication equipment developed to semi-mechanise the two methods, will be described.

5.2.1 IMMERSION-COATING

Immersion-coating is a relatively simple operation and is the preferred method when short membranes, *i.e.* 1,2m long, are produced. In this method a bundle of the support membranes is immersed first in the precursor solution, allowed to drain and then dipped in the cross-linking reagent solution, after which the membranes are dried in heated air.

Immersion-coating can easily be automated or semi-automated, and it is a technique used frequently in the plastics industry. The only complication is that the durations of immersion (or contact) in the precursor and cross-linking reagents as well as the periods allowed for drainage, are important and it must be possible to alter them, especially on research equipment where such flexibility is a definite requirement.

5.2.1.1 The immersion-coating machine

The equipment designed for immersion-coating consists of a central unit with a revolving carrier or carousel containing arms from which membranes are suspended. Spaced around the periphery of this unit are stands which raise and lower the vessels containing the coating solution (see Figure 5.8).

The equipment is pneumatically operated (see Figures 5.9 and 5.10) and electronic timing devices control the forward step motion of the carousel and the raising and lowering of the coating-solution vessels.

At any time, all of the following operations take place simultaneously at successive stations along the edge of the carrier.

Station 1:	Loading a set of wet-stored membranes onto one of the arms of the carousel carrier.
Station 2:	Draining off excess water.
Station 3:	Coating the membranes with the precursor by raising the precursor-containing vessel.
Station 4:	Draining off excess precursor.
Station 5:	Coating the membranes with the cross-linking reagent
Station 6:	Draining off excess cross-linking reagent
Station 7:	Off-loading the membranes for final conditioning in the oven.

The operation with the longest duration controls the forward step motion of the carousel. The carousel is locked into position after every step motion, which is the signal for the dipping action to commence. All the vessels move upwards simultaneously and remain raised according to individual timer settings. The carousel is

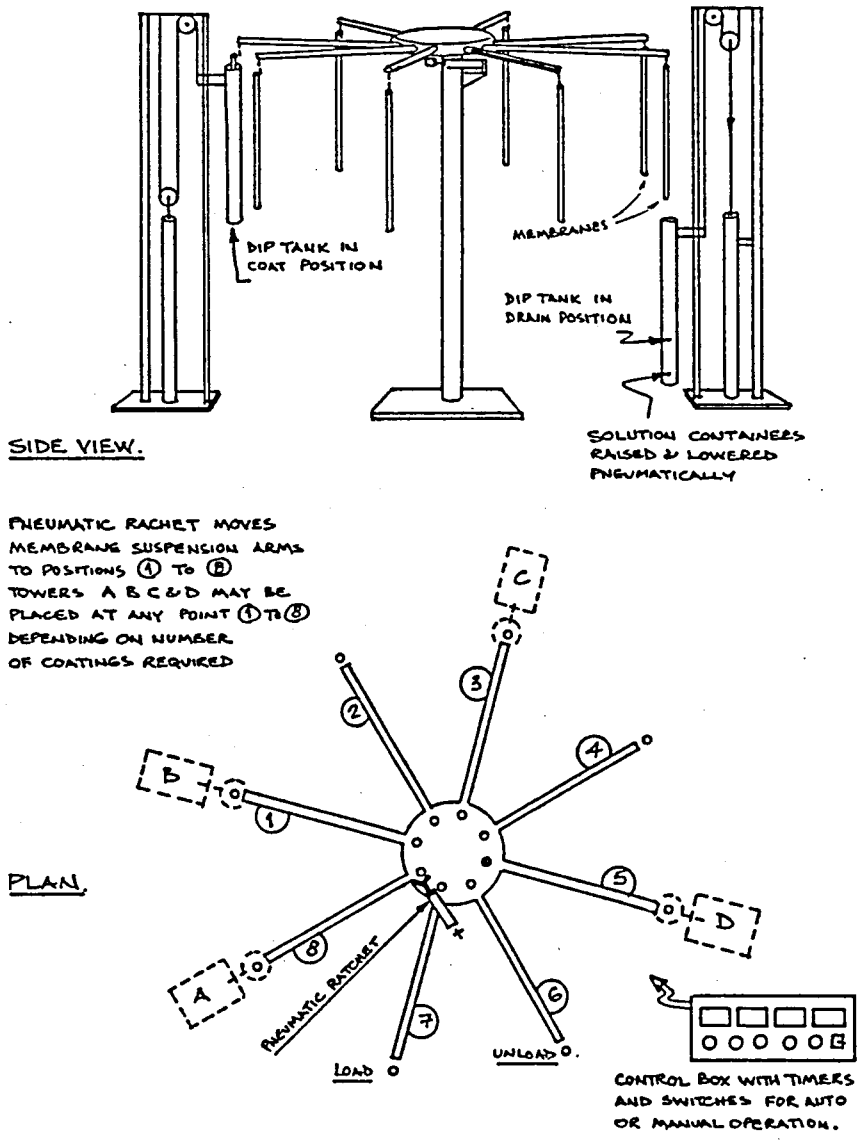

FIGURE 5.8: IMMERSION-COATING MACHINE FOR MEMBRANES UP TO 1,2m IN LENGTH

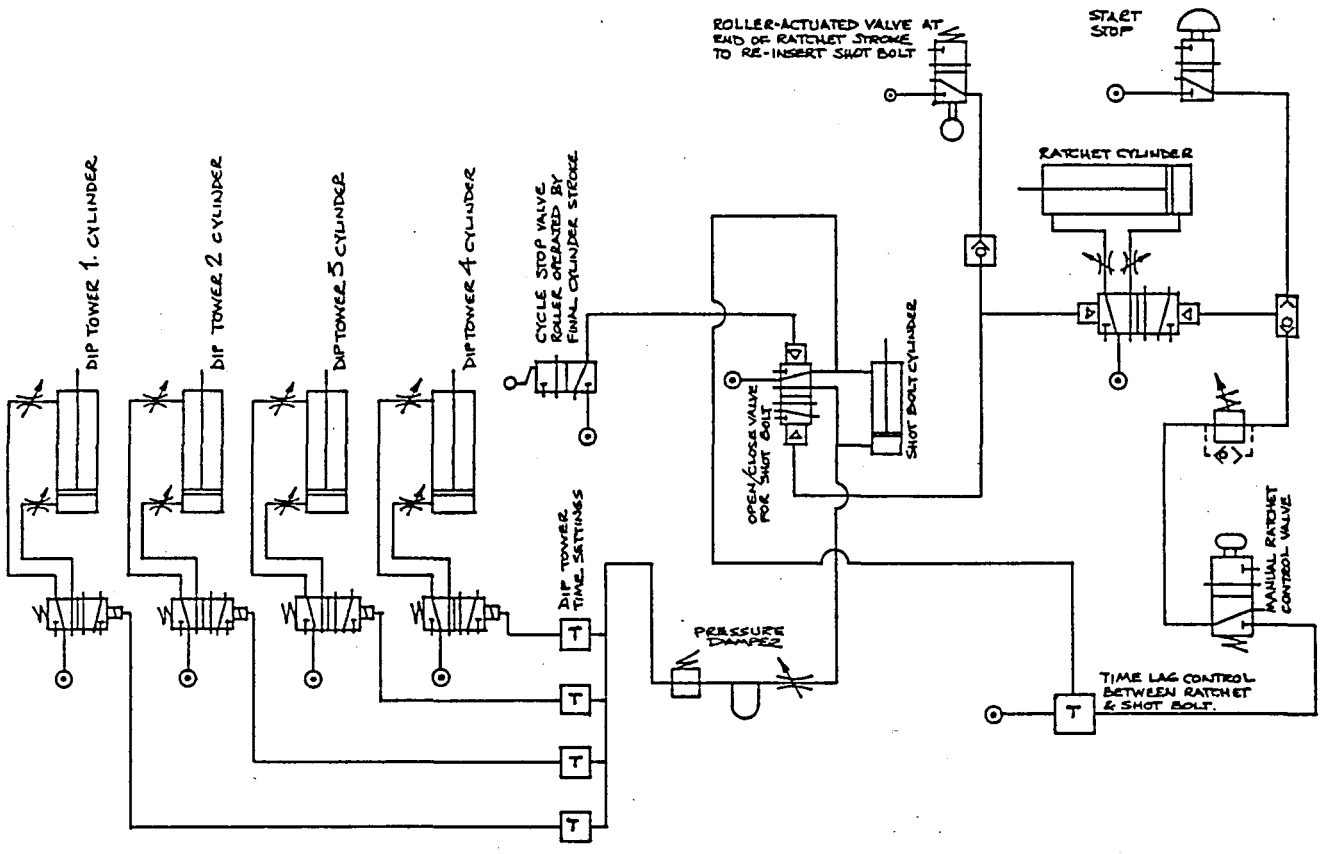

FIGURE 5.9: PNEUMATIC CIRCUIT OF THE IMMERSION-COATING MACHINE

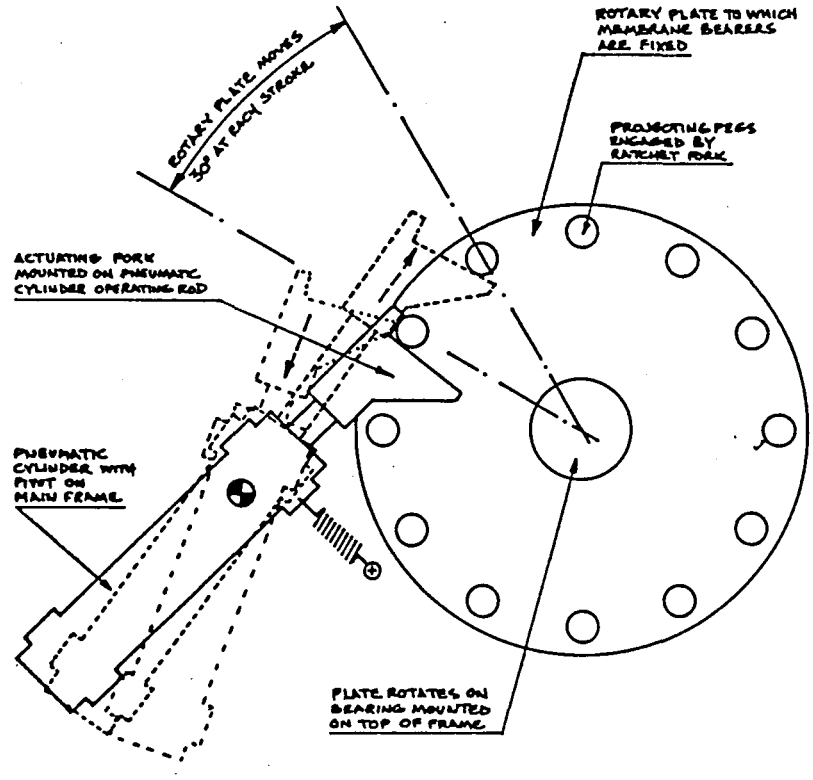

FIGURE 5.10: IMMERSION-COATING MACHINE RATCHET MECHANISM

signalled to rotate another step on the return of the last vessel to its rest position. The whole process of step motion and raising and lowering of the vessels is totally automated and is repeated continuously.

A drawback of the above operation is that the durations of specific actions are interdependent and immersion and drainage times cannot be changed at will. A problem will result, for example, if say, a precursor dip time of six minutes together with a precursor drainage time of three minutes is required. In this example, the step-time of the carousel will be six minutes, resulting also in a six minutes dwell-time drainage station. However, if two precursor dip tanks are used at successive stations, the dwell time can be reduced to the required three minutes.

Thus, by repeating the same action at two successive stations, some flexibility can be introduced into the duration of an operation. It has, however, the disadvantage that larger volumes of reagents are required.

The scheme below illustrates the amount of flexibility that can be introduced by repeating a single operation at two or more adjacent stations.

		Precursor		Cross-link		
6 Stations	*	*	*	*	*	*
	load	dip	drain	dip	drain	off-load
Load time (min)	6					6
Dip time		6		6		
Drain time			6		6	

		Precursor			Cross-link			
7 Stations	*	*	*	*	*	*	*	
	load	dip	dip	drain	dip	drain	off-load	
Load time (min)	3						3	
Dip time		(3 + 3)			2			
Drain time				3		(1 + 3)		

		Precursor				Cross-link			
8 Stations	*	*	*	*	*	*	*	*	*
	load	dip	dip	dip	drain	dip	drain	off-load	
Load time (min)	3							3	
Dip time		(2 + 2 + 2)				1			
Total drain		(1 + 1 + 1)			3		(2 + 3)		

Comments on immersion-coating

In summary, features of the immersion-coating technique are:

i) The method can be used to produce UTF composite RO membranes, as was proved during the study.

ii) It is costly to design and construct the equipment so as to allow absolute freedom with regard to the durations of the various operations, namely, the contact and draining periods. It is, however, possible.

iii) More than double the ultimate membrane length is necessary to provide head-space for the accommodation of the reagent vessels, membranes and membrane transport devices, which can make housing of such equipment difficult when three metre long membranes are produced.

iv) Since the whole membrane is wetted with the reagents, fiber debris originating from the fabric on the outside of the membrane support tube can contaminate the reagents. Continuous filtration is recommended.

v) The reagents have a limited shelf-life, especially the cross-linking reagent which hydrolyzes when it comes into contact with water. Provision must consequently be made for regular replenishment of large volumes of membrane reagents. The reagent tanks must also be cleaned thoroughly each day.

vi) The reagents are hazardous (irritants, sensitizers and carcinogens) and the fabrication area must be ventilated well. Proper care must be exercised to avoid direct human contact with the reagents and inhalation of their fumes.

vii) Temperature control is important since it affects the rate of the cross-linking reaction. An ambient temperature of 20 ± 2°C was ensured in the fabrication laboratory.

5.2.2 FILL-COATING

An investigation of the fill-coating technique, in which the tubular membranes are filled with, rather than immersed in, the membrane-forming solutions, was made to:

i) reduce the volumes of the chemicals used in the immersion-coating method to produce specified quantities of membranes;

ii) introduce time-dependent sequences of operation; and to

iii) reduce the risk of contaminating the membrane-forming solutions with foreign materials.

The prototype fill-coating equipment that has been designed and constructed for membrane fabrication is fully microprocessor-controlled, pneumatically operated and simple to operate. An important aspect of fill-coating is that only the inside of the membrane comes into contact with the membrane chemicals, which reduces the risk of contaminating the membrane chemicals with foreign material. It also ensures that less cross-linking reagent is used per batch of membranes produced, compared with the amount required in the immersion-coating process, where the cross-linking reagent also reacts with the precursor taken up by the support fabric.

The membranes are held at an angle of 15° from the horizontal during the filling operation, which limits the amount of aqueous precursor which weeps through the membrane. None of the cross-linking reagent is lost through weeping as a hydrocarbon is used as solvent.

5.2.2.1 Fill-coating machine

This machine, which is illustrated in Figure 5.11, consists of;

i) A support frame, above which a 3,2m-long tray is mounted on a horizontal pivot, rather like a large see-saw. This tray is pneumatically operated and may be tilted and locked in a number of different positions. The support membranes to be coated are positioned in grooves along the length of the chemically resistant epoxy-coated *(6)* tray.

ii) Two separate filler columns, each of which supports a carriage for the vessel that contains the membrane-forming solutions. The vessels may be raised and lowered pneumatically and halted at various positions as required. The vessels are connected by flexible tubing to manifolds at the ends of the tilting tray. The manifold outlets, in turn, are connected directly to the tubular membranes with the aid of connectors, illustrated in Figure 5.12.

iii) A microprocessor control unit, which controls all sequences of movement, may be programmed to (a) tilt and stop the tray containing the membranes at various positions, (b) raise and lower the filling vessels, (c) hold these vessels at pre-determined levels for computed times and oscillate the vessels to produce a washing effect inside the liquid-filled membranes.

The filling columns can be positioned one at each end or both at one end of the membrane tray since all the movements of the tray and filler vessels are programmable. The technique of fill-coating is illustrated in Figure 5.13, which shows the sequence of operations when the two filling columns are at the same end of the membrane tray.

The equipment functioned well and no insoluble problems arose in the operation of the equipment. Choice of the connector tube (between the cross-linking reagent vessel and the glass manifold) material did, however, pose a problem. This tube must be flexible, but plasticized PVC tubing was not used for fear of the extractable plasticizer affecting the chemical cross-linking reaction. Flexible PTFE tubing was a better choice.

Operation of the machine involves:

i) packing the tray with membranes and fitting riser tubes to one end of the membranes (the riser tubes remain in place until completion of the whole operation);
ii) connecting the precursor manifold to each individual support membrane, and activating the precursor sequence of filling and draining;
iii) disconnecting the precursor manifold to connect the cross-linking reagent manifold, after which the cross-linking reagent sequence of filling and draining is activated;
iv) removing the coated membranes from the tray for final heat treatment.

Comments

During the course of research on UTF composite membrane fabrication techniques and formulations, the consumption of the membrane forming chemicals, *i.e.* the precursor and cross-linking reagents, had to be adjusted so that they matched the rate of chemical production. As the materials are not commercially available, they had to be synthesized from raw materials, which was a study on its own *(1)*. The net effect was that the membrane materials were synthesized in rather small quantities, and as there were batch-to-batch variations in the physical and chemical properties of the materials produced, especially during the period of product development, the scale of membrane production was adjusted according to the volume of the batches of the materials produced.

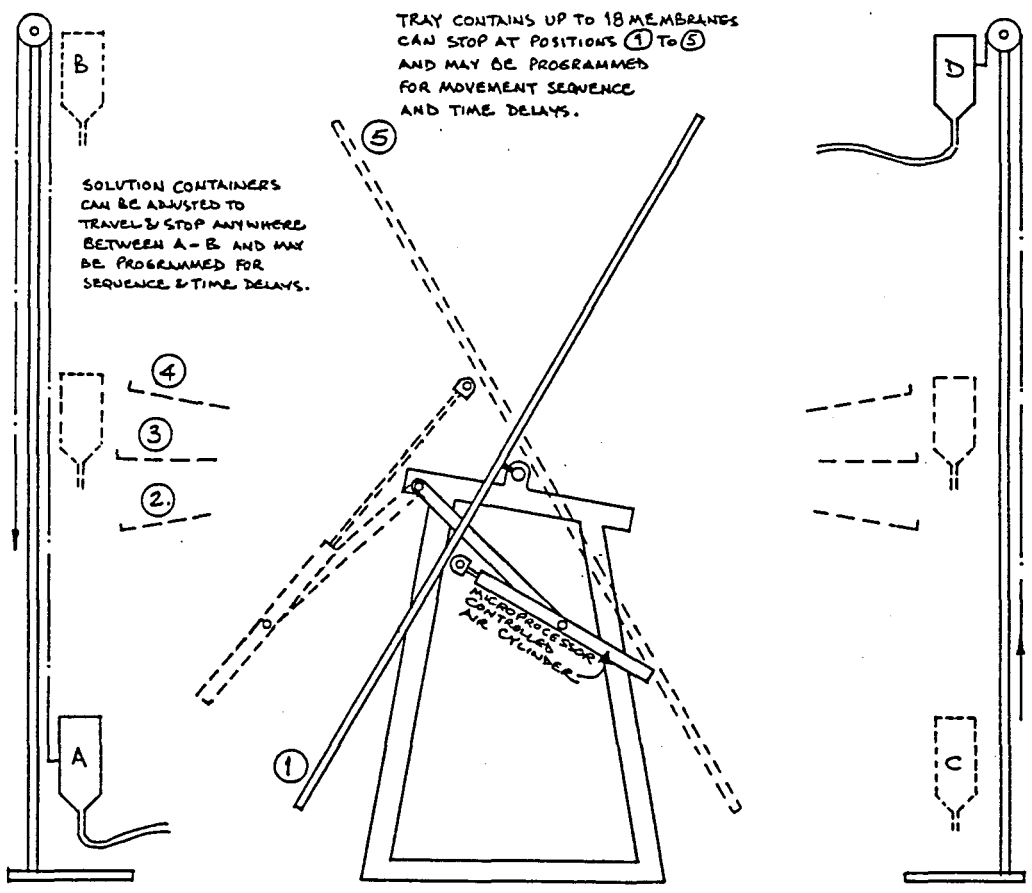

FIGURE 5.11: FIRST PROTOTYPE FILL-COATING MACHINE

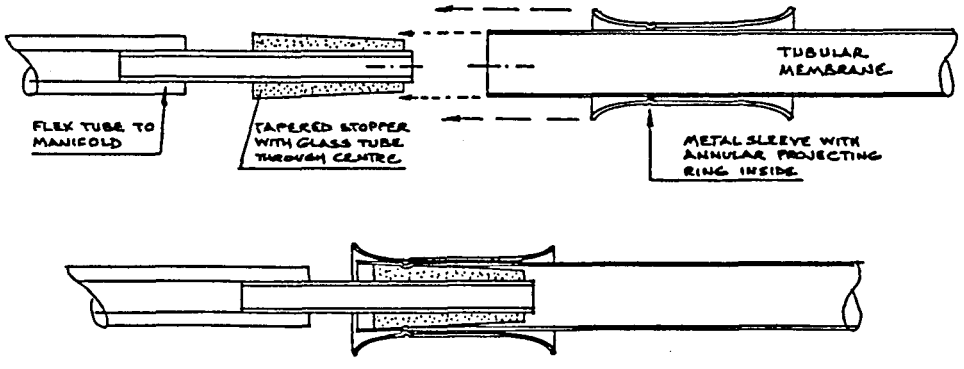

FIGURE 5.12: ILLUSTRATION OF THE MEMBRANE CONNECTOR PIECES

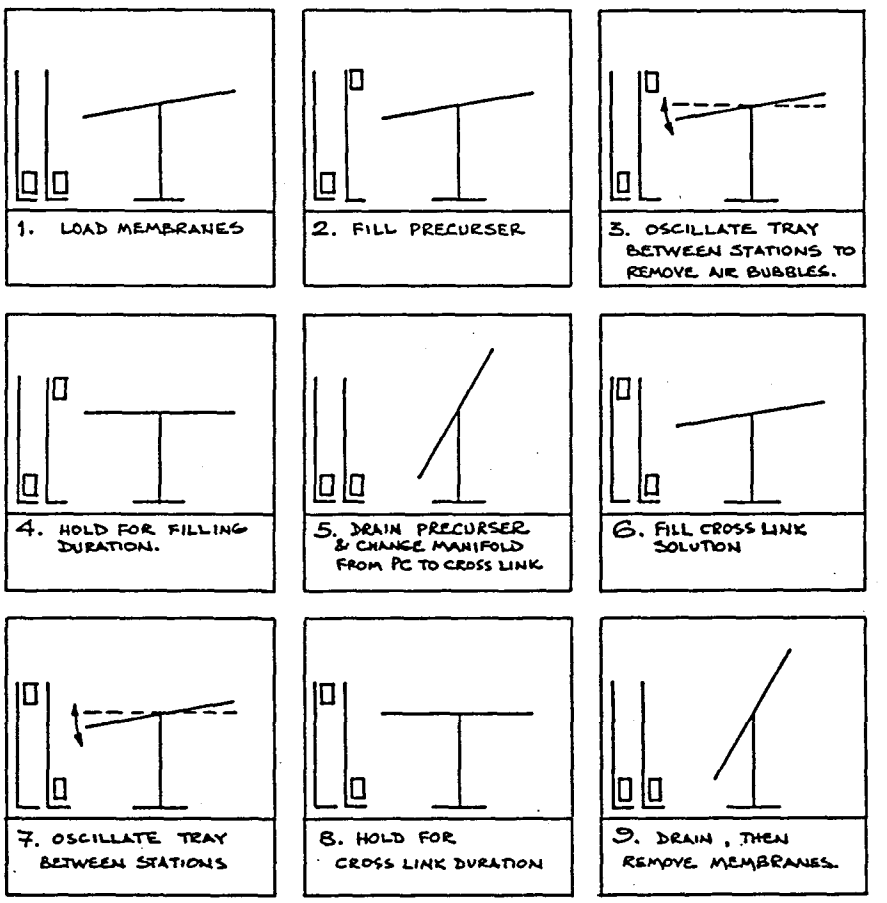

FIGURE 5.13: SEQUENCE OF FILL-COATING, TWO TOWERS AT ONE END

For this reason the bulk of the membranes produced during the period of experimentation were 1,2m long, and to further minimize chemical consumption, manual immersion-coating was used as the method of fabrication. The membranes were coated in 65mm diameter glass tanks, into which seven tubes fitted snugly. On average 90g of each of the membrane materials was used to produce up to ten sets of 1,2m membranes.

5.3 MEMBRANE DRYING AND CURING OVENS

Membrane drying or curing at elevated temperatures is the final step in creating the thin desalting matrix on the substrate membrane. Two kinds of oven were designed and used. The one oven operated on the hot air updraft principle, and the other was a horizontal radiation oven.

5.3.1 VERTICAL UPDRAFT OVEN

This oven consists of two sections, namely, a heating section at the bottom which contains the electrical heating elements, and the chimney section, in which the membranes are suspended.

The temperature is regulated by means of four PD temperature controllers, their respective probes being positioned at the bottom inlet into the chimney. Each controller controls a single bank of eight 500W heating elements. The total output per bank is determined by the manner in which the heating elements are connected, whether in series, in parallel, or combinations of the two. Two further banks of elements are reserved for boosting purposes, depending on ambient temperature conditions.

The temperature of the oven can reach 110°C within 15min of the ovens being switched on, and that temperature can be maintained to $\pm$0,5°C. The temperature difference between the bottom section of the insulated chimney and the top section is $\pm$1,5°C.

No problem has ever arisen due to fumes from the oven as these are exhausted at the chimney top, from where they rise to be extracted by the central ventilation system of the building.

5.3.2 HORIZONTAL OVEN

The tunnel oven was designed to permit the membranes to be treated in the horizontal position and to simplify the handling of 3m membranes. The design consists of a radiation oven section, placed over a transportation bed. The transportation bed was designed to rotate the membranes as they are transported through the oven to ensure even heating of the membranes. (See Figures 5.14 and 5.15).

The heating section has three banks of two infrared radiation heating elements each, which divide the oven into three heating zones, each with its own temperature controller. The maximum operating temperature of the oven is 150 $\pm$ 1°C.

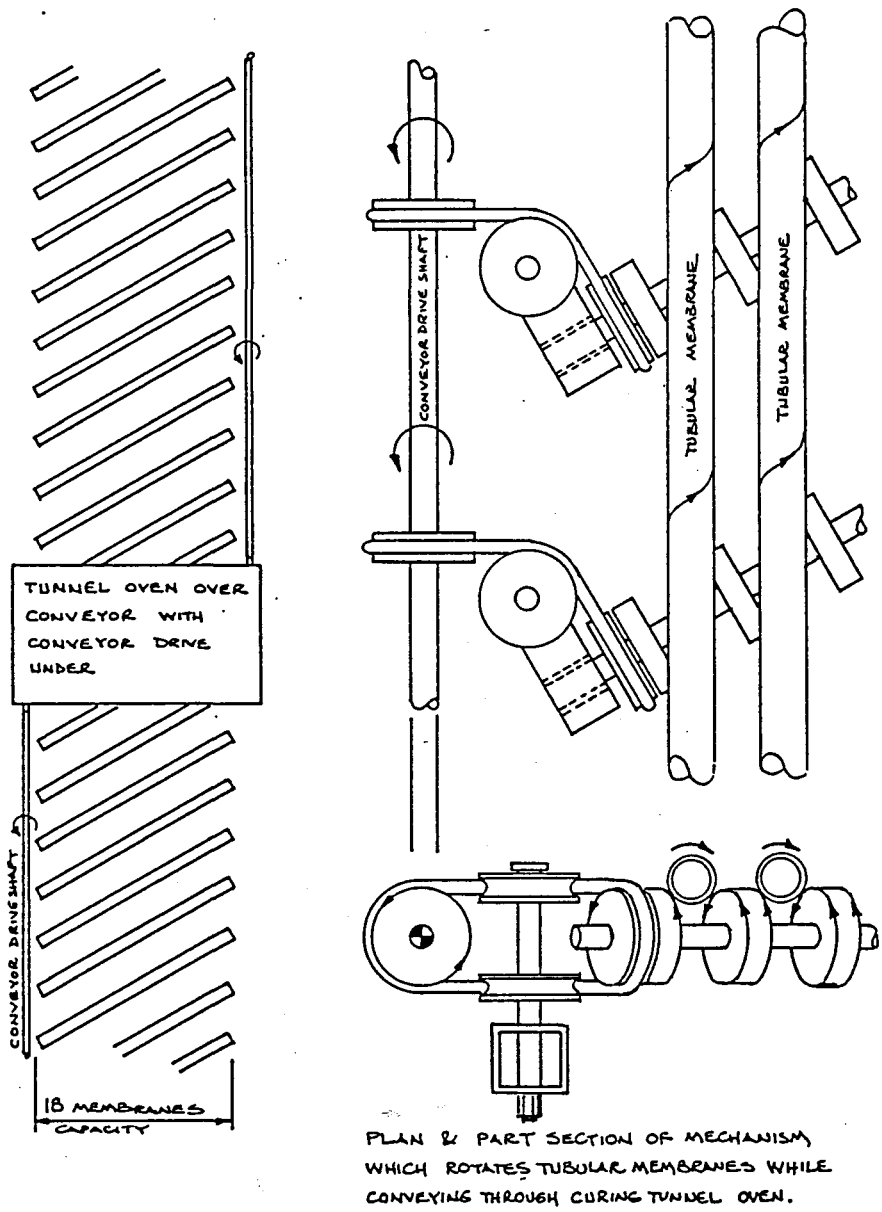

FIGURE 5.14: HORIZONTAL TUNNEL OVEN

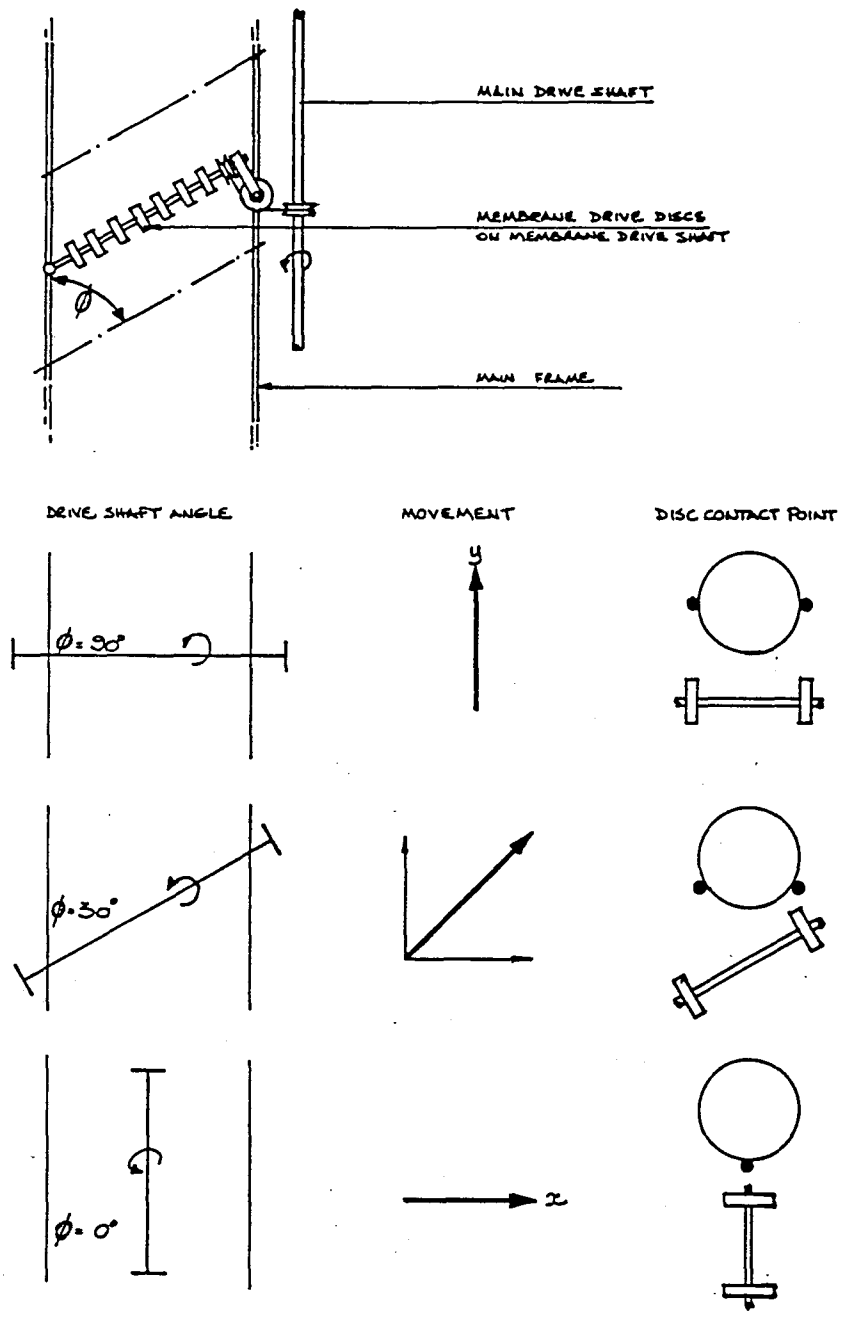

FIGURE 5.15: HORIZONTAL OVEN. PRINCIPLES OF TRANSPORTATION

The transportation bed, which extends 3,5m on either side of the oven, consists of a number of membrane drive shafts (spaced at 200mm centres) lying at an angle to the width of the bed. The membranes rest on disks that are spaced at 20mm centres along the lengths of these drive shafts. These disks propel the membranes forward, and there are 19 disks to allow for the accommodation of eighteen membranes. The retention time in the oven can be varied.

The speed of rotation relative to forward motion can be altered by changing the angle ϕ between the membrane drive shaft and the direction of travel. The principle of operation of the transportation bed is as follows:

If the angle ϕ shown in Figure 5.15, is 90°, no rotation will take place and the membranes would merely be transported forward. If the angle is decreased until the membranes touch the staggered drive disks on either side of it, the membranes will start rotating. The membranes will also be propelled forward by the component of force in the *y*-direction. The closer the points of contact between the two staggered disks are to the lowest point on the bottom contour of the membrane, the faster the membranes will rotate. When, therefore, the angle ϕ is 0° the membranes will merely rotate since the drive disks are aligned parallel to the membrane and there is no component of force in the *y*-direction.

It was difficult to extract fumes from this oven because of the size of the oven. As it was, the oven already added to the heating load of the air conditioning system which was barely able to cope with summer conditions and maintain an ambient temperature of 20°C in the laboratory. Extraction further increased the heat-load. A compromise was to set the room temperature to 22°C, partially extract the fumes, and to provide for breathing by wearing forced draft breathing masks.

5.4 MEMBRANE EVALUATION EQUIPMENT

The equipment used for the evaluation of membranes consists basically of a pressurized process fluid loop, connected to test cells within which the membranes are housed individually. The same equipment is used for both high- and low-pressure evaluation of membranes as is required in typical RO or UF performance studies.

5.4.1 PUMP SKID

The test system is pressurized by means of a triplex diaphragm pump, Hydra-Cell D10, which has a maximum delivery rate of 38lpm at a hydraulic head of 6,8MPa. The pump is connected to a 3kW electrical motor by means of twin V-belts. The pump is operated at a delivery rate of ≈20lpm which reduces noise and wear of the pump valves and seats. The linear flow-rate across the membranes is controlled by means of a by-pass ball-valve, and the operating pressure is controlled by means of a needle valve with a 6mm orifice.

The system is safeguarded against pressure surges by means of a double-contact pressure gauge, which automatically switches the system off when the system pressure exceeds set limits. The operating temperature

is controlled to ±0,2°C of set point by means of a 6m stainless steel cooling coil situated in the feed tank. Pressurized cooling water is allowed to pass through the cooling coil by the action of a solenoid valve, controlled by an RKC PB-96 temperature controller.

Figure 5.16 illustrates the flow diagram of the tubular membrane test equipment. Interconnecting flow-lines are from cloth-braided high-pressure rubber hoses, and all wetted metal parts are fabricated from 316L stainless steel.

5.4.2 TUBULAR TEST CELLS

A cross-sectional representation of the tubular test cell is given in Figure 5.17. The test cell was designed on the principle of the commercial pressure support design of Patterson Candy International in which the tubular membrane is housed within a perforated stainless steel tube. Rubber grommets are inserted into the ends of the membranes which seal under pressure to produce a leak-free assembly.

The test cells are designed to house membranes of 1m and 500mm lengths, excluding the dead area beneath the rubber grommets. The cells are mounted on racks and are arranged in sets of six, all connected in series. When two sets together are coupled together, twelve cells can be served by one pump skid. The operating pressure is set according to a calibrated pressure gauge situated between the two sets of membranes.

5.4.3 EVALUATION

Measurements by which membranes are evaluated and categorized are, for RO membranes, salt rejection and water permeability, and for UTF substrate membranes, pure water permeability [PWP].

Standard conditions of evaluation have been adopted for all these evaluation tests.

CA membranes. RO evaluation

Operating pressure	4,1	MPa
Linear flow velocity	1,5	m/s
Operating temperature	25	°C
Feed solution make-up	Distilled or RO permeate (<10μS/cm)	
NaCl feed additive	5	g/l
Duration of test	4 - 63	h

UTF composite membranes. RO evaluation

Operating pressure	2	MPa
Linear flow velocity	1,0	m/s
Operating temperature	20	°C
Feed solution make-up	Distilled or RO permeate (<10μS/cm)	
NaCl feed additive	2	g/l
Duration of test	18 - 63	h

Support membranes. PWP evaluation

Operating pressure	200	kPa
Linear flow velocity	0,5	m/s
Feed temperature	20	°C
Feed solution make-up	Distilled or RO permeate (<10μS/cm)	
Feed additive	None	
Duration of test	Instant flux, 5 min maximum	

5.4.3.1 Salt rejection measurements

The salt rejection capability of RO membranes is determined by differences between the conductivity of the feed solution (F_c) and that of the permeate (P_c), expressed as a percentage of the feed solution conductivity:

$$\text{Conductivity salt rejection} = (1 - P_c/F_c)100 \quad \%$$

A Radiometer flow-through conductivity cell, connected to a Radiometer CDC83 conductivity meter is used for conductivity determinations. Water at a controlled temperature (30 ± 0,1°C) is passed through the conductivity cell, and the appropriate corrections are made to relate the conductivity to that at 25°C. The test cell is calibrated daily by means of a standard KCl solution. The conductivity cell is cleaned when the cell constant correction deviates by more than 1% from the value given by the suppliers. The sodium chloride concentration of the sample is obtained from a regression model fitted to a NaCl/conductivity (25°C) calibration curve (accuracy ±2%).

5.4.3.2 Water permeability (flux) measurements

The water permeability of the membrane is expressed as the volume of the product which permeates through a unit of membrane area in a given period of time. In countries that have adopted the metric system, membrane flux is expressed as: litres per square metre per day, the quantity being abbreviated as lmd. (This notation is used throughout the text).

$$1 \text{ lmd} \equiv 1{,}157 \times 10^{-8} \ m^3 m^{-2} s^{-1}$$

In the determination of membrane flux, a stopwatch is used to measure the time-period within which a volumetric flask of known volume is filled to its mark. This rate of flow is multiplied by a membrane cell constant to obtain the membrane flux. The constant incorporates the membrane area and corrections for dimensions into one value.

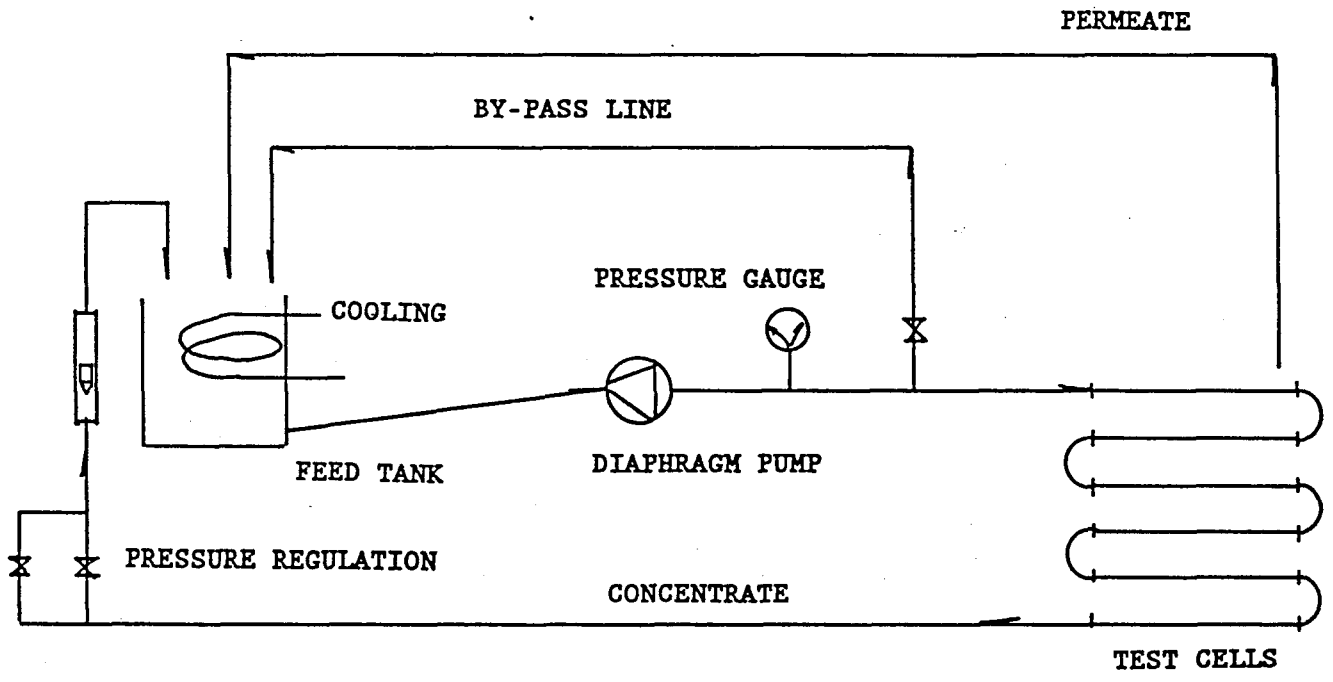

FIGURE 5.16: HIGH PRESSURE TEST LOOP FOR MEMBRANE EVALUATION

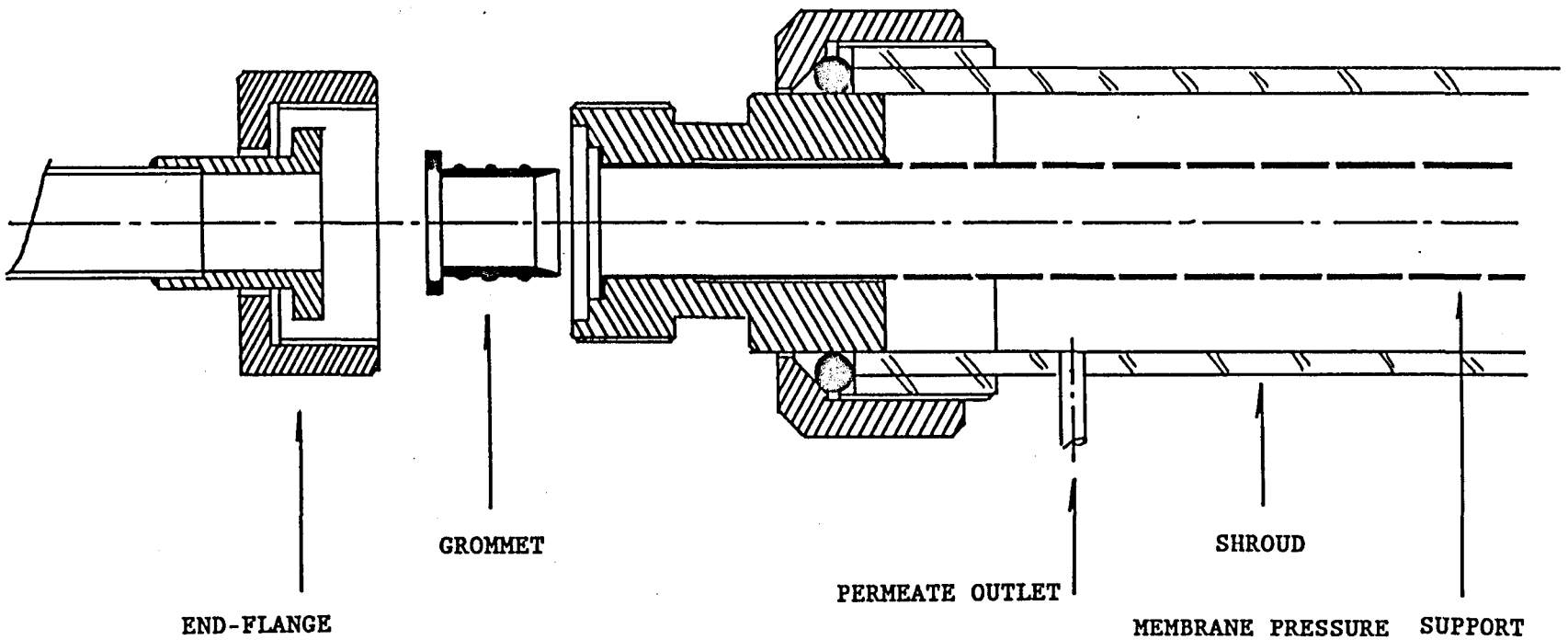

FIGURE 5.17: TUBULAR MEMRBANE TEST CELL

5.4.3.3 Membrane permeability coefficients

A method which can be used to compare the RO performance of membranes with different salt rejection and water permeability performances, was derived from the rejection model and the theories of Lonsdale *(7)*.

This was achieved by comparing the pure water permeability coefficient (A) and the salt permeability coefficient (B) of the different membranes at similar operating conditions, through the relationship A^2/B. The basic transport equations for these parameters, assuming that the fluxes are diffusional *(8)(9)*, are;

$$\text{Water flux:} \quad F_1 = A[\Delta P - (\pi_w - \pi_p)]$$

$$\text{Salt flux:} \quad F_2 = B(C_w - C_p)$$

where

A	membrane permeability coefficient for water
B	membrane permeability coefficient for salt
ΔP	pressure difference across the membrane
π_w	osmotic pressure at the membrane-brine interface
π_p	osmotic pressure of the product water
C_w	salt concentration at the membrane-brine interface
C_p	salt concentration in the product water

As desalinated product, water, is removed through the membrane, there is an increase in solute concentration at the membrane and brine interface. This concentration polarization effect can be determined from a mass balance on the convective flow of salt carried to the membrane surface by the bulk brine flow, diffusional back-flow of salt and salt flow through the imperfect membrane barrier. The extent of concentration polarization is defined by a ratio of the membrane wall solute concentration, C_w, to the bulk brine concentration, C_b. A higher concentration polarization ratio would obviously lead to a lower permeate flux due to an increase in π_w, and an increase in the salt flux, due to an increase in C_w. It is thus obvious that concentration polarization ratios have an effect on membrane performance and should be incorporated into the above performance equations.

For turbulent flow in tubular membranes the concentration polarization ratio is given by *(10)*:

$$C_w/C_b = 1/D_r + (1 - 1/D_r)\ \exp(F_1\ N_{Sc}^{0,67})/(U_b j_d)$$

$$D_r = D_b/D_p = 1/(1 - R)$$

where

C_w/C_b	concentration polarization
C_w	salt concentration at membrane/brine interface [g/cm^3]
C_b	salt concentration in bulk of flow [g/cm^3]
D_r	ratio of bulk brine concentration to product concentration
F_1	water flux [$cm^3cm^{-2}s^{-1}$]
N_{Sc}	Schmidt number for salt diffusion
U_b	bulk brine velocity [cm/s]
j_d	Chilton-Colburn (dimensionless) mass-transfer factor
R	membrane salt rejection [%]

$$N_{Sc} = \nu/D$$

where

ν	kinematic viscosity [cm^2/s]
D	salt diffusion coefficient [cm^2/s]

The Chilton-Colburn mass transfer factor is;

$$j_d = 0,023\ N_{Re}^{-0,17}$$

where

N_{Re}	Reynolds number (dimentionless)
d	tubular membrane inside diameter

expressed as;

$$N_{Re} = U_b d/\nu$$

After the necessary assumptions and substitutions have been made, concentration polarization is incorporated into the two performance equations and the following relationships result by which the A and B coefficients can be obtained *(11)*:

$$C_w/C_b = 1/D_r + (1 - 1/D_r)\ \exp\ (F_1\ \nu^{0,5} d^{0,17})/(0,023 U_b^{0,83})$$

$$F_2 = F_1 C_p \text{ (neglect density differences)}$$

$$F_1 = A[\Delta P - \pi_b(C_w/C_b) + \pi_b/D_r]$$

$$F_2 = BC_b(C_w/C_b - 1/D_r)$$

5.5 MEMBRANE SUPPORT FABRIC ADHERENCE

An Elcometer was used to determine quantitatively the adherence between the phase-inversion membrane and the support fabric. The Elcometer is normally used in the coatings industry to determine the bond-strength between various coatings and their substrates.

The instrument works on the principle that a force is applied to a stub, which is epoxy-glued to the specimen surface, against the action of a spring. A marker on a calibrated scale indicates the force applied the moment the coating breaks loose from the surface.

As the membrane support fabric is not a rigid structure, the procedure had to be modified to make provision for the flexibility of the support fabric when the membrane bond-strength was determined. A steel plate, containing a concentric hole, of diameter 1mm greater than that of the stub, was placed over the stub and onto the membrane surface. The tripod of the Elcometer rest on this plate.

5.6 VISCOSITY DETERMINATIONS

A Brookefield viscometer was used to obtain the viscosity of membrane casting solutions. All PS and PES casting solution viscosity measurements tabled, had been determined at a constant temperature of 20°C, with a no. 4 spindle.

Low shear mixing was used in the preparation of all polymer solutions. After the casting solution component was accurately weighed into glass containers on a two-decimal place Mettler electronic balance, they were slowly rotated until their contents were homogeniously mixed. The solutions were filtered through a 1μm stainless steel filter before use.

5.7 MICROSCOPY

5.7.1 SCANNING ELECTRON MICROSCOPY [SEM]

The cross-section morphology and surface characteristics of asymmetric membranes were investigated with the aid of a Hitachi, scanning electron microscope. The dry membrane samples were gold-palladium coated on a sputter-coater before analysis. Different techniques were employed to prepare CA and polysulphone membrane samples for gold-palladium alloy plating and SEM analysis.

The cross-section fracture surface of CA membranes were obtained by immersing the wet membrane sample, clamped in a SEM sample holder, in liquid nitrogen. At these temperatures the membrane became brittle and could be fractured with ease. This was not so with the PET support fabric, for which reason the CA membrane was preferably removed from the support fabric before being mounted. After the fracture surface

had been obtained, the water was removed from within the CA sample-structure by subliming the frozen water under vacuum.

PS and PES membrane samples were stored in the dry state. The membranes were rewetted with water by conditioning the samples in methanol/water mixtures. Membrane samples, supported or unsupported, were also fractured at liquid nitrogen temperatures, but because the membranes were not as brittle as the CA membranes, the fracture surface was obtained by cutting an immersed sample with a surgical knife in a smooth action. The entrapped frozen water reduced the tendency of the polymer to smear when cut.

The samples were analysed at acceleration voltages of 15kV to reduce the possibility of incurring damage to the membrane specimen.

5.7.2 OPTICAL MICROSCOPY

Optical investigations were performed on membrane samples with the aid of a three-dimensional optical microscope, which has an attachment for a camera. The equipment gave magnifications of up to 100x.

5.8 RATE OF MEMBRANE PHASE SEPARATION

A method used to determine the relative rates of membrane phase-separation from different polymer solutions, reproducibly, is to form a 110mm wide membrane of 0,2mm thickness, by means of a Gardener applicator, on a sheet of plate-glass. With another applicator a square section of 110mm is marked off by drawing the second applicator across the 110mm wide nascent film. The glass plate is immersed in a continuous motion in a coagulation bath of appropriate composition and temperature. The immersion procedure is timed from the moment the plate is introduced into the bath until the membrane becomes detatched from the glass plate.

An accuracy of $\pm 5\%$ can be obtained with relatively fast separations. The accuracy decreases as the rate of phase separation decreases. A directly related problem arises when membranes are cast from solutions of relatively high viscosity; the nascent film tends to be relatively thicker than a film cast from a solution of relatively low viscosity. By trial and error the casting blade can be set to produce membranes of comparative thickness.

LIST OF REFERENCES

1. Hurndall, M., PhD-thesis in preparation, Proposed Title "Polyvinylamidine RO membranes", (1988), Institute for Polymer Science, University of Stellenbosch
2. Jacobs, E.P., The design of a tubular RO element, MSc Thesis, (1980), University of Potchefstroom
3. Jacobs, E.P., Sanderson, R.D., Botha, G.R., Development of membrane support systems and modules, Final Report, (1982), Water Research Commission, Pretoria
4. Jacobs, E.P., Hurndall, M., Research on membrane development and fabrication for RO and UF, Final Report, (1986), Water Research Commission, Pretoria
5. Pienaar, H.S. The synthesis and physical properties of semipermeable polymeric membranes used in water purification by the process of RO, PhD thesis, (1977), University of Stellenbosch
6. Sanderson, R.D., Bardenhorst, J.B., SA Patent 83/1661 (1983)
7. Lonsdale, H.K., Desalination, 13(1976)317-325
8. Loeb, S., Rosenfeld, J., Turbulent region performance of RO desalination tubes., Experience at Coalinga pilot plant, Desalination Report no 10, (Oct. 1966), Water Resources Centre, Washington, DC
9. Merten, U., Lonsdale, H.K., Riley, R.L., Ind. Eng. Chem., Fund., 3(Aug. 1964)210
10. Brian, P.L.T., Influence of concentration polarization on RO system design, 1st Int. Symp., Water Desalination, (Oct. 1965), Washington, DC
11. Goel, V., McCutchan, J.W., Systems design of a tubular RO plant, Desalination Report no 64, (Jan. 1977), Desalination Centre, Washington, DC

CHAPTER VI

DESIGNED EXPERIMENTS, RESULTS AND DISCUSSION

6.0 INTRODUCTION

Aspects of the design and operation of prototype membrane fabrication and evaluation equipment were discussed in the previous chapter. In this chapter, which consists of three sections, aspects regarding RO membrane formulation studies, will be discussed. In the first section, the research on, and development of, formulations for producing asymmetric tubular CA RO membranes are covered. The design of asymmetric substrate UF membranes, used as support for the UTF composite RO membranes, is dealt with in the second section, and matters relating to the formulation of an UTF composite RO membrane is the subject of the last part of this chapter.

6.1 TUBULAR CELLULOSE ACETATE RO MEMBRANES

The formulation of cellulose acetate membranes, although extensively studied as mentioned in chapter II, was not as satisfactorily described in the literature for membranes of tubular geometry than for flat-sheet membranes. This therefore gave rise to an investigation of tubular cellulose acetate [CA] reverse osmosis [RO] membrane fabrication procedures and fabrication formulations.

Earlier research *(1)* revolved mainly around matters relating to the design and development of production and ancillary equipment, fabrication procedures and methods, and the selection of membrane materials. Three basic "tools", resulted from that work, namely;

i) the tube winding machine and extrusion-die design
ii) the technique, and
ii) a set of fixed fabrication conditions (Table 6.1).

These provided the foundation on which to base further investigative work. In this section, the second part of the investigation defined above, namely, that of formulating conditions for continuously produced tubular CA membranes, will be addressed.

This was the next logical step in the development of the tubular CA membrane in order to gain a more formal understanding of how fabrication variables affect membrane performance. The salt rejection capability of a

TABLE 6.1: FIXED CA MEMBRANE FABRICATION CONDITIONS

Linear casting speed	3,9 cm/s
Travel distance nascent membrane	140 mm
Annular extrusion gap	200 μm
Coagulation bath temperature	< 1,5 °C
Coagulation bath composition	deionized water
Gelation time allowed	2 h
Drying air	medical air
Annealing tank composition	deionized water, 0,5% glycerin, pH5
Annealing time	30 min
Support fabric material	Reemay 3396 (polyester)
CA membrane material	Eastman Kodak 400-25
Coagulation bath entry	Vertical

CA membrane can, for example, be improved by increasing the temperature at which the membrane is annealed. Membrane flux performance, however, is inversely related to salt rejection performance, and only a careful balance between fabrication variables will ensure a membrane with optimal flux performance at a given salt rejection. One approach which could have been followed in this study was to study membrane fabrication variables qualitatively; however, in order to relate membrane performance quantitatively to fabricating conditions, the use of experimental protocols based upon statistical design was essential.

The objective of the present study was therefore to relate the salt rejection and flux performances of CA membranes mathematically to fabrication conditions. To keep the number of experiments needed to support such an attempt to the minimum, two-level factorial-designed experiments were used through-out the study. Numerical optimization techniques (Box Complex algorithm) were used to forecast the expected optimum flux response for specified salt rejection performances in the range of interest (90, 93 and 95% in this case).

At this stage of the programme, membranes with very little batch to batch variation in their performances could be produced. It must be remembered however, that cost considerations dictated the use of a single-ply membrane support tube, rather than a more durable, but expensive, double-ply tube consisting of a smooth porous polyolefin inner ply, bonded to a polyester outer fabric *(2)*. The extent to which roll to roll variation in the quality of the fabric used could affect the reproducibility of membrane performances in the long run was not known.

Another aspect of the formulation study also caused reserve. A tubular membrane film must necessarily be extruded on the inside of a narrow-width channel, in an environment created by the air trapped between the extrusion-die and the coagulation medium (membrane cavity). A short time-period is permitted before the membrane enters the coagulation medium. It was known from the earlier study (Table 6.1) that reproducible membrane performance can only be ensured if *e.g.* the cast membrane entered the coagulation tank perpendicular to the coagulation-medium interface. However, to what extent other factors, such as non-stationary conditions which might exist within the membrane cavity (*e.g.*, moisture, temperature, acetone vapour concentration levels, *etc.*) could interfere with small changes brought about in membrane formulations, were unknown. All of these aspects put a dimension to tubular membrane formulation which is different to, and unaccounted for by, flat-sheet membrane formulation studies as described in the literature.

6.1.1 FIRST CA 400-25 DESIGNED EXPERIMENT

6.1.1.1 Selection of fabrication variables

Four factors which influenced the properties of the final membrane were chosen for the initial study and these, together with their variables, are listed in Table 6.2.

One variable was used to fix the composition of the ternary casting solution CA/acetone/formamide. The ternary phase diagram *(3)* for this system, was used in developing a formula for fixing the casting-solution composition (see Figure 6.1). The straight line, passing through the Manjikian composition (CA 25%, acetone

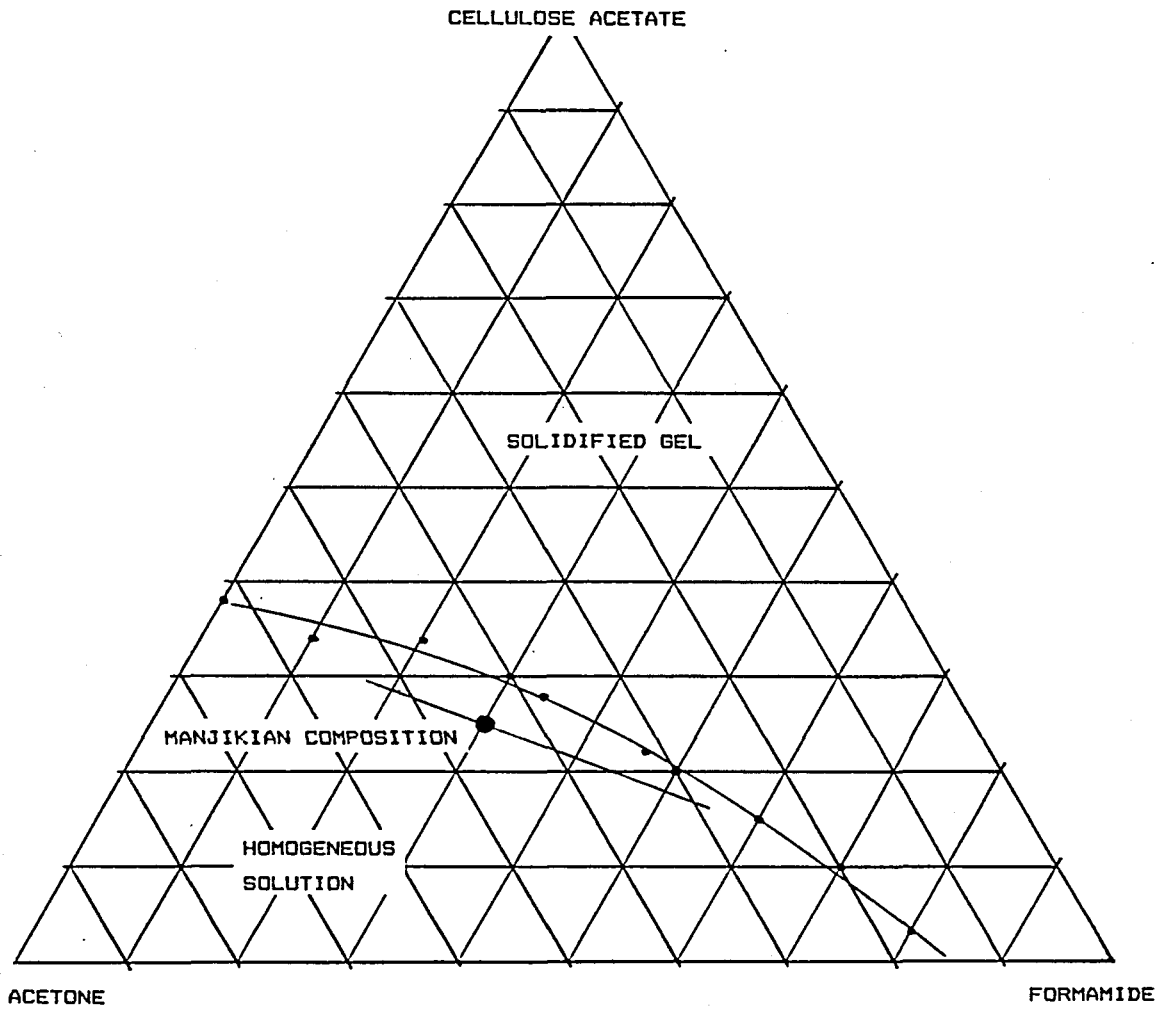

FIGURE 6.1: TERNARY PHASE DIAGRAM FOR THE CA/ACETONE/FORMAMIDE SYSTEM

45%, formamide 30%) represents a CA-to-acetone mass ratio of 0,556. When only the formamide concentration is varied, the composition of the casting solution is fixed along this line. The Manjikian composition was chosen as the base or mid-level *(4)*. CA grade 400-25 (Eastman Kodak) was used as membrane material and industrial grade acetone (distilled twice, 500mm vigereaux column) and Analar-grade formamide were used as solvents. All casting solutions were filtered through a 5μm sintered stainless steel filter on the day prior to use.

The membrane film was applied to the inside of the support tube by an extrusion process. The thickness of extruded film was not only a function of the annular extrusion gap between the extrusion die and the porous fabric support liner, but was also dependent on the viscosity of the solution and on the extrusion pressure. Excessive extrusion pressure resulted in the casting solution bleeding through the support fabric, especially in areas of low density, and an increase in film thickness; both are regarded as detrimental to the flux performance of membranes. Extrusion pressure was therefore incorporated into the study. As the low level for this factor, 1 000 kPa air pressure was used, which was 100kPa higher than the minimum pressure at which the extrusion-die-cavity would remain filled with casting solution at an extrusion rate of 3,9cm/s. The upper pressure was determined by system limitations.

As air is soluble in polymer solutions, care was taken to prevent direct contact of high pressure air with the casting solution, to avoid the dissolved gas forming small air bubbles at the low-pressure point of extrusion. For this reason the casting solution was dispensed to the extruder by means of a sealed piston inside a air-pressurized casting reservoir (see Figure 5.6).

Air-drying of the membrane before coagulation was another factor by which the membrane skin properties could be adjusted. The line in Figure 6.1 representing the casting solution composition, passes close to the gel region, and a small loss of acetone by evaporation should bring about gelation of the exposed nascent skin. Even if the amount of acetone evaporated is too small to bring about pre-gelation, it should have an effect on membrane surface characteristics and thus offer a means for controlling membrane-skin properties. The upper level for this variable was determined by the working range of the rotameter, the lower level being zero (no air drying).

The supply of air to the membrane cavity also served another purpose. A careful balance of the amounts of air supplied to, and withdrawn from (vacuum assisted), the cavity, enabled the relative height of the coagulation interface inside the tube to be controlled. A manometer was used to indicate the pressure difference and the stability of the liquid interface inside the tube (see Figure 5.6).

In order to render the CA membrane fit for use as an RO membrane, the membrane must be post-treated by heat treatment (annealed). As variables for this factor, the second relaxation temperature (77°C) and the temperature at which crystallization is favoured (93°C) were chosen, respectively, as the low and high levels for this factor *(5)*.

Ten full-length 3m membranes were produced at each treatment combination. Six 1,2m lengths were selected randomly from the long lengths for evaluation in 1m test cells. The mathematical averages of individual membrane performances were taken as representative of the response at the different treatment combinations.

6.1.1.2 Results

A complete randomized 2^4 factorial, without replication, was performed; the experimental observations and treatment combinations are shown in Table 6.3. The trials are listed in standard order in this table, although the various experiments were conducted randomly. Variable x_1 represents the transformed levels of factor A, x_2 that of factor B, x_3, factor C, *etc.* (see section 4.2.1) Three sets of membranes were produced at the centre-point of the design, and these results are also included in Table 6.3.

The main and interaction effects of the factors on the observed flux and rejection performances of the membranes are summarized in Table 6.4. Tables 6.5 and 6.6 list the details of an analysis of variance performed on the rejection and flux data.

Since each treatment was tested only once, there is no direct estimate of the experimental error variance by which the significance of the effects may be judged. However, it was assumed *a priori* that, subject to experimental confirmation, the three- and four-factor interaction mean squares may be combined to give an estimate of error variance as these interactions were regarded as being unlikely to be appreciable.

Thus, for Table 6.5, the mean square error [MSE] estimated from the three- and four-factor interactions was calculated as:

Sum of squares total	= 16,65
ϕ df	= 5
Mean square	= 3,33

At the 1% level the critical value of the F-statistic, $F(\phi_1,\phi_2)\alpha$, for $\phi_1 = 1$ and $\phi_2 = 5$ df is 16,3. Based on 1 df, mean squares are significant at the 1% level if they exceed the value of 16,3 x 3,33 = 54,28 (Table 6.5) and 16,3 x 13 388 = 218 224 (Table 6.6). At the 0,1% level $(F(1,5)_{0,001} = 47,2)$ the value of 47,2 x 3,33 = 157,18 must be exceeded (Table 6.5) for a mean square based on 1 df to be significant at the 0,1% level.

In the second last column in Tables 6.5 and 6.6, headed F-ratio, the mean squares for the main and interaction effects have been divided by the estimate of error variance. All the values in this column are based on 1 and 5 df and values that exceed 47,2 are significant at the 0,1% level. The levels of significance are given in the last columns of Tables 6.5 and 6.6.

6.1.1.3 Discussion

It is apparent from the results in Table 6.4 that the calculated effects and interaction effects had opposing signs for salt rejection and permeate flux responses. By implication this complicates optimization.

TABLE 6.2: FIRST DESIGNED EXPERIMENT, FACTOR LEVELS

	Factors		Factor level low	base	high	unit
A	Formamide concentration	[mm %]	27,6	30,0	32,4	2,4
B	Extrusion pressure	[kPa]	1 000	1 100	1 200	100
C	Air drying rate	[lpm]	0,0	0,2	0,4	0,2
D	Annealing temperature	[°C]	77	85	93	7

TABLE 6.3: RESULTS OF THE FIRST DESIGNED EXPERIMENT

Treatment Combination [TC]	Variable x_1	x_2	x_3	x_4	Response Rejection [%]	Flux [lmd]
I	-1	-1	-1	-1	85,9	1 077
a	+1	-1	-1	-1	61,1	2 410
b	-1	+1	-1	-1	84,5	1 161
ab	+1	+1	-1	-1	58,4	2 777
c	-1	-1	+1	-1	70,4	1 631
ac	+1	-1	+1	-1	52,6	2 718
bc	-1	+1	+1	-1	75,0	1 459
abc	+1	+1	+1	-1	51,6	2 703
d	-1	-1	-1	+1	94,6	475
ad	+1	-1	-1	+1	92,8	803
bd	-1	+1	-1	+1	93,1	519
abd	+1	+1	-1	+1	93,9	759
cd	-1	-1	+1	+1	95,9	196
acd	+1	-1	+1	+1	96,3	436
bcd	-1	+1	+1	+1	95,5	245
abcd	+1	+1	+1	+1	96,0	436
Mean					81,1	1 220
	0	0	0	0	88,0	1 112
	0	0	0	0	88,9	1 048
	0	0	0	0	88,4	1 043
Mean					88,6	1 068

TABLE 6.4: FIRST DESIGNED EXPERIMENT, EFFECT TOTALS AND EFFECTS

	Rejection performance		Flux performance	
Variation Source	Effect total	Effect	Effect total	Effect
Main effects				
A (formamide)	-92,2	-11,525	6 279	784,9
B (pressure)	-1,6	-0,200	313	39,1
C (air)	-31,0	-3,875	-157	-19,6
D (anneal)	218,6	27,325	-12 067	-1 508,6
Interaction effects				
AB	-4,2	-0,525	303	37,9
AC	11,6	1,450	-755	-94,4
AD	92,0	11,500	-4 281	-535,1
BC	7,4	0,925	-589	-73,6
BD	-0,6	-0,075	-215	-26,9
CD	49,6	6,200	-2 329	-291,4
ABC	-6,8	-0,850	-87	-10,9
ABD	9,6	1,200	-577	-72,1
ACD	-7,8	-0,975	481	60,1
BCD	-8,0	-1,000	687	85,9
ABCD	1,8	0,225	165	20,6
Response Total	1 297,6		19 805	

TABLE 6.5: FIRST DESIGNED EXPERIMENT, ANALYSIS OF VARIANCE, SALT REJECTION PERFORMANCE

Variation Source	SS	df	Mean SS	F-ratio	Sign. Level
Main effects					
A	531,30	1	531,30	159,50	0,1%
B	0,16	1	0,16	0,05	
C	60,06	1	60,06	18,00	1,0%
D	2 986,62	1	2 986,62	896,61	0,1%
Interaction effects					
AB	1,10	1	1,10	0,33	
AC	8,41	1	8,41	2,53	
AD	529,00	1	529,00	158,81	0,1%
BC	3,42	1	3,42	1,03	
BD	0,02	1	0,02	0,01	
CD	153,76	1	153,76	46,16	1,0%
ABC	2,89				
ABD	5,76				
ACD	3,80	=5	3,33		
BCD	4,00				
ABCD	0,20				

TABLE 6.6: FIRST DESIGNED EXPERIMENT, ANALYSIS OF VARIANCE, PERMEATE FLUX PERFORMANCE

Variation Source	SS	df	Mean SS	F-ratio	Sign. Level
Main effects					
A	2464115	1	2464115	184,1	0,1%
B	6123	1	6123	0,5	
C	1541	1	1541	0,1	
D	9100781	1	9100781	679,8	0,1%
Interaction effects					
AB	5738	1	5738	0,4	
AC	35627	1	35627	2,7	
AD	1145435	1	1145435	85,6	0,1%
BC	21683	1	21683	1,6	
BD	2889	1	2889	0,2	
CD	339015	1	339015	25,3	0,1%
ABC	473				
ABD	20808				
ACD	14460	=5	13388		
BCD	29498				
ABCD	1702				

An increase in formamide concentration (factor A) had a negative effect on salt rejection performance, *i.e.* higher concentrations of formamide lowered the salt rejection performance of the membrane on average. (The reverse was true for product flux, that is, higher formamide concentration levels in the casting solution led to membranes with increased permeate flux performances). Annealing temperature (factor D), on the other hand, showed a positive effect, which meant that rejection was improved on average by higher annealing temperatures.

The effect of the two-factor interaction AD, formamide/annealing temperature, on both salt rejection and flux performance was also highly significant (see Tables 6.5, 6.6 and 6.7). Higher formamide concentrations increased the permeability of the membrane, at the expense of selectivity, irrespective of annealing temperature. The change in skin morphology due to annealing was, on average, more pronounced with less dense skins, *i.e.* high formamide concentration level. The annealing temperature of 77°C was barely beyond the second relaxation temperature of CA and, on the average, densification of the membrane at this temperature was not as dramatic as that of the higher temperature, which tended to overpower the role of formamide to introduce greater permeability to some extent (Table 6.7). The effect which formamide concentration has on reducing salt rejection, was less at higher annealing temperatures, although an increase in formamide concentration still favoured the formation of membranes with higher flux performances.

The situation regarding air drying (factor C), needs closer examination. Air drying of flat-sheet membranes (section 2.2.1.4), is known to be used to increase the salt rejection expectancy of CA membranes. It was therefore expected for this factor to have a main effect which is positive for salt rejection and negative for permeate flux responses. However, the results shown in Table 6.4, where a negative main effect on salt rejection is implied, are not in agreement with the expected. From the analysis of variance performed (Tables 6.5 and 6.6), the main effect of this factor is significant (10% level), only in the case of salt rejection. From the above tables, it is apparent that air drying forms a significant interaction with annealing temperature (interaction CD). The effect of this interaction proves to be significant both for salt rejection (1% level) and permeate flux (0,1%) level. (Table 6.8 summarizes this interaction effect).

To gain some understanding of the observed anomaly of air drying, and not only discount it as being attributable to dissimilarities between membranes of flat and tubular geometry, the interaction effects of annealing temperature with both formamide concentration and air drying will be compared.

From Table 6.8, where the effect of the CD interaction has been summarized, it appears that at high annealing temperatures, membranes with, on average, better salt rejection performances result when air drying is at a high level. The reverse is true for permeate flux. This is in agreement with the general understanding that evaporation of a solvent causes the formation of more dense membranes.

However, at the low annealing temperature, the effect which air drying has on membrane performance is similar to that noted for formamide (Table 6.7), in other words, the membranes are, on average, less dense when air dried. Air drying therefore affects the characteristics of the membrane skin, a situation which is masked by densifying the membrane at high temperature.

TABLE 6.7: FORMAMIDE/ANNEALING TEMPERATURE INTERACTION

Rejection:

			Formamide [A]			
			low-level [-]		high-level [+]	
			27,6%		32,4%	
	A		85,9		61,1	
	n	[-]	84,5		58,4	
	n	77°C	70,4	Ave	52,6	Ave
	e		75,0	79,0	51,6	55,9
[D]	a					
	l		94,6		92,8	
	i	[+]	93,1		93,9	
	n	93°C	95,9	Ave	96,3	Ave
	g		95,5	94,8	96,0	94,8

Flux:

			Formamide [A]			
			low-level [-]		high-level [+]	
			27,6%		32,4%	
	A		1077		2410	
	n	[-]	1161		2777	
	n	77°C	1631	Ave	2718	Ave
	e		1459	1332	2703	2652
[D]	a					
	l		475		759	
	i	[+]	519		436	
	n	93°C	196	Ave	803	Ave
	g		245	359	436	609

TABLE 6.8: AIR DRYING/ANNEALING TEMPERATURE INTERACTION

Rejection:

			Air flow rate [C]			
			low-level [-]		high-level [+]	
			0 l/min		0,4 l/min	
	A		85,9		70,4	
	n	[-]	61,1		52,6	
	n	77°C	84,5	Ave	75,0	Ave
	e		58,4	72,5	51,6	62,4
[D]	a					
	l		94,6		95,9	
	i	[+]	92,8		96,3	
	n	93°C	93,1	Ave	95,5	Ave
	g		93,9	93,6	96,0	95,9

Flux:

			Air flow rate [C]			
			low-level [-]		high-level [+]	
			0 l/min		0,4 l/min	
	A		1077		1631	
	n	[-]	2410		2718	
	n	77°C	1161	Ave	1459	Ave
	e		2777	1856	2703	2128
[D]	a					
	l		475		196	
	i	[+]	803		436	
	n	93°C	519	Ave	245	Ave
	g		759	639	436	328

The moisture content of the air used was not monitored at the time of experimentation. Moist air was a possible cause of the anomaly noted. When the moisture content of the bottled medical air used in experimentation was analyzed, frost-point determinations showed wide differences in the moisture content of the air; frost points varied between -18°C to as high as 10°C. In subsequent experiments, the moisture contained in the air used for drying was removed by freezing, after which the air was equilibrated to room temperature by passing it through a glass column packed with silica gel and $CaCl_2$.

If the effect corresponding to a particular factor, *e.g.* the casting pressure, is small, it is possible that:

i) the system is independent of the level of this variable;
ii) the unit adopted for the factor is disproportionately small; or
iii) the base level chosen for this factor is near a conditional maximum, *i.e.* a maximum for this particular factor when all the other variables were held constant.

The casting pressure had no significant effect on either of the responses measured and (ii) is probably the reason for this. Therefore, because the system was independent of this factor over the practical pressure-range investigated, the casting pressure was excluded from further investigations, and was kept fixed at 1 000kPa.

6.1.1.4 Multiple linear regression

As is evident from Table 6.4, any effort made to increase the salt rejection performance of the CA membrane resulted in a decrease in permeate flux performance. By implication the question arises: "How then is the formulation of a membrane with an optimal permeate flux expectancy, for a given salt rejection performance, approached?" This problem can be resolved by employing numerical optimization techniques, once the membrane formulation variables have been related mathematically to the observed membrane performance responses by multiple linear regression.

One of the advantages of orthogonal designed experiments is the ease with which multiple linear regression is performed on the data (see section 4.4.2.2). These equations can be used to optimize one response, subject to an equality constraint for the other, or to construct multiple-dimension graphs to aid in visualizing the response surfaces.

The following regression equations were obtained (section 4.4.3), from a regression analysis performed on the data, for the observed flux and rejection responses shown in Table 6.3;

$$\text{Rejection} = 81{,}1 - 5{,}7625\ x_1 - 1{,}9375\ x_3 + 13{,}6625\ x_4 + 5{,}751\ x_1x_4 + 3{,}1\ x_3x_4$$

$$\text{Flux} = 1220{,}69 + 392{,}43\ x_1 - 754{,}31\ x_4 - 47{,}19\ x_1x_3 - 267{,}56\ x_1x_4 - 36{,}81\ x_2x_3 - 145{,}69\ x_3x_4$$

It is obvious from the regression coefficient estimates ($b_o \rightarrow \beta_o + \beta_{11} + \beta_{22} + \beta_{33} + \beta_{44}$), that these estimates are biased (especially in the case of salt rejection), when they are compared with the responses obtained at the centre of the design (Table 6.3). These first-order models were therefore not adequate, as the responses obtained from a numerically optimized set of fabrication conditions would not be experimentally

verifiable. However, they were used to map contour lines for the responses in the experimental region to obtain some insight into their behaviour.

In Figure 6.2 the flux and salt rejection responses have been plotted on the x_4 (annealing temperature) and x_1 (formamide concentration) axes. Three sets of maps were prepared, each for a different level of air-drying (x_3). This variable is represented on the vertical x_3-axis at co-ordinates levels -1, 0 and +1. (The casting pressure was fixed at x_2 = -1, *i.e.* 1 000kPa).

The complex algorithm of Box *(6)* was used to maximize the expression for flux, under the following inequality constraints;

$$-1 \leq x_1 \leq +1 \qquad i = 1, 2, 3, 4$$

and

$$R^I \leq \text{Rejection} < R^{II}$$

where R^I was a lower limit imposed on rejection (*e.g.* 90%) and R^{II} an arbitrarily selected upper limit (*e.g.* 90,2%). Optimized flux performances for seven specified rejections are shown in Table 6.9, together with the variable levels.

6.1.1.5 Conclusion

The numerical optimization data show that if high-flux performances are to be maintained, formamide concentration levels are in the upper region of its factor space, *i.e.* 31,98% for 90% rejection and 32,06% for 95% rejection (see section 4.2.1 and Table 6.2). The transformed values of annealing temperature were also in the upper region, since they varied between 90,1°C for a 90% rejection membrane to 93°C for a 95% rejection membrane.

The two-level factorial-designed experiment proved helpful in the location of a point of departure for further attempts to improve the mathematical modelling of the rejection and flux response surfaces closer to the 90-95% rejection region of interest.

The study confirmed the importance of being aware that random variation in replicating specific factor-levels (*e.g.* variation in the moisture content of drying air) can cause complications. Analysis of interaction effects proved helpful in gaining an understanding of the effect which interaction between factors have on the responses measured.

6.1.2 SECOND CA 400-25 DESIGNED EXPERIMENT

The first-order regression models resulting from the previous experiment were not regarded as adequate for two reasons. First, *e.g.* for the rejection model, the b_o estimate, 81,1 (*i.e.* average response) of β_o (response at the centre of the design) was biased, in that it was an underestimate of the average response at the centre of the design, 88,4 (See Table 6.3). This situation can be rectified if the regression model is expanded to include second-order terms. Second, as the experimental region was not within the rejection range of interest, namely

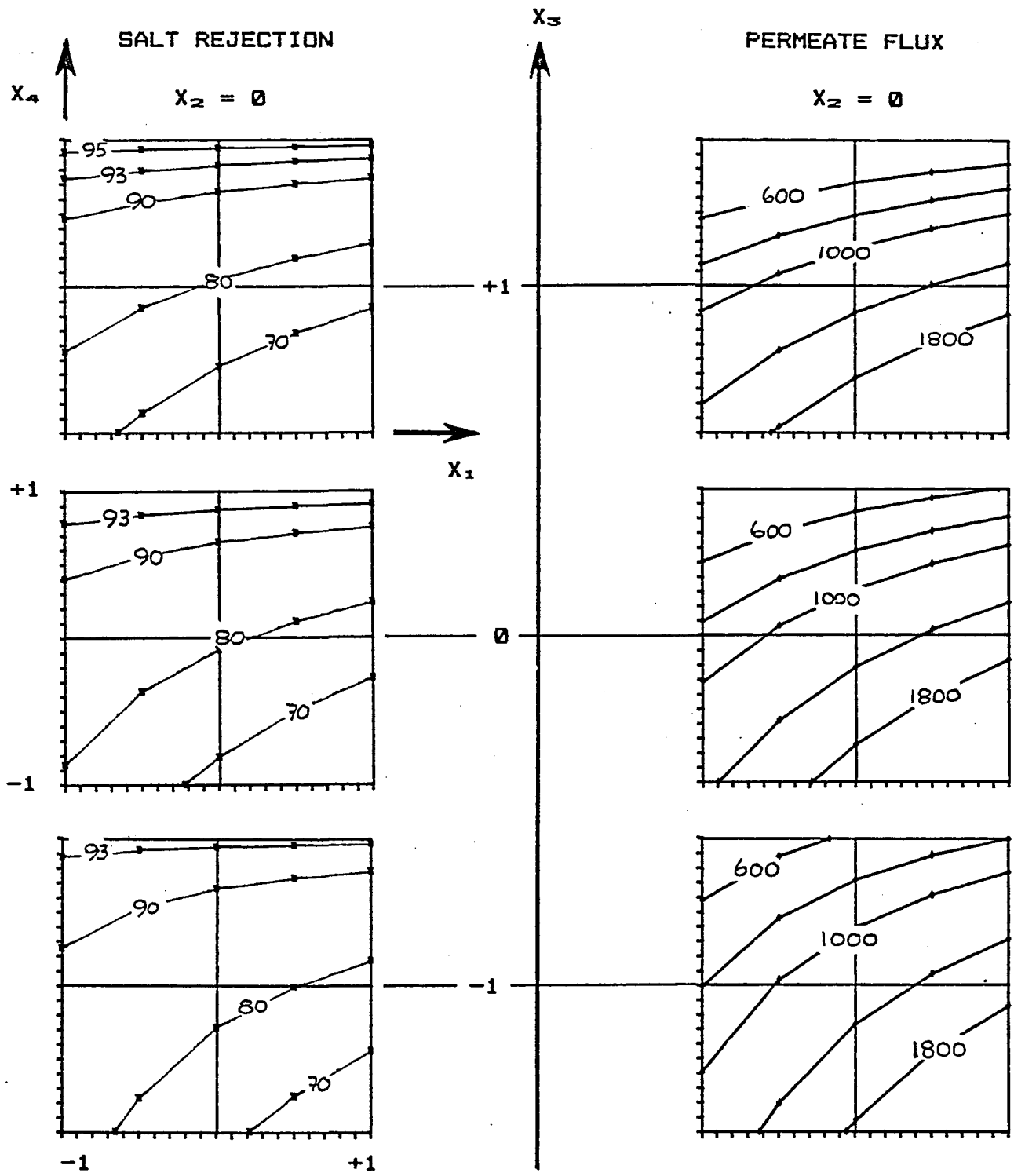

FIGURE 6.2: GRAPHICAL PRESENTATION OF THE FACTOR SPACE OF THREE FABRICATION VARIABLES, CA 400-25, FIRST EXPERIMENT

TABLE 6.9: OPTIMIZED FLUX RESPONSES FOR SPECIFIED SALT REJECTION PERFORMANCES

Rejection	Flux	x_1	x_2	x_3	x_4
90,0	933	0,826	0,511	-0,766	0,758
91,0	879	0,835	0,510	-0,763	0,822
92,0	827	0,843	0,509	-0,760	0,883
93,0	774	0,851	0,509	-0,757	0,945
94,0	705	0,858	0,508	-0,647	1,000
95,0	530	0,857	0,507	0,210	1,000
95,8	384	0,879	0,506	0,934	1,000

	Factor	Variable
A	Formamide concentration	x_1
B	Extrusion pressure	x_2
C	Air drying flow-rate	x_3
D	Annealing temperature	x_4

90 - 95% (see Figure 6.2), it was thought that a second designed experiment, in which a different experimental region was explored would be more beneficial than mere expansion of the first experiment to allow inclusion of second-order coefficients in the regression model.

6.1.2.1 Selection of variables

The factors which were selected for inclusion in this study were casting solution composition, air-drying flow rate, casting-room and annealing temperatures. Two variables were introduced to fix the casting-solution composition, as against the one used in the previous study. Consideration will be given to the choice of factors and their variable ranges in the following paragraphs.

Factor A: Mole ratio acetone/formamide (variable x_1)

Factor B: CA concentration (variable x_2)

From Table 6.9 and Figure 6.2 it can be concluded that improved membrane performance can be expected towards the upper limit used for factor A in the previous experiment. In Table 6.9, variable x_1 assumes the optimized value of 0,83 to 0,88 over the rejection performance range of 90 to 96%. By using the transformation;

$$X^* = c_1 x + c_2$$

X^*	factor level
x	variable level
c_1	unit
c_2	base

the transformed value of this variable (Table 6.2) becomes 32,1% at x_1 = 0,88. At a formamide concentration of 32,1% and an acetone/CA mass ratio of 0,556 (section 6.1.1.1), the mass percent acetone and CA present in the casting solution are, respectively, 43,6% and 24,3%. At these concentrations, the acetone/formamide mole ratio is 1,053. As the low level for factor A in this experiment, an acetone/formamide mole ratio of 1,0 was selected. The unit for this factor was arbitrarily chosen as 0,15.

The Manjikian concentration for CA of 25% by mass was again chosen as base for factor B, and the unit chosen, 1,2%, allowed this factor to be varied over a wider range than was possible in the previous experiment. To summarize, the levels for factors A and B are shown below. Table 6.10 shows all the possible casting solution compositions that can be obtained by considering these factors at two levels. The solution composition at the base of the experiment (0, 0) is also indicated in the table.

		Factor level			
	Factors	low	base	high	unit
A	Acetone/formamide mole ratio	1,0	1,15	1,3	0,15
B	CA concentration [mm%]	23,8	25,0	26,2	1,2

Factor C: Air drying (variable x_3)

Air-drying was initially introduced as a fabrication variable to allow for the removal of solvent vapour from the nascent membrane cavity. The air, which was used for removal of the vapour, was also a means for controlling the coagulation interface on the inside of the tubular membrane relative to the outside level of the coagulant. By adjusting the rate at which the air was withdrawn from the nascent membrane cavity, a pressure head of 2cm water was maintained inside the membrane. Depressing the liquid level inside the tube proved effective in preventing the leach front from being disturbed unduly when membranes were moved around in the leach tank.

At this stage, in the light of the seemingly confusing results obtained from the first experiment, the level of this factor could have been fixed, and the factor regarded as a casting parameter. However, as room temperature was to be introduced as another factor for analysis, there was a possibility of an interaction effect between the flow volume of the drying air and room temperature. The volumetric flowrate of the drying air was therefore maintained as a factor for study.

Factor D: Ambient temperature (variable x_4)

Ambient temperature was regarded as a random variable during the first experiment, due to lack of facilities for controlling the temperature of the casting area. As the first experiment was conducted during the early summer period, membranes were cast early, on only those mornings when the temperature ranged from 22 to 25°C. Temperature was introduced as a factor for study as a temperature-controlled room had been constructed around the casting equipment during the latter part of the first experiment.

Heat was extracted from the room by pumping chilled water at about -10°C, from a brine tank, installed to facilitate cooling of feed water during membrane evaluation, through a forced-draft heat exchanger. The volume of chilled water passing through the heat exchanger was controlled manually by means of a by-pass valve. This allowed the temperature of the room to be maintained at $\pm$0,3°C of set point by means of two temperature controllers each operating a bank of forced-draft electrical heaters.

The average of the mid-morning ambient temperature, outside the insulated casting-room measured over a number of days, was 26°C. This was taken as the base-level for casting room temperature.

Factor E: Annealing temperature (variable x_5)

Annealing is an essential aspect of CA RO membrane fabrication and was therefore kept as the fifth factor for analysis. The temperature range used in the first experiment was altered to have an upper-level limit of 91°C and a lower-level limit of 85°C. As the CA concentration was considered to be a variable in this experiment, it was reasoned that undue densification (crystallization) and loss of flux would result at the previously used upper limit of 93°C.

Table 6.11 summarizes the variables selected for the second experiment.

TABLE 6.10: SECOND DESIGNED EXPERIMENT - RANGE OF VARIABLES FOR FACTORS CONTROLLING CASTING SOLUTION COMPOSITION

Factor A	Factor B	Cellulose acetate	Acetone	Formamide
Variable x_1	Variable x_2		[mass%]	
-1	-1	23,8	42,9	33,3
+1	-1	23,8	47,8	28,4
-1	+1	26,2	41,6	32,2
+1	+1	26,2	46,3	27,5
0	0	25,0	44,8	30,2

Factor A: Acetone/formamide mole ratio
Factor B: Cellulose acetate [mass%]

TABLE 6.11: SECOND DESIGNED EXPERIMENT, FACTOR LEVELS

			Factor level			
	Factors		low	base	high	unit
A	Mole ratio acetone/formamide		1,0	1,15	1,30	0,15
B	CA concentration	[mm%]	23,8	25,0	26,2	1,2
C	Air drying rate	[lpm]	0,15	0,2	0,25	0,05
D	Room temperature	[°C]	23	26	29	3
E	Annealing temperature	[°C]	85	88	91	3

6.1.2.2 Results

A complete randomized 2^5 factorial was conducted. The observed salt rejection and flux performances associated with the various treatment combinations are listed in Table 6.12.

A summary is given in Table 6.13 of the main and two-factor interaction effects for both flux and salt rejection. The analysis of variance performed on the data is presented in Tables 6.14 and 6.15 for rejection and permeate flux, respectively. The experiment was again not replicated and the error-mean-square was estimated from three and more factor interaction terms, 16 df in total.

6.1.2.3 Discussion

Tables 6.13 to 6.15, illustrate clearly that the performance of CA membranes can be altered appreciably by making small alterations to the casting-solution composition. High acetone-to-formamide ratios (factor A) in the casting solution favour the formation of more dense membranes, with a resulting loss in permeability. The reverse, that is more porous membranes, results when the relative concentration of the non-solvent, formamide, is increased, which is the situation when factor A is at its low level (low acetone/formamide ratio). The main effect of factor A is therefore negative for flux and positive for salt rejection.

An increase in the concentration of the membrane-forming polymer (factor B) leads to an increase in the average salt rejection performance; but at a severe loss of permeability. A comparison of the magnitudes of the main effects on salt rejection and flux performance of factor B with that of factor A, showed that it seemed to be more appropriate (on average) to increase the acetone/formamide ratio to produce a higher salt rejection membrane, than to increase the polymer concentration.

The interaction effect between the acetone/formamide mole ratio and annealing temperature (factor E) is also significant. Table 6.16 illustrates the mean of the rejection and flux yields at the high and low levels of these two factors. On average, annealing seemed to have a more pronounced effect in tightening a porous membrane (low level, factor A), than one which is more dense (high level, factor A).

The interaction between polymer concentration (factor B) and room temperature (factor D) is significant, with respect to both flux and rejection performance. The interaction is illustrated in Table 6.17. On average, membranes with better performances were fabricated at higher polymer concentrations, but at lower ambient temperatures.

The degree to which interactions between fabrication variables are important underlines the necessity to consider all factors simultaneously in an optimization study. The optimal solution for the design of a membrane is a compromise between the opposing effects which the fabrication variables have on performance of the RO membrane. The problem is best solved by numeric optimization of response-surface regression equations.

TABLE 6.12: RESULTS OF THE SECOND DESIGNED EXPERIMENT

Treatment combination	Factor level					Response	
	x_1	x_2	x_3	x_4	x_5	Rejection [%]	Flux [lmd]
I	-1	-1	-1	-1	-1	83,4	1 592
a	+1	-1	-1	-1	-1	88,5	1 239
b	-1	+1	-1	-1	-1	89,0	1 038
ab	+1	+1	-1	-1	-1	91,5	891
c	-1	-1	+1	-1	-1	86,8	1 229
ac	+1	-1	+1	-1	-1	91,5	926
bc	-1	+1	+1	-1	-1	91,3	725
abc	+1	+1	+1	-1	-1	92,5	730
d	-1	-1	-1	+1	-1	88,7	1 166
ad	+1	-1	-1	+1	-1	92,3	887
bd	-1	+1	-1	+1	-1	88,0	970
abd	+1	+1	-1	+1	-1	91,6	700
cd	-1	-1	+1	+1	-1	90,9	891
acd	+1	-1	+1	+1	-1	92,1	700
bcd	-1	+1	+1	+1	-1	90,8	696
abcd	+1	+1	+1	+1	-1	93,5	509
e	-1	-1	-1	-1	+1	91,8	852
ae	+1	-1	-1	-1	+1	93,5	730
be	-1	+1	-1	-1	+1	95,3	426
abe	+1	+1	-1	-1	+1	95,9	446
ce	-1	-1	+1	-1	+1	93,6	504
ace	+1	-1	+1	-1	+1	94,4	485
bce	-1	+1	+1	-1	+1	95,6	304
abce	+1	+1	+1	-1	+1	96,8	284
de	-1	-1	-1	+1	+1	93,2	573
ade	+1	-1	-1	+1	+1	94,9	456
bde	-1	+1	-1	+1	+1	94,7	451
abde	+1	+1	-1	+1	+1	95,0	392
cde	-1	-1	+1	+1	+1	94,8	407
acde	+1	-1	+1	+1	+1	94,6	304
bcde	-1	+1	+1	+1	+1	95,5	310
abcde	+1	+1	+1	+1	+1	95,7	264
	Mean					92,4	693
Base	0	0	0	0	0	93,6	602
Base	0	0	0	0	0	92,8	730
	Mean					93,2	666

TABLE 6.13: SECOND DESIGNED EXPERIMENT, EFFECT TOTALS AND EFFECTS

Variation Source		Rejection performance: Effect total	Rejection performance: Effect	Flux performance: Effect total	Flux performance: Effect
Main effects					
A	(Ac/F ratio)	30,9	1,93	-2 275	-142,2
B	(CA conc)	27,7	1,73	-3 901	-243,8
C	(air)	23,1	1,44	-3 457	-216,1
D	(room temp)	14,9	0,93	-2 641	-165,1
E	(anneal)	72,9	4,56	-7 797	-487,3
Interaction effects					
AB		-6,3	-0,39	879	54,9
AC		-7,3	-0,46	379	23,7
AD		-4,7	-0,29	-397	-24,8
AE		-18,3	-1,14	1 355	84,7
BC		-1,7	-0,11	461	28,8
BD		-21,1	-1,32	1 525	95,3
BE		-0,3	-0,02	1 021	63,8
CD		-4,1	-0,26	597	37,3
CE		-9,7	-0,61	517	32,3
DE		-11,9	-0,74	881	55,1

TABLE 6.14: SECOND DESIGNED EXPERIMENT, ANALYSIS OF VARIANCE, SALT REJECTION

Variation Source	SS	df	Mean SS	F-ratio	Sign. level
Main effects					
A	29,84	1	29,84	49,72	0,1%
B	23,98	1	23,98	39,95	0,1%
C	16,68	1	16,68	27,78	0,1%
D	6,94	1	6,94	11,56	1,0%
E	166,08	1	166,08	276,72	0,1%
Interaction effects					
AB	1,24	1	1,24	2,07	
AC	1,67	1	1,67	2,77	
AD	0,69	1	0,69	1,15	
AE	10,47	1	10,47	17,44	0,1%
BC	0,09	1	0,09	0,15	
BD	13,91	1	13,91	23,18	0,1%
BE	0,00	1	0,00	0,00	
CD	0,53	1	0,53	0,88	
CE	2,94	1	2,94	4,90	5,0%
DE	4,43	1	4,43	7,37	5,0%
Three-factor	6,55	10			
Four-factor	2,94	5	0,60		
Five-factor	0,14	1			

TABLE 6.15: SECOND DESIGNED EXPERIMENT, ANALYSIS OF VARIANCE, PERMEATE FLUX PERFORMANCE

Variation Source	SS	df	MSS	F-ratio	Sign. level
Main effects					
A	161 738	1	161 738	77,99	0,1%
B	475 556	1	475 556	229,32	0,1%
C	373 464	1	373 464	180,09	0,1%
D	217 965	1	217 965	105,10	0,1%
E	1 899 788	1	1 899 788	916,09	0,1%
Interaction effects					
AB	24 145	1	24 145	11,64	1%
AC	4 489	1	4 489	2,16	
AD	4 925	1	4 925	2,38	
AE	57 376	1	57 376	27,67	0,1%
BC	6 641	1	6 641	3,20	10%
BD	72 676	1	72 676	35,04	0,1%
BE	32 576	1	32 576	15,71	1%
CD	11 138	1	11 138	5,37	5%
CE	8 353	1	8 353	4,03	10%
DE	24 255	1	24 255	11,70	1%
Three-factor	23 431	10			
Four-factor	8 900	5	2 074		
Five-factor	851	1			

TABLE 6.16: INTERACTION EFFECT BETWEEN ACETONE/FORMAMIDE RATIO AND ANNEALING TEMPERATURE

			Factor A Acetone/formamide ratio	
Rejection:			[-]	[+]
	Factor E Annealing Temperature	[-]	88,6	94,3
		[+]	91,7	95,1

			Factor A Acetone/formamide ratio	
Flux:			[-]	[+]
	Factor E Annealing Temperature	[-]	1 038	823
		[+]	478	420

TABLE 6.17: INTERACTION EFFECT BETWEEN POLYMER CONCENTRATION AND ROOM TEMPERATURE

			Factor B CA concentration	
Rejection:			[-]	[+]
	Factor D Room Temperature	[-]	90,4	93,5
		[+]	92,7	93,1

			Factor B CA concentration	
Flux:			[-]	[+]
	Factor D Room Temperature	[-]	945	606
		[+]	573	537

6.1.2.4 Regression analysis

By employing strategies similar to those mentioned earlier (section 4.4.3), the multiple linear regression equations given below were established for the CA 400-25 membrane system. In these equations:

x_1 = acetone/formamide mole ratio
x_2 = CA concentration
x_3 = air drying rate
x_4 = room temperature
x_5 = annealing temperature

Rejection:

$$R = 92{,}43 + 0{,}966\ x_1 + 0{,}866\ x_2 + 0{,}722\ x_3 + 0{,}466\ x_4 + 2{,}278\ x_5 - 0{,}197\ x_1x_2 - 0{,}228\ x_1x_3 - 0{,}572\ x_1x_5 - 0{,}659\ x_2x_4 - 0{,}303\ x_3x_5 - 0{,}372\ x_4x_5 + 0{,}228\ x_1x_2x_4 + 0{,}234\ x_2x_3x_4 + 0{,}228\ x_2x_4x_5$$

Flux:

$$F = 692{,}5 - 71{,}094\ x_1 - 121{,}91\ x_2 - 108{,}03\ x_3 - 82{,}53\ x_4 - 243{,}66\ x_5 + 27{,}47\ x_1x_2 + 42{,}34\ x_1x_5 + 14{,}41\ x_2x_3 + 47{,}66\ x_2x_4 + 31{,}91\ x_2x_5 + 18{,}66\ x_3x_4 + 16{,}16\ x_3x_5 + 27{,}53\ x_4x_5 - 13{,}47\ x_1x_2x_4 - 17{,}53\ x_2x_3x_4$$

As was mentioned earlier, b_o (the constants in the above models) is an estimate of the regression coefficient $\beta_o + \beta_{11} + \beta_{22} + \beta_{33} + \beta_{44} + \beta_{55}$. If the response surface is adequately modelled by a plane, or twisted plane, then b_o (the mean of the responses) will be an unbiased estimate of β_o (the response at the centre of the design). However, b_o will be an under- or overestimate of β_o, if the surface is concave or convex as a result of the effect of quadratic (self-interacting) terms. Two experiments were conducted at the centre (base) of the design (Table 6.12) and from the responses obtained, b_o seemed to be a reasonable estimate of β_o in the case of permeate flux, but an underestimate of salt rejection. The regression equations were however used in numerical optimization and forecasting of fabrication conditions.

6.1.2.5 Numerical approaches

In the first experiment the Box algorithm (7) was used to forecast the fabrication conditions for the preparation of a 95% rejection membrane (Table 6.9). The same procedure was followed and the solution to the following problem was obtained numerically;

Maximize flux: $F(x_1, x_2, x_3, x_4, x_5)$

subject to the following equality and inequality constraints;

$$\text{Rejection: } R(x_1, x_2, x_3, x_4, x_5) = 95$$

$$x_1 = 0$$
$$x_2 = 0$$
$$-1 \leq x_3 \leq 1$$
$$-1 \leq x_4 \leq 1$$
$$-1 \leq x_5 \leq 1$$

As a large quantity of stock casting solution of composition equivalent to $x_1 = 0$, $x_2 = 0$, was available, this restriction was also imposed on the problem. Under these restrictions, a maximized permeate flux of 402 lmd was forecast; the result is given in Table 6.18.

This formulation was verified experimentally. The temperature of the annealing system had to be controlled manually at the time and as a result deviated somewhat from ideal values as shown in Table 6.18. However, the performances of the three batches of membranes fabricated under the above conditions were in reasonable agreement with the forecast. The results (the annealing temperature given in square brackets) are listed below:

[93°C]	96,5 ± 0,1%	310 ± 12 lmd
[92°C]	95,6 ± 0,2%	400 ± 10 lmd
[91°C]	95,0 ± 0,2%	540 ± 27 lmd

Figure 6.3 illustrates the response surface behaviour close to conditions of the above forecast.

The optimization problem was defined differently in a second experiment, as rejection was maximized by introducing an inequality constraint for flux;

Maximize rejection: $R(x_1, x_2, x_3, x_4, x_5)$

subject to the following inequality constraints;

$$\text{Flux: } 550 \leq F(x_1, x_2, x_3, x_4, x_5) < 600$$

$$-1 \leq x_1 \leq 1$$
$$-1 \leq x_2 \leq 1$$
$$-1 \leq x_3 \leq 1$$
$$-1 \leq x_4 \leq 1$$
$$-1 \leq x_5 \leq 1$$

The maximized rejection thus obtained was 94,9% with a permeate flux of 569 lmd. The forecast conditions of fabrication are listed in Table 6.19, which also lists the actual experimental conditions of fabrication. As the table shows, two of the variables deviated from forecast values, and the expected performance of the membrane had to be recalculated by substituting the experimental conditions into the design regression equations. These predicted values are also indicated in Table 6.19.

The two batches of membranes fabricated under these conditions yielded average rejection performances of 94,8 ± 0,3% with permeate flux values of 579 ± 53 lmd.

6.1.2.6 Discussion

When the performances obtained with the computor formulated membranes are compared with the data shown in Table 6.12, the relative superiority of the formulated membranes is evident. With the aid of two-level factorial designed experiments and numerical techniques, the upper salt rejection target value of 95% had been reached.

This approach to membrane development and determination of fabrication conditions clearly had its advantages. In the planning and execution of a series of sequential experiments to achieve the maximum salt rejection capabilities of the CA membrane system, this technique is recommended, especially as the results indicate the importance of considering interaction between factors.

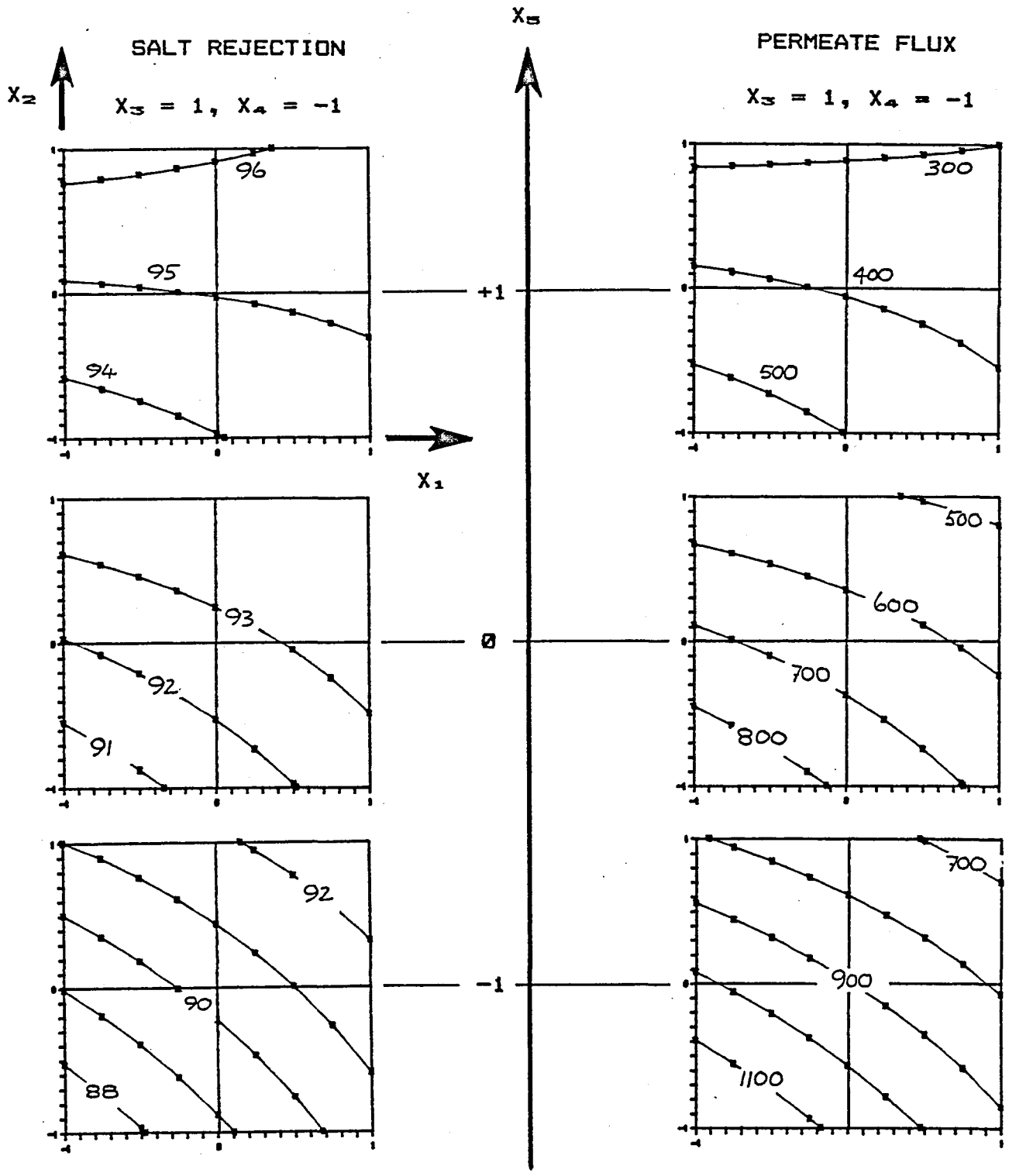

FIGURE 6.3: SECOND EXPERIMENT, ILLUSTRATION OF THE PERMEATE FLUX AND SALT REJECTION RESPONSE SURFACES

TABLE 6.18: CA 400-25, FORECAST OF FABRICATION CONDITIONS

Forecast conditions	Transformed values
$x_1 = 0$	1,15 mole ratio
$x_2 = 0$	25% CA 400-25
$x_3 = 0,968$	0,25 lpm drying air
$x_4 = -1$	23°C room temp.
$x_5 = 0,978$	90,9°C anneal temp.
Rejection: 95%	
Flux: 402 lmd	

TABLE 6.19: FABRICATION CONDITIONS, MAXIMIZED REJECTION FOR SPECIFIED FLUX

Forecast	Transformed	Experimental	Transformed	
$x_1 = 1$	1,3	$x_1 = -1$	1,0	mole ratio
$x_2 = 0,54$	25,65	$x_2 = 0,54$	25,7	CA %
$x_3 = -1$	0,15	$x_3 = -1$	0,15	air lpm
$x_4 = -1$	23	$x_4 = -1$	23	room T. °C
$x_5 = 0,77$	90,3	$x_5 = 1$	91	anneal T. °C
Forecast:	94,9%	569 lmd		
Recalculated:	94,6%	530 lmd		
Observed:	94,8 ± 0,3%	579 ± 53 lmd		

6.1.3 CELLULOSE ACETATE 398-10 EXPERIMENT

All stock of the CA 400-25 membrane material was depleted during the research described. As this material was unobtainable at the time, it had to be replaced by another grade of CA. The cellulose acetate material chosen (CA 398-10) had a slightly lower mean acetyl content (39,8% as opposed to 40,0%) and its viscosity and molecular mass were also lower. Because of the above it was expected that the permeate transport rates of the CA 398-10 membranes would be higher than that of the CA 400-25 membranes.

According to the transport model of Lonsdale (see section 2.1), salt transport across the membrane is uncoupled from water transport, and as a result of the diluting effect it has on the product salt concentration, higher salt rejections should accompany the assumed higher permeate transport rates.

For the purpose of verifying the above statements and thus the applicability of the fabrication regression equations developed for the CA 400-25 system, two batches of CA 398-10 membranes were made according to the predicted conditions of fabrication tabled in the first column of Table 6.19. The average performances obtained with these membranes were, 96,3 ± 0,3% salt rejection at permeate flux rates of 521 ± 21 lmd. These results were not in complete agreement with the performances predicted for the CA 400-25 membrane, which was 94,9% salt rejection at flux rates of 569 lmd.

The average of the observed responses of the CA 400-25 membrane system was in agreement with the results of trials replicated at the centre of the design, which indicated the absence of self-interaction effects (quadratic terms) of the factors investigated. If the earlier assumption that the permeate rate of transport of the CA 398-10 membrane was superior to that of the CA 400-25 membrane at equivalent salt rejection performance, it was possible that these terms might become important with the CA 398-10 membrane in a similar experimental region. For these reasons the conditions of fabrication of CA 398-10 membranes had to be reformulated.

6.1.3.1 Selection of variables

Table 6.20 lists the five factors and their associated levels which were to be used in a complete 2^5 factorial experiment, planned to elucidate the effects of the fabrication variables on membrane performance. The five factors chosen for this investigation remained as previously for the CA 400-25 membrane, namely;

Factor A:	x_1	acetone/formamide mole ratio	
Factor B:	x_2	CA concentration	[mass %]
Factor C:	x_3	air-drying flow rate	[lpm]
Factor D:	x_4	annealing temperature	[°C]
Factor E:	x_5	room temperature	[°C]

When these values are compared with those in Table 6.11, it will be noticed that the low-level mole ratio of 1:1 for factor A was kept, but that the unit for this factor was increased from 0,15 to 0,2. Increasing the level of this factor decreased the flux response, but increased the rejection response as the resulting membrane was more dense. On the assumption that the CA 398-10 membrane should on average be more permeable than

the CA 400-25 membrane, it was seen as a reason for increasing the salt rejection expectancy of the membrane by reducing its permeability, while still maintaining reasonable permeate flux transport rates.

The same argument applied to altering the range of factor B, 25 mass % being kept as the base for the polymer concentration, whereas the range was increased by increasing the unit from 1,2 to 2%. The range of this factor was increased to broaden the salt rejection expectancy of the membrane. (See Figure 6.9 at the end of section 6.1). As the upper set limits of the above two factors would lead to more dense membranes being formed, the annealing temperature was lowered; the base of the previous experiment (88°C) now became the upper limit and 3°C remained as unit for this factor.

The casting-room temperature range was also lowered to ensure more comfortable environmental conditions of fabrication for the researcher, 21°C being chosen as the base and 3°C as the unit. According to the analysis of variance performed on the data for the CA 400-25 membrane, room temperature had a significant positive effect on salt rejection, in other words, increasing the ambient temperature would improve the salt rejection performance of the membrane. Due to the inverse relationship which exists between the salt rejection and the rate of water transport, however, the membrane permeation rate would be increased by producing the membrane at a lower ambient temperature.

6.1.3.2 Screening of fabrication variables

The importance of controlling the moisture content of the air used for solvent evaporation and leach front depression had not been ellucidated experimentally. Rather than to introduce this variable formally as a sixth factor, it was decided to investigate its possible effect as part of a short study intended to determine whether the responses associated with the factor levels shown in Table 6.20 lay in the 90-95% salt rejection range of interest.

In the previous experiment, moisture was removed from the medical air used in the solvent-evaporation step, by passing the air through a cold-trap and a silica-gel packed column. In this way the frost point of the air was kept at temperatures below -10°C. For the purpose of this experiment, the dried air was rehumidified to an arbitrarily chosen high frost-point level of 6,5°C. The humidity was controlled by branching the air line after the moisture removal step, so that a portion of the air passed through a humidifier before it is rejoined with the unhumidified air. Rehumidification was achieved by bubbling the air through an ice-water trap, with the air being dispersed through a sintered glass diffuser. The flow rate of air through the diffuser was controlled by means of a needle valve. The frost point of the air was monitored by means of a thermoelectrically operated dew-point hygrometer. Before the air was introduced to the mandrel, it was passed through a heat exchanger to attain room temperature. (See Figure 5.6).

TABLE 6.20: FACTOR LEVELS FOR CA 398-10 EXPERIMENT

	Factor		Factor level low	base	high	unit
A	Mole ratio acetone/formamide		1,0	1,2	1,4	0,2
B	Cellulose acetate 398-10	[mm%]	23,0	25,0	27,0	3,0
C	Air flow rate	[lpm]	0,15	0,25	0,35	0,1
D	Annealing temperature	[°C]	82,0	85,0	88,0	3,0
E	Room temperature	[°C]	18,0	21,0	24,0	3,0

For the purpose of screening the six selected factors, a Plackett-Burman design matrix for the investigation of N - 1 factors in N = 12 experiments was chosen *(8)*. This plan, which permits the simultaneous study of 11 variables, is highly confounded, *i.e.* all main effects are confounded with second- and higher-order effects. Unless N, however, were an integral power of 2 (*i.e.* fractional replicate), the alias structure of this Plackett-Burman plan can not be determined.

As only six of the 11 factors were assigned in this experiment; the remaining five factors were treated as dummy factors, *i.e.* no changes were made corresponding to the levels of their factors. On the assumption that the interactions confounded with these dummy factors were non-existent and the other assigned factor levels were reproduced perfectly, the effect of these dummy factors should be zero. By argument, deviation from zero could be ascribed to experimental error and as such the effects of the dummy factors could be pooled in an estimate of experimental error.

Table 6.21 summarizes the observed responses according to the treatment combinations listed in that table and the factor levels shown in Table 6.20. The humidity of the air was introduced as Factor F (measured as frost point), the levels associated with -1 and +1, repectively, being -15°C and 6,5°C. The dummy variables are denoted by Z_{id}, i = 1, ...,5. The plus and minus signs, respectively, denote the high and low levels of each of the factors investigated.

As before, the effect of each factor was calculated as the mean difference between the sum of the responses at the high and low levels for each factor. Table 6.22 summarizes the calculated effects of the factors investigated on the two responses measured. The formulas below show how the effects calculated for the dummy factors are pooled in an estimate of their combined variance and standard error:

$$\text{Variance:} \quad V_{Eff} = \Sigma(Z_{id})^2/n$$

$$\text{Standard error:} \quad SE_{Eff} = \sqrt{V_{Eff}}$$

The significance of each effect was determined by using Student's t-test. The five dummy factors provided the 5 df for determining the tabulated values of t *(9)*, against which the calculated t-values were judged for significance.

$$t = \text{Effect}/SE_{Eff}$$

The critical value of t for 5 df was 4,77 (0,1% level), 4,03 (1% level), 2,57 (5% level), 2,01 (10% level) and 1,48 (20% level).

6.1.3.3 Discussion

It has been mentioned previously that the Plackett-Burman design matrix used in this experiment was highly confounded. This point is clearly illustrated by the large deviation from zero of the effect calculated for the last dummy factor entry (Z_{5d}) in Table 6.22. It was most probably as a result of a significant interaction confounded with this dummy variable. Because of the design matrix chosen (N not being an integer power of two), the alias structure could not be determined to give insight into the interactions confounded with Z_{5d}.

TABLE 6.21: DESIGN MATRIX FOR SCREENING FABRICATION VARIABLES

Factors											Rej	Flux
A	B	Z_{1d}	C	Z_{2d}	D	E	Z_{3d}	F	Z_{4d}	Z_{5d}	[%]	[lmd]
+	-	+	-	-	-	+	+	+	-	+	91,3	1 420
+	+	-	+	-	-	-	+	+	+	-	94,8	999
-	+	+	-	+	-	-	-	+	+	+	80,5	1 709
+	-	+	+	-	+	-	-	-	+	+	93,3	1 087
+	+	-	+	+	-	+	-	-	-	+	95,3	882
+	+	+	-	+	+	-	+	-	-	-	96,5	710
-	+	+	+	-	+	+	-	+	-	-	96,0	813
-	-	+	+	+	-	+	+	-	+	-	53,3	3 139
-	-	-	+	+	+	-	+	+	-	+	72,0	1 709
+	-	-	-	+	+	+	-	+	+	-	93,6	1 029
-	+	-	-	-	+	+	+	-	+	+	96,0	818
-	-	-	-	-	-	-	-	-	-	-	35,8	3 552

TABLE 6.22: SCREENING OF FABRICATION VARIABLES, CA 398-10

Factor		Effect on Rejection	t	Significance of effect
A	Mole ratio Ac/F	21,87	4,19	99%
B	CA concenctration	19,97	3,83	95%
C	Air flow rate	1,83	0,35	
D	Anneal temp.	16,07	3,08	95%
E	Room temp.	8,77	1,68	80%
F	Dew point	9,67	1,85	80%
Z_{1d}	Dummy	3,90		
Z_{2d}	Dummy	-2,67		
Z_{3d}	Dummy	1,57		
Z_{4d}	Dummy	4,10		
Z_{5d}	Dummy	9,73		

$V_{Eff} = [(3,90)^2 + (-2,67)^2 + (1,57)^2 + (4,10)^2 + (9,73)^2]/5$
$= 27,26$
$SE_{Eff} = \sqrt{27,26}$
$= 5,22$

Factor		Effect on Flux	t	Significance of effect
A	Mole ratio Ac/F	-936	4,66	99%
B	CA concenctration	-1 001	4,98	99,9%
C	Air flow rate	-102	0,51	
D	Anneal temp.	-923	4,59	99%
E	Room temp.	-278	1,38	
F	Dew point	-418	2,08	90%
Z_{1d}	Dummy	-19		
Z_{2d}	Dummy	82		
Z_{3d}	Dummy	-46		
Z_{4d}	Dummy	-51		
Z_{5d}	Dummy	-436		

$V_{Eff} = 40\ 388$
$SE_{Eff} = \sqrt{40\ 388}$
$= 200,9$

Further analysis of the results indicated that the fabrication variables most likely to affect the properties of the CA 398-10 membrane, were, as with the CA 400-25 membrane, acetone/formamide ratio mole ratio, CA concentration and annealing temperature. Room temperature showed hardly any significance as a variable with respect to salt rejection performance, but as mentioned in paragraph 6.1.1.3, this variable may have been at a conditional optimum.

The humidity of the drying air seemed to be more important as a variable than the volume flow rate of the drying air over the ranges investigated. This was most probably due to the effect which moisture had on enhancing phase-separation of the membrane film (water being a strong non-solvent for the casting system), by increasing super macromolecular aggregation on the surface of the cast film . If this factor was to be incorporated into the membrane design equations, strict control of the variable would be necessary. It proved rather cumbersome to fix the level of humidity of the drying air, and even though the indications were that the factor needed further investigation, it was decided only to take note of its possible importance. However, rather than treat this factor as a random variable, that is, allow it to fluctuate at will, control of this variable at frost-point levels below -10°C was maintained, a condition which did not prove difficult in practice during the previous CA 400-25 membrane experiments.

Air-drying did not seem to play a major role as a fabrication variable over the range considered, but as the air was also used for control of the leach front level inside the membrane, it was kept as a variable.

More important, however, the factor levels chosen gave rise to membranes with performances in the salt rejection range of interest and no adjustments were made to the initial levels chosen for the subsequent designed two-level factorial experiment.

6.1.3.4 2^5 Factorial design - CA 398-10

The variables selected for the purpose of modelling the salt rejection and flux response surfaces mathematically are listed in Table 6.20. A randomized complete 2^5 factorial was conducted and the responses observed are presented in Table 6.23 in the normal standard order. For the purpose of identifying the various entries, they are numbered in the table. The various trials were conducted at random and not according to the number scheme shown in the table.

The design was again not replicated, although some of the trials were repeated to enable an idea of the consistency in performance to be obtained of the membranes produced. The estimate of experimental error variance had therefore to be obtained from within the experiment, assuming negligible three- and higher-order interaction effects. It was noticed in the second CA 400-25 experiment that certain of the three-factor interactions were notably larger than the rest of the higher-order interactions. Two of these effects resulted from the interaction of the factors which control membrane-casting-solution composition (AB interaction) with both the casting-room and annealing temperature. The other effect resulted from the interaction between the polymer concentration, an the room and annealing temperatures. These three effects (ABD,

ABE, BDE) were therefore excluded from the estimate of error variance in order to judge their relative importance.

The effect totals calculated from the observed data in Table 6.23 are given in Table 6.24. By using the relationships:

$$\text{Effect} = [\text{Effect total}]/2^{5-1}$$

$$\text{Sum of squares} = [\text{Effect total}]^2/2^5$$

the main and interaction effects and the sum-of-squares entries, shown in Tables 6.24 and 6.25, are calculated from the effect totals.

In the estimate of error variance, both in the case of salt rejection and permeate flux, the three three-factor interaction effects mentioned earlier (ABD, ABE, BDE) were excluded. Because of the assumption that none of the remaining higher-order interactions contribute to the variation in observed results, they were combined for use in an estimate of experimental error. The number of degrees of freedom available for this estimate was thus reduced to 13, accounted for by the remaining seven three-factor, the five four-factor and one five-factor interactions. The critical variance ratio (F-ratio) that needed to be exceeded for significance for 1 and 13 df, is 17,1 at the 0,1% level, 8,86 (1% level), 4,60 (5% level) and 3,10 (10% level). From the analysis of variance (Table 6.25), it appeared that most of the effects were indeed significant, and that they should therefore be included in the membrane design equations.

The two multiple-linear first-degree regression equations derived from the calculated effect totals given in Table 6.24, are shown in Table 6.26. The same procedure was adopted as before for denoting the variables of the factors, *i.e.* factor A was represented by x_1, factor B by x_2 *etc.*

The membrane-design equations were used to predict the permeate flux and rejection responses corresponding to the treatment combinations shown in Table 6.23. The difference between observed and predicted responses (residual) are listed in Table 6.27. The lack of fit at the centre of the design was evident when the residuals, corresponding to the trials conducted at the centre of the design (ref. nos 33 to 39), were compared with those of the other trials.

The mean salt rejection response was an underestimate, and in the case of permeate flux, an over-estimate of the true response. This indicated the curved nature, especially of the salt rejection response surface.

6.1.3.5 Self-interacting effects

The Taylor series used as regression model therefore needed to be expanded to include second-degree terms to make allowance for curvature. The 2^5 factorial design was therefore supplemented with additional experimental points to complete a composite design. (See section 4.3.3.2). Ten further trials were performed along the five co-ordinate axis, all at a distance $\alpha = \pm\sqrt{2}$ away from the centre. The factor levels conforming to these variables were obtained by linear transformation, using as base and unit the values given in Table 6.20. The factor levels of the composite design are summarized in Table 6.28.

The experimental results are shown in Table 6.29. As entry in this table for the responses observed at the centre of the design, the mean of all the observations of the six trials replicated at the centre of the design (shown in Table 6.23) was taken as representative.

The method used to recalculate b_o (estimate of the regression coefficient $\beta_o + \beta_{11} + \beta_{22} + \beta_{33} + \beta_{44} + \beta_{55}$) shown in Table 6.26, by making allowance for the self-interaction between factors, was shown in detail in section 4.4.3.3. where the salt rejection response of this experiment was used as an example. The same procedure was followed in calculating the self-interacting effects for membrane permeate flux. The results are shown in Table 6.30.

The regression coefficient estimates given above replace the previously given estimate of b_o (Table 6.26). Bias in the former estimate of b_o was reduced by incorporating the self-interacting terms.

6.1.3.6 Discussion

The regression coefficients that are significant above the 5% level are shown in Table 6.26. The opposing signs of the rejection and flux regression coefficients again illustrate the inverse relationship between salt rejection and flux performances of membranes and, by implication, the problem it creates in the optimization of membrane performances. It is therefore not difficult to understand why different techniques based on statistical protocols are employed to design membranes with optimal performances *(10)(11)*.

All the main coefficients (shown in Table 6.26) were statistically important at the 0,1% level, and the degree to which their interactions were important suggests that membranes with similar rejection performances may be fabricated under differently defined conditions. Consider, for example, the membrane salt rejection performances of entries 4, 11, and 24 (≈95,3%), and 15, 16 and 28 (≈96,5%) in Table 6.23.

It is important to note that room temperature (x_5) had a significant effect on membrane performance. On average, the salt rejection was higher at room temperatures of 24°C than at 18°C when the sign of the x_5 regression coefficient was considered. Higher equilibrium temperatures will affect membrane properties as a result of its influence on the casting solution. A higher temperature will not only reduce the viscosity (and hence shear and orientation of the polymer on the extrusion land), but it will also enhance the rate of acetone evaporation. Although it has been suggested that high shear is necessary for the formation of good CA membranes *(12)* (shear is greater at low room temperature as the polymer chains are less coiled), the significance of the x_1x_5 interaction suggested that skin formation by evaporative loss of acetone played a greater role. The small x_3x_5 interaction coefficient (air drying/room temperature) was not contradictory, as the range over which the flow rate of air was varied was small. The importance of controlling room temperature was also manifest in the significant three-factor ($x_1x_2x_5$) interaction effect, which in essence can be regarded as a pseudo-two-factor interaction between the composition of the casting solution (x_1x_2) and casting-room temperature.

TABLE 6.23: COMPLETE 2^5 FACTORIAL - CA 398-10

Treatment combination	Ref. no.	Rej [%]	Flux [lmd]	Replicates Rej [%]	Replicates Flux [lmd]
I	1	35,8	3 552		
a	2	85,3	1 679		
b	3	79,3	1 817		
ab	4	95,1	994	94,7	1 029
c	5	35,2	3 678		
ac	6	86,8	1 670		
bc	7	82,8	1 646		
abc	8	94,7	989		
d	9	61,4	1 959		
ad	10	92,4	1 151	92,7	1 073
bd	11	95,3	901		
abd	12	96,5	710		
cd	13	69,1	1 802		
acd	14	93,3	1 087		
bcd	15	96,6	759	96,4	749
abcd	16	96,5	671		
e	17	52,7	2 831		
ae	18	90,9	1 455		
be	19	78,5	1 744	80,0	1 773
abe	20	94,9	901		
ce	21	53,3	3 139		
ace	22	90,4	1 455		
bce	23	80,0	1 729		
abce	24	95,3	882		
de	25	73,2	1 739		
ade	26	92,9	1 053		
bde	27	96,0	818		
abde	28	96,7	602	96,4	656
cde	29	75,9	1 641		
acde	30	94,5	989		
bcde	31	96,4	754		
abcde	32	97,0	558	96,8	607
Σ		2 654,7	47 355		
Mean		82,96	1 480		
Base point	33	92,4	1 248		
	34	92,9	1 233		
	35	90,5	1 336		
	36	91,3	1 299		
	37	92,1	1 630		
	38	92,4	1 266		
Mean		91,9	1 335		

TABLE 6.24 : SUMMARY OF EFFECT TOTALS AND EFFECTS - CA 398-10 EXPERIMENT

	Rejection performance		Flux performance	
Variation Source	Effect total	Effect	Effect total	Effect
Main effects				
A mole ratio	331,7	20,73	-13 663	-853,9
B CA conc.	288,5	18,03	-14 405	-900,3
C air drying	20,9	1,31	-457	-28,6
D annealing	192,7	12,04	-12 967	-810,4
E room temp.	62,5	3,91	-2 775	-173,4
Interaction effects				
AB	-208,1	-13,01	5 941	371,3
AC	-13,3	-0,83	-31	-1,9
AD	-139,9	-8,74	6 559	409,9
AE	-38,5	-2,41	663	41,4
BC	-6,9	-0,43	-541	-33,8
BD	-51,9	-3,24	3 109	194,3
BE	-66,5	-4,16	1 777	111,1
CD	8,9	0,56	-887	-55,4
CE	-6,9	-0,43	465	29,1
DE	-19,5	-1,22	1 003	62,7
ABC	0,5	0,03	601	37,6
ABD	25,9	1,62	-1 601	-100,1
ABE	46,9	2,93	-1 349	-84,3
ACD	-5,3	-0,33	531	33,2
ACE	6,5	0,41	-485	-30,3
ADE	5,1	0,32	-559	-34,9
BCD	-14,9	-0,93	729	45,6
BCE	3,3	0,21	-35	-2,2
BDE	28,3	1,77	-1 241	-77,6
CDE	-2,9	-0,18	-201	-12,6
ABCD	12,5	0,78	-609	-38,1
ABCE	1,5	0,09	-21	-1,3
ABDE	-12,7	-0,79	713	55,6
ACDE	7,3	0,46	201	12,6
BCDE	4,1	0,26	63	3,9
ABCDE	-10,5	-0,66	-27	-1,7

TABLE 6.25: SUMMARY OF ANALYSIS OF VARIANCE, CA 398-10 EXPERIMENT

Rejection

Source of variation	SS	df	MSS	F-ratio
Main effects	7 335,5	5	1 467,1	730,6
Interaction effects				
Two-factor	2 256,5	10	225,7	112,40
Three factor	114,7	3	38,2	19,02
Error estimate				
Three-factor	10,5	7		
Four-factor	12,2	5	2,01	
Five-factor	3,4	1		

Flux

Source of variation	SS	df	MSS	F-ratio
Main effects	17 819 819	5	3 563 964	551,4
Interaction effects				
Two-factor	2 933 807	10	293 381	45,39
Three factor	185 097	3	61 699	9,55
Error estimate				
Three-factor	55 124	7		
Four-factor	28 878	5	6 464	
Five-factor	23	1		

TABLE 6.26: FIRST-ORDER MULTIPLE LINEAR REGRESSION COEFFICIENTS, CA 398-10

Variable	Rejection coefficients	Flux coefficients
b_o	82,96	1 479,84
x_1	10,366	-427,00
x_2	9.016	-450,16
x_3	0,653	-14,28
x_4	6,022	-405,22
x_5	1,953	-86,72
$x_1 x_2$	-6,503	185,66
$x_1 x_3$	-0,416	
$x_1 x_4$	-4,372	204,97
$x_1 x_5$	-1,203	20,72
$x_2 x_3$	-0,216	-16,91
$x_2 x_4$	-1,622	97,16
$x_2 x_5$	-2,078	55,53
$x_3 x_4$	0,278	-27,72
$x_3 x_5$	-0,216	14,53
$x_4 x_5$	-0,609	31,34
$x_1 x_2 x_3$		18,78
$x_1 x_2 x_4$	0,809	-50,03
$x_1 x_2 x_5$	1,466	-42,16
$x_1 x_3 x_4$	-0,166	16,59
$x_1 x_3 x_5$	0,203	-15,16
$x_1 x_4 x_5$	0,159	-17,47
$x_2 x_3 x_4$	-0,466	77,78
$x_2 x_4 x_5$	0,884	-38,78

TABLE 6.27: DIFFERENCE BETWEEN OBSERVED AND PREDICTED RESPONSE VALUES (DATA FROM TABLE 6.23 AND 6.26)

	Membrane rejection			Membrane flux		
Ref.	Observed R	Predicted R^*	Residual $(R - R^*)$	Observed F	Predicted F^*	Residual $(F - F^*)$
1	35,8	35,8	0	3 552	3 479	73
2	85,3	86,4	-1,1	1 679	1 623	56
3	79,3	80,0	-0,7	1 817	1 867	-50
4	95,1	95,6	-0,5	994	1 048	-54
5	35,2	36,0	-0,8	3 678	3 707	-29
6	86,8	84,9	1,9	1 670	1 770	-100
7	82,8	81,3	1,5	1 646	1 641	5
8	94,7	95,0	-0,3	989	891	98
9	61,4	62,9	-1,5	1 959	2 033	-74
10	92,4	92,9	-0,5	1 151	1 201	-50
11	95,3	95,8	-0,5	901	854	47
12	96,5	97,1	-0,6	710	658	52
13	69,1	66,8	2,3	1 802	1 772	30
14	93,3	93,6	-0,3	1 087	992	95
15	96,6	96,9	-0,3	759	762	-3
16	96,5	95,1	1,4	671	768	-97
17	52,7	53,3	-0,6	2 831	2 834	-3
18	90,9	91,8	-0,9	1 455	1 361	94
19	78,5	79,8	-1,3	1 744	1 768	-24
20	94,9	95,0	-0,1	901	993	-92
21	53,3	51,9	1,4	3 139	3 181	-42
22	90,4	90,3	0,1	1 455	1 505	-50
23	80,0	79,5	0,5	1 729	1 660	69
24	95,3	94,4	0,9	882	834	48
25	73,2	73,8	-0,6	1 739	1 739	0
26	92,9	92,9	0	1 053	1 149	-96
27	96,0	96,0	0	818	795	23
28	96,7	98,3	-1,6	602	504	98
29	75,9	76,1	-0,2	1 641	1 597	44
30	94,5	93,7	0,8	989	938	51
31	96,4	95,6	0,8	754	822	-68
32	97,0	96,3	0,7	558	611	-53
33	92,4	83,0	9,4	1 248	1 480	-232
34	92,9	83,0	9,9	1 233	1 480	-247
35	90,5	83,0	7,5	1 336	1 480	-144
36	91,3	83,0	8,3	1 299	1 480	-181
37	92,1	83,0	9,1	1 630	1 480	150
38	92,4	83,0	9,4	1 266	1 480	-214

TABLE 6.28: FACTOR LEVELS TO ESTIMATE SELF-INTERACTING EFFECTS

	Factor		Factor level -√2	base	+√2	unit
A	Mole ratio acetone/formamide		0,92	1,2	1,48	0,2
B	CA 398-10	[mm%]	22,2	25,0	27,8	3,0
C	Air flow rate	[lpm]	0,10	0,25	0,40	0,1
D	Annealing temperature	[°C]	80,8	85,0	89,2	3,0
E	Room temperature	[°C]	16,8	21,0	25,2	3,0

TABLE 6.29: ADDITIONAL TRIALS TO FORM A COMPOSITE DESIGN TOGETHER WITH TABLE 6.23

x_1	x_2	x_3	x_4	x_5	Rejection	Flux
+√2	0	0	0	0	96,0 ± 0,2	985 ± 23
-√2	0	0	0	0	69,1 ± 0,7	1 959 ± 45
0	+√2	0	0	0	96,1 ± 0,1	907 ± 17
0	-√2	0	0	0	70,7 ± 1,1	2 090 ± 51
0	0	+√2	0	0	92,4 ± 0,4	1 257 ± 25
0	0	-√2	0	0	91,4 ± 0,3	1 300 ± 21
0	0	0	+√2	0	95,7 ± 0,3	877 ± 20
0	0	0	-√2	0	82,0 ± 0,4	1 807 ± 29
0	0	0	0	+√2	93,5 ± 0,6	1 180 ± 78
0	0	0	0	-√2	86,4 ± 0,5	1 504 ± 29
0	0	0	0	0	91,8 ± 0,9	1 284 ± 43

TABLE 6.30: RE-ADJUSTMENT OF THE b_o REGRESSION COEFFICIENT ESTIMATE (SELF-INTERACTING EFFECTS)

	Rejection	Flux
b_o	90,618	1 326,82
b_{11}	-3,927	73,27
b_{22}	-3,502	86,52
b_{33}	0,748	-23,48
b_{44}	-0,777	8,27
b_{55}	-0,227	8,27

When the significant two-factor interactions concerning acetone/formamide ratio (x_1) are considered, it appears that improvement in membrane performances were more pronounced when the membranes were made under conditions which favoured the formation of more porous membranes (low level x_1) than under conditions which favoured the formation of more dense membranes. Three interactions are compared in Table 6.31. The '+' and '-' signs shown in the table refer to the levels of the variables indicated, and the entries in each cell are the average membrane salt rejection and flux performances for that particular variable level combination. (Data taken from Table 6.23).

In all the interactions given in Table 6.31, high levels for both the x_1 and x_2 variables resulted in the formation of more dense membranes. With x_1, the concentration of the acetone solvent increased as the variable level approached the upper value limit of +1. (See Table 6.32). This decrease in non-solvent concentration, although relatively small, not only affects the coiled state of the polymer chains due to shifts within the solubility region (see Figure 6.1), and therefore a lesser state of supermolecular polymer aggregation, but also affected the specific gravity of the casting solution relative to that of the coagulation bath - a cause of modified membrane morphology which is often overlooked *(13)*. Acetone has a specific gravity and molar volume of 0,79 and 74,0, whereas those of formamide are 1,13 and 39,8 respectively. The greater the difference between the specific gravities of the solvent system and the coagulation medium, the more likely the instantaneous depletion and removal of the solvent from the cast membrane interface will be by convective flow (rather than diffusive exchange with water molecules), and a more dense membrane will result.

The three prime variables, in decreasing order of magnitude, seemed to be those that controlled the membrane casting-solution composition (*i.e.* acetone/formamide ratio (x_1) and CA concentration (x_2)) and annealing temperature (x_4), which controlled the final adjustment of membrane porosity. Figures 6.4 to 6.6, constructed with the aid of the design regression equations (Table 6.26 and 6.30), demonstrate how each of x_1, x_2 and x_4, considered in turn, affected the predicted response at common and fixed variable levels for all the other remaining variables. (In effect this study is comparable to a one-variable-at-a-time approach, but because it was conducted with the aid of the membrane design equations, tended to be more meaningful as such a study revolved around a sound selection of independent variables which were held constant).

The effect which variable x_1 had on membrane performance is shown in Figure 6.4. Along the line, denoted $x_i = 0$ for example, all the variables, except x_1 which is shown along the x-axis, took on the value of zero, *i.e.* base or mid-level value for these variables (see Table 6.11). As x_1 increased in value, the membrane morphology changed from porous (solvent-system specific gravity: 0,94 at $x_1 = -1$) to more dense at $x_1 = +1$ (solvent-system specific gravity: 0,88). However, as x_1 increased to its upper limit of +1, the overall porosity of the membrane decreased due to the higher acetone and polymer concentration, high annealing temperature and effect of room temperature, and the role which formamide played in creating supermolecular polymer aggregation was less pronounced with respect to rejection performance. However, higher permeate flux performances were still obtainable at comparable salt rejection performances at the relative higher formamide concentration level $x_1 = -1$.

TABLE 6.31: CA 398-10 INTERACTION EFFECTS

		X_1 Acetone/formamide ratio [-]	X_1 Acetone/formamide ratio [+]	
X_2 CA concentration	[-]	57,1	90,8	%
		2543	1317	lmd
	[+]	88,1	95,8	%
		1271	788	lmd

		X_1 Acetone/formamide ratio [-]	X_1 Acetone/formamide ratio [+]	
X_4 Annealing temp.	[-]	62,2	91,7	%
		2157	1264	lmd
	[+]	83,0	95,0	%
		1297	853	lmd

		X_1 Acetone/formamide ratio [-]	X_1 Acetone/formamide ratio [+]	
X_5 Room temperature	[-]	69,4	92,6	%
		2014	1119	lmd
	[+]	75,8	92,6	%
		1799	987	lmd

TABLE 6.32: TRANSFORMED X_1 AND X_2 VARIABLE LEVELS, CA 398-10, 2^5 FACTORIAL AND COMPOSITE DESIGN

Variable		CA	F	Ac
x_1	x_2	Mass percent		
-1	-1	23,8	33,3	42,9
+1	-1	23,8	27,1	49,1
-1	+1	26,2	32,2	41,6
+1	+1	26,2	26,3	47,5
0	$-\sqrt{2}$	22,2	30,5	47,3
0	$+\sqrt{2}$	27,8	28,3	43,9
$-\sqrt{2}$	0	25,0	34,2	40,8
$+\sqrt{2}$	0	25,0	25,8	49,2
0	0	25,0	29,4	45,6

Molecular mass acetone 58,08 g/mole
Molecular mass formamide 45,04 g/mole

CA Cellulose acetate
F Formamide
Ac Acetone

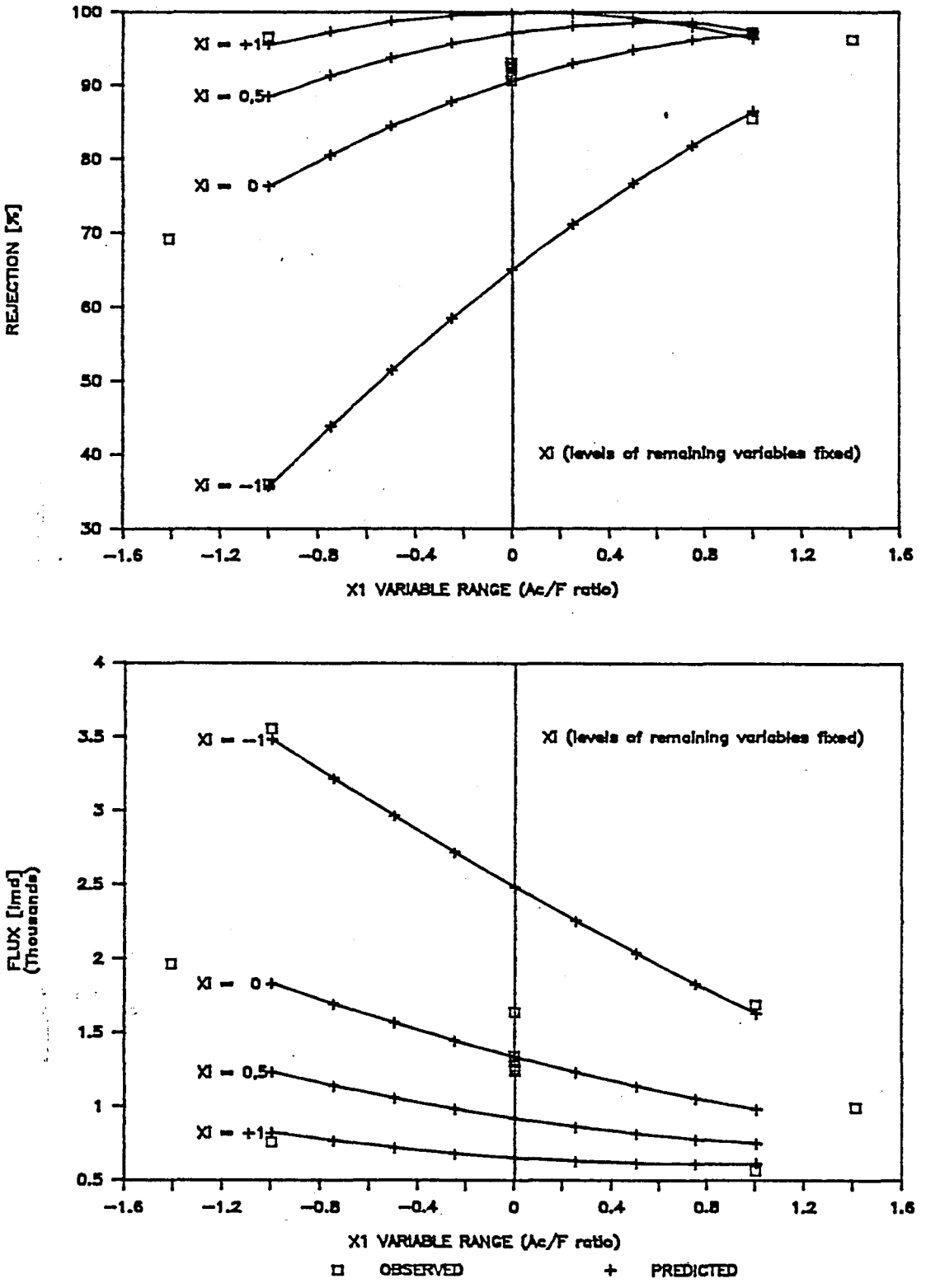

FIGURE 6.4: MEMBRANE PERFORMANCE *versus* ACETONE/FORMAMIDE RATIO

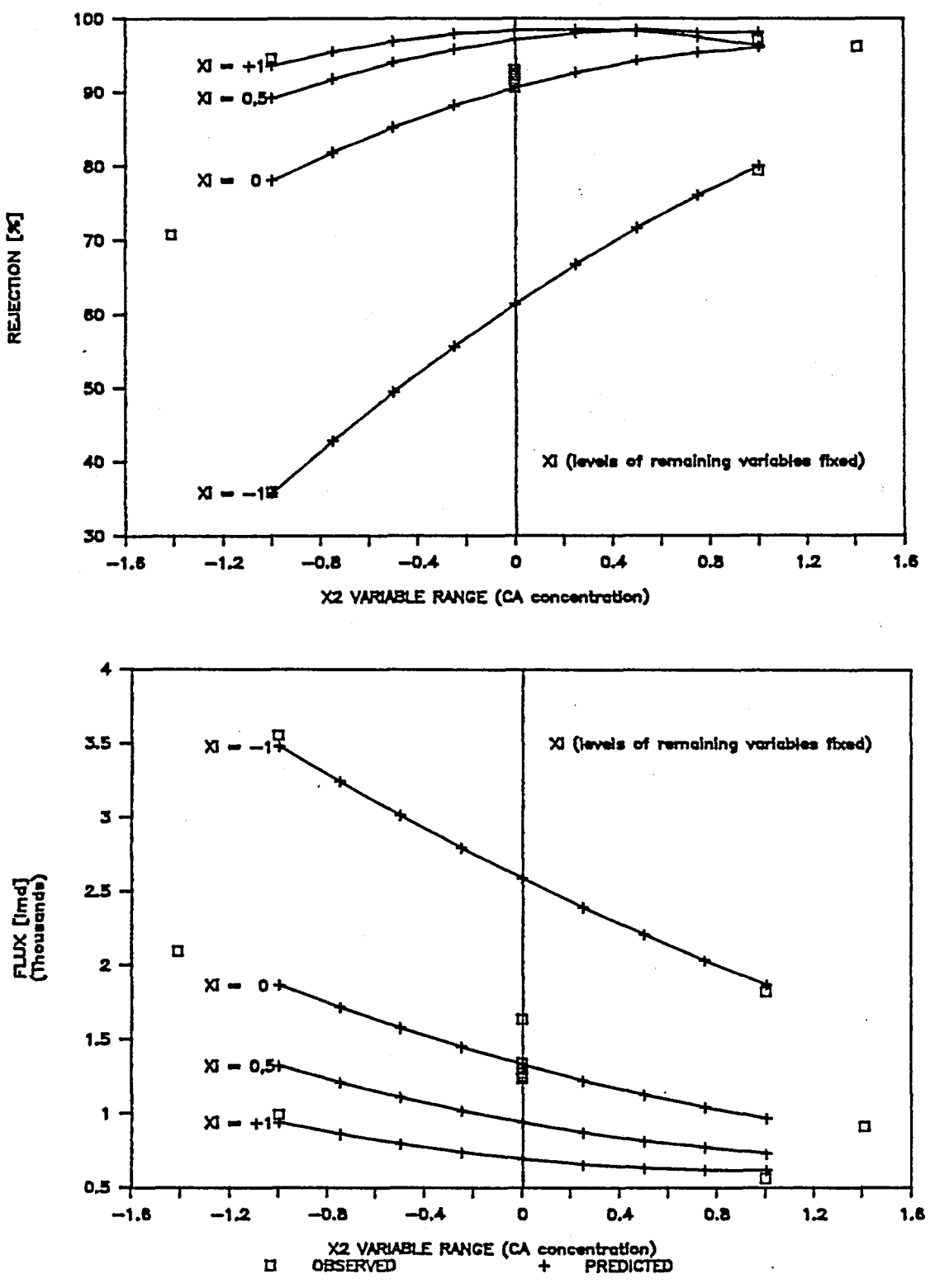

FIGURE 6.5: MEMBRANE PERFORMANCE *versus* POLYMER CONCENTRATION

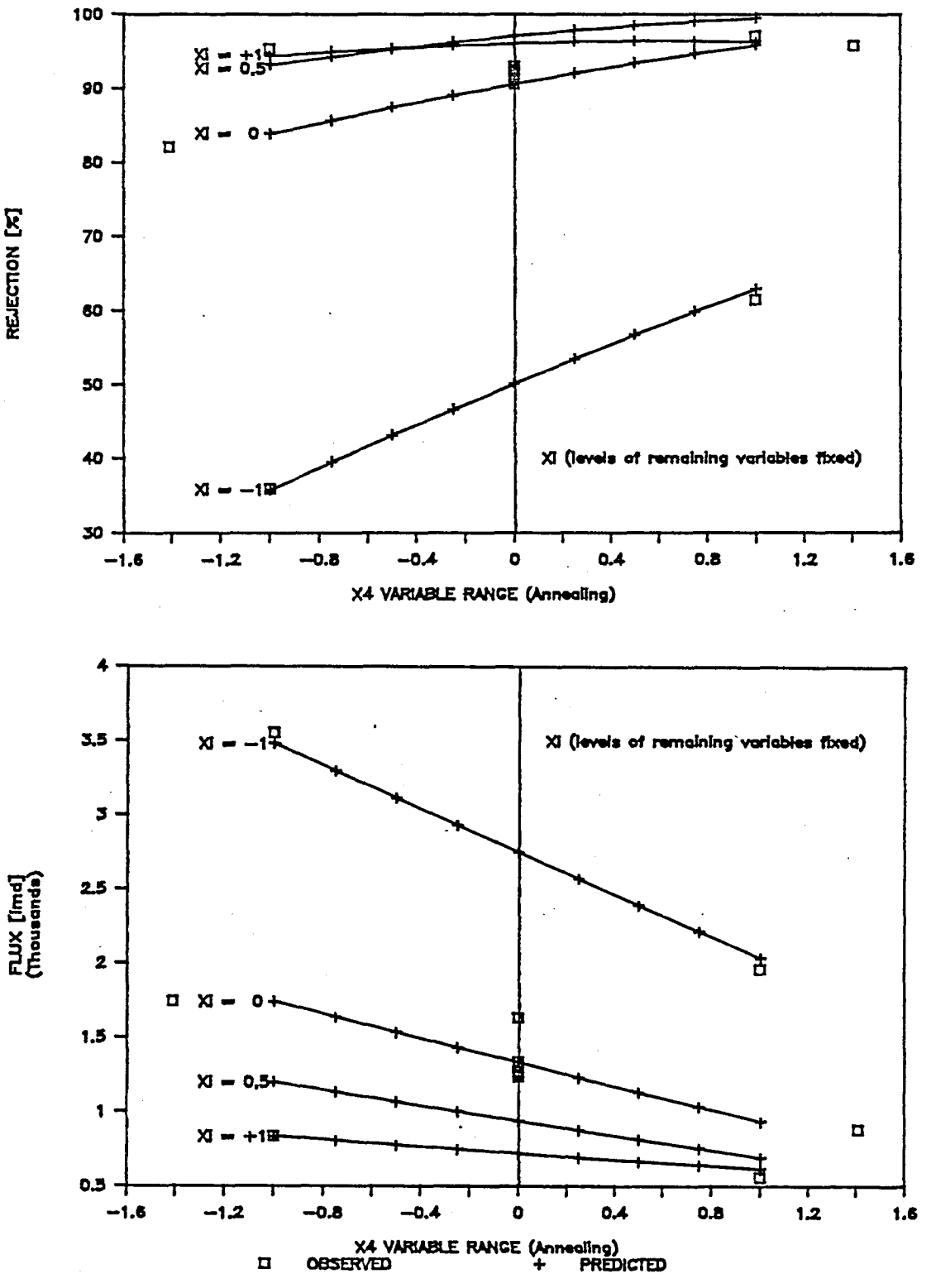

FIGURE 6.6: MEMBRANE PERFORMANCE *versus* ANNEALING TEMPERATURE

Solvents for CA with specific gravities closer to that of water, such as 1,4-dioxane (specific gravity 1,03) *(14)* and di-methyl sulphoxide *(15)*, were found to be useful to improve permeate flux performances of CA asymmetric membranes.

In Figure 6.5 the effect of polymer concentration, x_2, on membrane performance is illustrated. This is in agreement with other studies *(16)(17)* in that higher polymer concentrations in the casting solution led to the formation of smaller and fewer pores in the surfaces of membranes as well as a narrower pore size distribution; the salt rejection therefore increases. As a secondary effect, transport of water through the membrane will be reduced with increased polymer concentration as the void-volume ratio in the final structure will decrease with increasing polymer concentration. This variable (x_2), together with x_1 (Table 6.31), can be balanced against each other in order to adjust the final membrane morphology. (See Figure 4.8).

In the post-treatment annealing step (x_4) the membrane was tightened up (Figure 6.6) to improve its otherwise meagre salt rejecting characteristics *(5)*. When the membrane was heated in aqueous medium at temperatures above its second relaxation temperature, the thermal energy caused translational motion of the macro-molecules on the molecular level. This resulted in a permanent rearrangement of the polymer segments in that inter- and intra-di-pole bonds were formed between polar groups; coalescence of the structure and a reduction of the free energy as the total surface area was decreased.

The rejection *versus* the permeate flux performances of the CA 400-25 and CA 398-10 membranes associated with the factorial experiments shown in Tables 6.12 and 6.23, are compared in Figure 6.7. It is clear from these graphs that the permeate flux expectancy of CA 398-10 membranes was higher than those of CA 400-25 for equivalent salt rejections, for rejections above 90%. However, because of the higher rates of convective flow towards the membrane surface, concentration polarization, for these membranes, was also higher than for CA 400-25 membranes, for equivalent rejections. In Figure 6.8 the calculated concentration polarization factor (section 5.4.3.3), *i.e.* the factor by which the salt concentration at the upstream membrane interface is greater than that of the bulk stream, is plotted against the salt rejection performances of these two membranes.

The overall performances of these two membranes are compared in a log-log plot of the salt permeability coefficient *versus* the water permeability coefficient. The regression lines (Figure 6.9) clearly show the superiority in flux performance of the CA 398-10 membrane at rejections above 90%.

The predictions of the design equations developed in the laboratory for the CA 398-10 membrane system were also tested against the performances of membranes produced on a large scale by industry. A quality-control data sheet was taken at random from their files and the fabrication conditions listed were transformed appropriately. As the membrane evaluation conditions were similar, the performances predicted by the design equations could be interpreted as calculated. The conditions of membrane fabrication, the transformed variables, observed and predicted performances are shown below.

Factor level		Transformed variables	
Mole ratio Ac/F	1,304	$x_1 = (1,304 - 1,2)/0,2$	= 0,52
CA concentration	25,556	$x_2 = (25,556 - 25)/2$	= 0,278
Air drying		x_3	= 0
Annealing temp.	88	$x_4 = (88 - 85)/3$	= 1
Room temperature	20	$x_5 = (20 - 21)/3$	= -0,333

Predicted performance:	98,6%	782	lmd
Observed performance:	96,9 ± 0,4%	761 ± 37	lmd

The predicted performances were in reasonable agreement with observed responses, which was another illustration of the usefulness of membrane formulation and design equations.

6.1.4 CONCLUSIONS

In summary;

i) The results indicate that low variation in membrane properties is achievable by maintaining certain fabrication variables (Table 6.1) at a fixed level.

ii) A wide range of membrane properties can be achieved by altering five fabrication variables.

iii) Membranes with optimal performance can be tailor-made by numeric optimization of the design equations obtained through statistically designed experiments.

iv) Factorial experiments allow multiple linear regression analysis to be performed on data without large computational capacity. Although not part of this presentation, step-wise regression, performed on a main-frame computer on the same data, will reduce the residuals, shown in Table 6.27, even further and provide the researcher with an even better estimate of the response surface behaviour.

v) Experiments based on factorial design permit assessment of interactions between variables which is not possible in the one-variable-at-a-time approach.

vi) One-variable-at-a-time studies can be performed with the membrane design equations. This inverts the method otherwise used in that the response behaviour is known beforehand.

vii) Strict control of the five membrane design variables is imperative as small deviations in the space of these factors give rise to membranes with different performances.

viii) The Taylor series used as a regression model enabled a good approximation of the response surface to be made. Polynomials have the advantages that they are easy to fit and that they give a reasonable approximation of the true response behaviour within the bounds of the experiment, but extrapolation to regions beyond the bounds of the experiment should be treated with care.

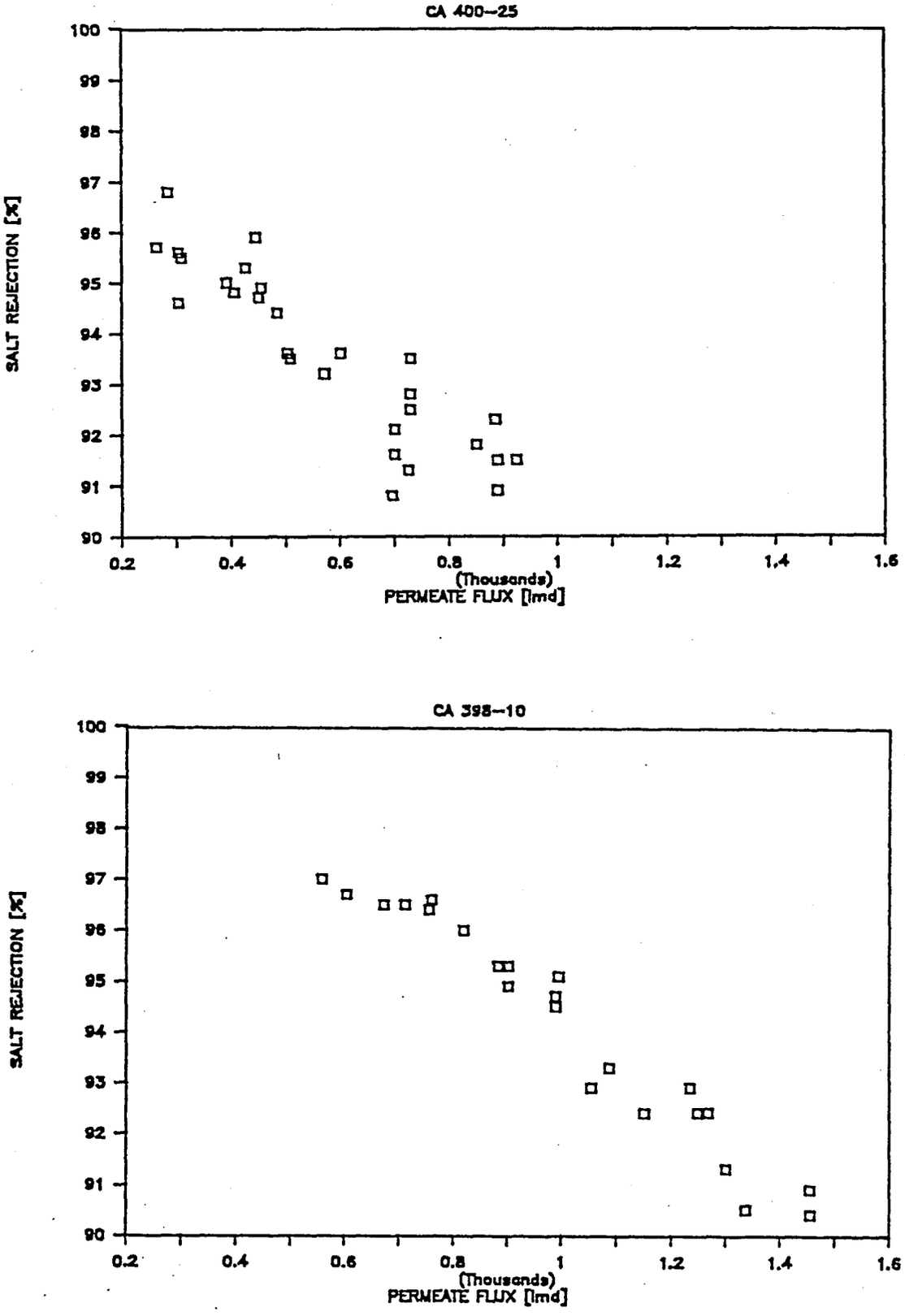

FIGURE 6.7: SALT REJECTION *versus* PERMEATE FLUX FOR CA 400-25 AND CA 398-10 MEMBRANES

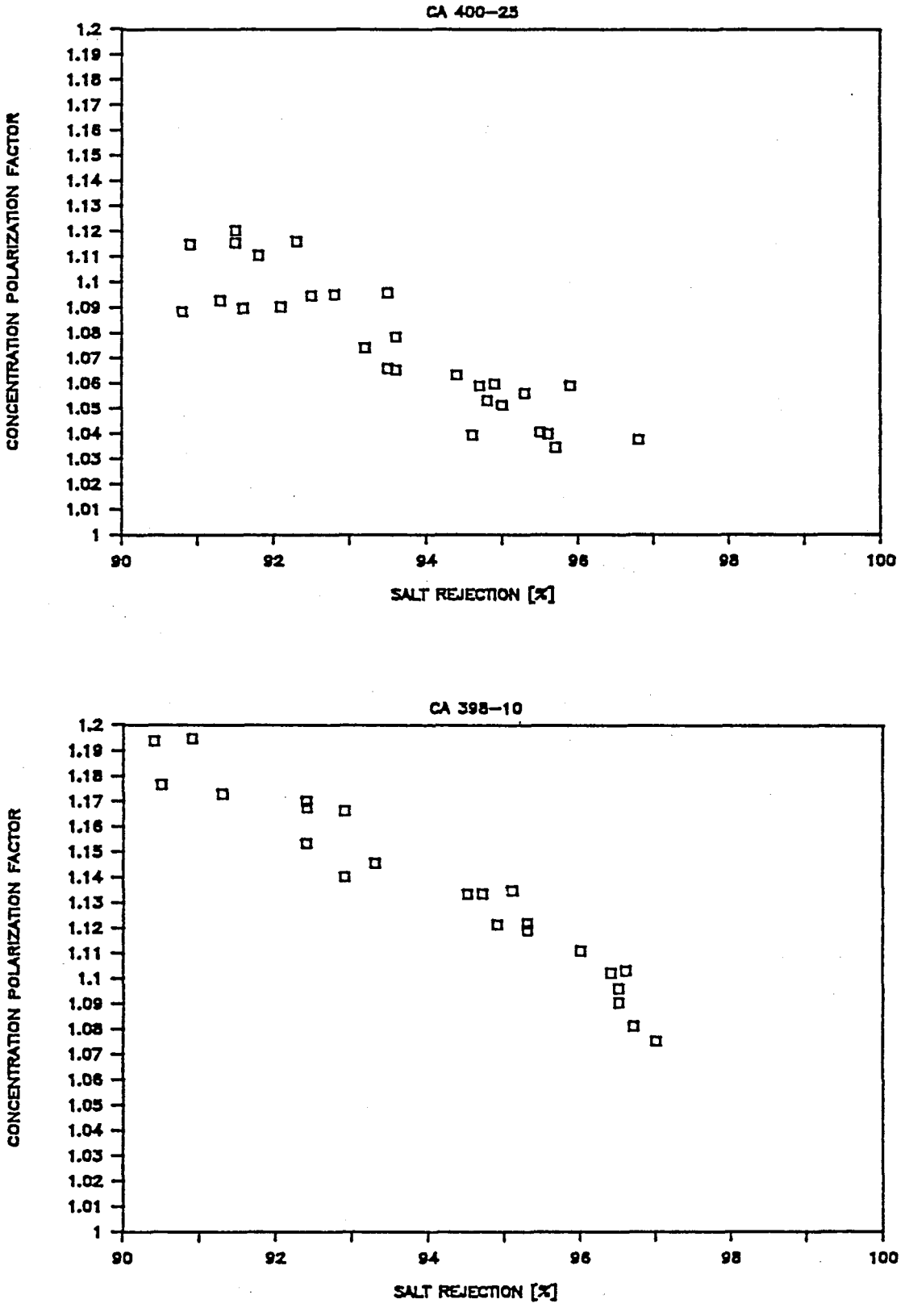

FIGURE 6.8: CONCENTRATION POLARIZATION versus SALT REJECTION FOR CA 400-25 AND CA 398-10 MEMBRANES

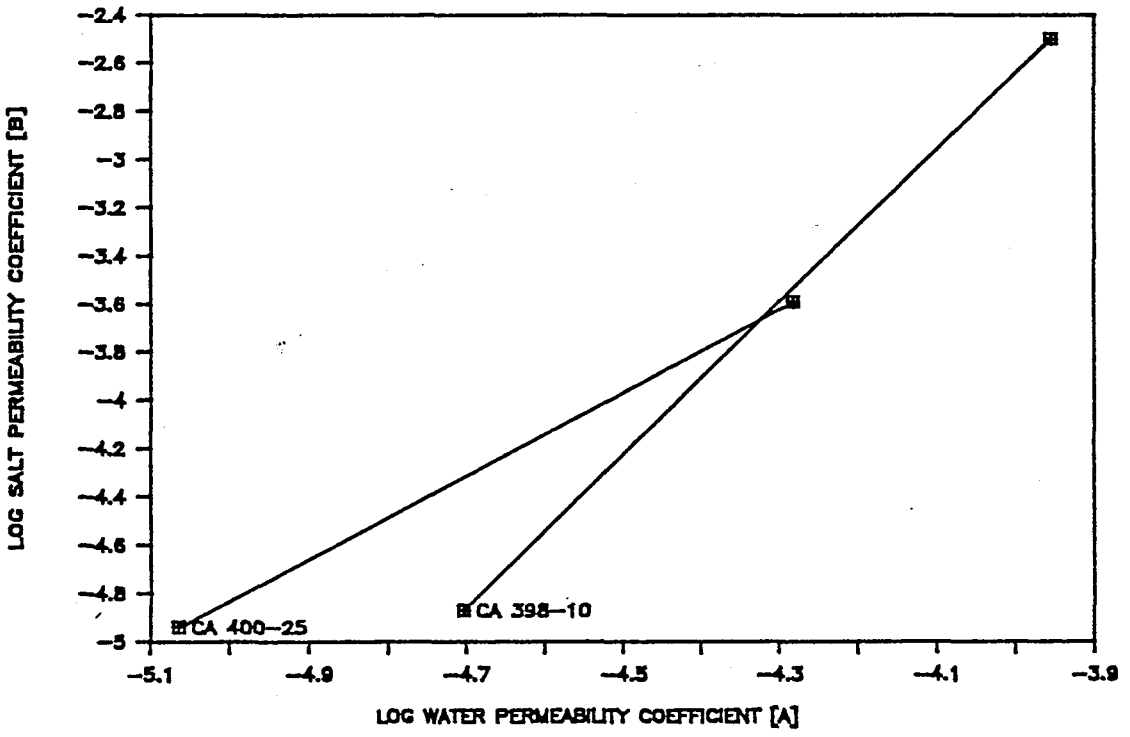

FIGURE 6.9: COMPARISON OF MEMBRANE PERMEABILITY COEFFICIENTS FOR THE CA 400-25 AND CA 398-10 MEMBRANE SYSTEMS

6.2 ASYMMETRIC SUBSTRATE MEMBRANES

It was shown earlier in Chapter III that dense, ultra-thin permselective barriers are deposited on asymmetric substrate membranes in the preparation of UTF composite RO membranes.

In this section aspects of the development of suitable fabrication conditions for tubular substrate membranes will be discussed. These synthetic micro-porous polymeric membranes may be regarded as ultrafiltration membranes, and, as such, this work also acted as a precursor for a study on the applicability of this membrane system in the process of ultrafiltration *per se (18)*.

In section 6.3 the reader will be introduced to the chemicals from which polyvinyl amidine [PVAM] ultra-thin film composite RO membranes were fabricated. The route followed in the synthesis and characterization of the polymeric amine compound(s) and cross-linking reagent *(19)* had to be researched and developed from start as these materials were not available commercially. It is thus understandable that the quality of the materials produced initially was not consistent and had therefore to be regarded as a random variable.

In a sense the situation was more resolved in the case of the substrate membrane. As a starting point in the development of this membrane, it was known from numerous publications on flat sheet composite membranes, that adequate composite RO substrate membranes can be fabricated from solutions of PS in DMF or DMAc *(20)(21)*. It was also known that the pure-water permeability coefficient (A-value) of flat-sheet substrate membranes, regarded as optimal in flat sheet composite RO membrane fabrication, was in the 2 000 to 4 000x10^{-5} *(20)* range, with surface pore radii in the 30 to 50nm range *(22)*. However, the applicability of these figures to membranes of the tubular type could initially only be assumed.

All the above uncertainties, together with the large number of possible fabrication variables associated with the complete UTF composite RO membrane system, added a different dimension to the problem of establishing fabrication formulations for the UTF composite RO membrane than was the case with the CA membrane system. As we were faced with at least two known random variables (*i.e.* the irreproducibility of membrane forming chemicals), a self-directing approach to optimization was followed. The initial experimental design was based on a Plackett-Burman design *(23)* (section 4.4.4.2).

The route followed in the development of the composite RO membrane was to consider the membrane as two separate entities: the substrate membrane and the permselective barrier (the ultra-thin film). At first, attention was to be paid to the substrate membrane itself, a study which involved: the selection of the polymeric membrane-forming material and membrane support fabric, choice of casting solution composition and of coagulation procedures, and elimination of imperfections. From these studies, two substrate membrane formulations resulted. These substrate membranes were used in the optimization study involving PVAM UTF composite membrane fabrication formulations (section 6.3.3 and 6.3.4).

6.2.1 SUBSTRATE MEMBRANE MATERIALS

Criteria for the choice of a suitable synthetic substrate membrane polymer can be based on:

i) physical properties: molecular mass (intrinsic viscosity of the polymer), wettability (hydrophobic/hydrophylic balance);
ii) chemical properties: resistance to solvents, chemical resistance (oxidizing agents, acids and alkalis);
iii) mechanical integrity: resistance to compaction (deformation).

A further obvious criterion is that the membrane polymer should yield a film with anisotropic morphology when solution-cast by the wet phase-inversion process. Polymers which fall within this class of usable materials are, inter alia: poly(bisphenol-A-sulphone) [PS], -(arylether sulphone) [PES], -(vinylidene fluoride) [PVDF], -(acrylonitrile) [PAN] and -(dimethyl phenylene oxide) [PPO] ().

6.2.1.1 Membrane support fabric

The above criteria also hold for the tubular membrane support-fabric material. Poly(ethylene terephthalate) [PET] has withstood the test of time as a competent membrane support material and is widely used for this purpose. PET fabrics (), suitable as support materials for flat-sheet membranes, are available from various sources, both as spun-bonded or wet-laid non-woven fabrics, or as woven fabrics ().

Woven or non-woven filter fabrics of any thickness may be used to support flat-sheet membranes, as long as it offers adequate mechanical support to the membrane. Normally, as these membranes are housed in spiral-wrap configurations (rolled-up form), where the packing density of the membrane is important, thinner support fabrics are used. Single-ply tubular membranes, on the other hand, require that heavier and thicker fabrics are used to give greater mechanical strength to the tubular element.

Various materials have been investigated as possible materials for the fabrication of tubular membrane support elements *(1)*. Of all the non-woven products investigated, only two were regarded as satisfactory for fabrication of a single-ply support-element, namely, a spun-bonded fabric (Reemay™ 3396) from Eaton-Dikeman (USA) and a wet-laid fabric (Viledon™ FO 2406) from Carl-Freudenberg (Germany). The former was extensively used during the CA-membrane development program, whereas a switch was made to the latter at the start of the composite-membrane program.

6.2.1.2 Substrate membrane polymers and solvents

Of the membrane polymer materials mentioned earlier, poly(bisphenol A sulphone) [PS] is the most widely used as a substrate membrane for UTF composite RO membranes. The choice of this synthetic material is historic *(27)* and based mainly on the relative ease with which solutions of the polymer can be transformed into asymmetric membranes by the wet phase inversion process. This hydrophobic material also offers resistance against attack by oxidizing chemicals, acids and alkalis. In fact, under harsh membrane-cleaning conditions (*e.g.* pH 11), the integrity of the PET material is questionable, rather than that of the PS

membrane. The polymer (a product of Union Carbide) has a high T_g [195°C] and has otherwise found widespread application as a high-impact-resistant engineering thermoplastic. The two grades of this material which have found application as membrane-forming polymers are Udel 1700P and 3500P. (Udel 1700P is the lower molecular-mass equivalent of 3500P).

Some aspects regarding the use of polysulphone as a wet-phase-inversion membrane material:

i) The polymer can be classed as hydrophobic, and when wet-stored over a period of time, some permanent loss of permeability (densification) occurs when its performance is compared with flux performances of freshly produced membranes. This tendency is reduced by hot rinsing (50°C for 60min) the membranes after the coagulation step *(28)*. This loss of permeability has been ascribed to diffusion of solvent from dead-end pores, the hydrophobic nature of the polymer preventing water from exchanging with the solvent, which results in a densification of the membrane structure.

ii) Polysulphone membranes need to be stored wet to retain their ability to pass water at pressures just above atmospheric. Once dried out completely, hydrodynamic pressures in the 0,5 to 1MPa pressure range need to be applied as "breakthrough" pressure to restore permeation *(29)*.

iii) The viscosity of binary PS casting solutions (*i.e.* polymer and a solvent) depends on the solvent used, but as the molecular mass of polysulphones is not high, the viscosity is not drastically increased by increasing the polymer concentration over the useful 13 to 18% mass range.

iv) N,N-dimethyl formamide [DMF] is well known as a solvent in the preparation of PS membranes. Unfortunately, DMF-based casting solutions turn milky within two to three days after preparation due to precipitation of lower molecular mass fractions of the polymer. The homogeneity of the solution can be restored by heating at 90°C. However, once milky, solutions have a storage-life of about seven days, beyond which heat treatment does not help in restoring the original homogeneity.

Different moderately polar aprotic solvents, other than DMF, may be used to dissolve PS, examples are N,N-dimethyl acetamide and 2-pyrrolidone. Another solvent, which gives stable polymer solutions, is N-methyl, 2-pyrrolidone [NMP].

NMP became the preferred solvent for use towards the end of the study, due primarily to its higher solvating power for the polymer. Other advantages of the NMP-based solvent system were the extended shelf-life of polysulphone casting solutions and lower toxicity-levels relative to that of DMF.

PS is not the only member of the polysulphone family which can be used for the formation of asymmetric support membranes. Poly(arylether sulphone) [PES] (Victrix, a product of ICI, England) *(30)*, has also found acceptance as an UF membrane forming material *(31)*. The material is slightly more polar than PS, as is indicated by higher equilibrium water adsorption at 20°C *(32)* (see Table 6.33), and should offer higher thermal stability as a result of its higher glass transition temperature.

The chemical structure of the two polymers, Udel [PS] and Victrex [PES], are given below.

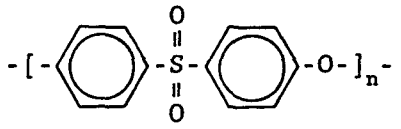

Victrex: 4800G [PES]

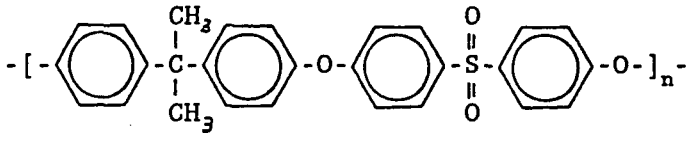

Udel: 1700P, 3500P [PS]

In Figure 6.10 the viscosity of Victrex and Udel, dissolved in NMP, are shown as a function of polymer concentration. Of the three polymers, PES has the lowest relative (Brookefield) viscosity. Figure 6.11 shows that NMP gives PES polymer solutions of higher viscosities than DMF does. This may be regarded as an indication of the higher solvating power of NMP.

This statement is supported by the volume of non-solvent coagulant (water) which ternary, NMP-based, solutions of PS and PES can tolerate, relative to those of DMF-based solutions, before the first sign of liquid-liquid phase separation (cloud-point). In the determination of the cloud-point titration volumes [CPTV] (section 2.2.1.3) shown in Table 6.34, 100ml of homogeneous ternary solutions containing two mass percent polymer, an additive (mass percentage as indicated in Table 6.34) and either NMP or DMF, were prepared and titrated (20°C) with water as the non-solvent. It is evident from the entries in Table 6.34 that NMP-based solutions show a greater tolerance to added water than do DMF-based casting solutions. According to Kai *et al (31)*, the permeability of a particular membrane can be adjusted by adjusting the CPTV of the casting solution; in general, the lower the CPTV for a specific solvent system, the greater the sensitivity of the casting solution to non-solvent addition, and the higher the rate of water transport through the resulting membrane *(33)*.

The effect which the solvent and additives have on casting solution viscosity is also evident from Table 6.34. Viscosity determinations were performed on casting solutions containing 18% polymer; the mass ratio between solvent and additive was similar to that indicated for CPTV determinations in the table.

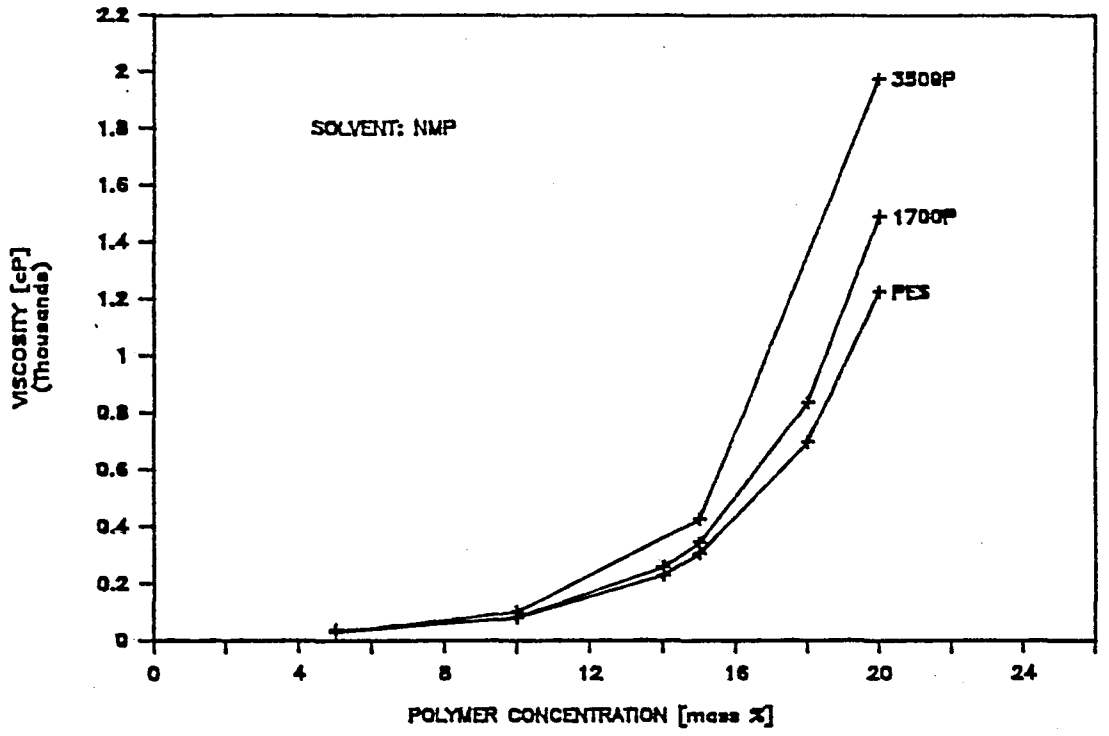

FIGURE 6.10: VISCOSITY INCREASE OF POLY(BISPHENOL-A-SULPHONE) CASTING SOLUTIONS AS A FUNCTION OF POLYMER CONCENTRATION

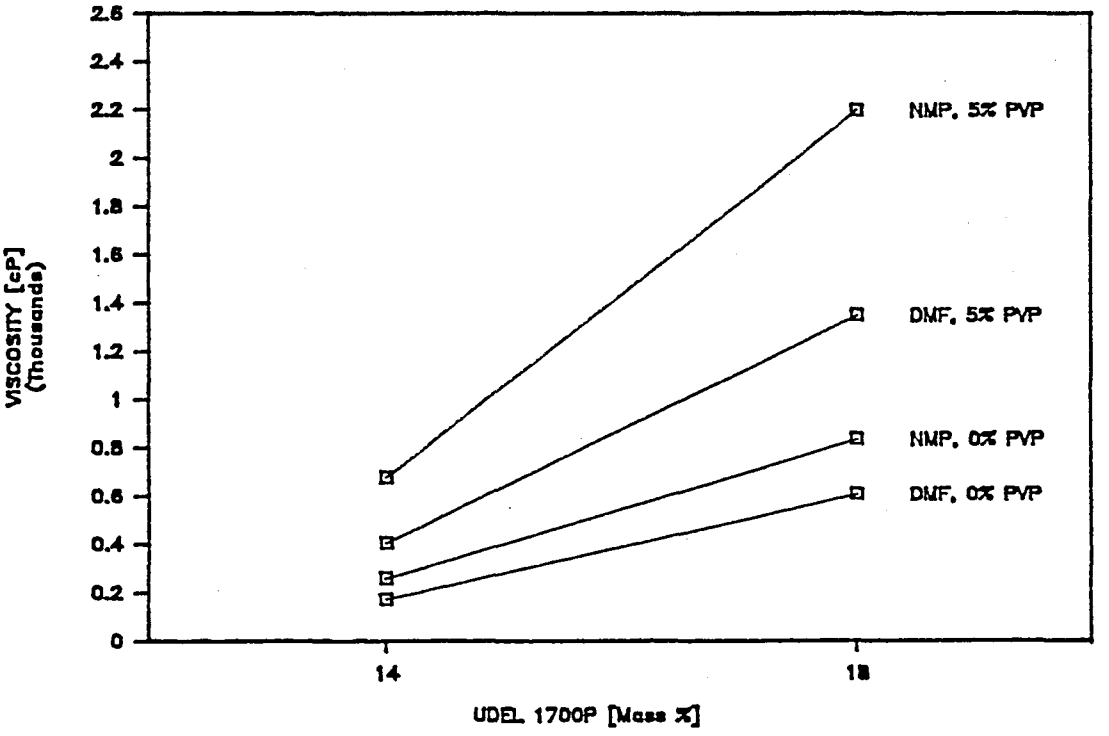

FIGURE 6.11: EFFECT OF 5% PVP ADDITION ON CASTING SOLUTION VISCOSITY

TABLE 6.33: PROPERTIES OF PS AND PES

	PS	PES
Glass transition temperature	190°C	225°C
Equilibrium water adsorption	0,85%	2,1%

TABLE 6.34: CLOUD-POINT TITRATION VOLUMES [CPTV], 20°C

Udel 3500P/NMP

Additive	[mass%]	CPTV ml	Visc. cP
Acetone:	11,95	7,32	760
Acetone:	47,80	1,76	500
LiCl :	0,40	7,72	1 260
LiCl :	2,32	5,74	2 250
PVP/44K:	1,20	7,92	1 260
PVP/44K:	5,98	6,11	2 560

Udel 3500P/DMF

Additive	[mass%]	CPTV ml
Acetone:	11,95	0,86
LiCl :	0,47	1,00
PVP/44K:	1,20	1,55
Dioxane:	5,98	1,94

Victrex 4800G/NMP

Additive	[mass%]	CPTV ml	Visc. cP
Acetone:	11,95	14,15	430
Acetone:	47,80	6,39	240
LiCl :	0,65	14,84	850
LiCl :	3,23	12,71	1 980
PVP/44K:	1,20	14,97	860
PVP/44K:	5,98	13,23	1 880
Dioxane:	5,98	15,21	680
Dioxane:	17,93	14,14	590

Victrex 4800G/DMF

Additive	[mass%]	CPTV ml	Visc. cP
Acetone:	5,98	6,38	265
Acetone:	11,95	5,80	
LiCl :	0,64	6,06	370
LiCl :	2,15	4,84	550
PVP/40K:	1,20	6,60	370
PVP/40K:	5,98	6,11	1 420
Dioxane:	5,98	7,41	280
Dioxane:	17,93	6,97	275

It was noticed that the contents of the leach tank turned hazy (micro-bead formation) *(34)* during leaching, particularly of PES/NMP membranes (high CPTV) at low PES concentration. The cause of this phenomenon is most probably lower molecular mass polymer fractions which can remain solvated in thermodynamically poorer solvents, in instances where the higher molecular mass fractions had already precipitated. This will have caused lower-molecular mass fractions to stay in solution and grow with the polymer-poor phase during phase inversion. These fractions therefore do not form part of the coherent solid-rich phase and precipitate as micro-beads from the polymer-poor phase once their solubility limit was exceeded by further intrusion of non-solvent. This milky "latex" is expelled from the structure during the final stages of coagulation when the gelled structure starts to contract.

Membranes with different morphologies can be created by modifying the solvent, additive and additive concentration, polymer and polymer concentration *etc.* Subsurface morphologies can even be altered further by producing the membranes on different substrate surfaces. Figure 6.12 shows electron-micrographs (420x magnification) of three flat sheet membranes, fabricated in similar fashion from three different casting solutions, but on four different substrate surfaces. The four substrate materials, from left to right in the micro-graphs are a polyolefinic fabric (Tyvek 1085D), two PET fabrics, Viledon FO2406 and Reemay 3396 and a plate-glass surface. The membranes were all coagulated in 20°C RO treated Stellenbosch tap water. The membranes in the figure were cast respectively from;

(a) 18% Victrex 4800G PES, 0,54% LiCl and DMF,
(b) 18% Victrex 4800G PES, 2,7% LiCl and NMP, and
(c) 18% Udel 3500P PS, 0,54% LiCl and NMP.

The support membranes used during the optimization of variables in the fabrication of UTF composite PVAM RO membranes evolved from earlier work *(35)*, and were produced from either 12% 3500P (series 224) or 13% 1700P PS (series 221) solutions in 3,5:1 mass ratio NMP:1,4-dioxane. These membranes had mean permeate flux performances corresponding to A-values, respectively, of $1\,600 \times 10^{-5}$ and $1\,400 \times 10^{-5}$ $[g.cm^{-2}s^{-1}atm^{-1}]$.

6.2.1.3 Coagulant-miscible casting solution additives

The tendency for large cavities or micro-voids to be formed in the membrane sub-surface can be reduced substantially by increasing the casting-solution viscosity, according to Cabasso *(36)*; this is a situation which retards the rate at which the respectively rich phases grow during liquid-liquid phase separation. The viscosity can, however, be increased simply by increasing the polymer concentration as was seen earlier in the case of CA membranes, but at the expense of a severe reduction in permeate volume output.

To overcome this problem, coagulant-miscible polymers are added to increase the viscosity of casting solutions. Normally neutral polymers, when mixed, exhibit positive enthalpy of mixing, with little gain in the entropy of mixing and, as such, exhibit little gain in free energy of mixing. Solutions of such polymer mixtures will phase-separate spontaneously when left to stand undisturbed *(37)*.

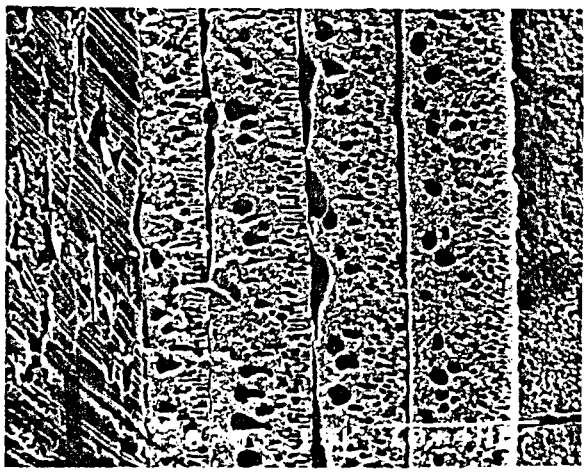

18% Victrex 4800G PES, 0,54% LiCl and DMF

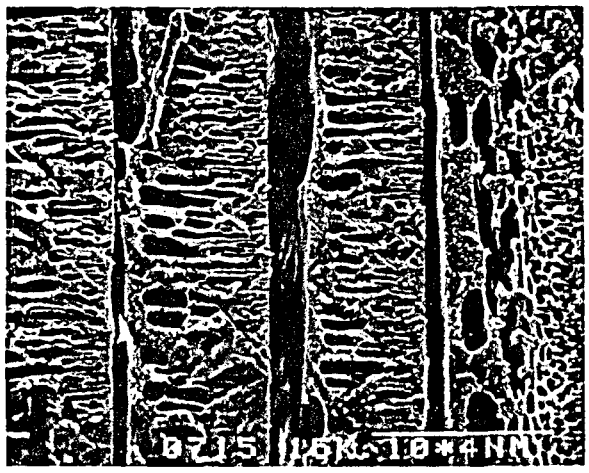

18% Victrex 4800G PES, 2,7% LiCl and NMP

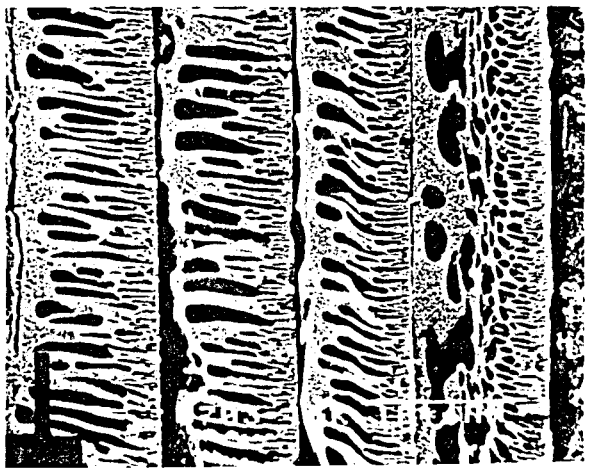

18% Udel 3500P PS, 0,54% LiCl and NMP

FIGURE 6.12: ELECTRON MICROGRAPHS OF SUPPORT MEMBRANES PRODUCED FROM DISSIMILAR CASTING SOLUTIONS ON DIFFERENT SUPPORT SURFACES

Poly(vinyl pyrrolidone) [PVP] is thermodynamically compatible with both PS and PES in solution and can be used in solids concentration ratios of up to 2 to increase the viscosity of such solutions. (See Figure 6.12). PVP is widely used as an additive in the preparation of the extremely high viscosity (about 50 000cP) solutions necessary for the production of hollow fine-fiber PS membranes *(38)*. Low-molecular-mass poly-(ethylene glycol) [PEG] is another example of a polymer which is compatible both with polysulphone casting solutions and the coagulant.

Inorganic compounds such as LiCl and $LiNO_3$ are also miscible with PES and PS casting solutions in concentrations of up to 5% of polymer mass, depending on the solvents used. Inorganic additives have been used in the preparation of, *e.g.* CA and polyimide *(39)* casting solutions. These compounds tend to increase the casting solution viscosity and decrease the CPTV, which in turn affects the surface pore characteristics and hence hydraulic permeability of the membranes.

6.2.2 MEMBRANE/FABRIC COMPATIBILITY

Tubular substrate membranes produced from binary, PS/DMF, solutions are particularly prone to the formation of blisters when they are dried at elevated temperatures, which is a final step in the fabrication of UTF composite RO membranes. The problem arose as a result of the poor bonding between these substrate membranes and the Reemay 3396 support fabric. Other researchers have also been confronted with membrane/fabric bonding problems *(40)*. In first attempts at rectifying the situation, the smoother Reemay 3396 fabric was substituted for the coarser Viledon FO2406 material. However, adhesion between PS membranes produced from binary NMP/1,4-dioxane solvent mixtures and this fabric, although greater than obtained with PS/DMF membranes, remained low and never exceeded values of 0,5kg/cm^2 (determined with the aid of an Elcometer, as described in section 5.5).

The blisters which formed during oven-curing of composite RO membranes produced on the Viledon FO2406 material were small enough to prevent the membrane from tearing when it was pressurized during RO evaluation. However, it was still necessary to adopt careful start-up procedures during membrane evaluation. Once the membranes were pressurized, no further problems arose with the evaluation of the membranes on laboratory equipment. As will be seen, excellent RO membranes could be produced on Viledon FO2406-supported substrate membranes cast from ternary PS/NMP/1,4-dioxane solutions. From the point of view of evaluating membranes in the field *(41)(42)*, the presence of such blisters (potentially substandard substrate membranes) was less acceptable, especially as the membrane module design does not allow for replacement of individual membranes.

A study was therefore conducted to investigate the possibility of improving the adherence between the substrate membrane and the support fabric. For reasons already mentioned, the support tube design and the material used were fixed, *i.e.* a single-ply tube produced from a non-woven fabric, the material of choice being

Viledon FO2406. This reduced possible factors which could be investigated to:

i) membrane-forming polymers;
ii) base solvents;
iii) casting-solution additives (coagulant-miscible; organic, inorganic and polymeric); and
iv) coagulation system (temperature, additives)

6.2.2.1 Membrane shrinkage

During a screening study *(43)*, conducted on flat-sheet membranes, it was noticed that the addition of PVP (44k molecular mass) to PES and NMP casting solutions improved the adherence of PES membranes to the Viledon fabric markedly. The same did not apply to PS.

PS and PES films cast from DMF-based solutions were humidity-sensitive and tended to gel, the initially clear film turns opaque, within 60s when exposed to ambient temperatures of 20°C and 50% relative humidity. Such partially air-gelated binary PS/DMF and PES/DMF flat-sheet films exhibited better adherence to the support fabric than non-exposed (directly leached) films, or *e.g.*, films produced from PS/NMP/1,4-dioxane mixtures.

Polysulphone membrane films contract considerably during gelation. Flat-sheet membranes may even curl up towards the skin side to release stress caused by shrinkage. In similar circumstances, with tubular membranes, this tendency will become manifest in release of the film from the support fabric as stress, caused by shrinkage, is released.

A possible reason for this was that poor membrane/fabric bonding was aggravated by excessive shrinkage of the membrane. In order to determine the magnitude of the problem, a series of flat sheet membranes was produced from various casting solutions according to the design matrix of a 2^4 factorial. In this experiment, a comparison was made between the shrinkage behaviour of PS and PES membranes, cast from NMP-based solutions. As it was known that addition of PVP improved adherence, it was used as one casting solution additive. LiCl was used as another additive. As the experiment designed was a two-level factorial experiment, the factors were all tested at two levels. The concentrations of the two membrane-forming polymers were tested at 14 and 18 mass percent, and that of the additives, LiCl and PVP^{44K} at zero and 0,2, and 1 and 10 mass percent, respectively.

The factor levels chosen and measured responses for this replicated 2^4 factorial experiment were given earlier in chapter IV, section 4.2.3.3 and in Table 4.13. The analysis of variance performed on the data was shown in Table 4.14.

In this replicated experiment, membrane films, 200μm thick, were cast on a glass plate, exposed to air for a maximum of 4 sec, and coagulated in unstirred RO treated Stellenbosch tap water (20°C) for 2h. The final width of the coagulated films was determined with a micrometer and expressed as a percentage of nascent (initial, as cast) width.

TABLE 6.35: LINEAR MEMBRANE SHRINKAGE - RESPONSES EXTRACTED FROM TABLE 4.13

Treatment combination	Polymer mass %	PVP^{44K} mass %	Shrinkage %	Mean shrinkage
I	PS 14%	1%	12,0	
b	PS 14%	1%	11,6	11,8
d	PES 14%	1%	13,6	
bd	PES 14%	1%	13,1	13,3
c	PS 14%	10%	12,5	
bc	PS 14%	10%	12,3	12,4
cd	PES 14%	10%	12,9	
bcd	PES 14%	10%	12,9	12,9
a	PS 18%	1%	11,5	
ab	PS 18%	1%	11,3	11,4
ad	PES 18%	1%	12,2	
abd	PES 18%	1%	12,4	12,3
ac	PS 18%	10%	11,8	
abc	PS 18%	10%	11,9	11,8
acd	PES 18%	10%	12,7	
abcd	PES 18%	10%	12,0	12,3

When the results given earlier (Table 4.13), were compared, it appeared that a membrane cast from a 14% solution of PS (solvent NMP) with 1% PVP as additive (treatment combination '*d*') had, on average, the highest shrinkage namely, (100 - 172,8/2) = 13,6%. On the other hand, the addition of 0,2% LiCl to a PS casting dope containing 18% PS and 1% PVP (treatment '*ab*'), resulted in a membrane with the lowest shrinkage on average, *i.e.* 11,3%. From the analysis of variance performed on the data (shown in Table 4.14), the only significant factors contributing to a reduction in membrane shrinkage appears to be polymer concentration (18% favoured) and the choice of polymer (PS favoured). The CD interaction effect (PVP concentration and membrane-forming polymer), although the largest among the interaction effects, was not significant with respect to membrane shrinkage.

The adherence of flat sheet membrane films produced from ternary PS/PVP/NMP solutions on Viledon FO2406 were, however, not as good as those films produced from PES/PVP/NMP solutions. It appeared from this data that linear shrinkage of PS and PES membranes is not the only cause of poor bonding, as the data in Table 6.35 (taken from Table 4.13) indicate that PS films shrink less on average than PES films do. (From the analysis of variance performed on the data, Table 4.14, LiCl appears not to have made a significant contribution to the observed variation in the responses shown in Table 4.13. However, those treatment combinations that contain the letter '*b*' in the first column of Table 6.35 indicate LiCl containing casting solutions. The same argument applies to PVP. Similarly, those treatment combinations that contains the letter '*c*' indicate a 10% PVP concentration level and the absence of '*c*' a 1% PVP concentration level).

6.2.2.2 Membrane gelation time

In another experiment, the rates of gelation of PS/NMP and PES/NMP membranes were compared according to the method outlined in section 5.8. Other factors investigated in this *24* factorial experiment (see chapter IV, Table 4.8 and 4.11) were the concentrations of the membrane-forming polymer, and two casting-solution additives, PVP and LiCl. The flat-sheet membranes were coagulated in a bath containing RO permeate, maintained at 20°C. The mean of five observations was taken for each treatment combination in this nonreplicated experiment.

From the analysis of variance (Table 4.12) performed on the data, the indications were that the significant contributing factors to longer gelation time of the membrane films were:

i) higher polymer concentration (0,1% level), Figure 4.3,
ii) higher PVP concentration (1% level), and
iii) lower level of factor D, *i.e.* PS (1% level), Figure 4.3.

The interaction effect between PVP concentration and membrane polymer (CD interaction) was also significant, albeit at the 5% level (Table 4.9, section 4.2.3.1). Barely significant, at the 10% level, were the interaction effects between membrane polymer concentration (factor A) and, respectively, PVP concentration (AC interaction) and membrane-forming polymer (*i.e.* PS, PES), AD interaction. Although LiCl had an effect on membrane shrinkage, it appeared to be insignificant as a variable in affecting gelation time.

When the signs of the effects (last column in Table 4.11), which correspond to the significant main and interaction effects above, *i.e.* A, C, D and CD, were compared, the following deductions were made:

i) Higher membrane-polymer concentration (factor A, positive sign), on average, increases the time it takes for the membrane films to gelate. Higher polymer content also increases the viscosity of the nascent film, which may slow down migration and growth of the two phases during liquid-liquid phase separation *(24)*. According to Yasuda *et al (44)*, higher polymer concentration leads to the formation of smaller and fewer pores in the PS membrane skin, thus imposing a restriction on diffusive flow of coagulant/solvent species across the gelled membrane skin.

ii) Higher PVP concentration (factor C, positive sign) slows down the rate at which the membrane phase separates, which may result in the formation of smaller pores in the skin surface. Again, as PVP affects the viscosity of casting solutions markedly, this may be attributed to viscosity effects. This factor also shows a significant interaction with the choice of membrane polymer, CD interaction. This interaction effect was summarized previously in Table 4.9. From this table it appears that PVP has a more pronounced effect on the rate at which PS membranes phase-separate than is the case with PES membranes.

iii) The sign of the main effect of factor D (choice of polymer) is negative. This implies that, on average, PS films (the lower level of factor D) take longer to coagulate than PES membranes do. On the basis of CPTVs listed in Table 6.34, this may appear to be a contradiction, as PS/NMP solutions are more sensitive to included water than PES/NMP solutions are. However, when the relative viscosities of the two membrane systems are compared, it again appears as if the viscosity of the casting solution causes the difference in the rates of phase-separation. CPTV values should therefore not be used indiscriminately.

6.2.2.3 Tubular substrate membranes

Up to this stage, all screening investigations were conducted with membranes in flat-sheet form. In the following paragraphs the outcome of a fractional factorial experiment, planned to elucidate the effect which fabrication variables have on the flux and adherence performance of tubular membranes will be discussed.

Nine fabrication variables were selected for this study. The number of experiments associated with a complete 2^9 factorial would have been beyond management. It was therefore necessary to reduce the size of the experiment to more manageable levels; this resulted in the design of a $1/16^{th}$ replicate of a 2^9 factorial (2^{9-4} fractional factorial) which reduced the number of experimental treatment combinations (trials) from 512 to a more manageable 32 trials. Unfortunately, because of this reduction, some information regarding interaction effects was lost (see section 4.3), but the system of confounding chosen still permitted assessment of all the main, and at least some, of the two-factor, interaction effects. The mechanics of generating the matrix of treatment combinations for a $1/16^{th}$ replicated 2^9 factorial was illustrated in section 4.3, paragraph 4.3.4.2.

The factors chosen for this investigation were divided into two groups, namely, those that affected membrane-casting procedures and leach-tank composition, and that which affected the casting-solution composition. The nine factors are listed in Table 6.36, together with their respective levels.

Rather than extend the number of factors studied to beyond nine, the following factors were maintained at a fixed level;

i) Choice of solvent. (NMP was chosen).
ii) Membrane thickness. (250μm used).
iii) Choice of fabric. (Viledon FO2406 used).
iv) Rate of production. The casting rate of 4,3 cm/s used in the experiment was the maximum rate at which quality weld seams could be ensured during continuous production.
v) Room temperature. (20°C was chosen).
vi) Coagulant make-up, RO permeate (Stellenbosch tap water).

The design of the mandrel used for membrane fabrication allowed for air-drying (see Figure 5.3). At treatment combinations with this factor (factor A) at the low level (*i.e.* no air-drying), the mandrel was vented and the membranes were cast directly into the leach tank at the prescribed rate of 4,3 cm/s. With the factor at the high level, the 3m membranes were cast in air for the required period, after which they were slit and introduced manually into a coagulation tank inclined at 45°. Air was passed into the membrane cavity at a flow rate to maintain a stationary column of priorly dried air inside the membrane.

Water permeabilities were determined within 24h of production of the membranes. Adherence tests were performed with an Elcometer, for which purpose the membranes were allowed to dry out completely at ambient conditions. The two responses measured, pure-water permeability (PWP, A-value) (mean of twelve observations) and membrane/fabric adhesion (mean of three observations), are listed in Table 6.37, together with the respective 2^{9-4} factorial treatment combinations. The calculated main and interaction effects, and their respective levels of significance are presented in Table 6.38.

A slightly different approach was adopted in the calculation of the variance of the factorial effects on the two responses presented in Table 6.38. In both cases two-factor interaction effects had to be pooled in an estimate of error variance as no outside source of error variation was available. However, as it was expected that some of the interaction effects which involved PVP (factor H) were real for membrane adherence, these effects were excluded from the error-variance estimate. On the other hand, all two-factor interactions effects were pooled in the estimate of membrane permeability error variance.

The variance (V_{Eff}) and standard error (SE_{Eff}) of effects, in the case of membrane adherence, are calculated as;

$$\begin{aligned} V_{Eff} &= \Sigma(Eff)^2/n \\ &= [(0,5)^2 + (1,4)^2 + \ldots + (0,4)^2]/8 \\ &= 0,45 \end{aligned}$$

$$SE_{Eff} = \sqrt{V_{Eff}} = 0,67$$

TABLE 6.36: PES MEMBRANE FABRICATION CONDITIONS, 2^{9-4} FRACTIONAL FACTORIAL

			Factor level		
	Factor		low	base	high
A	Air drying time	[sec]	0	35	70
B	NaCl content, leach tank	[mg/l]	0	2500	5000
C	NMP content, leach tank	[mass%]	0	2,5	5
D	Temperature, leach tank	[°C]	5	12,5	20
E	Surfactant [SLS], leach tank	[mg/l]	0	500	1000
F	Casting dope, PEG400	[mass%]	0	1	2
G	Casting dope, PES 4800G	[mass%]	14	16,0	18
H	Casting dope, PVP^{44K}	[mass%]	0	2,5	5
J	Casting dope, LiCl	[mass%]	0	0,1	0,2

SLS = sodium laurel sulphate

TABLE 6.37: TUBULAR SUBSTRATE MEMBRANES, WATER PERMEABILITY AND ADHESION RESPONSES, 2^{9-4} FACTORIAL

Treatment combination	Adhesion kg/cm^2	PWP (A-value) $x10^5$
I	3,7	3 630
abcd	2,9	2 110
cdef	0,8	4 940
abef	4,1	1 110
bceg	4,5	1 260
adeg	1,0	1 650
bdfg	1,3	1 990
acfg	2,6	1 790
bdeh	6,6	3 510
aceh	8,8	2 350
bcfh	6,0	1 890
adfh	8,0	1 790
cdgh	2,5	1 640
abgh	15,6	513
efgh	10,7	1 310
abcdefgh	14,8	917
bdej	1,4	2 210
acej	5,6	1 230
bcfj	5,5	1 770
adfj	4,1	1 330
cdgj	3,6	1 340
abgj	5,6	900
efgj	5,8	702
abcdefgj	2,9	1 110
hj	6,6	1 670
abcdhj	10,1	1 490
cdefhj	7,9	3 330
abefhj	9,7	1 620
bceghj	10,2	1 420
adeghj	14,0	640
bdfghj	10,0	1 460
acfghj	12,3	620

TABLE 6.38: SUBSTRATE MEMBRANE FABRICATION VARIABLES, MAIN AND INTERACTION EFFECTS, LEVELS OF SIGNIFICANCE

Membrane adherence		Level	Pure-water permeability		Level
Main effects			Main effects		
A Air	2,2	5%	A Air	-806	0,1%
B NaCl	0,8		B NaCl	-293	
C NMP	-0,4		C NMP	198	
D Temp.	-1,6	5%	D Temp.	480	5%
E SLS	0,5		E SLS	211	
F PEG	0,2		F PEG	7	
G PES	1,6	5%	G PES	-1 045	0,1%
H PVP	6,2	0,1%	H PVP	-181	
J LiCl	1,3	10%	J LiCl	-597	1%
Confounded interactions			Confounded interactions		
AF, BE, CG	-0,9		AF, BE, CG	-82	
AG, DE, CF	0,3		AG, DE, CF	434	5%
FG, AC, BD	0,2		FG, AC, BD	60	
BG, DF, CE	0,7		BG, DF, CE	277	
EG, AD, BC	0,8		EG, AD, BC	-367	10%
EF, CD, AB	0,3		EF, CD, AB	89	
AE, BF, DG	-0,6		AE, BF, DG	-201	
Two-factor interaction effects			Two-factor interactions, estimate of error variance		
AH	1,9	5%	AH	20	
BH	0,7		BH	226	
CH	-0,6		CH	-55	
DH	0,8		DH	-57	
EH	0,9		EH	292	
FH	0,4		FH	-44	
GH	1,7	5%	GH	-96	
Two-factor interactions, estimate of error					
AJ	-0,5		AJ	186	
BJ	-1,4		BJ	432	
CJ	0,6		CJ	24	
DJ	0,7		DJ	-107	
EJ	-0,6		EJ	-1	
FJ	-0,1		FJ	123	
GJ	0,1		GJ	238	
HJ	-0,4		HJ	389	

For 8 df, the critical t-values at the 10%, 5%, 1% and 0,1% levels are 1,86, 2,31, 3,36 and 3,83, respectively. A factorial effect mean, in the case of membrane adherence, must therefore exceed the value of (0,67)(1,86) = 1,25 to be significant at the 10% level, and 1,55, 2,25 and 2,57 for significance at the 5%, 1% and 0,1% levels, respectively.

In the case of membrane permeability, all the measurable two-factor interactions were pooled to determine their variance (V_{Eff} = 40 713) and standard error (SE_{Eff} = 202). For 15 df in this case, the critical t-values at the 10%, 5%, 1% and 0,1% levels were 1,75, 2,13, 2,95 and 3,29, respectively. A factorial effect mean, in the case of membrane permeability, must therefore exceed the value of (202)(1,75) = 353 to be significant at the 10% level, and 430, 595 and 664, for significance at the 5%, 1%, and 0,1% levels, respectively.

6.2.2.4 Discussion

Ignoring for the present the levels of significance associated with the effects of factors and their interactions on both of membrane adherence and permeability (Table 6.38), the coincidence that the signs of all the effects (except SLS and PEG400) are opposite for the two responses is too great to ignore. The adherence of the substrate membrane, therefore, appears to be inversely related to membrane permeability; hence it appears that there is a balance between substructure morphology and porosity (permeability of the membrane) on the one hand and adherence on the other. (See Table 6.39).

The most important factor which contributed to the improvement of membrane/fabric adherence was an increase in the casting solution solids concentration by an addition of at least 5% PVP (factor H). Increasing the solids content of the casting solution by the addition of membrane-forming polymer (factor G) also improved adherence, but at the cost of a significant loss of permeability. Although PVP had a negative effect on flux performance, this effect was small enough to be ascribed to chance fluctuation. The hydraulic permeability of these membranes could therefore be improved by substituting PVP for PES in the casting solution, as was also reported for hollow fine-fibre PS membranes *(45)(46)*. Both these factors increase the casting solution viscosity as well as the membrane gelation time.

LiCl also improved membrane adhesion, albeit at the 10% level of significance. Its presence in the casting solution caused a significant loss of membrane hydraulic permeability. It indicated, however, the possibility of altering membrane porosity by the addition of very small amounts of soluble inorganic electrolytes. This could be of possible use in adjusting membrane cut-off rejections in the case of UF membranes *per se*.

It is interesting to note that the addition of 5% (by mass) of NMP solvent to the coagulation tank did not have a significant effect on either membrane permeability or adherence. The addition of 2% casting solution solvent to the coagulation medium is commonly accepted practice in the case of flat-sheet membrane fabrication, the reason being that it leads to higher hydraulic permeability by reducing the steep solvent concentration gradient at the membrane interface, thereby retarding the membrane skin gelation rate. The effect of this factor was probably masked in that coagulant which entered the tube, as it passed down the coagulation bath, remained trapped inside the membrane. As a result, the leach-front solvent content

increased rapidly anyway, and no difference in permeability was noticed which would indicate whether factor C was originally at a high or a low level. The addition of much larger quantities of solvent to the coagulation medium would definitely have had an effect on membrane morphology and performance, as seen in Figure 6.13, which shows the effect of coagulating flat-sheet membranes in a 1:1 solvent/non-solvent (RO permeate) coagulant mixture.

The significant effect of air exposure is interesting since NMP is a high-boiling-point solvent, and evaporative loss of solvent over the 60s period (room temperature 20°C) allowed can be disregarded, which cannot be done with evaporation of acetone from CA membranes. Exposure to air, although no moisture was present in the air and although the air column inside the tubular membrane was kept stationary, had a substantial negative effect on membrane hydraulic permeability rates. This was primarily due to a noticeably deeper penetration of the casting solution into the fabric, and encapsulation of larger volumes of support fabric fibers, which increased the pressure drop across the membrane, and therefore permeation rate.

The fabrication variables, which were significant over the ranges investigated, appeared to be air-exposure time, coagulation tank temperature, PES concentration, PVP concentration and the concentration of LiCl. The addition of a surfactant, sodium lauryl sulphate, to the coagulation medium had no effect on the membrane properties examined, but its use was continued as it did have an effect on membrane skin topography and membrane wettability *(47)*.

The confounded effects are numerically equivalent. Of these the effect of the interactions AG, DE, CF on PWP were significant at the 5% level. One way of examining these interactions was to create two-way comparison tables for the individual interactions. The three interaction tables in Table 6.39, were constructed from the data given in Table 6.37. The values given in Table 6.39 represent the mean pure-water permeabilities observed at the conditions indicated in the table.

6.2.3 CONCLUSIONS

Initial experimentation led to the use of ternary PS/NMP/1,4-dioxane casting solutions which had PWP rates of $\approx 1\ 500 \times 10^{-5}$, but with a measure of adherence (<0,5 kg/cm^2) which, as far as membrane-element integrity was concerned, proved to be inadequate in field studies. These membranes were, however, used extensively during RO composite membrane research and in the optimization of UTF PVAM composite membrane fabrication formulations.

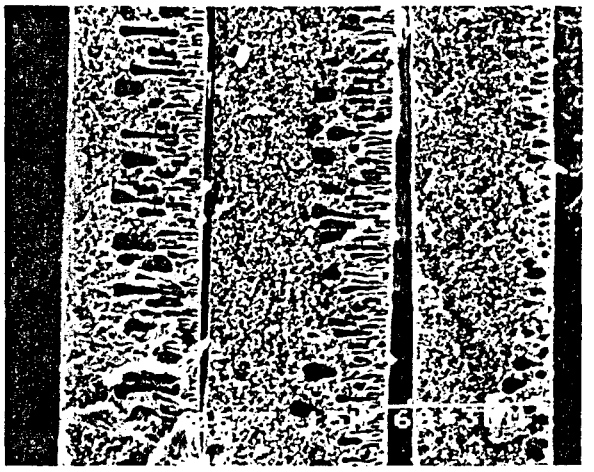

18% 4800G PES in DMF, coagulated in 25%, 50%, 75% - DMF/water mixture

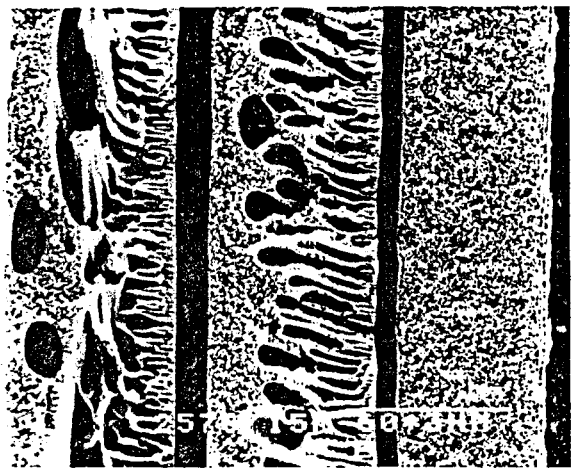

18% 4800G PES in NMP, coagulated in 25%, 50%, 75% - NMP/water mixture

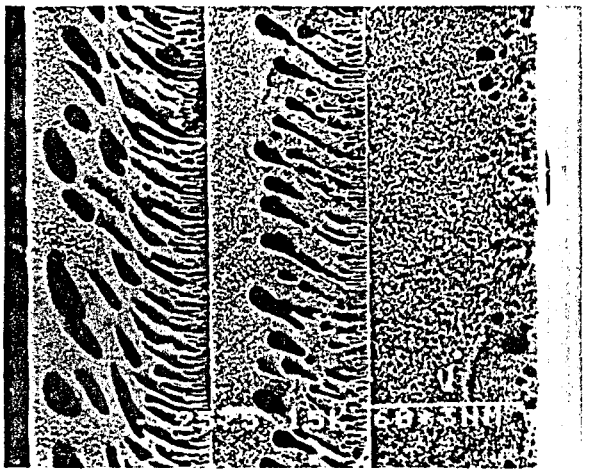

18% 4800G in 1:1 DMF:NMP, coagulated in 1:1 25%, 50%, 75% - DMF:NMP/water mixture

FIGURE 6.13: SOLVENT ADDITION TO COAGULANT - EFFECT ON MEMBRANE SUBSURFACE MORPHOLOGY

TABLE 6.39: SUBSTRATE MEMBRANE FABRICATION EXPERIMENT, CONFOUNDED INTERACTION EFFECTS, AVERAGE PWP RESPONSE

AG interaction

PES concentration	Air exposure None	Air exposure 60 sec
14%	2869	1629
18%	1390	1017

DE interaction

SLS concentration	Coagulant temperature 5°C	Coagulant temperature 20°C
None	1598	1643
1g/l	1375	2288

CF interaction

PEG400 concentration	NMP in coagulant None	NMP in coagulant 5%
None	1840	1605
2%	1414	2045

TABLE 6.40: SUMMARY OF SUBSTRATE MEMBRANE CASTING SOLUTION FORMULATIONS (MASS PERCENTAGES)

	Series 200		Series 700		
Components	221	224	712	714	719
1700P PS	13,0				
3500P PS		12,0			
4800G PES			18,0	16,0	19,0
DMF					2,0
NMP	76,7	68,4	76,8	80,4	68,8
1,4-Dioxane	19,3	19,6			
PVP^{40K}			5,0	2,5	10,0
LiCl		0,1	0,2	0,2	
A-value ($x10^5$)	1 400	1 600	700	1 780	900
Adherence [kg/cm^2]	<0,5	<0,5	13,5	10,3	14,5

With the introduction of PES/PVP composition casting-solutions, adhesion of the membrane to the Viledon fabric was improved by more than an order of magnitude. Towards the end of the programme, two substrate membranes (designated series 719 and 714), with mean bond-strengths of 14,5 and 10,3 kg/cm^2 respectively, were produced routinely. The membranes (casting-solution formulas shown in Table 6.40) were coagulated in 20°C RO permeate containing 50 mg/l Triton X-100 surfactant. The casting-solution composition of the series 714 membrane corresponded to the base composition of the 2^{9-4} factorial experiment. This membrane had a higher mean PWP coefficient (1 780x10^5 g.cm^{-2}s^{-1}atm^{-1}) than did the series 719 membrane, produced from a higher solids-content casting solution, but a lower adhesion rating.

As the study progressed, substrate membranes were developed which adhered excellently to the support fabric, and which gave PWP-values in agreement with those for the PS/NMP/1,4-dioxane membranes (series 221 and 224 membranes), used in the optimization of PVAM composite-membrane formulations.

Although the PWP coefficient of the 714 series membrane agrees with that of the 224 and 221 membranes, (see Table 6.40) the RO performance of PVAM UTF composite membranes produced on this series 700 membrane was lower, as will be seen later. (The formulations used to fabricate the UTF composite RO membrane on the series 700 substrate membranes were developed from optimization studies conducted on the series 200 membranes). This indicates the importance of optimizing the composite membrane fabrication variables on either a specific substrate membrane, or of combining all composite membrane fabrication variables (*i.e.* substrate and desalting barrier) in one large experiment. If a routinely produced UF membrane is available, the obvious choice would be the first one.

6.3 ULTRA-THIN FILM [UTF] PVAM REVERSE OSMOSIS MEMBRANES

In this section aspects relating to the creation of a low-pressure brack-water permselective matrix on the skin-surfaces of PS and PES substrate membranes will be discussed. The approach adopted to formulate the conditions for fabrication of PVAM membranes with optimal performance, was different from the one used in the development of tubular CA membranes, in which regression models of the salt rejection and water permeability response surfaces were used. The reason for selecting a self-directing optimization [SDO] approach, as opposed to the regression approach, came about as a result of the following considerations;

i) The number of factors involved in composite membrane fabrication was large *(48)*.
ii) No knowledge of tubular PVAM membrane fabrication techniques existed at the start of the programme, so that a pre-planned, 2-level factorial experiment, where the outcome of the experiment could be judged only at the completion of all the experimental trials, was regarded as ungainly and unnecessarily time-consuming.
iii) The strength of the 2-level factorial experimental designs lay in their orthogonal character. To maintain orthogonality though, factor levels must be replicated with care. To have accommodated the known variability which existed in the initial batch quality of PVAM and SCL synthesized, block-confounding would have had to be introduced, causing additional degrees of freedom to be lost in the analysis of factorial effects (section 4.3.1).

iv) The simplex method of SDO is less prone to the effect which random error variation has on the response(s) measured, because it is self-adjusting (self-correcting) (section 4.3.4.2).

v) A further advantage of the multi-variable SDO technique is that progress, in achieving improved membrane properties, can be judged on a day-to-day basis, as opposed to ii) above, for the more formal factorial designs.

The following reasons are given for initializing the PVAM UTF membrane study directly with an attempt at obtaining an optimum formulation through SDO:

i) A composite UTF membrane system, fabricated from a given set of cross-linking and precursor reagents, should show an intrinsic maximum salt rejection capability when operated at specific conditions.

ii) The intended purpose of use of the PVAM UTF membrane was in low-pressure desalination applications.

iii) The intrinsic salt rejection capability of tubular membranes produced from PVAM-chemistry had therefore to be tested at low-pressure conditions, to determine the viability of the chemistry, and system geometry, for this application.

iv) An optimized UTF membrane could be regarded as a membrane with the best mechanical, and physical properties achievable from the membrane chemicals used.

iv) Fabrication formulations which result in the formation of sub-optimum membranes could therefore affect the durability of the desalting barrier.

v) The intention with the SDO study was to establish the feasibility of the membrane system, in the light of the above points, within the smallest possible number of experiments.

6.3.1 POLYVINYLAMIDINE [PVAM] PRECURSOR

As mentioned earlier, the polymeric precursor used in the formulation of the UTF permselective barrier is not commercially available. Its synthesis and characterization formed a study on its own; this is described in detail elsewhere *(19)*. For the sake of completion though, some of the findings are summarized below.

The procedure followed in synthesizing PVAM involves;

i) synthesis of polyacrylonitrile [PAN] from acrylonitrile monomer, and

ii) amination of PAN with ethylene diamine to produce PVAM.

Two methods are described by which the second of the above synthesizing steps was accomplished, each of which resulted in a different product of PVAM, namely PVAM-OD and PVAM-FD. The idealized structure of PVAM homopolymer is shown in Figure 6.14. However, the two polymer products synthesized and used in UTF membrane formulations, are said not to be homopolymers of PVAM, but a copolymer mixture of PVAM and its hydrolyzed form. PVAM-FD is regarded as the purer of the two polymer products as it contains significantly lower levels of hydrolyzed groups than PVAM-OD does.

Both these two polymers react readily with m-chlorosulphonyl benzoylchloride [SCL] (also a non-commercially available reagent), which is used as a cross-linking reagent to insolubilize the water-soluble PVAM. Hydrochloric acid is formed as a condensation product.

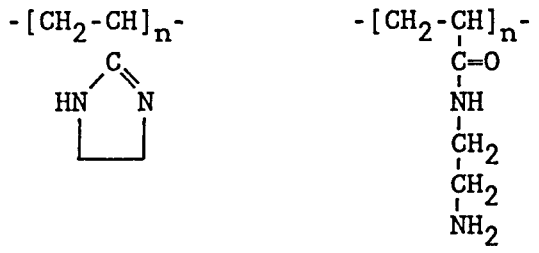

PVAM Hydrolyzed PVAM

FIGURE 6.14: IDEALIZED CHEMICAL STRUCTURE OF PVAM AND HYDROLYZED PVAM REPEAT UNITS

6.3.2 SELECTION OF PVAM-OD UTF MEMBRANE FABRICATION VARIABLES

Some understanding of ultra-thin film [UTF] membrane fabrication formulations had been gained earlier by experimentation with flat-sheet membranes *(19)*. These formulations allowed initial selections to be made of factors and their levels. However, to what extent fabrication conditions of the small-section (10 x 5cm) flat-sheet membranes could be extrapolated to membranes of tubular geometry and lengths of up to 3m, was unknown.

The critical step in the formation of polyvinylamidine UTF membranes on the surface of a microporous substrate membrane, depends on the reaction of PVAM with m-chlorosulphonyl benzoylchloride [SCL]. The procedure of creating a UTF composite RO membrane involves three basic steps:

i) Preparation of the microporous PS substrate membrane (section 6.2) on the tube winding machine (section 5.1).
ii) Coating (section 5.2) the surface of the substrate membrane with an aqueous solution of the amine-type precursor, followed by draining the solution and insolubilizing the film by an interfacial cross-linking reaction performed *in-situ* with a solution of SCL in n-hexane.
iii) Thermal treatment (section 5.3) of the film to induce further cross-linking by a condensation reaction between primary amines.

6.3.2.1 Substrate membrane

The substrate membranes used in the fabrication of UTF PVAM membranes were produced in 3m lengths, at a casting rate of 4,3cm/s. The casting solutions (series 224, Table 6.40) were filtered (1μm stainless steel filter) before use. The prototype fabrication and ancillary equipment were described in section 5.1 and Figures 5.3 and 5.6. The membranes were cast on Viledon FO2406 fabric liner and gelled in RO permeate at 20°C (controlled). The coagulant was circulated throughout the fabrication run by means of a small centrifugal pump (Figure 5.6). Coagulant was furthermore drained from the coagulation tank during the operation. To make up for lost volume and to prevent solvent concentration levels from building up at the surface of the tank, fresh coagulant was supplied continuously to the tank at a flow-rate of ≈2 l/min. The

membranes were removed 2-3h after fabrication for extended leaching in running RO permeate, before they were used for UTF membrane fabrication.

Two methods were used to create a film of PVAM on the surface of the substrate membrane, namely, immersion-coating (section 5.2.1) and *in situ*-coating (section 5.2.2). The former became the preferred technique for the production of 1,2m and shorter membranes, and the latter was used for the production of 3m-long membranes. Irrespective of the coating technique used, the PVAM film was formed by simply draining excess polymer solution from the substrate tube. The expression for film thickness under gravity action of Newtonian fluids, neglecting inertial and capillary effects, is given by *(49)*:

$$\delta = \sqrt{[\nu x/gt]}$$

d	film thickness
ν	kinematic viscosity
x	distance from the top of the draining surface
t	time
g	gravity acceleration

It is obvious from the above equation that greater variation between the thickness of the film at the top and at the bottom end of the tube was to be expected with the longer membranes. The effect which this could have on the variability of the performance of longer membranes was a matter of concern at the time.

Substrate membrane length, precursor wetting and draining times were therefore selected as three independent variables.

6.3.2.2 Interfacial condensation reactions

The second step in the formation of the UTF was the interfacial cross-linking reaction between the water-soluble PVAM film on the substrate membrane surface and SCL. The reaction was effected by wetting the substrate membrane with a solution of SCL in hexane (industrial grade, distilled). As the precursor solvent, water, and hexane were not miscible, the aqueous precursor film remained *in situ* when the substrate membrane surface was wetted with the cross-linking solution.

According to Morgan *(50)*, the reaction actually occurs in the organic phase. Migration of the polymer into the organic phase would, however, become increasingly difficult as the cross-linking reaction progresses, since segmental movement of the polymer would become physically hindered due to restraints imposed by cross-linking. It was expected, therefore, that the cross-linked UTF would have an asymmetric structure, with the polymer becoming progressively more cross-linked towards the solution interface. On the basis of this argument, it was expected that film thickness of the nascent precursor would play a part in the effectiveness of the cross-linking reaction.

In chemical reactions, temperature, contact time and concentration of the reactants affect the rate and extent of reaction and must, therefore, be regarded as potential formulation variables. The temperature of the

fabrication room was controlled to 22°C, while the concentration of the precursor and cross-linking reagent, as well as the contact time, were regarded as independent variables.

Hydrochloric acid forms as a condensation product during the cross-linking reaction. To reduce the extent of occurrence of salt formation with the amine precursor which would inhibit cross-linking, acid acceptors were added to the precursor solution. The two acid acceptors which were selected were tri-ethyl amine [TEA] and trisodium phosphate [TSP]. NaOH is also effective as an acid acceptor *(51)*.

Work on flat-sheet membranes *(19)* indicated that the permeate flux of PVAM membranes was lower when isophthaloyl chloride [IPC] is used as the cross-linking reagent, as opposed to SCL. The work also showed that SCL cross-linked membranes gave higher salt rejection in comparison with IPC cross-linked membranes. Small percentages of IPC was included in the cross-linking reagent solution to determine whether the finding also holds true for tubular membranes.

6.3.2.3 Thermal treatment

As a last step in formulating the UTF RO membrane, the membranes were air dried after the SCL reaction, and heated (section 5.3) to complete cross-linking *(52)*. The three variables regarded here as important were, SCL draining-time, oven residence-time and oven temperature.

6.3.2.4 Evaluation

The UTF RO membranes were evaluated on equipment similar to that used for CA membrane evaluation. Different operating conditions were used, however, (section 5.4.3) as the purpose was to determine the low-pressure brack-water desalting performances of the membranes. The membranes were therefore evaluated at a pressure of 2MPa, using an NaCl feed solution of 2g/l at an operating temperature of 20°C.

When short-length, *i.e.* 0,6m or 1,2m, membranes were produced by the immersion-coating technique, seven membranes were produced in each batch, of which six were installed for evaluation. When long membranes, *i.e.* three-metre, were produced by the fill-coating technique, the membranes were fabricated in batches of three; the top and bottom 1,2m sections of each long membrane were used for installation and evaluation in 1m test cells.

The salt rejection and flux performances of the set of six membranes were measured individually. The performance of the set was calculated as the arithmetic mean of the individual observations. The mean salt rejection and flux performances of a set of membranes were used in the calculation of their overall performance (A^2/B-value, section 5.4.3.3). The performance of a set of membranes was judged according to their A^2/B-value, which combines the conductivity salt rejection and flux performances into a single unbiased figure.

6.3.3 SELF-DIRECTING OPTIMIZATION, PVAM-OD RO MEMBRANE FORMULATIONS

6.3.3.1 Results

The twelve factors investigated in the SDO study of PVAM-OD UTF membrane formulations (see Table 6.41) were introduced in the previous section 6.3.2. In the first simplex design matrix these factors were introduced at two levels, as for two-level factorial designs, *i.e.* a high and a low level. The factor-levels chosen (co-ordinates) for the initial simplex experiment *(53)* are shown in Table 6.41. It is necessary to define only the starting co-ordinates of the first simplex, as those for the second are derived from the first, the third from the second, *etc.* (see section 4.4.2).

The matrix of experimental points (co-ordinates of the first simplex) according to which the initial fourteen sets of UTF PVAM-OD membranes were fabricated, *i.e.* trials OD1 to OD14, are shown in the top part of Table 6.42. These fourteen trials were replicated three times, and in each replicate, sets of membranes of different lengths were produced by either the fill-coating or immersion-coating methods. This allowed comparisons to be made of the performances of 3m-long membranes produced on the fill-coating machine, and 0,6m and 1,2m membrane lengths produced by immersion-coating.

The salt rejection and flux performances of the sets of membranes of different lengths are given in Table 6.43. The data contained in Tables 6.42 and 6.43 have been ranked in descending order of the A^2/B-value of the 3m membranes. (The A^2/B entries in the last column in Table 6.42 were calculated from the mean performances of the 3m membranes given in Table 6.43). As the different sets of membranes were rated according to the value of this parameter, the A^2/B-value was also used as a criterion in the generation of new co-ordinate points for subsequent simplexes.

A two-way analysis of variance (section 4.1.4.2) was performed on the salt rejection and flux performance data given in Table 6.43 for membranes of lengths 0,6m, 1,2m and 3m, in order to establish whether the differences in the respective performances of the membranes were significant. From this analysis, summarized in Table 6.44, it was concluded that there was not enough evidence on which to reject the null hypothesis (the means of the responses observed are equal) in the case of membrane permeate flux. It can be concluded, although only at the 10% level however, that the mean of the salt rejection performances observed for the three sets differed. From inspection of the data in Table 6.43, it may be concluded that the average performances of the 3m membranes appears to be better than that of the 0,6 and 1,2m membranes.

However, the PVAM-OD material was still being produced in relatively small laboratory quantities, and the volumes of materials synthesized were not high enough to have supported an optimization study conducted on 3m membranes. For this reason it was decided to take note that the mean performances of 3m fill-coated membranes appeared to be better, but to continue the SDO study with membranes of 0,6m lengths, produced by the immersion-coating method, to reduce the consumption of membrane-forming reagents.

TABLE 6.41: FACTOR LEVELS FOR FIRST SDO EXPERIMENT CONDUCTED ON PVAM-OD/SCL MEMBRANE

	Factor		Factor level low	high
A	Concentration PVAM-OD	[mass%]	0,8	3,0
B	Surfactant [SLS]	[mass%]	0	0,4
C	Acid acceptor [TEA]	[mass%]	0,1	0,5
D	Acid acceptor [TSP]	[mass%]	0	0,1
E	Precursor contact time	[min]	15	30
F	Precursor draining time	[min]	7	11
G	Concentration SCL	[mass%]	0,9	2,5
H	Concentration IPC	[mass%]	0	0,4
J	Crosslink reagent contact	[min]	3	6
K	Post crosslink air dry time	[min]	5	10
L	Oven temperature	[°C]	90	115
M	Oven residence time	[min]	7	12

TABLE 6.41: FIRST SIMPLEX DESIGN MATRIX, PVAM-OD/SCL MEMBRANE

	Fabrication variables												
Trial no.	A	B	C	D	E	F	G	H	J	K	L	M	A^2/B-value 3m membranes
Co-ordinate points for first simplex													
OD12	3,0	0	0,5	0,1	15	7	0,9	0	6	5	114	11,67	$2,56 \times 10^{-5}$
OD 9	3,0	0	0,1	0	15	11	2,5	0	6	5	90	6,5	$2,46 \times 10^{-5}$
OD11	3,0	0	0,5	0	30	7	2,5	0,4	3	5	115	7,0	$2,39 \times 10^{-5}$
OD14	3,0	0,4	0,1	0,1	15	7	2,5	0	3	10	91	10,5	$2,30 \times 10^{-5}$
Mean	3,0	0,1	0,3	0,05	18,8	8	2,1	0,1	4,5	6,25	102,5	8,92	
2xMean	6,0	0,2	0,6	0,1	37,5	16	4,2	0,2	9	12,5	205	17,84	
OD13	3,0	0,4	0,1	0	30	7	0,9	0,4	6	10	91	7,0	$1,83 \times 10^{-5}$
OD 4	0,8	0	0,5	0,1	30	11	2,5	0	3	10	92	7,0	$1,75 \times 10^{-5}$
OD10	3,0	0	0,1	0,1	30	11	0,9	0,4	3	5	89	11,5	$1,39 \times 10^{-5}$
OD 1	0,8	0	0,1	0	30	7	0,9	0	3	10	116	7,5	$1,21 \times 10^{-5}$
OD 2	0,8	0	0,1	0,1	15	7	2,5	0,4	6	10	116	7,0	$1,12 \times 10^{-5}$
OD 3	0,8	0	0,5	0	15	11	0,9	0,4	6	10	84	12,0	$1,04 \times 10^{-5}$
OD 8	0,8	0,4	0,5	0,1	15	7	0,9	0,4	3	5	91	7,0	$0,76 \times 10^{-5}$
OD 6	0,8	0,4	0,1	0,1	30	11	0,9	0	6	5	115	7,0	$0,54 \times 10^{-5}$
OD 7	0,8	0,4	0,5	0	30	7	2,5	0	6	5	90	12,0	$0,47 \times 10^{-5}$
OD 5	0,8	0,4	0,1	0	15	11	2,5	0,4	3	5	116	15,0	$0,33 \times 10^{-5}$
Co-ordinate points generated for second simplex													
OD15	3,0	0	0,5	0,1	7,5	9	3,3	0	3	2,5	114	10,84	from OD13
OD16	4,0	0,2	0,1	0	7,5	5	1,7	0,2	6	2,5	113	10,84	from OD 4
OD17	3,0	0,2	0,5	0	7,5	5	3,3	0	6	7,5	116	6,34	from OD10
OD18	4,0	0,2	0,5	0,1	7,5	9	3,3	0,2	6	2,5	89	10,34	from OD 1
OD19	4,0	0,2	0,5	0	22,5	9	1,7	0	3	2,5	89	10,84	from OD 2
OD20	4,0	0,2	0,1	0,1	22,5	5	3,3	0	3	2,5	121	5,84	from OD 3
OD21	4,0	0	0,1	0	22,5	9	3,3	0	6	7,5	114	10,84	from OD 8
OD22	4,0	0	0,5	0	7,5	5	3,3	0,2	3	7,5	90	10,84	from OD 6
OD23	4,0	0	0,1	0,1	7,5	9	1,7	0,2	3	7,5	115	5,84	from OD 7
OD24	4,0	0	0,5	0,1	22,5	5	1,7	0	6	7,5	89	2,84	from OD 5

(Mirror-image values have been taken where the signs of new points generated were negative)

- A Concentration PVAM-OD
- B Surfactant [SLS]
- C Acid acceptor [TEA]
- D Acid acceptor [TSP]
- E Precursor contact time
- F Precursor draining time
- G Concentration SCL
- H Concentration IPC
- J Crosslink reagent contact
- K Post crosslink air dry time
- L Oven temperature
- M Oven residence time

TABLE 6.43: PVAM-OD/SCL MEMBRANE PERFORMANCE, 0,6m, 1,2m AND 3m MEMBRANE LENGTHS (SIMPLEX 1)

	3m membranes Fill-coated		1,2m membranes Immersion-coated		0,6m membranes Immersion-coated	
Trial no.	Rejection [%]	Flux [lmd]	Rejection [%]	Flux [lmd]	Rejection [%]	Flux [lmd]
OD12	86,7 ± 1,7	1000 ± 61	90,8 ± 1,1	590 ± 85	90,4 ± 1,0	430 ± 54
OD9	89,1 ± 1,4	790 ± 46	83,5 ± 0,8	720 ± 45	86,7 ± 0,5	610 ± 23
OD11	94,5 ± 1,2	400 ± 89	89,6 ± 1,0	270 ± 29	89,8 ± 0,3	190 ± 14
OD14	95,1 ± 0,7	230 ± 39	95,9 ± 0,4	250 ± 20	94,1 ± 1,7	180 ± 8
OD13	91,9 ± 0,9	430 ± 14	92,5 ± 1,0	400 ± 42	90,0 ± 0,3	360 ± 48
OD4	89,8 ± 1,2	520 ± 10	75,0 ± 1,8	820 ± 31	74,7 ± 4,1	810 ± 18
OD10	81,0 ± 0,8	790 ± 25	81,9 ± 2,7	840 ±125	84,6 ± 1,5	750 ± 66
OD1	79,7 ± 0,8	740 ± 31	76,8 ± 1,1	900 ± 59	66,8 ± 1,5	1300 ±105
OD2	81,0 ± 1,5	650 ± 67	76,5 ± 1,6	560 ± 18	75,8 ± 1,5	650 ± 93
OD3	75,9 ± 2,4	750 ± 19				
OD8	64,3 ± 2,5	850 ± 37	63,4 ± 3,0	920 ±116	54,0 ± 1,8	1300 ± 82
OD6	76,0 ± 1,0	380 ± 59	78,1 ± 2,5	270 ± 48	78,9 ± 1,4	260 ± 67
OD7	68,8 ± 3,7	440 ± 5	55,4 ± 4,4	700 ± 84	44,1 ± 3,6	710 ±141
OD5	33,7 + 3,7	530 +190	49,8 + 1,4	520 + 50	39,2 + 0,7	670 +202
Mean	79,4	596	77,6	597	74,5	632

TABLE 6.44: TWO-WAY ANALYSIS OF VARIANCE (DATA TABLE 6.43)

	Rejection					Flux				
Source variation	SS	df	MSS	F	Level	SS	df	MSS	F	Level
Membrane length	154,26	2	77,13	2,78	10%	11092	2	5546	0,21	
Treatments	9104,46	12	758,70	27,38	1%	2291241	12	190937	7,31	1%
Error	665,06	24	27,71			626774	24	26116		
Total	9923,77	38				2929108	38			

$F(2,24)_{0,1} = 2,54$

$F(12,24)_{0,1} = 1,83$

$F(12,24)_{0,01} = 3,03$

TABLE 6.45: SUMMARY OF BEST PERFORMANCE PVAM-OD/SCL MEMBRANES

Trial	A^2/B-value	Rejection [%]	Flux [lmd]	Simplex no
OD12	$2,56 \times 10^{-5}$	86,7 ± 1,7	1000 ± 61	1
OD 9	$2,46 \times 10^{-5}$	89,1 ± 1,4	790 ± 46	
OD11	$2,39 \times 10^{-5}$	93,9 ± 1,0	420 ± 78	
OD12	$2,56 \times 10^{-5}$	86,7 ± 1,7	1000 ± 61	2
OD 9	$2,46 \times 10^{-5}$	89,1 ± 1,4	790 ± 46	
OD23	$1,06 \times 10^{-5}$	86,4 ± 0,7	420 ± 27	
OD12	$2,56 \times 10^{-5}$	86,7 ± 1,7	1000 ± 61	3
OD 9	$2,46 \times 10^{-5}$	89,1 ± 1,4	790 ± 46	
OD26	$0,77 \times 10^{-5}$	81,6 ± 1,6	420 ± 24	
OD47	$5,75 \times 10^{-5}$	96,1 ± 0,3	650 ± 46	4
OD41	$3,21 \times 10^{-5}$	96,4 ± 0,5	330 ± 29	
OD46	$2,49 \times 10^{-5}$	87,5 ± 0,9	920 ± 69	
OD61	$6,37 \times 10^{-5}$	97,2 ± 0,2	500 ± 38	5
OD47	$5,75 \times 10^{-5}$	96,1 ± 0,3	650 ± 46	
OD52	$4,92 \times 10^{-5}$	97,1 ± 0,7	410 ± 19	
OD74	$8,98 \times 10^{-5}$	97,1 ± 0,1	730 ± 24	6
OD65	$7,88 \times 10^{-5}$	97,2 ± 0,1	620 ± 38	
OD66	$7,87 \times 10^{-5}$	98,0 ± 0,2	440 ± 33	

TABLE 6.46: OPTIMUM PVAM-OD/SCL MEMBRANE FABRICATION FORMULATION (TRIAL OD74)

	Factor		Level
A	Concentration PVAM-OD	[mass%]	5,0
B	~~Surfactant [SLS]~~		
C	Acid acceptor [TEA]	[mass%]	1,1
D	Acid acceptor [TSP]	[mass%]	0,14
E	Precursor contact time	[min]	43
F	Precursor draining time	[min]	1,5
G	Concentration SCL	[mass%]	4,5
H	~~Concentration IPC~~		
J	Crosslink reagent contact	[min]	3
K	Post crosslink air dry time	[min]	10
L	Oven temperature	[°C]	95
M	Oven residence time	[min]	5,4

The calculations performed to generate new co-ordinate points for the second simplex are illustrated in the bottom half of Table 6.42. There is some advantage in discarding the optimum number of trial points for every move of the simplex. The optimum number to discard is easily determined by a calculation *(54)* which is best illustrated in the light of the calculated A^2/B-values shown in Table 6.42.

As a first step, the responses are ranked in descending order. (See last column of A^2/B-values in Table 6.42). The column of data is next classified into two groups, namely, the "worst" and the "best" response groups. Next, the differences between the mean responses of the two groups are calculated. For example, 0,33 (the last entry), is ranked as member of the "worst" group and the remaining entries, 2,56, ..., 0,47 as members of the "best" group. The difference in the mean values between these two groups is 1,19. The process is repeated, grouping 0,33 and 0,47 next as members of the "worst" group, and 2,56,..., 0,54 as members of the "best" group, *etc.* Grouping trials OD12, OD9, OD11 and OD14 as members of the "best", maximizes the difference between the means of the two groups, and the remainder of the trials (group of "worst") are therefore used in turn to generate the new set of experimental points for the next simplex. The calculation performed to generate a new formulation in place of the discarded trial is illustrated in Table 6.42 as, simply, twice the average of the "best", minus the "worst".

Table 6.45 illustrates how the average performances of the membranes improved from simplex to simplex as the SDO experiment progressed. In this table, the performances of the three membrane sets with the "best" performance rating obtained from each of the six simplexes conducted are shown. No further improvement could be obtained beyond simplex 6, and the optimization study on PVAM-OD membranes was terminated. The fabrication formulations, corresponding to the "best" trial, OD74, are listed in Table 6.46.

6.3.3.2 Discussion

Only moderately high salt-rejection performances were realized with the PVAM-OD material, although a substantial improvement in the performance of the low-pressure membrane was obtained. As mentioned earlier, the precursor material used is not a homopolymer of vinyl amidine, but rather a mixture of the amidine and its hydrolysis product (Figure 6.14) *(35)*. The degree to which PVAM-OD hydrolyzes during synthesis and product recovery cannot be controlled, and the resulting batch-to-batch variation in the pure product content of this polymer had to be accepted *(19)*. However, even in a situation where the synthesis route to the precursor material was under development, the performance of the UTF RO membrane formulated with it could be improved, which was proof of the potential of the simplex SDO method of approach in membrane research and development.

Trial runs OD74, OD65 and OD66 (see Table 6.45) were replicated in subsequent experiments with PVAM-OD originating from a batch different from the one used in simplex 6. The performances obtained in the replicated trials are shown in Table 6.47. Although the salt-rejections of the membranes were in reasonable agreement with those shown in Table 6.45, the flux performances were lower.

Two factors were excluded early from further study (simplex 3), as there was an indication that they had a detrimental effect on membrane performance. These two factors were SLS (surfactant) and IPC (cross-linking reagent). Omission of IPC from the tubular membrane study only confirmed earlier findings, based on work with flat sheet membranes, *(19)* that PVAM/SCL membranes out-performed PVAM/IPC membranes.

In retrospect, the use of an anionic surfactant, SLS in this case, should not have been considered, due to the cationic nature of PVAM. The sporadic occurrence of patched take-up of Congo red dye on membrane surfaces, in some of the cases where SLS was added to the precursor formulations, is possible evidence of its effect on the homogeneity of the cross-linked film. Reporting on surface-acting cleaning agents, Riley *(55)* and Leban *(56)* mentioned the detrimental effects which anionic surfactants have on the performances of poly(ether/urea) and polyvinyl amine UTF composite membranes. The addition of surfactants to the precursor formulation was discontinued altogether. The use of a non-ionic surfactant was, however, continued in substrate membrane fabrication.

The movement in the variable-space as optimum membrane performance is approached, is indicated in Table 6.48 for each of the remaining ten factors investigated. In this table, the means of the variables for the three "best" membranes (Table 6.45) from each of the six simplexes are shown (first simplex Table 6.42).

An interesting feature of the formulation shown in Table 6.48 for trial OD74 (regarded as optimum), is the high (5% by mass) precursor concentration that originated from the SDO study (Factor A). This concentration was regarded as being unduly high, especially when it was compared with solids levels indicated for other UTF composite membrane systems based on polymeric precursors, which varied between 0,7 to 2% by mass *(57)(58)*. This could be ascribed to the poor film-forming properties of the PVAM-OD material. The viscosity of the polymer solution per unit solids is regarded as an important parameter in the formation of an adequate film *(55)*. The molecular mass of the starting material [PAN] from which PVAM was synthesized was controlled which, ideally, should control the viscosity of the PVAM-OD end-product to within certain limits. However, hydrolysis during synthesis caused a significant reduction in the intrinsic viscosity of the PVAM-OD material *(19)*.

The active role which the acid-acceptors played in the formulation, became manifest in the increase in concentration levels of both TEA and TSP (factors C and D) above their respective starting values. This indicated that the hydrochloric acid freed during the condensation reaction was detrimental to the membrane structure and that neutralization was necessary to increase the extent of the cross-linking reaction.

At the average temperatures and residence times cited in Table 6.48 for simplexes 5 and 6 (Factors L and M) and for that of the final formulation (trial OD74), the membranes passed out of the tunnel oven while they were still damp. This indicated that (i) the membranes actually do not need high curing temperatures for optimum performance which, in turn, indicates that (ii) chemical cross-linking plays a primary role in establishing the final PVAM-OD membrane matrix and that (iii) thermal fusion of primary amines plays a secondary role.

TABLE 6.47: REPLICATIONS OF TRIALS IN SIMPLEX 6 (TABLE 6.44)

Trial Repeat	Rejection [%]	Flux [lmd]	A^2/B-value
OD74Rep	97,4 ± 0,7	310 ± 11	$4,36 \times 10^{-5}$
OD74Rep	97,5 ± 0,1	230 ± 14	$3,30 \times 10^{-5}$
OD65Rep	96,9 ± 1,7	410 ± 13	$4,92 \times 10^{-5}$
OD65Rep	97,7 ± 0,1	330 ± 35	$5,29 \times 10^{-5}$
OD66Rep	96,1 ± 0,3	200 ± 7	$1,80 \times 10^{-5}$
OD66Rep	94,8 ± 0,1	250 ± 57	$1,68 \times 10^{-5}$
Simplex 6 (Table 6.45)			
OD74	97,1 ±0,1	730 ± 24	$8,98 \times 10^{-5}$
OD65	97,2 ± 0,1	620 ± 38	$7,88 \times 10^{-5}$
OD66	98,0 ± 0,2	440 ± 33	$7,87 \times 10^{-5}$

TABLE 6.48: MEAN TRENDS IN THE VARIABLE-SPACE OF FACTORS INVESTIGATED (PVAM/OD/SCL)

Simplex	Factors									
no	A	C	D	E	F	G	J	K	L	M
1	3,0	0,37	0,03	20,0	8,33	1,97	5,0	5,0	106	8,4
2	3,3	0,23	0,07	12,5	9,00	1,70	5,0	5,8	106	8,0
3	3,0	0,37	0,03	15,0	9,67	1,43	7,0	3,7	106	8,7
4	4,0	0,56	0,05	22,5	7,66	1,90	6,0	2,3	109	6,1
5	4,3	0,97	0,09	30,0	3,35	2,93	8,7	6,1	88	2,3
6	5,3	1,32	0,19	34,3	2,00	4,64	5,0	11,7	80	3,2
Trial OD74	5,0	1,10	0,14	43	1,5	4,5	3,0	10	95	5,4

Legend			Simplex 1 (base) Table 6.41
A	Concentration PVAM-OD	[mass%]	1,9
C	Acid acceptor [TEA]	[mass%]	0,3
D	Acid acceptor [TSP]	[mass%]	0,05
E	Precursor contact time	[min]	22,5
F	Precursor draining time	[min]	9
G	Concentration SCL	[mass%]	1,7
J	Crosslink contact time	[mass%]	4,5
K	Post crosslink air dry time	[min]	7,5
L	Oven temperature	[°C]	102
M	Oven residence time	[min]	9,5

On the other hand, it is possible that thermal curing induces stress in the brittle UTF due to (i) substrate membrane densification and (ii) shrinkage of the UTF upon the loss of water from within their respective structures. As a result, micro-cracks could form in the UTF, which in turn, would cause leakage of salt, a situation which would result in lower potential salt-rejection performance. (Micro-crack formation was clearly observed when films of PVAM/SCL, produced on glass plates and cured at 110°C for 10 min, were investigated on an optical microscope).

6.3.4 SDO, PVAM-FD UTF RO MEMBRANE FORMULATIONS

As was mentioned earlier, two PVAM polymers were synthesized in the course of the research programme, namely, the PVAM-OD polymer, discussed in the previous paragraphs, and PVAM-FD. Batches of powdered PVAM-FD material showed little variation in its light cream colour, as opposed to variations in the shades of brown of the PVAM-OD material. Without any analytical information that the PVAM-FD material was chemically different, UTF membranes were prepared from the PVAM-FD material to determine whether this was so.

The best formulation for tubular PVAM UTF membranes available at the time originated from the SDO investigations performed on PVAM-OD, and specifically that from trial OD47, obtained in simplex no 4 (Table 6.45). The formulation for trial OD47 (shown in Table 6.49) was replicated, using PVAM-FD as precursor.

In the first replicate involving the PVAM-FD material, the conditions shown in Table 6.49 were duplicated on 0,6m long series 224 support membranes. At the standard operating pressure of 2MPa, however, no water permeated the PVAM-FD desalting barrier. This situation was rectified in subsequent replicates by reducing the polymer content of the precursor solution. The results are summarized in Table 6.50.

The preliminary results shown in Table 6.50 indicated what analytical evidence later confirmed, namely, that the two precursor materials were different. An important result of this experiment was the difference in precursor concentrations that resulted in PVAM-FD and PVAM-OD membranes of apparently similar performances. This was encouraging from the point of view that at such low solids concentration levels the supply of laboratory quantities of PVAM-FD would not be overtaken by the demand, and full 3m-long PVAM-FD membranes could therefore be fabricated on the fill-coating machine in the ensuing SDO formulation study.

6.3.4.1 Results

At the start of the research programme on the PVAM UTF tubular membrane system, no prior knowledge existed of either membrane formulations or of tubular membrane performance expectations. The situation was clearer at the start of the PVAM-FD self-directing optimization programme as formulations originating from the study on the PVAM-OD membrane could be used as a guide in setting initial variable ranges.

TABLE 6.49: FORMULATIONS FOR TRIAL OD47, PVAM-OD/SCL MEMBRANE

	Factor		Factor Level
A	Concentration PVAM polymer	[mass%]	4,0
B	~~Surfactant - [SLS]~~		
C	Acid acceptor [TEA]	[mass%]	0,73
D	Acid acceptor [TSP]	[mass%]	0,07
E	Precursor contact time	[min]	22,5
F	Precursor draining time	[min]	6,33
G	Concentration SCL	[mass%]	2,17
H	~~Concentration - IPC~~		
J	Crosslink reagent contact	[min]	8,0
K	Post crosslink air dry time	[min]	4,8
L	Oven temperature	[°C]	100
M	Oven residence time	[min]	1,9

Performance:			
	Rejection	96,1 ± 0,3	%
	Flux	650 ± 46	lmd
	A^2/B-value	$5,75 \times 10^{-5}$	

TABLE 6.50: FIRST EXPERIMENTAL PVAM-FD MEMBRANES (FORMULATION OD47, TABLE 6.49)

PVAM-FD [mass%]	Rejection [%]	Flux [lmd]	A^2/B-value
4,0		nil	
1,0	97,5 ± 0,5	370 ± 22	$5,18 \times 10^{-5}$
0,5	68,6 ± 4,1	690 ± 146	$0,72 \times 10^{-5}$

The ten factors in the final PVAM-OD membrane formulation were kept unchanged for the SDO study on the PVAM-FD membrane, and are listed in Table 6.51, together with their proposed levels. The use of IPC as a cross-linking additive and the addition of a surfactant to the precursor solution was not considered. With respect to the PVAM-OD membrane formulation, shown in Table 6.46;

i) The solids level of the PVAM-FD precursor was reduced as result of the above experiments.
ii) *In situ* coating performed on the fill-coating machine was accomplished under a slight average internal pressure of 200mm. Wetting of the pores on the surface of the substrate membrane was therefore enhanced by convective flow of precursor, and not only on diffusive flow as with dip-coated membranes. The base level for this factor (precursor wetting time), was therefore made lower.
iii) Short precursor drainage times could not be achieved on the fill-coating machine due to the time required for connecting up the cross-linking reagent solution manifold to individual membranes. The intrinsic viscosity of the PVAM-FD material was higher *(59)* than that of PVAM-OD, and on these grounds it was expected that longer drainage times would be required to obtain films of similar thicknesses. The levels for this factor (precursor draining time) were chosen accordingly.

The PVAM-FD UTF membranes were prepared according to formulations (first simplex) shown in Table 6.52. Series 224 substrate membranes, similar to those used in the PVAM-OD SDO study, were used. The substrate membranes were again stored wet before use, and a 10min pre-draining period was again allowed before coating of the membranes commenced. The membranes were dried in the tunnel oven.

The membranes were evaluated under conditions similar to those for the 0,6m dip-coated PVAM-OD membranes. Three 3m membranes were prepared simultaneously on the fill-coating machine at each experimental point. Six membranes were evaluated at each experimental point, for which purpose 1,2m test specimens were taken from the top-section (as prepared on the fill-coating machine) and bottom-section of each 3m membrane.

The performances in the first simplex of the SDO experiment, conducted on the PVAM-FD/SCL membrane system, are summarized in Table 6.52. The trials are ranked in the table according to decreasing order of their A^2/B-values. From this table a second simplex was generated. When only trial FD11 was considered as a member of the "best" group, and the remainder of the trials as members of the "worst" group, the difference between the mean A^2/B-values of the two groups was maximized. All the trials, except FD11, were therefore discarded and new formulations generated in their place. (See Table 6.52).

Three SDO experiments were conducted in all, and as can be seen in Table 6.53, in which the performances of the four "best" membranes from each simplex are summarized, there was no further improvement in the performance of the membranes after the second simplex. The formulation of membrane FD14, regarded as optimum, is shown in Table 6.54.

TABLE 6.51: FACTOR LEVELS FOR FIRST SDO EXPERIMENT CONDUCTED ON THE PVAM-FD/SCL MEMBRANE

Factor			Factor level	
A	Concentration PVAM-OD	[mass%]	0,8	1,6
B	Acid acceptor [TEA]	[mass%]	0,2	0,5
C	Acid acceptor [TSP]	[mass%]	0,1	0,3
D	Precursor contact time	[min]	15	25
E	Precursor draining time	[min]	5	8
F	Concentration SCL	[mass%]	1	2
G	Crosslink reagent contact	[min]	2	4
H	Post crosslink air dry time	[min]	4	8
J	Oven temperature	[°C]	95	105
K	Oven residence time	[min]	2	8

TABLE 6.52: FIRST SIMPLEX DESIGN MATRIX, PVAM-FD/SCL MEMBRANE

Trial no	Factors A	B	C	D	E	F	G	H	J	K	Rejection [%]	Flux [lmd]	A^2/B-value
FD11	0,8	0,2	0,3	15	8	2	4	4	95	2	98,4 ± 0,3	280 ± 28	$6,25 \times 10^{-5}$
Mean	0,8	0,2	0,3	15	8	2	4	4	95	2			
2xMean	1,6	0,4	0,6	30	16	4	8	8	190	4			
FD10	1,6	0,2	0,1	25	5	2	4	8	95	2	98,4 ± 0,3	160 ± 46	$3,51 \times 10^{-5}$
FD 3	0,8	0,5	0,3	25	5	1	2	8	93	2	79,4 ± 3,8	730 ± 95	$1,20 \times 10^{-5}$
FD 6	1,6	0,2	0,1	15	8	1	2	8	96	8	65,0 ± 1,9	1300 ±164	$1,14 \times 10^{-5}$
FD 7	0,8	0,2	0,1	25	5	1	4	4	102	8	92,0 ± 2,8	250 ± 97	$1,09 \times 10^{-5}$
FD 4	1,0	0,5	0,3	15	5	1	4	4	96	8	67,9 ± 1,2	880 ± 55	$0,89 \times 10^{-5}$
FD 9	0,8	0,5	0,1	15	8	1	4	8	102	2	76,8 ± 4,8	610 ± 97	$0,89 \times 10^{-5}$
FD 1	1,6	0,5	0,3	25	8	2	4	8	107	8	75,5 ± 8,3	260 ± 53	$0,37 \times 10^{-5}$
FD 2	1,6	0,2	0,3	25	8	1	2	4	104	2	66,9 ± 4,1	140 ± 23	$0,15 \times 10^{-5}$
FD 5	1,6	0,5	0,1	15	5	2	2	4	103	2	74,4 ± 6,9	73 ± 10	$0,10 \times 10^{-5}$
FD 8	0,8	0,2	0,3	15	5	2	2	8	107	8	76,4 ± 5,2	60 ± 23	$0,09 \times 10^{-5}$
Co-ordinate points generated for the second simplex													
FD12	1,2	0,2	0,5	5	11	2	4	3	95	2			
FD13	0,8	0	0,3	5	11	3	6	3	97	2			
FD14	1,2	0,2		0,5	185	3	6	3	94	4			
FD15	0,8	0,2	0,5	5	11	3	4	4	88	4			
FD16	0,6	0	0,3	15	11	3	4	4	94	4			
FD17	0,8	0	0,5	15	8	3	4	3	88	2			
0D18	1,2	0	0,3	5	8	2	4	3	83	4			
0D19	1,2	0,2	0,3	5	8	3	6	4	86	2			
FD20	1,2	0	0,5	15	11	2	6	4	87	2			
FD21	0,8	0,2	0,3	15	11	2	6	3	83	4			

Legend:
- A Concentration PVAM-OD
- B Acid acceptor [TEA]
- C Acid acceptor [TSP]
- D Precursor contact time
- E Precursor draining time
- F Concentration SCL
- G Crosslink reagent contact
- H Post crosslink air dry time
- J Oven temperature
- K Oven residence time

TABLE 6.53: SUMMARY OF BEST PERFORMANCE PVAM-FD/SCL MEMBRANES

Trial	A^2/B-value	Rejection [%]	Flux [lmd]	Simplex no
FD11	$6,25 \times 10^{-5}$	98,4 ± 0,3	280 ± 28	1
FD10	$3,51 \times 10^{-5}$	98,4 ± 0,3	160 ± 46	
FD 3	$1,20 \times 10^{-5}$	79,4 ± 3,8	730 ± 95	
FD 6	$1,14 \times 10^{-5}$	65,0 ± 1,9	1300 ± 164	
FD14	$10,90 \times 10^{-5}$	98,2 ± 0,7	560 ± 150	2
FD18	$9,96 \times 10^{-5}$	99,2 ± 0,1	220 ± 100	
FD17	$8,83 \times 10^{-5}$	98,8 ± 0,4	310 ± 230	
FD20	$8,61 \times 10^{-5}$	98,9 ± 0,2	260 ± 147	
FD14	$10,90 \times 10^{-5}$	98,2 ± 0,7	560 ± 150	3
FD18	$9,96 \times 10^{-5}$	99,2 ± 0,1	220 ± 100	
FD17	$8,83 \times 10^{-5}$	98,8 ± 0,4	310 ± 230	
FD20	$8,61 \times 10^{-5}$	98,9 ± 0,2	260 ± 147	

TABLE 6.54: OPTIMUM PVAM-FD/SCL MEMBRANE FABRICATION FORMULATION (TRIAL FD14)

	Factor	Level	level
A	Concentration PVAM-OD	[mass%]	1,2
B	Acid acceptor [TEA]	[mass%]	0,2
C	Acid acceptor [TSP]	[mass%]	0,5
D	Precursor contact time	[min]	15
E	Precursor draining time	[min]	8
F	Concentration SCL	[mass%]	3
G	Crosslink reagent contact	[min]	6
H	Post crosslink air dry time	[min]	3
J	Oven temperature	[°C]	95
K	Oven residence time	[min]	4

6.3.4.2 Discussion

When the formulations shown in Tables 6.46 (PVAM-OD) and 6.54 (PVAM-FD) are compared, it is evident that different formulations resulted from the SDO studies on the two membrane systems. As was shown with the CA membrane system, interactions between fabrication variables introduce another dimension in finding optimum levels for fabrication variables; it is theoretically possible to obtain membranes with similar performances from different formulations.

On the other hand, it was shown (Table 6.50) that the two membrane precursor starting materials differed to such an extent that formulations designed for one membrane did not apply to the other. A further indication that the materials differed, and also of the suggested superiority of PVAM-FD as a membrane material, was that the first 99% salt rejection membrane (FD18, Table 6.53) was produced from this material, as opposed to a maximum salt rejection of 98% (OD66, Table 6.45) of the PVAM-OD material.

An observation made from the data, was that the standard deviation of salt rejection performances decreased as the salt rejections approached 99%. This was regarded as an indication of the greater homogeneity of these cross-linked matrices.

In comparison with the PVAM-OD membrane system, fewer experimental trials were conducted in the SDO of PVAM-FD formulations before the simplex converged to a solution. There were three possible reasons: reduced variability in the quality of the two reagents used, the performance of membranes produced on the fill-coating machine was more consistent, and the base-points of the first simplex was chosen closer to the respective maximas of the factors. (Ideally, if time permits, another simplex could be generated at co-ordinates away from that of the solution, to determine if a second SDO study would converge to the same solution).

The concentrations of the acid-acceptors included in the precursor solution were lower in the FD14 formulation than in the OD74 formulation. A possible explanation for this occurrence is the presence of unreacted ethylene diamine in the freeze-dried PVAM-FD product. In the synthesis of PVAM-FD, PAN is dissolved in excess ethylene diamine, which is recovered from the polymer product by freeze-drying. Techniques were established towards the end of the programme (i) to determine the relative concentration of ethylene diamine in the PVAM-FD product, and (ii) to ensure minimal concentration of the di-functional monomer in the polymer product *(19)*. It was evident from these analyses that ethylene diamine, in severe cases, could remain present in the product at concentration levels of up to 10%.

On the one hand, the ethylene diamine could act as an acid-acceptor, but its reactivity with SCL caused another problem. At a stage in the cross-linking reaction at which the mobility of PVAM-FD is hindered due to cross-linking, unreacted ethylene diamine retains its mobility and can diffuse towards the interface to interfere with the cross-linking reaction. As SCL and ethylene diamine are both di-functional, a linear polymer will result from a reaction between the two species. Cross-linking results only if the end-groups on the linear polymer-chain are joined up with the PVAM-FD matrix. This chemical modification of the desalting matrix resulted in lower salt rejection performances.

Fortunately, in the absence of any quantitative technique to determine the relative concentration of ethylene diamine in the PVAM-FD product at the time, it was soon learnt through experience to use the colour of the precursor solution as an indication that the concentration of ethylene diamine had exceeded acceptable limits. Acceptable precursor solutions were brown. In this subjective test, a batch of precursor solution was discarded when any shade of green, an indication of the presence of ethylene diamine, was noticed.

The situation regarding oven-drying times and temperatures was the same as experienced with PVAM-OD; the membranes left the oven while they were still damp. The post cross-link reaction air-drying time obtained from the SDO study was too short for complete evaporation of the hexane. The low flash-point of this solvent was a matter of concern and the period allowed for hexane evaporation was extended later in the programme from 3 to 16min, which ensured complete evaporation of hexane (section 6.3.5.2).

6.3.5 ROLE OF THE SUBSTRATE MEMBRANE

Variation in the performance of 3m UTF membranes was particularly noticeable when the performances observed for membrane specimens taken from the top-section of the long membrane were compared with those of specimens taken from the bottom section. The variation was also more noticeable in the flux performances of the membrane sections than in the salt rejection performances. This was ascribed to the precursor film at the top section of the drain-coated membranes being thinner than at the bottom section. (Swabbing the membranes *(48)* with a foam ball, after the drain-coating step to obtain precursor films of more uniform thicknesses, was not considered as it would have complicated the fabrication process further).

It is evident from the data in Table 6.55 to what extent variations can be expected to occur as a result of (i) uneven thickness of drain-coated films, (ii) characteristics of the substrate membrane and (iii) synthesized PVAM-FD precursor. Two membrane formulations (FD18 and FD14, Table 6.52) were replicated on three different batches of series 224 substrate membranes produced under similar conditions (substrate casting runs 99T, 101T and 107T). The PVAM polymer used originated from three different synthesized batches, namely, PVAM-3, PVAM-4 and PVAM-6. Six 1,2 membranes were slit from the bottom and top sections of three 3m fill-coated membranes for evaluation.

6.3.5.1 Replication on PS substrate membranes

Substrate membranes make an important contribution to both the quality and reproducibility of UTF RO membranes. Dye solutions are added to precursor formulations in flat sheet membrane production *(60)* in order to simplify the location and manual masking of micro-flaws in the UTF desalting barrier. The geometry of the tubular membranes makes difficult the visual inspection of the UTF for the presence of irregularities. Evaluation of the membrane for RO properties therefore remains the only means for determining the quality of the product. The addition of Congo red in milligram quantities to the 40 litres feed tank during evaluation helps to reveal imperfections in the desalting barrier. Any form of flaw in the perm-selective barrier is revealed as a red mark on the outside of the membrane.

TABLE 6.55: REPLICATED PVAM-FD UTF MEMBRANES

Support batch	A-value [x10^5]	PVAM batch	UTF trial	UTF membrane Section: Top Rejection	Top Flux	Bottom Rejection	Bottom Flux
99T	1 900	PVAM-3	FD18	98,3	170	98,5	190
				99,2	180	96,3	200
				99,0	200	97,9	210
				98,8 ± 0,5	183 ± 15	97,6 ± 1,1	200 ± 10
101T	1 450	PVAM-4	FD18	99,1	320	99,1	480
				99,2	300	98,9	480
				99,1	440	99,0	560
				99,1 ± 0,1	350 ± 75	99,0 ± 0,1	510 ± 46
101T	1 450	PVAM-4	FD14	99,0	380	98,2	290
				99,0	340	99,2	200
				98,9	380	98,8	330
				99,0 ± 0,1	370 ± 23	98,7 ± 0,5	270 ± 67
107T	1 050	PVAM-6	FD14	99,4	590	91,0	670
				99,3	660	96,3	560
				99,5	360	95,6	520
				99,4 ± 0,1	540 ±157	94,3 ± 2,9	580 ± 78

TABLE 6.56: PVAM-FD UTF RO MEMBRANES, DIFFERENT SUBSTRATE MEMBRANE BATCHES

Substrate lot code	Rejection [%]	Flux [lmd]	A^2/B-value
102T35S224	99,0 ± 0,1	340 ± 39	$12,8 \times 10^{-5}$
103T35S224	98,5 ± 0,3	390 ± 169	$9,8 \times 10^{-5}$
107T35S224	99,4 ± 0,1	500 ± 103	$28,7 \times 10^{-5}$
107T35S224	99,2 ± 0,2	490 ± 103	$22,7 \times 10^{-5}$
108T35S225	99,2 ± 0,6	470 ± 76	$19,5 \times 10^{-5}$
108T35S225	99,4 ± 0,4	450 ± 88	$26,6 \times 10^{-5}$

TABLE 6.57: OVEN PRE-DRYING OF DIFFERENT SUBSTRATE MEMBRANES

Substrate lot code	Drying method	Rejection [%]	Flux [lmd]	A^2/B-value
118T35S224	Control	99,4 ± 0,2	176 ± 37	$10,6 \times 10^{-5}$
(12% 3500P)	4min/95°C	99,0 ± 0,5	270 ± 91	$9,9 \times 10^{-5}$
121T35S227	Control	98,5 ± 0,6	130 ± 18	$3,1 \times 10^{-5}$
(14% 3500P)	4min/95°C	98,1 ± 0,7	229 ± 57	$4,4 \times 10^{-5}$
120T35S226	Control	95,4 ± 4,0	109 ± 18	$0,8 \times 10^{-5}$
(16% 3500P)	4min/95°C	97,7 ± 1,2	127 ± 25	$1,9 \times 10^{-5}$
	8min/95°C	98,2 ± 0,3	445 ± 40	$9,4 \times 10^{-5}$

Post-coating the UTF RO membrane with the precursor solution, followed by a re-baking process (*i.e.* if the precursor contains primary amines) is one method *(48)* by which flaws in the UTF can be masked. The other methods are *in situ* coating techniques which are applied while the membrane is in operation, and in which polymeric substances such as tannic acid *(61)* and proprietary materials *(5)* are relied upon to seal imperfections.

Imperfections in the UTF desalting matrix, resulting from inadequate substrate membrane support, are caused by;

i) Imperfections in the substrate membrane skin due to vibration of the casting equipment or leach front disturbances which cause lines to form on the skin surface of the substrate membrane.
ii) Pinholes in the membrane skin due to unfiltered casting solution, air bubbles in the casting solution and support fabric fibre intrusion.
iii) Areas of low density of support fabric fibres, or poor calendering, which cause bleed-through of low-viscosity casting solutions, resulting in gross imperfections on the opposite skin-side of the substrate membrane.
iv) Blow-out of the substrate membrane skin in regions where it is inadequately supported by the sub-surface matrix due to the presence of large macro-voids in the sub-surface region.
v) Presence of micro-beads (low-molecular-mass fractions of the substrate membrane polymer) on the surface of the substrate membrane.

Notwithstanding these problems, excellent PVAM UTF has been replicated repeatedly, as shown by data in Table 6.56. The performance results shown in the table were obtained from 3m fill-coated membranes, produced according to formulation FD14 (Table 6.54). The substrate membranes were cast into 20°C RO permeate from solutions with a solvent mass ratio of 3,5 to 1, NMP to 1,4-dioxane and either 12% 3500P PS (series 224) or 11,5% 3500P PS (series 225).

As a rule, the wet substrate membranes were pre-drained for the standard 10min to remove excess water. In an experiment to determine whether this 10min time-period could be reduced, membranes were passed through the tunnel oven, set for a 4min pass at an oven temperature of 95°C. The membranes were produced in 3m lengths from the same precursor (batch PVAM-7) by the fill-coating method. The substrate membrane casting solutions used differed in their solids contents (solvent system NMP/1,4-dioxane, mass ratio 3,5:1). The membranes were drained for 10min as control for the experiment. The data contained in Table 6.57 reflects that the manner in which the substrate membrane moisture was removed had an effect on the end-performance of the UTF RO membrane.

Any trend, which thermally assisted removal of moisture brought about in the observed pure-water permeability [PWP] (A-values) of the support membranes, was masked by the large standard deviations noted in PWP tests conducted on such membranes. Some trend was noticed, however, when the RO performances of UTF composite membranes produced on semi-damp substrate membranes, are compared. In the case of the low polymer-content substrate membranes (lots 118T and 121T), thermally assisted removal of moisture seemed to have little effect on the ultimate performance of the UTF membranes. The substrate membrane cast from a higher solids content solution (lot 121T, 16% solids) showed a marked improvement in the

permeability of the resulting UTF membrane (Table 6.57). It is known *(16)* that substrate membranes prepared from higher solids-containing solutions have relatively smaller surface pore sizes than those cast from solutions containing lower amounts of solids. It was therefore possible that as moisture was removed from the substrate, the substrate shrank, causing enlargement of smaller pores, or even caused micro-cracks to form in the substrate membrane surface skin. This situation is transient, as the low-pressure hydrodynamic permeability (200kPa) of the substrate membrane drops away drastically, upon further drying, to leave the membrane unfit for use as a UTF substrate membrane *(62)*.

6.3.5.2 Discussion

It has been shown in the above experiment, that the substrate membrane characteristics may be altered by thermal treatment, thereby affecting the RO properties of the UTF membrane. In both the SDO studies conducted on the PVAM/SCL membrane system, the membranes left the oven in a still damp condition, an indication that thermal treatment either did not lead to an improvement of the RO properties of the UTF membrane, or, in the light of the above findings, possibly led to some other adverse effects, *e.g.* unnecessary densification of the substrate membrane, or even stress-induced cracking. However, optical microscopy performed on PVAM films cured at 110°C on glass-slides revealed cracks which had formed in the film during the curing process. When the films were wetted, they showed a tendency to redissolve, an indication of the unability of the PVAM-FD material to undergo self-curing under thermal treatment.

An early finding in studies conducted on flat-sheet polyvinylamidine UTF composite membranes *(63)*, were that thermal curing was a necessary step in the formulation of the RO membrane. In this regard, two possibilities offer themselves:

i) If thermal treatment brings about structural changes in the substrate membrane, the tendency will be aggrevated in the case of tubular membranes because of their different geometry.
ii) The chemistry of the polyvinylamidine material has advanced from an initial mixture of materials, to PVAM-OD and PVAM-FD products which were relatively more homogeneous in their content.

That the difference in geometry between flat-sheet and tubular membrane configurations can lead to different membrane formulations, had been addressed in the opening paragraphs to this chapter. Here is an example where this difference manifested itself.

6.3.5.3 Replication on PES substrate membranes

At this stage of the UTF membrane-development programme, it was realized that the bond-strength between the PS substrate membrane and the Viledon fabric led to membrane/module adaptation problems, a situation which made the membrane unsuitable for field tests. The research was redirected to improve the bond-strength of the substrate membrane. Part of this study was introduced earlier in section 6.2.2. A study was conducted simultaneously to determine to what extent the substrate membrane casting formulations (substrate

membrane factor levels were shown in Table 6.36) influenced the performance of UTF PVAM-FD membranes.

UTF membranes (formulation FD14/mod) were fabricated on each of the different sets of membranes developed in the adhesion study discussed in section 6.2.2.3. The UTF membrane formulation used in this experiment (FD14/mod), differed from the formulation given earlier in Table 6.54 in that the precursor draining-time was reduced to 4min and the post cross-linking time was increased to 16min to allow complete evaporation of hexane. The manually dip-coated membranes were dried in the vertical oven at 90°C for 4min, and not in the tunnel-oven at 95°C for 4min as previously. The membranes were produced in 1,2m lengths. All UTF solutions were made up freshly on the day of use, and filtered through Whatman filter paper just prior to use.

The membranes were evaluated at the standard UTF membrane test conditions. The results obtained in this study are summarized in Table 6.58.

By employing the technique described in section 4.2.3.1 (method I), the main and interaction effects of the contributing factors were calculated from the data contained in Table 6.58. These effects are listed in Table 6.59, together with the calculated estimates of error variance, obtained by pooling all measurable two-factor interactions. Student's t-test was performed to determine the levels of significance of the main effects. For 15df, the critical t-values at the 10%, 5% and 1% levels were 1,75, 2,13 and 2,95, respectively. A factorial effect mean must therefore, in the case of rejection, exceed the absolute value of (3,14)(2,95) = 9,26 for significance at the 1% level, and 6,69 and 5,49, respectively, for significance at the 5% and 10% levels.

6.3.5.4 Discussion

The statistical analysis of results indicated that substrate membrane fabrication formulations do have an effect on the RO performance of UTF RO membranes. If formulations for the UTF matrix were to be studied jointly with substrate membrane formulations, the five important factors which have been isolated in this experiment, would at least have to be included in such a study, namely:

i) length of exposure to air of the substrate membrane,
ii) coagulant temperature,
iii) addition of surfactant to the coagulation medium, (anionic SLS was used during this experiment, but was later replaced by non-ionic Triton X-100, for reasons already given),
iv) concentration of the membrane-forming polymer.

The addition of PVP to the casting solution formulation had no apparent significant effect on the UTF membrane properties, but as it enhanced membrane/fabric compatibility (Table 6.38), it should be present in the membrane-casting formulation. In a joint study of UTF and substrate membrane formulations, the concentration of PVP can therefore be kept fixed at the 5 or 10 mass percent levels (see Table 6.40 for series 719 substrate membrane formulation.

TABLE 6.58: PVAM-FD UTF MEMBRANES, PES SUBSTRATE MEMBRANE, SALT REJECTION, RO WATER FLUX AND A^2/B-VALUE, 2^{9-4} FACTORIAL

Treatments	Rejection [%]	Flux [lmd]	A^2/B-value [x10^5]
I	33,9	1160	0,24
abcd	94,1	350	2,09
cdef	96,7	400	4,52
abef	94,6	420	2,82
bceg	96,3	550	5,71
adeg	96,7	300	3,35
bdfg	97,7	410	6,94
acfg	96,7	360	4,08
bdeh	92,5	410	1,95
aceh	98.4	360	8,53
bcfh	71,4	1100	1,19
adfh	98,1	320	6,27
cdgh	95,5	540	4,54
abgh	96,8	290	3,39
efgh	98,5	370	9,50
abcdefgh	96,7	210	2,24
bdej	95,8	400	3,21
acej	98,6	330	9,18
bcfj	62,5	890	0,60
adfj	96,8	360	4,15
cdgj	97,1	390	5,07
abgj	99,0	290	10,90
efgj	98,6	330	8,95
abcdefgj	98,7	210	5,94
hj	85,9	420	0,97
abcdhj	98,1	340	6,49
cdefhj	97,1	370	4,82
abefhj	98,3	350	7,71
bceghj	98,6	580	16,90
adeghj	97,1	280	3,63
bdfghj	98,8	390	13,00
acfghj	95,9	300	2,71

A Air drying period
B NaCl concentration, leach tank
C NMP concentration, leach tank
D Temperature, leach tank
E Surfactant [SLS], leach tank
F Casting dope, PEG400 concentration
G Casting dope, PES 4800G concentration
H Casting dope, PVP^{44K} concentration
J Casting dope, LiCl concentration

TABLE 6.59: SUBSTRATE MEMBRANE CASTING VARIABLES, EFFECT ON UTF RO MEMBRANE PERFORMANCE

		Rejection [%]		Flux [lmd]		A^2/B-value	
Factor		Effect	Level	Effect	Level	Effect	Level
A	Air	8,63	5%	-227,5	1%	-0,29	
B	NaCl	0,49		37,5		0,66	
C	Solvent	0,86		48,8		-0,15	
D	Temperature	7,69	5%	-151,3	1%	-0,95	
E	Surfactant	8,41	5%	-127,5	5%	1,65	10%
F	PEG	1,44		-12,5		-0,04	
G	PES	9,14	5%	-136,3	1%	2,63	1%
H	PVP	4,02		-32,5		1,01	
J	LiCl	3,87		-82,5	10%	2,30	5%
Confounded two-factor interactions							
AF, BE, CG		-1,82		11,3		-1,41	
AG, DE, CF		-9,07	5%	62,5		-4,01	1%
FG, AC, BD		-0,88		-67,5		0,03	
BG, DF, CE		0,32		-30,0		2,24	5%
EG, AD, BC		-7,94	5%	110,0	5%	-0,95	
EF, CD, AB		-0,74		-56,3		-0,70	
AE, BF, DG		-7,96	5%	108,8	5%	-1,23	
Two-factor interactions (pooled for estimate of error variance)							
AH		-3,49		11,3		-1,20	
AJ		-2,57		63,8		-0,06	
BH		-2,41		51,3		0,83	
BJ		-2,71		46,3		2,50	
CH		-2,64		72,5		0,27	
CJ		-3,77		25,0		0,05	
DH		-3,93		37,5		-0,05	
DJ		-2,48		57,5		-0,50	
EH		-3,82		31,3		0,44	
EJ		-2,37		61,3		0,41	
FH		-2,46		36,3		0,17	
FJ		-4,33		33,8		-1,01	
GH		-4,38		47,5		-0,38	
GJ		-2,76		50,0		1,11	
HJ		-1,13		11,3		0,02	
V_{Effect}		9,85		2107,6		0,77	
SE_{Effect}		3,14		45,91		0,88	

Ten factors were isolated as being important in the initial study of PVAM-FD formulations (Table 6.54). Combining these with the five factors considered significant in the formulation of the substrate membrane, will result in fifteen factors which should be studied jointly; this would be a manageable situation, as has been illustrated throughout the text.

It has been shown that quality membranes can be produced reproducibly from formulations FD14 (Table 6.54) and FD14/mod. With these formulations and those listed in Table 6.38 for substrate membranes, research was directed at isolating other factors which could also play important roles in the preparation of UTF membranes.

6.3.6 PVAM-FD PRECURSOR

Although studies involving the PVAM precursor material as such fell within the scope of another study *(19)*, two aspects of the material were considered to have bearing on membrane formulation studies, namely, the molecular mass of the material, and the shelf-life of prepared precursor solutions. These two aspects will receive attention in the next paragraphs.

6.3.6.1 Molecular mass

When UTF membranes are fabricated from monomeric amines, it is sometimes preferable *(64)* to produce an oligomeric version of the amine compound, prior to membrane manufacture, to ensure greater homogeneity in the thin-film matrix.

The PVAM materials used in the fabrication of UTF membranes, have molecular mass averages in the range 20 000 to 40 000. It is, however, possible to produce PVAM materials of differing molecular mass, simply by varying the molecular mass of the synthesized PAN starting material.

In Table 6.60 performances are shown for membranes produced from PVAM-FD precursors of different molecular mass on series 224-support membranes (Table 6.40) using a manual immersion-coating method and UTF formulation FD14. From the data it appeared that the molecular mass of the precursor could have an affect on membrane performance. Higher-molecular-mass polymers seem to be preferable.

This has revealed another factor which could be considered in future formulations of the PVAM/SCL UTF RO membrane.

6.3.6.2 Ageing

Once prepared, precursor solutions are stored under nitrogen gas in dark, capped, containers. Even when these precautions are taken, the solutions have a limited shelf-life, and membranes should preferably be made from freshly prepared solutions. An experiment was performed to determine what effect precursor solution-ageing has on UTF membrane properties. Membranes were prepared from a solution stored under the above conditions, after periods of storage as indicated in Table 6.61. Series 224 substrate membranes and

formulation FD14/mod were used. The control set of six 1,2m manually dip-coated membranes was prepared from the freshly-made stock solution.

6.3.7 CHEMICAL MODIFICATION OF PVAM-FD/SCL FILMS

The chemical reactions performed thus far in creating the UTF permselective matrix were liquid-liquid interfacial condensation reactions. It has been mentioned earlier that certain surfactants had a deleterious effect on membrane performance ratings, and the question arose to what extent the performance properties of the PVAM membrane could be adjusted beneficially by performing a solid/liquid post-reaction with the membrane film after its formation.

The three cases presented in the following paragraphs indicate the importance of giving consideration to post-treatment as a fabrication step in the formulation of UTF composite membranes.

6.3.7.1 Modification by reaction with aldehydes

The basis of formation of UTF composite membranes is the cross-linking reaction which insolubilizes the water-soluble monomeric, oligomeric or polymeric precursor materials (see chapter III), either by complete reaction with a cross-linking reagent or partial reaction with the cross-linking reagent, followed by thermal curing of the precursor. Increase in the cross-linking density will improve the permselectivity of the desalting matrix, at the cost of a reduction in hydraulic permeability. In general, very high cross-linking densities will lead to the formation of brittle films, whereas insufficient cross-linking will lead to the formation of PVAM UTFs which will show excessive swelling and low salt rejection.

In the optimization studies on PVAM membranes, the final oven temperature and retention time arrived at can hardly be described as suitable for inducing thermal cross-linking, *i.e.* if primary amines were present in appreciable proportions. (Primary amines will condense and, if contained in a polymer, cause cross-linking, at 110°C).

The remarkable degree to which the hydrophilic PVAM/SCL cross-linked film will swell in water was evident from examination of samples of the film on glass slides. (Salts of the acid form at amine sites which further increases the water-uptake capability of the film). It was concluded that the mechanical integrity of the film could be improved by reducing the swelling capacity of the desalting matrix by increasing the degree of cross-linking (*58*).

Aldehydes such as formaldehyde *(61)* have been used as cross-linking-enhancing reagents in the formation of composite UTF RO membranes. In order to increase the cross-linking density of the UTF, the membranes were treated, after initial reaction with SCL, with an aqueous solution of glyoxal, a di-aldehyde. Cross-linking the UTF with the aldehyde cause a reduction in the swelling capacity of the film, when exposed to water, relative to that of the untreated films.

TABLE 6.60: EFFECT OF PAN MOLECULAR MASS (PRECURSOR IN PVAM SYNTHESIS) ON PVAM-FD MEMBRANE PERFORMANCE

PAN mol mass	Rejection [%]	Flux [lmd]
PVAM-FD-6	98,4 ± 0,8	96 ± 32
48 000	98,4 ± 0,4	220 ± 42
100 000	98,8 ± 0,2	430 ± 30

TABLE 6.61: PVAM-FD PRECURSOR SHELF-LIFE

Days aged	Solution pH	Rejection [%]	Flux [lmd]	A^2/B [x10^5]
Control	12,0	98,4 ± 0,2	370 ± 52	8,9
1	11,8	98,9 ± 0,3	270 ± 51	8,0
12	11,3	98,5 ± 0,1	230 ± 5	5,4
26	11,2	90,2 ± 1,0	1 540 ±114	7,3

Even though the reaction increased the cross-linking density of the film, the functionality introduced into the membrane structure increased the hydrogen-bonding capacities of the matrix, leading to higher hydraulic permeabilities of treated membranes. Tables 6.62 and 6.63 illustrate how conditioning of PVAM-FD membranes in glyoxal solutions for 21h affected the performance of the membranes. The UTF PVAM-FD membranes used in these experiments were produced in 1,2m lengths by immersion-coating series 714 substrate membranes according to formulation FD14/mod. The UTF membranes were dried in the vertical oven. After all the membranes had been fabricated, sets of six were selected randomly for conditioning according to each of the conditions listed in Tables 6.62 and 6.63.

The control membranes were not post-treated and were evaluated directly after having been rinsed in RO permeate. The 1% (by mass) glyoxal solutions were made up by dissolving the appropriate amount of a 40% solution of glyoxal (BASF) in RO permeate, after the pH of the water had been adjusted to 9 and 11, respectively, by the addition of NaOH. The membranes were immersed in the respective solutions for 21h, at a controlled ambient temperature of 22°C. The membranes were rinsed in RO permeate before evaluation.

The same procedure was followed in preparing the membranes listed in Table 6.63. In this case however, different glyoxal concentrations and immersion periods were used. The conditioning solutions were prepared by the addition of the appropriate amounts of glyoxal to RO permeate, previously buffered *(65)* to pH values of 4, 7, and 10.

6.3.7.2 Modification by reaction with aromatic diamines

PVAM-FD UTF RO membranes can also be modified chemically by being conditioned in a solution containing a di-functional amine. This post-treatment reaction was initially introduced as a means for dye-staining the surface of the membranes. The colour of the untreated PVAM-FD/SCL UTF changed permanently (*i.e.* under prevailing RO evaluation conditions) from a very light yellow, to a darker red-brown when the membranes were brought into contact with an aqueous 0,7 mass percent solution of 1,3-diamino benzene for 21h. This allowed visual inspection of the UTF for homogeneity.

However, it also allowed the membranes to be stored in a dried-out state, as opposed to their normally being stored wet in neutral pH RO permeate.

The results of two experiments are shown in Table 6.64. The UTF PVAM-FD membranes were produced on 1,2m series 221 support membranes by the immersion-coating technique, according to formulation FD14/mod, and dried in the tunnel oven for four minutes at 95°C. The control membranes were selected randomly and rinsed in RO permeate before being tested. The treated membranes were immersed in a 0,7 mass percent solution of 1,3-diamino benzene for 21h at a controlled temperature of 22°C. After having been conditioned, a set of six membranes was selected randomly for evaluation (Rx control), while the remainder were stored open in the laboratory for the periods indicated in the table. As 1,3-diamino benzene discoloured the feed water, the membranes were rinsed thoroughly after being installed for evaluation to remove all traces of 1,3-diamino benzene from the feed solution.

TABLE 6.62: GLYOXAL CONDITIONING OF UTF PVAM-FD MEMBRANES

Conditioning	Rejection [%]	Flux [lmd]	A^2/B-value
Control	97,8 ± 0,9	380 ± 50	$6,5 \times 10^{-5}$
21h, RO permeate	98,3 ± 0,2	540 ± 50	$12,2 \times 10^{-5}$
21h, RO permeates, 1% glyoxal	98,1 ± 0,3	1110 ±216	$26,3 \times 10^{-5}$
21h, pH 9 RO permeate, 1% glyoxal	98,5 ± 0,3	1090 ±220	$33,5 \times 10^{-5}$
21H, pH 11 RO permeate, 1% glyoxal	98,5 ± 0,3	980 ±194	$28,7 \times 10^{-5}$
21h, 2% Na_2CO_3, 1% glyoxal	96,4 ± 1,7	1230 ± 81	$15,6 \times 10^{-5}$
Control	96,1 ± 2,5	170 ± 10	$1,5 \times 10^{-5}$
21h, RO permeate, 1% glyoxal	97,8 ± 0,7	850 ± 80	$16,1 \times 10^{-5}$
21h, pH 9 RO permeate, 1% glyoxal	98,5 ± 0,5	670 ±230	$17,9 \times 10^{-5}$
21H, pH 11 RO permeate, 1% glyoxal	98,3 ± 0,5	750 ±230	$19,0 \times 10^{-5}$
21h, 2% Na_2CO_3, 1% glyoxal	97,3 ± 1,5	840 ±150	$13,4 \times 10^{-5}$

TABLE 6.63: DIFFERENT GLYOXAL POST-TREATMENT CONDITIONS

Glyoxal solution (pH RO make-up water)

Glyoxal Concentration		pH 4	pH 7	pH 10		Conditioning time
	1,0%	98,7 % 530 lmd [15,4]	98,4 % 550 lmd [13,1]	97,2 % 500 lmd [7,0]	1h	
	0,5%	98,5 % 950 lmd [27,7]	98,6 % 940 lmd [29,6]	98,3 % 850 lmd [20,9]	21h	
	1,0%	97,8 % 490 lmd [8,7]	97,6 % 560 lmd [9,5]	97,0 % 540 lmd [7,1]	21h	

[Figure in square brackets denotes $A^2/Bx10^5$]

TABLE 6.64: 1,3-DIAMINOBENZENE CONDITIONING OF PVAM-FD/SCL UTF COMPOSITE MEMBRANES

Storage	Rejection [%]	Flux [lmd]	A^2/B-value
Control	98,9 ± 0,3	270 ± 51	$8,0 \times 10^{-5}$
Rx control	98,9 ± 0,4	270 ± 17	$9,3 \times 10^{-5}$
14 days	99,3 ± 0,2	300 ± 35	$16,6 \times 10^{-5}$
Control	98,3 ± 0,2	320 ± 11	$6,9 \times 10^{-5}$
Rx control	94,7 ± 1,6	230 ± 19	$1,5 \times 10^{-5}$
7 days	97,2 ± 0,3	230 ± 9	$2,9 \times 10^{-5}$
5 months	97,0 ± 0,6	300 ± 21	$3,6 \times 10^{-5}$

6.3.7.3 Modification of the UTF film by neutralization and thermal treatment

The performance of a UTF PVAM-FD membranes is affected if the membranes are stored in buffered (pH 11) RO permeate for a period. Generally, the salt rejection remained at its initial value, but the hydraulic permeability increased. This was ascribed to slow hydrolysis *(59)* of PVAM-FD at high pH, which caused a chemical modification of the membrane matrix, leaving the structure more hydrophilic (see Figure 6.14).

In an experiment to determine the effect of high-pH conditioning, 1,2m PVAM-FD UTF membranes were made according to formulation FD14/mod, by immersion-coating series 712 (Table 6.40) substrate membranes. The membranes were conditioned, for the periods shown in Table 6.65, in RO permeate, which had been buffered to pH 11 before they were immersed. After the required period of conditioning, the membranes were removed and rinsed in RO permeate. One set (six membranes) was tested directly, and the other set was cured at 110°C for 10min in the vertical oven before evaluation. The control membranes were rinsed after fabrication, but one set was cured under the above conditions before evaluation.

The performance data showed that high-pH conditioning affected the hydraulic permeability of both cured and uncured membranes. Thermal curing had a negative effect on the rejection performance of the control membranes, which was not surprising in the light of the results of the SDO PVAM membrane formulation studies. Thermal curing decreased the hydraulic permeability performance of conditioned membranes, which indicated that there was thermally induced condensation cross-linking between neighbouring primary amine groups. The performance of thermally cured, pH 11-conditioned membranes, appeared to be better than that of the control membrane.

In another experiment, UTF PVAM-FD membranes were conditioned under different conditions for 21h hours and were evaluated in either the cured (vertical oven, 10min at 110°C) or uncured states. Six sets of membranes were dip-coated according to formulation FD14/mod on series 719 substrate membranes. Membranes selected at random from the total production batch were treated according to the scheme below. All the membranes were rinsed in RO permeate before being conditioned and before evaluation (Table 6.66).

1) Control membranes - evaluated directly (no conditioning)
2) Conditioned in a solution containing 1% glyoxal and 2% Na_2CO_3 in RO permeate for 21h.
3) Conditioned in a solution containing 1% glyoxal and 2% Na_2CO_3 in RO permeate for 21h. The membranes were rinsed in RO permeate before curing.
4) Conditioned in RO permeate for 21h containing 1% glyoxal by mass. The pH of the permeate was raised to 11 with NaOH before the glyoxal was mixed in.
5) Similar to no. 4 above, except that the membranes were cured for 10min at 110°C.
6) Conditioned for 21h in RO permeate, buffered to pH 11. The membranes were heat-cured for 10min at 110°C.

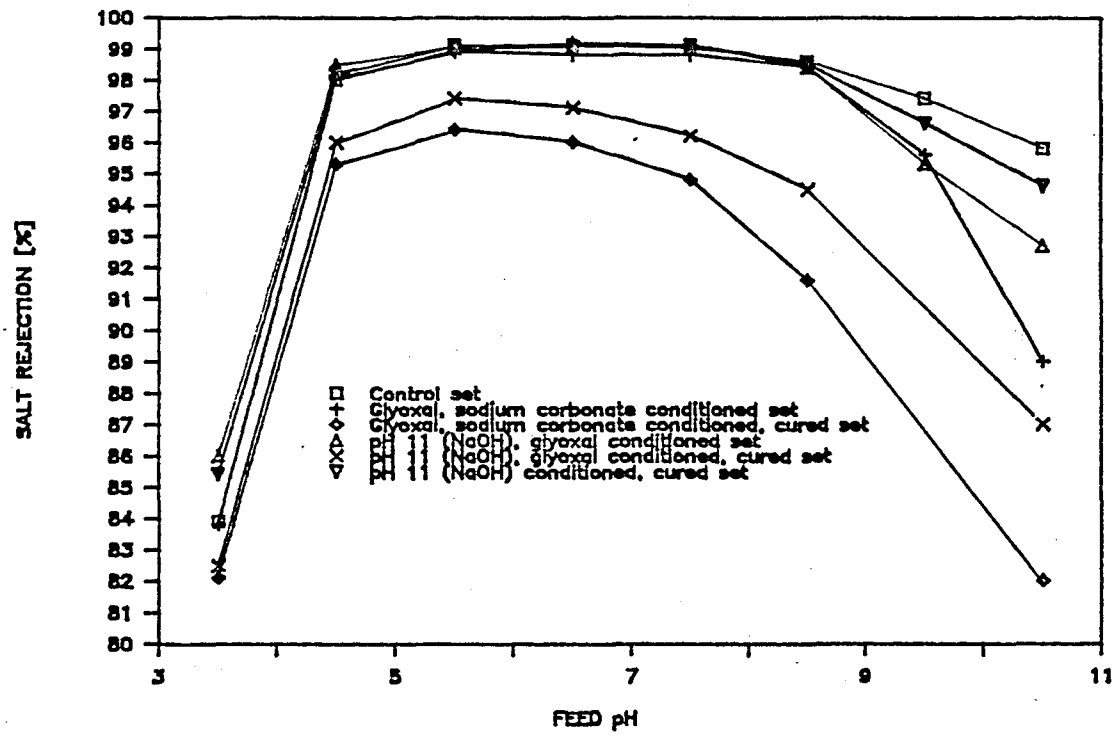

FIGURE 6.15: CONDUCTIVITY REJECTION PERFORMANCE OF "MODIFIED" PVAM MEMBRANES (TABLE 6.66)

TABLE 6.65: pH 11 CONDITIONING OF PVAM-FD UTF COMPOSITE MEMBRANES

	Control	pH 11 3 days	pH 11 7 days	pH 11 28 days	
Tested	95,7 ± 1,2	96,2 ± 1,2	97,9 ± 0,6	95,4 ± 2,2	%
Uncured	280 ± 78	290 ± 30	380 ± 55	800 ±145	lmd
	2,8 E-5	2,8 E-5	7,0 E-5	7,1 E-5	A^2/B
Tested	91,5 ± 3,7	95,2 ± 1,1	98,3 ± 1,0	96,3 ± 0,3	%
Cured	200 ± 34	170 ± 22	250 ± 49	390 ± 28	lmd
	0,8 E-5	1,3 E-5	5,6 E-5	3,8 E-5	A^2/B

TABLE 6.66: POST-TREATMENT OF PVAM-FD UTF COMPOSITE MEMBRANES

	Control	1% glyoxal 2% Na_2CO_3 21h	1% glyoxal pH 11 21h	pH 11 21h	
Tested	98,9 ± 0,1	99,1 ± 0,1	98,9 ± 0,5		%
Uncured	330 ± 47	860 ±104	800 ± 83		lmd
	10,8 E^{-5}	43,0 E^{-5}	32,2 E^{-5}		A^2/B
Tested		96,1 ± 0,5	97,5 ± 0,6	98,8 ± 0,1	%
Cured		980 ±170	740 ±140	250 ± 32	lmd
		10,9 E^{-5}	12,2 E^{-5}	8,1 E^{-5}	A^2/B

From the results above it appears again that the chemistry of the PVAM-FD membrane can be modified by post-treatment, a point worth noting when membrane formulations are considered for further optimization. The rejection performance behaviour of the six sets of membranes were not the same over a pH range of 4,5 to 8,5. The conductivity rejection performance of the membranes that underwent glyoxal treatment, before curing, appeared to decline more rapidly as the pH of the feed water was raised than happened with the other membranes. Figure 6.15 indicates that membrane properties may be modified by neutralizing (hydrolysis) at high pH, and thermal curing, post-treatment steps.

6.3.7.4 Discussion

The chemistry of the UTF PVAM-FD/SCL membrane system appears to be complicated, as judged only by the relative performances of treated membranes. The desalting matrix remained chemically reactive after the cross-linking step, which allowed further post-reaction steps to be incorporated into the formulation procedure for the final product.

Although the indications are that swelling of the UTF matrix occurred when the film was subjected to acidified feed water, the swelling was not destructive when the membranes were operated at pH values down to 4,5. The membrane performances recovered when the pH of the feed was readjusted to optimum pH values of 6,5 to 7,5.

LIST OF REFERENCES

1. Jacobs, E.P., Design of a tubular RO element, M.Sc. Thesis, (1980), Potchefstroom University
2. Banfield, D.L., British Patent No. 704834, (July 1969)
3. Saline Water Conversion Report, for 1969-1970, Office of Saline Water, US Dept. of Interior, p449 (1971), Washington, DC
4. Manjikian, S., Loeb, S., McCutchan, J.W., Proc. 1st Int. Symp. Desal., (1965), 2(1967)159, Washington, DC
5. Pienaar, H.S., The synthesis and physical properties of semi-permeable polymeric membranes used in water purification by the process of RO, Ph.D. thesis, (1977), University of Stellenbosch
6. Kuester, J.L., Mize, J.H., Optimization techniques with Fortran, (1973), McGraw-Hill, NY
7. Jacobs, E.P., Sanderson, R.D., Botha, G.R., Development of membrane support systems and modules, Final Report (1982)233-301, Water Research Commission, Pretoria
8. Stowe, R.A., Mayer, R.P., Ind. Eng. Chem.,58(1966)36-40
9. Kreyszig, E. Introductory to mathematical statistics, Table 8, p454, (1970) John Wiley & Sons, Inc., NY
10. Grethlein. H.E., Statistical design of experiments for optimizing the casting variables for CA membranes, Ch. 6., Ed. Sourirajan, S., RO and synthetic membranes, (1977),
11. Fang, H.H.P., Chian, E.S.K., J. Appl. Pol. Sci., 20(1976)303-314
12. Matz, R., Frommer, M.A., The mechanism of skin formation in CA RO membranes, Rep. no. 774(1972), Office of Saline Water Research, Washington, DC
13. Cabasso, I., Zimny, B.L., Development of novel porous substrates for UF, desalination and water reclamation - Part III, U.S. Dept. of Interior, OWRT, Rep. no PB 283 4220 (1981), Washington, DC
14. Wafilin B.V., Netherlands Patent Appl. 78 12,664 (Dec. 1978)
15. Masahiro, K., Ryozo, H., Eur. Pat. Appl. 12,630 (25 Jun. 1980), Teijin Ltd.
16. Yasuda, H., Tsai, J.T., J. Appl. Polym. Sci., 18(1974)805-819
17. Yasuda, H., Tsai, J.T., J. Appl. Polym. Sci., 19(1975)2529-2536
18. Strohwald, H. MSc-thesis in Preparation, Title: The development of PES UF membranes and its modular applications, (1988), University of Potchefstroom
19. Hurndall, M., PhD-thesis in preparation, Proposed Title "Polyvinylamidine RO membranes", (1988), Institute for Polymer Science, Univ. Stellenbosch
20. Riley, R.L., Lyons, C.R., Milstead, C.E., Seroy, M.W., Tagami, M., Wrasidlo, W.J., Res. and dev. on a spiral-wound membrane system for single-pass seawater desalination, NTIS Report no. PB-81 151938, (1976), OSW contract 14-30-3303
21. Richardson, J.L., Williams, R.H., Segovia, G., Tubular RO membrane research, NTIS Report PB-23943 (1974), OSW contract 14-30-2884
22. Rozelle, L.T., Cadotte, J.E., King, W.L., Senechal, A.J., Nelson, B.R., Development of ultra-thin RO membranes for desalination, Res. & Dev. Prog. Rep. 659, (1971), OSW, Washington, DC
23. Plackett, R.L., Burman, J.P., Biometrika, 33(1946)305
24. Cabasso, I., Practical aspects in the development of a polymer matrix for UF, Ed. Cooper, R., UF membranes and applications, (1980), Plenum Press, NY
25. Sudak, R.G., Chirrick, J.M., Fox, R.L., Mckee, M.E., Bott, J.B., Tomaschke, J.E., Development of chlorine resistant membranes, asymmetric polyimide membranes and porous substrates, NTIS Report PB81-142242, (Sept. 1980), OWRT Contract 14-34-0001-9515, Washington, DC
26. Buckfelder, J.J., Schleinitz, H.M., US Patent 4454176, (Jun. 1984)
27. Riley, R.L., Fox, R.L., Lyons, C.R., Milstead, C.E., Seroy, W.M., Tagami, M., Desalination, 19(1976)113
28. Kesting, R.E., Development of dry process microporous PS supports for ultra-thin film composites, NTIS Rep. PB-300 488, (1979), Washington, DC
29. Cabasso, I., Development of novel porous substrates for UF, desalination and water reclamation, NTIS Report PB81-14787, (1980), OWRT Contract no. 14-34-0001-8521, Washington, DC
30. Rose, J.B., Discovery and development of the "Victrex" poly(arylether sulphone), PES, and poly(arylether ketone), PEEK., Dept. Chem., Univ. Surrey, England, Anon.
31. Kai, M., Ishii, K., Tsugaya, H, Miyano, T., Development of polyether sulphone UF membranes, ACS Symp. Series (1975)21
32. Dreger, D.R., Mach. Des., 50(1978)114
33. Guillotin, M., Lemoyne, C., Noel, C., Monnerie, L., Desalination, 21(1977)165-181
34. Cadotte, J.E., King, R.S., Sand, J.E., Petersen, R.J., Improved porous supports for thin-film composite RO membranes, NTIS Report PB-82 197997, (1981), OSW Contract 14-34-0001-0443, Washington, DC
35. Jacobs, E.P., Hurndall, M., Research on membrane development and fabrication for RO and UF, Final Rep. (1983 - 1985), (Feb. 1986), Water Res. Comm., Pretoria
36. Cabasso, I., Development of a polymer matrix for UF, Ed. Cooper, A.R., UF membranes and applications, Polym. Sci. and Techn., Vol 13, Plenum Press, NY
37. Barton, A.M.F., Handbook of solubility parameters, p15 (1983), CRC Press, Inc., Florida
38. Cabasso, I., Klein, E., Smith, J.K., Research and development of NS-1 and related PS hollow fibers for RO desalination of sea water, NTIS Rep. PB-248666, (July 1975), OSW contract 14-30-3165
39. Fox, R.L., US Patent 4 307 135 (Dec. 1981)
40. Riley, R.L., Milstead, C.E., Research and development on spiral-wound thin-film composite membrane systems, NTIS Report PB83-167825, (Sept. 1982), OSW Contract DI-14-34-0001-1481, Washington, DC
41. Private communications, J.P. Barnard, Membratek Division, Bintech (Pty)(Ltd), Paarl
42. Barnard, J.P, Molnar, O., Hattingh, P.A., USA Patent Application no 084-208, Filed (Oct. 1987)
43. Strohwald, H., Marshall, G., Development of a UF and TFC support membrane, Internal Report, (1986), Institute Polymer Science, Univ. Stellenbosch
44. Yasuda, H., Tsai, J.T., J. Appl. Polym. Sci., 18(1974)805-918
45. Cabasso, I, Klein, E., Smith, J.K., J. Appl. Polym. Sci., 20(1976)2377
46. Cabasso, I, Klein, E., Smith, J.K., J. Appl. Polym. Sci., 21(1977)165
47. Cabasso, I, Klein, E., Smith, J.K., Research and development of NS-1 and related PS hollow fibers for RO desalination of sea water, NTIS Rep. no. PB-248666, (July 1975), OSW Contract 14-30-3165, Washington, DC

48. Zadak, A., Hoover, P., Gollan, A., Goldsmith, R.L., Development of a low-cost tubular RO module for one-pass sea water desalting, NTIS Report PB-242967, (June 1975), OWRT Contract 14-30-3251
49. Groenveld, P., Journal AIChE, 17(1971)489-490
50. Morgan, P.W., Condensation polymers by interfacial and solution methods, (1965), Interscience Publishers
51. Cadotte, J.E., Evolution of composite RO membranes, Lloyd, D.R., Ed., Material Science of Synthetic Membranes, ACS Symp. Ser. 269(1985)273-294
52. Teijin, Pty., Ltd., Eur. Patent Appl. no. 80304742.2, (Dec. 1980)
53. Private Discussions, Sanderson, R.D., Hurndall, M., Institute for Polymer Science, Stellenbosch University
54. Hendrix,C.D., Empirical optimization in research and development, Internal Report, Union Carbide Corporation, South Charleston, West Virginia, USA
55. Riley, R.L., Milstead, C.E., Research and development on a spiral-wound membrane system for single-stage sea water desalination, NTIS Report PB81-213191, (April 1981), OWRT Contract 14-34-0001-9529, Washington, DC
56. Leban, M.I., Environ. Sci. Techn., 18(1984)778-780
57. Baker, R.W., Barss, R.P., Composite membranes for RO, NTIS Rep. PB83-140947, (May 1981), Dept. of Interior, PAT-APPL-6-259349, Washington, DC
58. Teijin, Pty., Ltd., Eur. Patent Appl. no. 80304742.2, (Dec. 1980)
59. Private Discussions, Sanderson, R.D., Institute for Polymer Science, University of Stellenbosch
60. Riley, R.L., Milstead, C.E., Research and development on a spiral-wound membrane system for single-stage seawater desalination, NTIS Rep. PB81-105918, (Aug. 1977), OWRT Contract DI-14-34-0001-6516, Washington, DC
61. Riley, R.L., Milstead, C.E., Research and development on a spiral-wound membrane system for single-stage seawater desalination, NTIS Rep. PB80-114705, (Oct. 1979), OWRT Contract 14-34-0001-7543, Washington, DC
62. Rozelle, L.T., Cadotte, J.E., Nelson, B.R., Ultra-thin membranes for RO water desalination, Res. & Dev. Prog. Rep. no. 725, (Dec. 1971), Contract no. 14-01-0001-1969, US. Dept. of the Interior, Washington, DC
63. Hurndall, M., Flat-sheet PVAM studies, Unpublished Research results, Institute for Polymer Science, University of Stellenbosch
64. Lu, E.K., Babcock, W.C., Novel composite membranes, NTIS Rep., PB83-243170 (Apr. 1983), OWRT Contract, Washington, DC
65. Weast, R.C., Ed., Handbook of Chemistry and Physics, (1976)D-134, CRC Press

CHAPTER VII

CONCLUSIONS

The science of any membrane system involves an examination of a multitude of formulation variables. Consequently, membrane research involves a study of these variables and their interactions in order either to generate an understanding of the science involved, or to exercise control over desired properties.

With this goal in mind, the study proved successful in a number of ways, namely:

<u>Tubular cellulose acetate membranes</u>

i) The applicability of statistical techniques and statistical designed experiments to the generation of fabrication formulations for tubular cellulose acetate membranes was illustrated. (Sections 6.1.2 and 6.1.3)

ii) It was proved that the multiple-linear regression models, which were developed to represent the permeate flux and salt rejection responses of tubular cellulose acetate membranes, can be manipulated mathematically to predict fabrication formulations to achieve optimal permeate flux performances for specified salt rejections. (Sections 6.1.2.4 and 6.1.2.5).

iii) A Taylor series, expanded to include quadratic terms, proved sufficient for modelling the permeate flux and salt rejection responses of tubular cellulose acetate membranes. (Section 6.1.3.5).

iv) It was shown further that by changing the grade of cellulose acetate used from 398-10 to 400-25, a different set of design equations, which showed better performance in different ranges of usage, was obtained. (Preamble to section 6.1.3 and 6.1.3.6).

<u>Asymmetric micro-porous tubular substrate membranes</u>

i) Although micro-porous substrate membranes, used in ultra-thin film composite membrane fabrication, were successfully produced from the well documented Udel 1700P and 3500P poly(bisphenol A sulphone) dissolved in a mixture of N-methyl, 2-pyrrolidone and 1,4-dioxane, the adhesion of these membrane systems to the porous non-woven Viledon FO2406 poly(ethylene terephthalate) support fabric was as unsatisfactory. This inadequacy in membrane adherence was overcome by the use of a different substrate membrane which was developed from a study of membrane-forming polymers, casting solution compositions and fabrication conditions. These membranes were produced from Victrex 4800G poly(arylether sulphone), dissolved in either N-methyl, 2-pyrrolidone or a mixture of N-methyl, 2-pyrrolidone and N,N-dimethyl formamide, with polyvinyl-pyrrolidone and lithium chloride additives. The bond-strength of these membranes to the

support fabric was more than twenty times greater than that of the Udel 1700P and 3500P membranes. (Section 6.2.2.4).

ii) In a simultaneous study of nine factors (Section 4.3.4), only thirty-two experiments were needed to establish that an inverse relationship existed between the substrate membrane permeate flux performance and the adherence of the substrate membrane to the non-woven support tube.

Ultra-thin film polyvinylamidine membranes

i) It was demonstrated with the polyvinylamidine ultra-thin film composite reverse osmosis membrane system that up to twelve membrane formulation variables can be studied simultaneously in a self-directing optimization approach to yield a membrane with optimum performance. (Sections 6.3.2 and 6.3.3). This study was successfully concluded even though the synthesis of the polyvinylamidine precursor was still under development and random variability in the quality of the material was known to exist.

ii) It was shown that ultra-thin film composite membranes with extremely good reverse osmosis properties (in the optimum case a sodium chloride salt rejection of 99,1% and a permeate flux performance of 860 liters per square metre per day), can be fabricated in tube form. (Section 6.3.7.3). Although the ultra-thin film composite membrane study was mainly directed towards a better understanding of factors at play in the formulation of the membrane it was shown unequivocally that a novel ultra-thin film tubular composite membrane can be made with more than adequate performance characteristics to warrant its use as a commercial brack-water desalting membrane.

iii It was also shown that the chemistry of the approximately 200 nanometre ultra-thin membrane film can be changed or improved by further post-chemical reaction(s). Examples were the improved permeate flux performance which resulted by reaction of the membrane with glyoxal, and the improved dry storage-life obtained with diaminobenzene treatment. (Section 6.3.7).

Future research

i) A strong correlation was found between factors that control the morphology of the poly(arylether sulphone) substrate membrane and the final performance of the polyvinylamidine ultra-thin film composite membrane (section 6.3.5.2). It is suggested that any future planning of research to optimize the properties of an ultra-thin film composite membrane on poly(arylether sulphone) substrate membranes should take this fact into account. The ideal would be to combine all factors that proved to have an effect on the reverse osmosis properties of the ultra-thin film membrane for simultaneous study. (See sections 6.3.4.1 and 6.3.5.2).

ii) A number of factors that affect the adherence and permeability of the asymmetric poly(arylether sulphone), poly(ethylene terephthalate) supported membranes were isolated. (Section 6.2.2.3). No attempt was made in this study to qualify these findings. If further scientific advances are to be made

in the area of membrane/support fabric adherence, it is suggested that the phase diagrams which evolved from this particular phase-inversion process be studied to obtain a deeper insight into the mechanisms which control membrane phase separation and morphology.

Contribution to membrane literature

i) It has been clearly indicated that the technique of modelling membrane performance response surfaces by means of statistically designed experiments, and the design of fabrication conditions by numerical techniques, apply equally to membranes in tubular form, as was reported in the literature on flat-sheet membranes. The validity of the expanded Taylor series as regression model was proved. These simple approaches can allow custom design of reverse osmosis membrane performance for specific applications.

ii) The value of statistically designed experiments as a tool in improving membrane properties, was demonstrated during the course of a study aimed at the improvement of the bond-strength which initially existed between an asymmetric micro-porous substrate membrane and its support fabric. Of the original nine factors which were considered for study, five proved to contribute significantly to membrane adhesion. In this case a sixteenth fractional replicate of a 2^9 factorial was used, which reduced the number of experiments from 512 (full 2^9 factorial) down to a more manageable 32 experiments.

iii) The simplex method of self-directing optimization can be used to optimize the performance properties of an intricate membrane such as the ultra-thin film composite membrane, without prior knowledge of tubular membrane formulations, and in the face of known random variation in the quality of the membrane chemicals synthesized initially. When the variability in the quality of the membrane materials was reduced by improving the route followed in chemical synthesis, membrane properties could be improved even further, within fewer experiments.